University of Nottingham
UK | CHINA | MALAYSIA

The Ecological and Evolutionary Significance of Functional Variation in Mitochondria in the Three-spined Stickleback.

Thesis submitted to the University of Nottingham for the degree of Doctor of Philosophy

March 2025

Megan Barnes

Student ID: 10271374

Supervisors: Andrew MacColl and Lisa Chakrabarti

School of Life Sciences

University of Nottingham

Abstract

Mitochondria are widely known as the ‘powerhouse of the cell’ due to their importance in energy metabolism, and the mitochondrial DNA (mtDNA) plays a central role as it encodes subunits of the oxidative phosphorylation pathway, responsible for the majority of this energy production when oxygen is available. Despite this fundamental role, the adaptive significance of mtDNA variation has often been overlooked. It is now well established that the mitogenome is not evolving neutrally as once assumed, with studies across numerous taxa identifying evidence of positive selection, or showing that mtDNA variation has functional consequences which can be associated with adaptation. However, pure mitochondrial effects have rarely been separated from nuclear genetic effects in natural study systems, mainly due to a lack of populations or species wherein variation in the mtDNA can be studied independent of potentially confounding variation in the nuclear genetic background. In this thesis, I focus on Atlantic three-spined stickleback (*Gasterosteus aculeatus*) on the Scottish island of North Uist, where, in migratory populations, two deeply diverged mitochondrial lineages segregate against a common nuclear genomic background. I show that the stickleback provides a valuable model to determine the adaptive significance of mtDNA variation. I first assessed the development of migratory stickleback, and examined the effect of anaesthetics on mitochondrial function. I then focused on variation between the two highly diverged mitochondrial lineages that likely diverged in allopatry on opposite sides of the Atlantic, but are now both widespread. Migratory populations were a mix of the two lineages, but resident populations in fresh water and saltwater lagoons were predominantly one lineage, suggesting differing adaptive potential. Using phylogenetic selection analyses, I found evidence that the mitogenomes of the Atlantic three-spined stickleback evolved under positive selection, so the mtDNA variation itself may be adaptive. Unlike previous work in natural populations, I was able to show that mtDNA variation had temperature-dependent consequences for mitochondrial respiration independent of the nuclear genetic background. By combining phylogeography, ecology, selection analyses and mitochondrial physiology, I show that mitochondrial variation makes an important contribution to the ecology and evolution of the Atlantic three-spined stickleback. To my knowledge, this research may be the first to explicitly link mtDNA variation to physiological mitochondrial differences and adaptive potential in natural populations, independent of the nuclear genome.

Acknowledgements

I would firstly like to thank my supervisors Professor Andrew MacColl and Professor Lisa Chakrabarti for their guidance. I am extremely grateful that they have shared their knowledge and ideas and encouraged me throughout my PhD.

The MacColl lab group has given me so much support; Laura Dean, Iain Hill, Henry Lewis, Francis Gyapong, Harry Bodkin, Ann Lowe, Anthony Ducker and Ben Fisher have provided help in the field, lab and aquarium, and have offered valuable advice. Henry has been there since day one of my PhD, through the ups and downs, and I am extremely grateful for his ongoing support, motivation and the constant laughs he brings to the group. My experience would not be the same without him.

The Chakrabarti lab group has helped with mitochondrial biology and experimental design using the O2k; their input has helped shape my research. I am also grateful to all of the evolutionary ecology researchers at the University of Nottingham, and in particular those who I have shared an office with, who have always been there for advice, discussions and to offer motivation.

My PhD has included stickleback samples and mitochondrial genomes from across the Atlantic which have kindly been provided by collaborators. I am very grateful to Daniel Bolnick, Alison Bell, Antoine Paccard, Grant Haines and Felicity Jones for their contributions.

I would also like to thank NERC and the Envision doctoral training partnership for funding this project and providing valuable training opportunities.

I am lucky to have been supported by so many people throughout my PhD. My family and friends have always believed in me and pushed me to fulfil my potential, which I am incredibly grateful for. I would finally like to thank Matt, who has given so much love, encouragement, and understanding throughout my PhD.

Contents

Chapter 1: General Introduction

The adaptive significance of mitochondrial DNA (mtDNA) variation has often been overlooked. Separating mitochondrial from nuclear genetic effects is difficult as mitochondria rely on both genomes for efficient function, so despite the potential association of mtDNA variation with adaptive potential, most research to date has been unable to directly connect mtDNA substitutions to physiology and fitness. To measure any direct effects of mtDNA variation, comparisons of individuals with different mtDNA variants but the same nuclear genetic background ('conplastic' experiments) have begun to be explored in model organisms such as *Drosophila* and mice, but it is extremely rare to find natural populations where two deeply diverged mitochondrial lineages segregate against a common nuclear background. I show that the three-spined stickleback (*Gasterosteus aculeatus*, 'stickleback') in the Atlantic is a valuable model to assess the ecological and evolutionary significance of mtDNA variation as migratory populations segregate only by their mtDNA, which provides an ideal natural system to study the role of mtDNA variation in adaptation independent to the nuclear genome.

I first provide some background on the role of the mtDNA and how sequence variation could impact mitochondrial function, before giving a brief overview of the techniques used to measure mitochondrial respiration and how these are being used in the field of ecology. I discuss the potential role of mtDNA variation in adaptation from studies identifying evidence of positive selection across the mitogenome and research into the functional consequences of mtDNA variation, highlighting the lack of direct connections between mitochondrial sequence variation and physiology or fitness in natural populations due to the difficulty in separating pure mitochondrial from nuclear or mitonuclear effects in most study systems. I show that direct mitochondrial effects can be measured in the Atlantic stickleback as there are two highly diverged mitochondrial lineages which, in migratory populations, segregate against a common nuclear background, evidencing the stickleback as a valuable model to assess the significance of mtDNA variation.

1.1 Mitochondrial DNA variation

Mitochondrial DNA (mtDNA) is a widely used marker in population genetics (Avise et al., 1987). Features that make it a useful tool include its small size, high mutation rate,

maternal inheritance and lack of recombination, in comparison to the nuclear genome (Moritz et al., 1987). Importantly, the mtDNA has long been assumed to evolve neutrally (Avise et al., 1987; Ballard and Kreitman, 1995). However, given the functional importance of the peptides encoded by the mtDNA, which are subunits of the enzyme complexes involved in oxidative phosphorylation (OXPHOS, **Figure 1.1**, **Table 1.1**) and the electron transfer system (ETS), and are responsible for producing the majority of a cell's ATP production when oxygen is available, there is increasing research into understanding the importance of mtDNA variation. It is now generally believed that the mtDNA is not neutral; variation in mtDNA sequence may have key implications for fitness, with selection acting on this variation to promote mitochondrial sequences that provide an advantage in environments that affect metabolic processes.

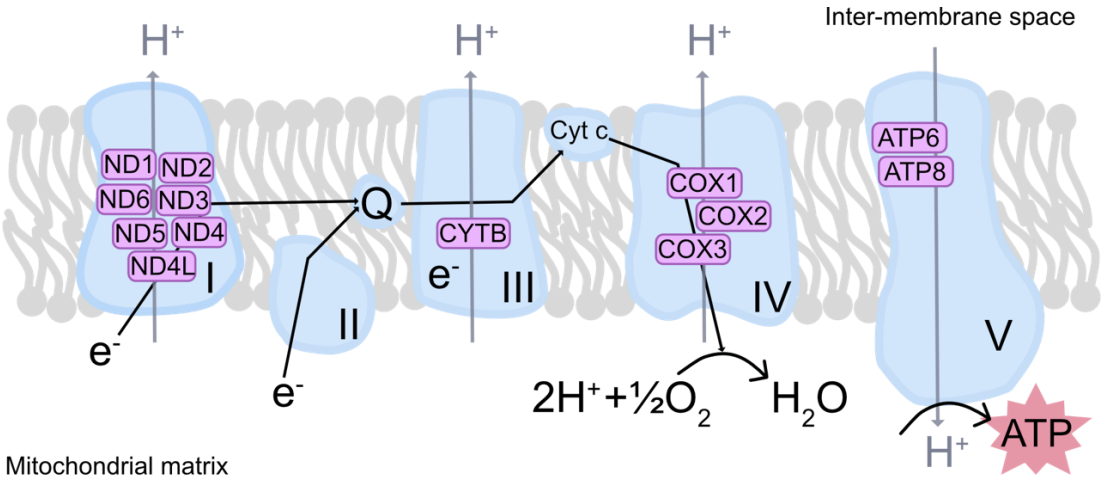

Figure 1.1: OXPHOS. Schematic showing the enzyme complexes of the ETS with subunits encoded by the mitochondrial genome in purple. Electrons are donated from NADH and $FADH_2$ (products of glycolysis, fatty acid metabolism and the Krebs cycle) and are transported through the enzyme complexes before being transferred to oxygen, the terminal electron acceptor, producing water. This is coupled to the pumping of protons from the mitochondrial matrix to the intermembrane space, which creates an electrochemical gradient, driving ATP synthesis at complex V, ATP synthase.

Table 1.1: Mitochondrial protein coding genes.

Name	Protein product	Complex
ND1	NADH dehydrogenase subunit 1	I
ND2	NADH dehydrogenase subunit 2	I

ND3	NADH dehydrogenase subunit 3	I
ND4	NADH dehydrogenase subunit 4	I
ND4L	NADH dehydrogenase subunit 4L	I
ND5	NADH dehydrogenase subunit 5	I
ND6	NADH dehydrogenase subunit 6	I
CYTB	Cytochrome b	III
COX1	Cytochrome c oxidase subunit I	IV
COX2	Cytochrome c oxidase subunit II	IV
COX3	Cytochrome c oxidase subunit III	IV
ATP6	ATP synthase F0 subunit 6	V
ATP8	ATP synthase F0 subunit 8	V

Any variation in the mtDNA sequence could alter the conformation, structure or interactions of the core protein components of OXPHOS, impacting their function. Mitochondria are not self-supporting entities and rely on many nuclear-encoded factors to function. Enzyme complexes I, III, IV and V consist of peptides encoded by both the nuclear and mitochondrial genomes (**Figure 1.1**), so mitochondrial function relies on the two genomes working efficiently together (Bettinazzi et al., 2024; Nguyen et al., 2020; Rank et al., 2020). An emerging field studies these mitonuclear interactions (Barreto et al., 2018; Burton, 2022; Burton and Barreto, 2012; Hill, 2015) and the coevolution of the mitochondrial and nuclear genomes (Barreto et al., 2018; Hill, 2020, 2016). This makes studying the influence of the mitochondrial genome difficult as the nuclear genetic background plays such a pivotal role and is near impossible to completely control for in most study systems. The mitochondrial genome also encodes 22 tRNAs and 2 rRNAs which are necessary for the translation of mRNA. As well as being vital to the generation of the OXPHOS complexes, these may also play a role in additional processes linked to the mitochondria, including ageing (Jang et al., 2018), apoptosis (Tait and Green, 2013) and signalling (Chandel, 2014).

1.2 Measuring mitochondrial function

The role of mitochondria in ageing and disease has long been investigated (Horan et al., 2012), but with the development of new techniques to measure mitochondrial function there has been increasing interest in studying mitochondrial bioenergetics in evolutionary ecology (McKenzie et al., 2019) and conservation biology (Thoral et al.,

2024). One such technique is high-resolution respirometry (HRR), using the Oxygraph 2k (O2k, Oroboros® Instruments) or Seahorse XF Flux Analyzer (Agilent Technologies, Santa Clara, CA), which allows small changes in mitochondrial function to be measured. By combining HRR with ecology, previous work has evaluated how mitochondria respond to changes in energy demand (Coulson et al., 2024) and the environment (Salin et al., 2018; Steffen et al., 2023; Thoral et al., 2021), and mitochondria have also been implemented in the adaptation to new environments (Devaux et al., 2019; Greenway et al., 2020; Pfenninger et al., 2014; Willis et al., 2021). Although this work highlights the role that differences in mitochondrial function may have in adaptation, research in this field has only just begun to explore the genetic changes behind this, perhaps due to the complexity of the mitochondrial pathways involved.

1.3 Natural selection across the mitogenome

Variation in the mtDNA was long assumed to be neutral (Avise et al., 1987; Ballard and Kreitman, 1995). As the mitochondrial genes encode peptides involved in such a fundamental and conserved process, any mtDNA mutations that arose were thought to disrupt mitochondrial function so would be eliminated from the population by purifying selection. Although purifying selection is the main driver of mitogenome evolution (Popadin et al., 2013), more recent evidence suggests that some mtDNA variants could be beneficial in particular environments so may evolve under positive selection (Foote et al., 2011; Morales et al., 2015; Noll et al., 2022) and it is now more widely accepted that the mtDNA can be adaptive (Bazin et al., 2006; Ruiz-Pesini et al., 2004). The environment can alter an organism's metabolic demands due to factors such as temperature, altitude and diet, meaning an individual may adjust its energy usage and nutrient acquisition in response to changes in conditions (Salin et al., 2018; Thoral et al., 2021). Long-term changes may result in selection for optimal metabolic function in these conditions, which may be due to mtDNA variation altering OXPHOS or mitochondrial function.

Studies across numerous taxa have demonstrated that the mitochondrial genome can evolve under natural selection (Foote et al., 2011; Li et al., 2018; Melo-Ferreira et al., 2014; Morales et al., 2015). Multiple methods have been developed to look for evidence of selection, which have been utilised to detect positive selection across the mitochondrial protein coding genes (PCGs). Methods are based on the ratio of non-synonymous to synonymous mutations (dN/dS), where a higher value indicates an

increase in amino acid substitutions, suggesting that positive selection may have acted on the gene of interest (Bazin et al., 2006). CODEML, which is implemented in PAML (Yang, 2007), is one such method and is able to detect specific positively selected sites which may have otherwise been masked by overwhelming signals of purifying selection across the mitochondrial PCGs (Awadi et al., 2021; Noll et al., 2022; Zhang et al., 2021). Alternative methods can utilise the physiochemical properties of amino acids, predicting whether amino acid substitutions are likely to alter protein function which could be selected for (Bahbahani et al., 2023; Mukundan et al., 2022; Zhao et al., 2022); TreeSAAP (Woolley et al., 2003) is one example. By using methods in combination, studies have found strong evidence that positive selection acts across the mitogenome in many species (Awadi et al., 2021; Lamb et al., 2018; Noll et al., 2022; Zhao et al., 2022).

Some studies have attempted to link this evidence of positive selection in the mitogenome to adaptive consequences, but with limited success. mtDNA variation that alters metabolic function in certain environments may be beneficial and be selected for. Positive selection in the mitogenome has been associated with altitude (Li et al., 2018; Yu et al., 2011; Zhou et al., 2014), temperature (Baltazar-Soares et al., 2021; Melo-Ferreira et al., 2014; Sebastian et al., 2020), deep sea (Shen et al., 2019; Yang et al., 2021; Zhang et al., 2017) and diet (Aw et al., 2018; Ballard and Youngson, 2015; Towarnicki and Ballard, 2018). One common approach to assess the role of the mitogenome in adaptation to new environments is to compare the mitogenomes of species or populations inhabiting different environments, for example low and high-altitude adapted fishes (Wang et al., 2016), birds (Zhou et al., 2014) and insects (Li et al., 2018). This method has identified positively selected sites in the mitochondrial PCGs that may have played a role in adaptation, but how these amino acid substitutions affect mitochondrial function or individual fitness generally remains unknown.

1.4 Functional consequences of mtDNA variation

Studies have linked variation in the mitochondrial genome to phenotypic differences in model systems, with most work utilising cybrid cell lines (Gómez-Durán et al., 2012, 2010; Wilkins et al., 2014), conplastic mouse strains (Latorre-Pellicer et al., 2016; Scotece et al., 2021; Yu et al., 2009), or comparing *Drosophila* mitochondrial haplogroups (Ballard et al., 2007; Camus et al., 2017; James et al., 2003; Pichaud et al., 2013) to identify any physiological or fitness consequences. It has been more

difficult to explicitly link mtDNA variation to specific phenotypes in natural populations as it is harder to conduct experiments and control for variation in the nuclear genetic background, although differences in fitness have been found between mitochondrial haplogroups in some insects (Dahlhoff et al., 2019; Sun et al., 2019). Most work assessing the role of the mitochondria in adaptation in natural systems has compared mitogenomes and mitochondrial function between populations or species from two contrasting environments.

The bar-headed goose (*Anser indicus*) has become a key example showing the role of the mitochondrial genome in high-altitude adaptation (Scott et al., 2015, 2011). A comparative analysis of the high-altitude adapted bar-headed goose and two low-land species, the pink-footed goose (*Anser brachyrhynchus*) and barnacle goose (*Branta leucopsis*), found that cytochrome c oxidase (COX, complex IV) of the bar-headed goose had lower activity levels and a higher affinity for cytochrome c than the low-land species (Scott et al., 2011). By comparing the mitogenomes, Scott et al. identified a nonsynonymous substitution in COX3 of the bar-headed goose which was otherwise conserved in vertebrates. This was predicted to alter the interaction between COX3 and COX1, which could explain the observed difference in complex IV kinetics. It was hypothesised that these changes in complex IV activity could be beneficial at high-altitude as they may reduce reactive oxygen species (Scott et al., 2015, 2011). Although the bar-headed goose has other key adaptations that allow flight at high-altitude where oxygen availability is limited (Black and Tenney, 1980; Scott et al., 2015; Scott and Milsom, 2007) and further work is necessary to decipher how complex IV differences can be advantageous for altitude adaptation, this work demonstrates that variation in the mitogenome can provide a functional advantage which may be selected for in certain environments. Phylogenetic selection analyses on the mitochondrial PCGs were not possible in this study as the divergence between the mitogenomes of the species assessed was too low (Scott et al., 2011). A similar alteration of mitochondrial enzyme activities has been found in mammals adapting to high-altitude, with cytochrome c oxidase and citrate synthase (catalyses the first step in the Krebs cycle) having enhanced activity in highland populations of deer mice (*Peromyscus maniculatus*) compared to low-land relatives (*Peromyscus leucopus*) (Cheviron et al., 2012; Lui et al., 2015). By linking mtDNA variation to changes in mitochondrial function and the environment, these studies show that the mitogenome can have a role in adaptation. Disentangling these findings from the nuclear genome and any mitonuclear interactions can be difficult with such study systems and

approaches as nuclear genetic divergence will be high between species, which can also influence OXPHOS (Baris et al., 2016; Edmands and Burton, 1999; Ellison and Burton, 2006; Hill, 2015). Mitochondrial sequence variation alone could not be linked to the observed physiological differences.

Examples explicitly linking mtDNA variation to physiological mitochondrial changes must control or account for the nuclear genetic background. While this is not possible in most study systems, *Drosophila* have become a valuable model in developing our understanding of the evolutionary and ecological implications of mtDNA variation (reviewed in Dowling and Wolff, 2023) as mtDNA variants can be expressed alongside different nuclear genetic backgrounds. This has allowed the assessment of mitonuclear incompatibilities (James et al., 2003; Meiklejohn et al., 2013; Montooth et al., 2010) and the functional consequences of mtDNA variation when assessed in the same nuclear background (Aw et al., 2018; James et al., 2003; Wolff et al., 2016). This shows the important role of mitochondrial gene-by-environment interactions, including temperature (Hoekstra et al., 2013; Pichaud et al., 2013) and diet (Aw et al., 2018; Ballard and Youngson, 2015; Zhu et al., 2014), demonstrating that mtDNA effects may be context or environment dependent. More recent studies have utilised conplastic mouse strains to compare individuals with different mtDNA variants but the same nuclear genetic background (Latorre-Pellicer et al., 2016; Scotece et al., 2021; Yu et al., 2009). Although these findings confirm the influence of mtDNA haplotype on mitochondrial function (Latorre-Pellicer et al., 2016), by combining the mtDNA of one strain with the nuclear genome of another, the interactions of the two genomes likely influence findings.

Natural study systems are beginning to be explored; those where strong nuclear gene flow occurs between mitochondrial haplogroups offer the most potential for the exploration of mtDNA variation, as this minimises any differences in the nuclear genome (Baris et al., 2016; Sun et al., 2019). Ideal populations consist of two diverged mitochondrial lineages that segregate against a common nuclear genetic background, but such populations are rare in natural study systems. Unlike artificial conplastic strains, studying natural populations ensures that mitonuclear combinations are compatible and mtDNA variants are compared in an admixed nuclear background. Genetic studies of mitochondrial and microsatellite markers of the European sardine (*Sardina pilchardus*) found that it formed an almost panmictic population around the Iberian Peninsula, but CYTB and ATP6 haplotypes were negatively correlated with minimum sea surface temperature (Baltazar-Soares et al.,

2021), and more recent work found evidence of positive selection across some sites in the mitogenome (Vieira et al., 2024). Whether mitochondrial haplotypes and positively selected amino acid substitutions alter mitochondrial physiology or function under certain conditions remains unexplored however. Mitochondrial genome variation has also been associated with climate and latitude (Sun et al., 2015) and phenotype (Sun et al., 2019) in the small brown planthopper (*Laodelphax striatellus*), with differences in mtDNA copy number, cold tolerance and fecundity identified between mitochondrial haplogroups, despite strong nuclear gene flow between populations (Sun et al., 2019, 2015). The differences in mtDNA copy number were independent from the nuclear genetic background and could be traced to non-synonymous substitutions in the mitochondrial genome, highlighting the functional importance of mtDNA variation. But fecundity and cold resistance were dependent on the nuclear genetic background (Sun et al., 2019), so the small brown planthopper may be a valuable model to study mitonuclear interactions and their role in maintaining mtDNA diversity.

Perhaps the most comprehensive series of work comparing mitochondrial haplogroups was conducted on the Atlantic killifish (*Fundulus heteroclitus*). There are two haplogroups near the Hudson River in Mantoloking, NJ, USA, where a northern group experiences temperatures approximately 12ºC colder than the southern. Initial studies assessed the mitochondrial genome within the species, identifying 5 amino acid differences between the northern and southern haplotypes, but found no evidence of positive selection across the mitogenomes (Whitehead, 2009). To determine whether OXPHOS function differed between the two haplogroups and whether this was dependant on temperature, HRR was conducted on permeabilised heart tissue (Baris et al., 2016). Importantly, fish from a single admixed population containing high frequencies of both haplotypes were selected as this meant that both haplogroups experienced the same environmental conditions and minimised any nuclear genetic differences. OXPHOS was measured at different acute temperatures in fish previously acclimatised to either 12 or 28ºC and the mitochondrial haplotype affected many of the measured OXPHOS parameters, but findings were complex and dependant on both the acute and acclimatisation temperature (Baris et al., 2016). These results demonstrated that mtDNA variation had temperature-dependant physiological consequences for cardiac OXPHOS function. Additional work compared the nuclear genomes of the two mitochondrial haplogroups from this same population by assigning the two mitochondrial haplogroups as independent populations and

calculating F_{ST} values to measure the amount of genetic differentiation among these. This method identified over 300 single nucleotide polymorphisms (SNPs) that had large F_{ST} values that were classed as statistical outliers and four of these were in genes that were likely to influence OXPHOS (Baris et al., 2017). Differences in mitochondrial respiration were only apparent between mitochondrial haplotypes with outlier single nucleotide polymorphisms (SNPs) associated with their own ancestral lineage, and not between haplotypes in a mixed nuclear background (Baris et al., 2017). So together, these results suggested that the observed differences in cardiac mitochondrial respiratory parameters were due to both mitochondrial and nuclear differences and their potential interactions (Baris et al., 2017, 2016; McKenzie et al., 2019). This series of studies highlights the potential functional consequences of mtDNA variation for OXPHOS, but this could not be disentangled from the nuclear genetic background.

1.5 The three-spined stickleback as a model

To link mtDNA variation to differences in mitochondrial physiology, organism fitness, and to any ecological and evolutionary consequences of this independent of the nuclear genetic background, utilising further non-model and natural systems is necessary. By assessing mitochondrial genomes for evidence of natural selection, numerous studies across a wide range of organisms have suggested that the mtDNA is adaptive (Foote et al., 2011; Li et al., 2018; Melo-Ferreira et al., 2014; Morales et al., 2015), but the majority fail to test whether positively selected amino acid substitutions have physiological consequences that could be selected for, instead relying on predictions from protein structures or previous work (Garvin et al., 2011; Zhang et al., 2024). This is due to the lack of natural model systems that allow mtDNA variation to be assessed independent to the nuclear genome. Where selection has been detected across the mitochondrial genome, species or populations from different environments have been compared (Li et al., 2018; Wang et al., 2016; Zhang et al., 2024; Zhou et al., 2014), or mitochondrial lineages had very little gene flow (Noll et al., 2022), resulting in divergence in the nuclear genomes. Any differences in mitochondrial function in these systems could be from mitochondrial or nuclear genetic differences, or their interactions. We also know that mitochondrial sequence and functional variation can influence numerous fitness parameters from studies of cybrid cell lines (Gómez-Durán et al., 2012, 2010; Wilkins et al., 2014), *Drosophila* (Aw et al., 2018; James et al., 2003; Wolff et al., 2016), and mice (Latorre-Pellicer et al., 2016; Scotece et al., 2021; Yu et al., 2009), and this is increasingly being applied

to natural populations including in high-altitude adaptation in birds and mammals (Cheviron et al., 2012; Lui et al., 2015; Scott et al., 2015, 2011) and in temperature tolerance in fish (Baris et al., 2017, 2016; Whitehead, 2009). These examples provide consistent evidence that mitochondria are important in adaptation, but again, these findings cannot be explicitly linked to variation in mtDNA sequence as there were also nuclear genetic differences between the populations studied. Ideal study systems would allow the comparison of mtDNA variants in the same nuclear genetic background, as in studies of *Drosophila* and mice.

Here, we propose that the three-spined stickleback (*Gasterosteus aculeatus*, 'stickleback') is a good model to investigate mtDNA variation. The stickleback is a small teleost fish widely distributed throughout the Northern Hemisphere and ancestrally marine stickleback have repeatedly colonised freshwater habitats (Bell and Foster, 1995; Jones et al., 2012). There are two well-studied mitochondrial lineages in the Atlantic with greatly diverged mitochondrial genomes (Dean et al., 2019; Mäkinen and Merilä, 2008): European ('*Eu*') and trans-Atlantic ('*At*'). Previous research on North Uist, Scottish Western Isles, found differences in the frequencies of these lineages between stickleback ecotypes which inhabit different environments (Dean et al., 2019), which may suggest different adaptive propensities. Migratory populations were generally an almost equal mix of two lineages, while non-migratory ('resident') stickleback that had permanently colonised fresh water and saltwater lagoons were predominantly the *Eu* lineage (Dean et al., 2019). As there are differences in energy requirements between such environments (due to differences in temperature, diet and salinity for example) and lifestyles (migratory versus non-migratory), the variation in mtDNA between lineages could explain these differences in adaptive potential. No work to our knowledge has investigated whether natural selection has played a role in the evolution of the stickleback mitogenome in the Atlantic or determined the physiological or fitness consequences of the mtDNA variation between lineages.

As previously discussed, current research into the consequences of mtDNA variation has identified natural selection acting on the mitogenome but is often unable to disentangle mitochondrial from nuclear genetic effects which limits tests of how mtDNA variation influences physiology and fitness. Migratory stickleback populations, at least on North Uist, segregate into approximately equal frequencies of the two mitochondrial lineages (Dean et al., 2019), but to the best of our knowledge are freely interbreeding and nuclear genetic differences are unlikely. This results in two mtDNA

variants in the same nuclear genetic background, experiencing the same environmental conditions. As a consequence, any physiological or morphological differences between lineages from these populations could be traced back to the mtDNA differences. This provides a natural study system to investigate the ecological and evolutionary consequences of mtDNA variation. The stickleback can be raised in aquaria (Divino et al., 2014), where factors that can influence mitochondrial function in fish can be controlled, including diet (Salin et al., 2021; Závorka et al., 2021), temperature (Chouinard-Boisvert et al., 2024; Dawson et al., 2022; Michaelsen et al., 2021) and salinity (Brijs et al., 2017; Zikos et al., 2014), so any consequences of mtDNA variation can be assessed independently or in addition to these variables. The stickleback has a high-quality reference genome (Nath et al., 2021; Peichel et al., 2020, 2017), with genetic studies widely conducted to answer a range of ecological and evolutionary questions (Dean et al., 2019; Jones et al., 2012; Reid et al., 2021; Roberts Kingman et al., 2021). A major area of research has been on the stickleback's repeated adaptation to fresh water across the Northern Hemisphere (Colosimo et al., 2005; Ishikawa et al., 2021; Jones et al., 2012) but little work has focused on the mitochondrial genome (but see Beck et al., 2022; Karlsen et al., 2024) other than as a marker of population structure (Mäkinen and Merilä, 2008; Orti et al., 1994), which we believe may have also played an important role in adaptation.

1.6 Study system

We sampled wild populations of stickleback from North Uist in the Western Isles of Scotland, UK (57.5704, -7.2812, **Figure 1.2**). North Uist is a well-studied system for stickleback ecology, evolution and behaviour (Dean et al., 2019; MacColl et al., 2013; Magalhaes et al., 2016; Robertson et al., 2016; Spence et al., 2013). The stickleback is widely distributed across the Northern Hemisphere and previous research has looked at the mitochondrial lineages across multiple locations in the Atlantic (see **Table 4.2**). We were therefore able to not only look at the adaptive consequences of mtDNA variation on North Uist, which may be specific to the colonisation history of the island, but to expand our survey across the Atlantic. We were also able to build upon this dataset by including the further sampling we conducted on North Uist, and samples from collaborators in North America (Nova Scotia, Newfoundland, Quebec, Lubec), Iceland and Portugal (see **Figure 1.2** for locations). In combination, this provides a large study area across the stickleback's Atlantic distribution.

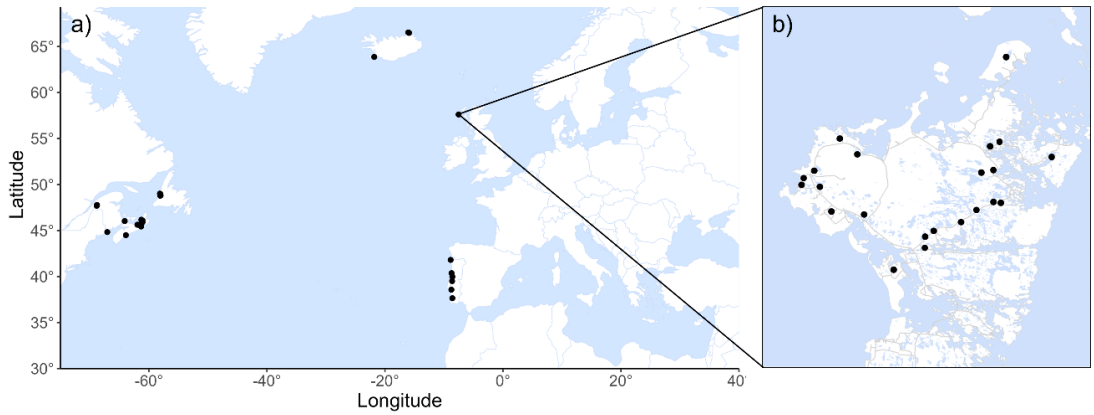

Figure 1.2: Stickleback sampling sites. Map of the northern Atlantic (a) and North Uist (b) with points showing sites where stickleback samples were collected. See individual chapters for further details.

1.7 Thesis outline

In this research I aim to show that the two mitochondrial lineages of the stickleback in the Atlantic differ in adaptive potential by combining phylogeography, ecology, selection analyses and HRR. I will provide evidence that the mtDNA variation between *Eu* and *At* stickleback has physiological consequences for mitochondrial function independent of the nuclear genome, and that natural selection may have acted upon this variation resulting in differences in adaptive potential between *Eu* and *At* stickleback.

Chapter 2: Development of Resident and Migratory Three-spined Stickleback, *Gasterosteus aculeatus*. A large part of this work included assessing and raising migratory populations from North Uist as these are an approximately equal mix of the two mitochondrial lineages. Very few studies have assessed the development, fertilisation and hatching success of migratory populations (Kirschman et al., 2023); instead, the focus has been on freshwater populations (Kuntz and Radcliffe, 1917; Vrat, 1949) and at a higher temperature than stickleback experience in North Uist (Swarup, 1958). Noting this gap in the literature, I raised migratory and resident clutches and compared their development in order to inform raising stickleback in aquaria and provide a baseline for future studies.

Chapter 3: A Common Anaesthetic, MS-222, Alters Measurements Made Using High-Resolution Respirometry in the Three-Spined Stickleback (*Gasterosteus aculeatus*). To compare mitochondrial function between the two Atlantic stickleback mitochondrial lineages, I first needed to optimise a protocol for the O2k as few studies

had previously conducted HRR on stickleback tissue (Chouinard-Boisvert et al., 2024; Cominassi et al., 2022; Shama et al., 2014). From the literature, it was apparent that the effects of anaesthetics used for the euthanasia of fish on mitochondrial function had not previously been investigated, with over 50% of HRR studies using the O2k having used an anaesthetic without investigating any effects on the mitochondria (from https://wiki.oroboros.at/, 6th February 2025). As I used MS-222 for stickleback euthanasia, I first assessed the physiological effects of MS-222 on stickleback mitochondrial respiration, finding that this altered specific respiratory states in the brain.

Chapter 4: Repeated association of mitochondrial lineage with habitat in Atlantic three-spined stickleback. I first designed an assay to reliably distinguish the *Eu* and *At* stickleback mitochondrial lineages to assess their distribution across the Atlantic. I provide evidence that the two Atlantic mitochondrial lineages are associated with adaptive potential, and highlight the Atlantic three-spined stickleback as a model for further investigations into the physiological and evolutionary consequences of mtDNA variation.

Chapter 5: Positive selection in the mitochondrial protein coding genes of the three-spined stickleback. To test whether the evolution of the stickleback mitochondrial lineages and freshwater adaptation was accompanied by selection acting on mitochondrial function, I assembled and analysed stickleback mitogenomes using multiple phylogenetic selection analyses. I show that sites within the complex I genes were likely candidates for positive selection, with amino acid substitutions predicted to alter protein structure and function.

Chapter 6: Physiological consequences of mitochondrial DNA variation in the three-spined stickleback. I next tested whether the mtDNA variation between the two Atlantic mitochondrial lineages has physiological consequences that could be selected for. I show that the two mitochondrial lineages in the Atlantic have temperature-dependent differences in mitochondrial function, in particular respiration via complex I.

Chapter 7: General discussion. I highlight and link the key findings from this thesis, focussing on the ecological and evolutionary consequences of mtDNA variation in the Atlantic three-spined stickleback.

1.8 References

Avise, J.C., Arnold, J., Martin Bal, R., Bermingham, E., Lamb, T., Neigel, J.E., Reeb, C.A., Saunders, N.C., 1987. Intraspecific phylogeography: The Mitochondrial DNA Bridge Between Population Genetics and Systematics. *Ann. Rev. Ecol. Sys.* **18**, 489–522. https://doi.org/10.1146/annurev.es.18.110187.002421

Aw, W.C., Towarnicki, S.G., Melvin, R.G., Youngson, N.A., Garvin, M.R., Hu, Y., Nielsen, S., Thomas, T., Pickford, R., Bustamante, S., Vila-Sanjurjo, A., Smyth, G.K., Ballard, J.W.O., 2018. Genotype to phenotype: Diet-by-mitochondrial DNA haplotype interactions drive metabolic flexibility and organismal fitness. *PLoS Genet.* **14**, e1007735. https://doi.org/10.1371/JOURNAL.PGEN.1007735

Awadi, A., Ben Slimen, H., Schaschl, H., Knauer, F., Suchentrunk, F., 2021. Positive selection on two mitochondrial coding genes and adaptation signals in hares (genus *Lepus*) from China. *BMC Ecol. Evol.* **21**, 100. https://doi.org/10.1186/S12862-021-01832-7

Bahbahani, H., Al-Zoubi, S., Ali, F., Afana, A., Dashti, M., Al-Ateeqi, A., Wragg, D., Al-Bustan, S., Almathen, F., 2023. Signatures of purifying selection and site-specific positive selection on the mitochondrial DNA of dromedary camels (*Camelus dromedarius*). *Mitochondrion*. **69**, 36–42. https://doi.org/10.1016/J.MITO.2023.01.004

Ballard, J.W., Youngson, N.A., 2015. Review: can diet influence the selective advantage of mitochondrial DNA haplotypes? *Biosci. Rep.* **35**, e00277. https://doi.org/10.1042/BSR20150232

Ballard, J.W.O., Kreitman, M., 1995. Is mitochondrial DNA a strictly neutral marker? *Trends in Ecology & Evolution,* **10**, 485-488. https://doi.org/10.1016/S0169-5347(00)89195-8

Ballard, J.W.O., Melvin, R.G., Katewa, S.D., Maas, K., 2007. Mitochondrial DNA variation is associated with measurable differences in life-history traits and mitochondrial metabolism in *Drosophila simulans*. *Evolution.* **61**, 1735–1747. https://doi.org/10.1111/J.1558-5646.2007.00133.X

Baltazar-Soares, M., Lima, A.R. de A., Silva, G., 2021. Targeted sequencing of mitochondrial genes reveals signatures of molecular adaptation in a nearly

panmictic small pelagic fish species. *Genes.* **12**, 91. https://doi.org/10.3390/genes12010091

Baris, T.Z., Blier, P.U., Pichaud, N., Crawford, D.L., Oleksiak, M.F., 2016. Gene by environmental interactions affecting oxidative phosphorylation and thermal sensitivity. *Am. J. Physiol. Regul. Integr. Comp. Physiol.* **311**, R157–R165. https://doi.org/10.1152/ajpregu.00008.2016

Baris, T.Z., Wagner, D.N., Dayan, D.I., Du, X., Blier, P.U., Pichaud, N., Oleksiak, M.F., Crawford, D.L., 2017. Evolved genetic and phenotypic differences due to mitochondrial-nuclear interactions*. PLoS Genet.* **13**, e1006517. https://doi.org/10.1371/journal.pgen.1006517

Barreto, F.S., Watson, E.T., Lima, T.G., Willett, C.S., Edmands, S., Li, W., Burton, R.S., 2018. Genomic signatures of mitonuclear coevolution across populations of *Tigriopus californicus*. *Nat. Ecol. Evol.* **2**, 1250–1257. https://doi.org/10.1038/s41559-018-0588-1

Bazin, E., Gle, S., Galtier, N., 2006. Population Size does not Influence Mitochondrial Genetic Diversity in Animals. *Science.* **312**, 570–572. https://doi.org/10.1126/science.11220

Beck, E.A., Bassham, S., Cresko, W.A., 2022. Extreme intraspecific divergence in mitochondrial haplotypes makes the threespine stickleback fish an emerging evolutionary mutant model for mito-nuclear interactions. *Front. Genet.* **13**. https://doi.org/10.3389/fgene.2022.925786

Bell, M.A., Foster, S.A., 1995. The Evolutionary Biology of the Threespine Stickleback. *J. Anim. Ecol.* **64**, 418-419. https://doi.org/10.2307/5902

Bettinazzi, S., Liang, J., Rodriguez, E., Bonneau, M., Holt, R., Whitehead, B., Dowling, D.K., Lane, N., Camus, M.F., 2024. Assessing the role of mitonuclear interactions on mitochondrial function and organismal fitness in natural *Drosophila* populations. *Evol. Lett.* **8**, 916–926. https://doi.org/10.1093/EVLETT/QRAE043

Black, C.P., Tenney, S.M., 1980. Oxygen transport during progressive hypoxia in high-altitude and sea-level waterfowl. *Respir. Physiol.* **39**, 217–239. https://doi.org/10.1016/0034-5687(80)90046-8

Brijs, J., Sandblom, E., Sundh, H., Gräns, A., Hinchcliffe, J., Ekström, A., Sundell, K., Olsson, C., Axelsson, M., Pichaud, N., 2017. Increased mitochondrial coupling

and anaerobic capacity minimizes aerobic costs of trout in the sea. *Sci. Rep.* **7**, 45778. https://doi.org/10.1038/srep45778

Burton, R.S., 2022. The role of mitonuclear incompatibilities in allopatric speciation. *Cell. Mol. Life Sci.* **79**, 103. https://doi.org/10.1007/S00018-021-04059-3

Burton, R.S., Barreto, F.S., 2012. A disproportionate role for mtDNA in Dobzhansky–Muller incompatibilities? *Mol. Ecol.* **21**, 4942–4957. https://doi.org/10.1111/MEC.12006

Camus, M.F., Wolff, J.N., Sgrò, C.M., Dowling, D.K., 2017. Experimental Support That Natural Selection Has Shaped the Latitudinal Distribution of Mitochondrial Haplotypes in Australian *Drosophila melanogaster*. *Mol. Biol. Evol.* **34**, 2600–2612. https://doi.org/10.1093/MOLBEV/MSX184

Chandel, N.S., 2014. Mitochondria as signaling organelles. *BMC Biol.* **12**, 34. https://doi.org/10.1186/1741-7007-12-34

Cheviron, Z.A., Bachman, G.C., Connaty, A.D., McClelland, G.B., Storz, J.F., 2012. Regulatory changes contribute to the adaptive enhancement of thermogenic capacity in high-altitude deer mice. *PNAS.* **109**, 8635–8640. https://doi.org/10.1073/PNAS.1120523109

Chouinard-Boisvert, S., Ghinter, L., St-Pierre, A., Mortz, M., Desrosiers, V., Dufresne, F., Tardif, J.-C., Huard, J., Sirois, P., Fortin, S., Blier, P.U., 2024. Mitochondrial functions and fatty acid profiles in fish heart: an insight into physiological limitations linked with thermal tolerance and age. *J. Exp. Biol.* **227**, jeb247502. https://doi.org/10.1242/JEB.247502

Colosimo, P.F., Hosemann, K.E., Balabhadra, S., Villarreal, G., Dickson, H., Grimwood, J., Schmutz, J., Myers, R.M., Schluter, D., Kingsley, D.M., 2005. Widespread parallel evolution in sticklebacks by repeated fixation of ectodysplasin alleles. *Science*. **307**, 1928–1933. https://doi.org/10.1126/SCIENCE.1107239

Cominassi, L., Ressel, K.N., Brooking, A.A., Marbacher, P., Ransdell-Green, E.C., O'Brien, K.M., 2022. Metabolic rate increases with acclimation temperature and is associated with mitochondrial function in some tissues of threespine stickleback. *J. Exp. Biol.* **225**, jeb244659. https://doi.org/10.1242/JEB.244659

Coulson, S.Z., Guglielmo, C.G., Staples, J.F., 2024. Migration increases mitochondrial oxidative capacity without increasing reactive oxygen species

emission in a songbird. *J. Exp. Biol.* **227**, jeb246849. https://doi.org/10.1242/JEB.246849

Dahlhoff, E.P., Dahlhoff, V.C., Grainger, C.A., Zavala, N.A., Otepola-Bello, D., Sargent, B.A., Roberts, K.T., Heidl, S.J., Smiley, J.T., Rank, N.E., 2019. Getting chased up the mountain: High elevation may limit performance and fitness characters in a montane insect. *Funct. Ecol.* **33**, 809–818. https://doi.org/10.1111/1365-2435.13286

Dawson, N.J., Millet, C., Selman, C., Metcalfe, N.B., 2022. Inter-individual variation in mitochondrial phosphorylation efficiency predicts growth rates in ectotherms at high temperatures. *The FASEB Journal* **36**, e22333. https://doi.org/10.1096/FJ.202101806RR

Dean, L.L., Magalhaes, I.S., Foote, A., D'Agostino, D., McGowan, S., MacColl, A.D.C., 2019a. Admixture between Ancient Lineages, Selection, and the Formation of Sympatric Stickleback Species-Pairs. *Mol. Biol. Evol*. **36**, 2481–2497. https://doi.org/10.1093/MOLBEV/MSZ161

Devaux, J.B.L., Hedges, C.P., Birch, N., Herbert, N., Renshaw, G.M.C., Hickey, A.J.R., 2019. Acidosis Maintains the Function of Brain Mitochondria in Hypoxia-Tolerant Triplefin Fish: A Strategy to Survive Acute Hypoxic Exposure? *Front. Physiol.* **9**. https://doi.org/10.3389/FPHYS.2018.01941

Divino, Jeffrey and Schultz, Eric. 2015. Juvenile threespine stickleback husbandry: standard operating procedures of the Schultz lab. https://doi.org/10.13140/RG.2.1.4232.5605.

Dowling, D.K., Wolff, J.N., 2023. Evolutionary genetics of the mitochondrial genome: insights from *Drosophila*. *Genetics.* **224**, iyad036. https://doi.org/10.1093/GENETICS/IYAD036

Edmands, S., Burton, R.S., 1999. Cytochrome C Oxidase Activity in Interpopulation Hybrids of a Marine Copepod: A Test for Nuclear-Nuclear or Nuclear-Cytoplasmic Coadaptation. *Evolution.* **53**, 1972-1978. https://doi.org/10.2307/2640456

Ellison, C.K., Burton, R.S., 2006. Disruption of Mitochondrial Function in Interpopulation Hybrids of *Tigriopus Californicus*. *Evolution.* **60**, 1382-1391. https://doi.org/10.1554/06-210.1

Foote, A.D., Morin, P.A., Durban, J.W., Pitman, R.L., Wade, P., Willerslev, E., Gilbert, M.T.P., Fonseca, R.R.D., 2011. Positive selection on the killer whale mitogenome. *Biol. Lett*. **7**, 116–118. https://doi.org/10.1098/rsbl.2010.0638

Garvin, M.R., Bielawski, J.P., Gharrett, A.J., 2011. Positive Darwinian Selection in the Piston That Powers Proton Pumps in Complex I of the Mitochondria of Pacific Salmon. *PLoS One.* **6**, e24127. https://doi.org/10.1371/JOURNAL.PONE.0024127

Gómez-Durán, A., Pacheu-Grau, D., Martínez-Romero, I., López-Gallardo, E., López-Pérez, M.J., Montoya, J., Ruiz-Pesini, E., 2012. Oxidative phosphorylation differences between mitochondrial DNA haplogroups modify the risk of Leber's hereditary optic neuropathy. *BBA Molecular Basis of Disease.* **1822**, 1216–1222. https://doi.org/10.1016/J.BBADIS.2012.04.014

Gómez-Durán, Pacheu-Grau, D., López-Gallardo, E., Díez-Sánchez, C., Montoya, J., López-Pérez, M.J., Ruiz-Pesini, E., 2010. Unmasking the causes of multifactorial disorders: OXPHOS differences between mitochondrial haplogroups. *Hum. Mol. Genet.* **19**, 3343–3353. https://doi.org/10.1093/hmg/ddq246

Greenway, R., Barts, N., Henpita, C., Brown, A.P., Rodriguez, L.A., Rodríguez Peña, C.M., Arndt, S., Lau, G.Y., Murphy, M.P., Wu, L., Lin, D., Tobler, M., Kelley, J.L., Shaw, J.H., 2020. Convergent evolution of conserved mitochondrial pathways underlies repeated adaptation to extreme environments. *PNAS.* **117**, 16424–16430. https://doi.org/10.1073/pnas.2004223117

Hill, G.E., 2020. Mitonuclear Compensatory Coevolution. *Trends in Genetics.* **36**, 403–414. https://doi.org/10.1016/j.tig.2020.03.002

Hill, G.E., 2016. Mitonuclear coevolution as the genesis of speciation and the mitochondrial DNA barcode gap. *Ecol. Evol.* **6**, 5831–5842. https://doi.org/10.1002/ece3.2338

Hill, G.E., 2015. Mitonuclear ecology. *Mol. Biol. Evol.* **32**, 1917–1927. https://doi.org/10.1093/molbev/msv104

Hoekstra, L.A., Siddiq, M.A., Montooth, K.L., 2013. Pleiotropic effects of a mitochondrial-nuclear incompatibility depend upon the accelerating effect of temperature in *Drosophila*. *Genetics*. **195**, 1129–1139. https://doi.org/10.1534/GENETICS.113.154914

Horan, M.P., Pichaud, N., Ballard, J.W.O., 2012. Review: Quantifying Mitochondrial Dysfunction in Complex Diseases of Aging. *The Journals of Gerontology: Series A*. **67**, 1022–1035. https://doi.org/10.1093/GERONA/GLR263

Ishikawa, A., Stuart, Y.E., Bolnick, D.I., Kitano, J., 2021. Copy number variation of a fatty acid desaturase gene Fads2 associated with ecological divergence in freshwater stickleback populations. *Biol. Lett.* **17**, 20210204. https://doi.org/10.1098/RSBL.2021.0204

James, A.C., William, J., Ballard, O., Dean, K.J., Ballard, A., Glass, J.W.O., 2003. Mitochondrial Genotype Affects Fitness in *Drosophila simulans*. *Genetics*. **164**, 187–194. https://doi.org/10.1093/GENETICS/164.1.187

Jang, J.Y., Blum, A., Liu, J., Finkel, T., 2018. The role of mitochondria in aging. *J. Clin. Invest.* **128**, 3662–3670. https://doi.org/10.1172/JCI120842

Jones, F.C., Grabherr, M.G., Chan, Y.F., Russell, P., Mauceli, E., Johnson, J., Swofford, R., Pirun, M., Zody, M.C., White, S., Birney, E., Searle, S., Schmutz, J., Grimwood, J., Dickson, M.C., Myers, R.M., Miller, C.T., Summers, B.R., Knecht, A.K., Brady, S.D., Zhang, H., Pollen, A.A., Howes, T., Amemiya, C., Baldwin, J., Bloom, T., Jaffe, D.B., Nicol, R., Wilkinson, J., Lander, E.S., Di Palma, F., Lindblad-Toh, K., Kingsley, D.M., 2012. The genomic basis of adaptive evolution in threespine sticklebacks. *Nature*. **484**, 55–61. https://doi.org/10.1038/nature10944

Karlsen, B.O., Adhikari, D., Jørgensen, T.E., Hanssen, I.K., Moum, T.B., Nordeide, J.T., Johansen, S.D., 2024. Two Distinct Maternal Lineages of Threespine Stickleback (*Gasterosteus aculeatus*) in a Small Norwegian Subarctic Lake. *Fishes*. **9**, 285. https://doi.org/10.3390/FISHES9070285

Kirschman, L.J., Khadjinova, A., Ireland, K., Milligan-Myhre, K.C., 2023. Early Life Disruption of the Microbiota Affects Organ Development and Cytokine Gene Expression in Threespine Stickleback. *Integrative and Comparative Biology*. **63**, 250-262. https://doi.org/10.1093/icb/icaa136

Kuntz, A., Radcliffe, L., 1917. Notes on the Embryology and Larval Development of Twelve Teleostean Fishes. *NOAA Fisheries.* **35**.

Lamb, A.M., Gan, H.M., Greening, C., Joseph, L., Lee, Y.P., Morán-Ordóñez, A., Sunnucks, P., Pavlova, A., 2018. Climate-driven mitochondrial selection: A test in Australian songbirds. *Mol. Ecol.* **27**, 898–918. https://doi.org/10.1111/MEC.14488

Latorre-Pellicer, A., Moreno-Loshuertos, R., Lechuga-Vieco, A.V., Sánchez-Cabo, F., Torroja, C., Acín-Pérez, R., Calvo, E., Aix, E., González-Guerra, A., Logan, A., Bernad-Miana, M.L., Romanos, E., Cruz, R., Cogliati, S., Sobrino, B., Carracedo, Á., Pérez-Martos, A., Fernández-Silva, P., Ruíz-Cabello, J., Murphy, M.P., Flores, I., Vázquez, J., Enríquez, J.A., 2016. Mitochondrial and nuclear DNA matching shapes metabolism and healthy ageing. *Nature*. **535**, 561–565. https://doi.org/10.1038/nature18618

Li, X.D., Jiang, G.F., Yan, L.Y., Li, R., Mu, Y., Deng, W.A., 2018. Positive Selection Drove the Adaptation of Mitochondrial Genes to the Demands of Flight and High-Altitude Environments in Grasshoppers. *Front. Genet.* **9**. https://doi.org/10.3389/fgene.2018.00605

Lui, M.A., Mahalingam, S., Patel, P., Connaty, A.D., Ivy, C.M., Cheviron, Z.A., Storz, J.F., McClelland, G.B., Scott, G.R., 2015. High-altitude ancestry and hypoxia acclimation have distinct effects on exercise capacity and muscle phenotype in deer mice. *Am. J. Physiol. Regul. Integr. Comp. Physiol.* **308**, R779-R791. https://doi.org/10.1152/AJPREGU.00362.2014

MacColl, A.D.C., Nagar, A. El, De Roij, J., 2013. The evolutionary ecology of dwarfism in three-spined sticklebacks. *J. Anim. Ecol.* **82**, 642-652. https://doi.org/10.1111/1365-2656.12028

Magalhaes, I.S., D'Agostino, D., Hohenlohe, P.A., MacColl, A.D.C., 2016. The ecology of an adaptive radiation of three-spined stickleback from North Uist, Scotland. *Mol. Ecol.* **25**, 4319–4336. https://doi.org/10.1111/MEC.13746

Mäkinen, H.S., Merilä, J., 2008. Mitochondrial DNA phylogeography of the three-spined stickleback (*Gasterosteus aculeatus*) in Europe-Evidence for multiple glacial refugia. *Mol. Phylogenet. Evol.* **46**, 167–182. https://doi.org/10.1016/j.ympev.2007.06.011

McKenzie, J.L., Chung, D.J., Healy, T.M., Brennan, R.S., Bryant, H.J., Whitehead, A., Schulte, P.M., 2019. Mitochondrial Ecophysiology: Assessing the Evolutionary Forces That Shape Mitochondrial Variation. *Integr. Comp. Biol.* **59**, 925–937. https://doi.org/10.1093/ICB/ICZ124

Meiklejohn, C.D., Holmbeck, M.A., Siddiq, M.A., Abt, D.N., Rand, D.M., Montooth, K.L., 2013. An Incompatibility between a Mitochondrial tRNA and Its Nuclear-

Encoded tRNA Synthetase Compromises Development and Fitness in *Drosophila*. *PLoS Genetics*. **9**, e1003238. https://doi.org/10.1371/journal.pgen.1003238

Melo-Ferreira, J., Vilela, J., Fonseca, M.M., Da Fonseca, R.R., Boursot, P., Alves, P.C., 2014. The Elusive Nature of Adaptive Mitochondrial DNA Evolution of an Arctic Lineage Prone to Frequent Introgression. *Genome Biol. Evol.* **6**, 886–896. https://doi.org/10.1093/GBE/EVU059

Michaelsen, J., Faro, A., Bundgaard, A., 2021. High temperature impairs mitochondrial function in rainbow trout cardiac mitochondria. *J. Exp. Biol.* **224**, jeb242382. https://doi.org/ 10.1242/jeb.242382

Montooth, K.L., Meiklejohn, C.D., Abt, D.N., Rand, D.M., 2010. Mitochondrial-nuclear epistasis affects fitness within species but does not contribute to fixed incompatibilities between species of *Drosophila*. *Evolution*. **64**, 3364-3379. https://doi.org/10.1111/J.1558-5646.2010.01077.X

Morales, H.E., Pavlova, A., Joseph, L., Sunnucks, P., 2015. Positive and purifying selection in mitochondrial genomes of a bird with mitonuclear discordance. *Mol. Ecol.* **24**, 2820–2837. https://doi.org/10.1111/MEC.13203

Moritz, C., Dowling, T.E., Brown, W.M., 1987. Evolution of animal mitochondrial DNA: Relevance for population biology and systematics. *Ann. Rev. Ecol. Sys.* **18**, 269-292. https://doi.org/10.1146/annurev.es.18.110187.001413

Mukundan, L.P., Sukumaran, S., Raj, N., Jose, A., Gopalakrishnan, A., 2022. Positive selection in the mitochondrial protein coding genes of teleost regional endotherms: Evidence for adaptive evolution. *J. Mar. Biol. Ass. India.* **64**, 1. https://doi.org/10.6024/jmbai.2022.64.1.2320-02

Nath, S., Shaw, D.E., White, M.A., 2021. Improved contiguity of the threespine stickleback genome using long-read sequencing. *G3 Genes*|*Genomes*|*Genetics* **11**, jkab007. https://doi.org/10.1093/G3JOURNAL/JKAB007

Nguyen, T.H.M., Sondhi, S., Ziesel, A., Paliwal, S., Fiumera, H.L., 2020. Mitochondrial-nuclear coadaptation revealed through mtDNA replacements *in Saccharomyces cerevisiae*. *BMC Evol. Biol.* **20**, 128. https://doi.org/10.1186/S12862-020-01685-6

Noll, D., Leon, F., Brandt, D., Pistorius, P., Le Bohec, C., Bonadonna, F., Trathan, P.N., Barbosa, A., Rey, A.R., Dantas, G.P.M., Bowie, R.C.K., Poulin, E., Vianna,

J.A., 2022. Positive selection over the mitochondrial genome and its role in the diversification of gentoo penguins in response to adaptation in isolation. *Sci. Rep.* **12**, 3767. https://doi.org/10.1038/s41598-022-07562-0

Orti, G., Bell, M.A., Reimchen, T.E., Meyer, A., 1994. Global survey of mitochondrial DNA sequences in the threespine stickleback: evidence for recent migrations. *Evolution.* **48**, 608–622. https://doi.org/10.1111/J.1558-5646.1994.TB01348.X

Peichel, C.L., McCann, S.R., Ross, J.A., Naftaly, A.F.S., Urton, J.R., Cech, J.N., Grimwood, J., Schmutz, J., Myers, R.M., Kingsley, D.M., White, M.A., 2020. Assembly of the threespine stickleback y chromosome reveals convergent signatures of sex chromosome evolution. *Genome Biol.* **21**, 177. https://doi.org/10.1186/S13059-020-02097-X

Peichel, C.L., Sullivan, S.T., Liachko, I., White, M.A., 2017. Improvement of the Threespine Stickleback Genome Using a Hi-C-Based Proximity-Guided Assembly. *Heredity*. **108**, 693–700. https://doi.org/10.1093/JHERED/ESX058

Pfenninger, M., Lerp, H., Tobler, M., Passow, C., Kelley, J.L., Funke, E., Greshake, B., Erkoc, U.K., Berberich, T., Plath, M., 2014. Parallel evolution of cox genes in H2S-tolerant fish as key adaptation to a toxic environment. *Nat. Commun.* **5**, 3873. https://doi.org/10.1038/ncomms4873

Pichaud, N., Ballard, J.W.O., Tanguay, R.M., Blier, P.U., 2013. Mitochondrial haplotype divergences affect specific temperature sensitivity of mitochondrial respiration. *J. Bioenerg. Biomembr.* ***45***, 25–35. https://doi.org/10.1007/S10863-012-9473-9

Popadin, K.Y., Nikolaev, S.I., Junier, T., Baranova, M., Antonarakis, S.E., 2013. Purifying selection in mammalian mitochondrial protein-coding genes is highly effective and congruent with evolution of nuclear genes. *Mol. Biol. Evol.* **30**, 347–355. https://doi.org/10.1093/molbev/mss219

Rank, N.E., Mardulyn, P., Heidl, S.J., Roberts, K.T., Zavala, N.A., Smiley, J.T., Dahlhoff, E.P., 2020. Mitonuclear mismatch alters performance and reproductive success in naturally introgressed populations of a montane leaf beetle. *Evolution*. **74**, 1724–1740. https://doi.org/10.1111/EVO.13962

Reid, K., Bell, M.A., Veeramah, K.R., 2021. Threespine Stickleback: A Model System For Evolutionary Genomics. *Ann. Rev. Genomics Hum. Genet.* **22**, 357-383. https://doi.org/10.1146/ANNUREV-GENOM-111720-081402

Roberts Kingman, G.A., Vyas, D.N., Jones, F.C., Brady, S.D., Chen, H.I., Reid, K., Milhaven, M., Bertino, T.S., Aguirre, W.E., Heins, D.C., Von Hippel, F.A., Park, P.J., Kirch, M., Absher, D.M., Myers, R.M., Palma, F. Di, Bell, M.A., Kingsley1, D.M., Veeramah, K.R., 2021. Predicting future from past: The genomic basis of recurrent and rapid stickleback evolution. *Sci. Adv.* **7**, 5285–5303. https://doi.org/10.1126/SCIADV.ABG5285

Robertson, S., Bradley, J.E., Maccoll, A.D.C., 2016. Measuring the immune system of the three-spined stickleback - investigating natural variation by quantifying immune expression in the laboratory and the wild. *Mol. Ecol. Resour.* **16**, 701-713. https://doi.org/10.1111/1755-0998.12497

Ruiz-Pesini, E., Mishmar, D., Brandon, M., Procaccio, V., Wallace, D.C., 2004. Effects of Purifying and Adaptive Selection on Regional Variation in Human mtDNA. *Science*. **303**, 223–226. https://doi.org/10.1126/SCIENCE.1088434

Salin, K., Mathieu-Resuge, M., Graziano, N., Dubillot, E., Le Grand, F., Soudant, P., Vagner, M., 2021. The relationship between membrane fatty acid content and mitochondrial efficiency differs within- and between- omega-3 dietary treatments. *Mar. Environ. Res.* **163**, 105205. https://doi.org/10.1016/J.MARENVRES.2020.105205

Salin, K., Villasevil, E.M., Anderson, G.J., Auer, S.K., Selman, C., Hartley, R.C., Mullen, W., Chinopoulos, C., Metcalfe, N.B., 2018. Decreased mitochondrial metabolic requirements in fasting animals carry an oxidative cost. *Funct. Ecol.* **32**, 2149–2157. https://doi.org/10.1111/1365-2435.13125

Scotece, M., Rego-Pérez, I., Lechuga-Vieco, A.V., Cortés, A.C., Jiménez-Gómez, M.C., Filgueira-Fernández, P., Vaamonde-García, C., Enríquez, J.A., Blanco, F.J., 2021. Mitochondrial DNA impact on joint damaged process in a conplastic mouse model after being surgically induced with osteoarthritis. *Sci. Rep.* **11**, 9112. https://doi.org/10.1038/s41598-021-88083-0

Scott, G.R., Hawkes, L.A., Frappell, P.B., Butler, P.J., Bishop, C.M., Milsom, W.K., 2015. How bar-headed geese fly over the Himalayas. *Physiology*. **30**, 107–115. https://doi.org/10.1152/physiol.00050.2014

Scott, G.R., Milsom, W.K., 2007. Control of breathing and adaptation to high altitude in the bar-headed goose. *Am. J. Physiol. Regul. Integr. Comp. Physiol.* **293**, R379-R391. https://doi.org/10.1152/AJPREGU.00161.2007

Scott, G.R., Schulte, P.M., Egginton, S., Scott, A.L.M., Richards, J.G., Milsom, W.K., 2011. Molecular Evolution of Cytochrome c Oxidase Underlies High-Altitude Adaptation in the Bar-Headed Goose. *Mol. Biol. Evol.* **28**, 351–363. https://doi.org/10.1093/MOLBEV/MSQ205

Sebastian, W., Sukumaran, S., Zacharia, P.U., Muraleedharan, K.R., Dinesh Kumar, P.K., Gopalakrishnan, A., 2020. Signals of selection in the mitogenome provide insights into adaptation mechanisms in heterogeneous habitats in a widely distributed pelagic fish. *Sci. Rep.* **10**, 9081. https://doi.org/10.1038/s41598-020-65905-1

Shama, L.N.S., Strobel, A., Mark, F.C., Wegner, K.M., 2014. Transgenerational plasticity in marine sticklebacks: Maternal effects mediate impacts of a warming ocean. *Funct. Ecol.* **28**, 1482–1493. https://doi.org/10.1111/1365-2435.12280

Shen, X., Pu, Z., Chen, X., Murphy, R.W., Shen, Y., 2019. Convergent Evolution of Mitochondrial Genes in Deep-Sea Fishes. *Front. Genet.* **10**, 925. https://doi.org/10.3389/FGENE.2019.00925

Spence, R., Wootton, R.J., Barber, I., Przybylski, M., Smith, C., 2013. Ecological causes of morphological evolution in the three-spined stickleback. *Ecol. Evol.* **3**, 1717–1726. https://doi.org/10.1002/ECE3.581

Steffen, J.B.M., Sokolov, E.P., Bock, C., Sokolova, I.M., 2023. Combined effects of salinity and intermittent hypoxia on mitochondrial capacity and reactive oxygen species efflux in the Pacific oyster*, Crassostrea gigas. J. Exp. Biol.* **226**, jeb246164. https://doi.org/10.1242/JEB.246164

Sun, J.T., Duan, X.Z., Hoffmann, A.A., Liu, Y., Garvin, M.R., Chen, L., Hu, G., Zhou, J.C., Huang, H.J., Xue, X.F., Hong, X.Y., 2019. Mitochondrial variation in small brown planthoppers linked to multiple traits and probably reflecting a complex evolutionary trajectory. *Mol. Ecol.* **28**, 3306–3323. https://doi.org/10.1111/MEC.15148

Sun, J.T., Wang, M.M., Zhang, Y.K., Chapuis, M.P., Jiang, X.Y., Hu, G., Yang, X.M., Ge, C., Xue, X.F., Hong, X.Y., 2015. Evidence for high dispersal ability and mito-

nuclear discordance in the small brown planthopper, *Laodelphax striatellus*. *Sci. Rep.* **5**, 8045. https://doi.org/10.1038/srep08045

Swarup, H., 1958. Stages in the Development of the Stickleback *Gasterosteus aculeatus* (L.). *Development*. **6**, 373–383. https://doi.org/10.1242/DEV.6.3.373

Tait, S.W.G., Green, D.R., 2013. Mitochondrial Regulation of Cell Death. *Cold Spring Harb. Perspect. Biol.* **5**. https://doi.org/10.1101/CSHPERSPECT.A008706

Thoral, E., Dawson, N.J., Bettinazzi, S., Rodríguez, E., 2024. An evolving roadmap: using mitochondrial physiology to help guide conservation efforts. *Conserv. Physiol.* **12**, coae063. https://doi.org/10.1093/CONPHYS/COAE063

Thoral, E., Roussel, D., Chinopoulos, C., Teulier, L., Salin, K., Thoral, E., 2021. Low oxygen levels can help to prevent the detrimental effect of acute warming on mitochondrial efficiency in fish. *Biol. Lett.* **17**, 20200759. https://doi.org/10.1098/RSBL.2020.0759

Towarnicki, S.G., Ballard, J.W.O., 2018. Mitotype Interacts With Diet to Influence Longevity, Fitness, and MitochondriaTowarnicki, S. G., & Ballard, J. W. O. (2018). Mitotype Interacts With Diet to Influence Longevity, Fitness, and Mitochondrial Functions in Adult Female *Drosophila*. *Front. Genet.* **9**, 593. https://doi.org/10.3389/FGENE.2018.00593

Vieira, A.R., de Sousa, F., Bilro, J., Viegas, M.B., Svanbäck, R., Gordo, L.S., Paulo, O.S., 2024. Mitochondrial genomes of the European sardine (*Sardina pilchardus*) reveal Pliocene diversification, extensive gene flow and pervasive purifying selection. *Sci. Rep.* **14,** 30977. https://doi.org/10.1038/s41598-024-82054-x

Vrat, V., 1949. Reproductive Behavior and Development of Eggs of the Three-Spined Stickleback (*Gasterosteus aculeatus*) of California **15**, 252–260. https://doi.org/10.2307/1438375

Wang, Y., Shen, Y., Feng, C., Zhao, K., Song, Z., Zhang, Y., Yang, L., He, S., 2016. Mitogenomic perspectives on the origin of Tibetan loaches and their adaptation to high altitude. *Sci. Rep.* **6**, 29690. https://doi.org/10.1038/srep29690

Whitehead, A., 2009. Comparative mitochondrial genomics within and among species of killifish. *BMC Evol. Biol.* **9**, 11. https://doi.org/10.1186/1471-2148-9-11

Wilkins, H.M., Carl, S.M., Swerdlow, R.H., 2014. Cytoplasmic hybrid (cybrid) cell lines as a practical model for mitochondriopathies. *Redox Biol.* **2**, 619-631. https://doi.org/10.1016/J.REDOX.2014.03.006

Willis, J.R., Hickey, A.J.R., Devaux, J.B.L., 2021. Thermally tolerant intertidal triplefin fish (*Tripterygiidae*) sustain ATP dynamics better than subtidal species under acute heat stress. *Sci. Rep.* **11**, 11074. https://doi.org/10.1038/s41598-021-90575-y

Wolff, J.N., Pichaud, N., Camus, M.F., Côté, G., Blier, P.U., Dowling, D.K., 2016. Evolutionary implications of mitochondrial genetic variation: Mitochondrial genetic effects on OXPHOS respiration and mitochondrial quantity change with age and sex in fruit flies. *J. Evol. Biol.* **29**, 736–747. https://doi.org/10.1111/jeb.12822

Woolley, S., Johnson, J., Smith, M.J., Crandall, K.A., McClellan, D.A., 2003. TreeSAAP: Selection on Amino Acid Properties using phylogenetic trees. *Bioinformatics*. **19**, 671–672. https://doi.org/10.1093/BIOINFORMATICS/BTG043

Yang, M., Dong, D., Li, X., 2021. The complete mitogenome of *Phymorhynchus* sp. (Neogastropoda, Conoidea, Raphitomidae) provides insights into the deep-sea adaptive evolution of Conoidea. *Ecol. Evol.* **11**, 7518–7531. https://doi.org/10.1002/ECE3.7582

Yang, Z., 2007. PAML 4: Phylogenetic Analysis by Maximum Likelihood. *Mol. Biol. Evol.* **24**, 1586–1591. https://doi.org/10.1093/MOLBEV/MSM088

Yu, L., Wang, X., Ting, N., Zhang, Y., 2011. Mitogenomic analysis of Chinese snub-nosed monkeys: Evidence of positive selection in NADH dehydrogenase genes in high-altitude adaptation. *Mitochondrion*. **11**, 497–503. https://doi.org/10.1016/j.mito.2011.01.004

Yu, X., Gimsa, U., Wester-Rosenlöf, L., Kanitz, E., Otten, W., Kunz, M., Ibrahim, S.M., 2009. Dissecting the effects of mtDNA variations on complex traits using mouse conplastic strains. *Genome Res.* **19**, 159–165. https://doi.org/10.1101/GR.078865.108

Závorka, L., Crespel, A., Dawson, N.J., Papatheodoulou, M., Killen, S.S., Kainz, M.J., 2021. Climate change-induced deprivation of dietary essential fatty acids can reduce growth and mitochondrial efficiency of wild juvenile salmon. *Funct. Ecol.* **35**, 1960–1971. https://doi.org/10.1111/1365-2435.13860

Zhang, B., Zhang, Y.H., Wang, X., Zhang, H.X., Lin, Q., 2017. The mitochondrial genome of a sea anemone *Bolocera* sp. exhibits novel genetic structures potentially involved in adaptation to the deep-sea environment. *Ecol. Evol.* **7**, 4951–4962. https://doi.org/10.1002/ECE3.3067

Zhang, J., Shu, L., Peng, Z., 2024. Adaptive evolution of mitochondrial genomes in *Triplophysa* cavefishes. Gene **893**, 147947. https://doi.org/10.1016/j.gene.2023.147947

Zhang, L., Sun, K., Csorba, G., Hughes, A.C., Jin, L., Xiao, Y., Feng, J., 2021. Complete mitochondrial genomes reveal robust phylogenetic signals and evidence of positive selection in horseshoe bats. *BMC Ecol. Evol.* **21**, 199. https://doi.org/10.1186/S12862-021-01926-2.

Zhao, D., Guo, Y., Gao, Y., 2022. Natural selection drives the evolution of mitogenomes in *Acrossocheilus. PLoS One*. **17**, e0276056. https://doi.org/10.1371/JOURNAL.PONE.0276056

Zhou, T., Shen, X., Irwin, D.M., Shen, Y., Zhang, Y., 2014. Mitogenomic analyses propose positive selection in mitochondrial genes for high-altitude adaptation in galliform birds. *Mitochondrion*. **18**, 70–75. https://doi.org/10.1016/j.mito.2014.07.012

Zhu, C.T., Ingelmo, P., Rand, D.M., 2014. G×G×E for Lifespan in *Drosophila*: Mitochondrial, Nuclear, and Dietary Interactions that Modify Longevity. *PLoS Genet.* **10**, e1004354. https://doi.org/10.1371/JOURNAL.PGEN.1004354

Zikos, A., Seale, A.P., Lerner, D.T., Grau, E.G., Korsmeyer, K.E., 2014. Effects of salinity on metabolic rate and branchial expression of genes involved in ion transport and metabolism in Mozambique tilapia (*Oreochromis mossambicus). Comp. Biochem. Physiol. A. Mol. Integr. Physiol.* **178**, 121–131. https://doi.org/10.1016/J.CBPA.2014.08.016

Chapter 2: Development of Resident and Migratory Three-spined Stickleback, *Gasterosteus aculeatus*

Megan Barnes[1], Lisa Chakrabarti[2,3], Andrew D.C. MacColl[1]

[1] School of Life Sciences, University of Nottingham, Nottingham NG7 2RD, UK.

[2] School of Veterinary Medicine and Science, Sutton Bonington Campus, University of Nottingham, Loughborough LE12 5RD, UK.

[3] Medical Research Council Versus Arthritis Centre for Musculoskeletal Ageing Research, Nottingham NG7 2RD, UK.

2.1 Statement of contribution

I planned the project, collected and analysed the data, prepared the figures and tables, and wrote and compiled the manuscript. Andrew MacColl supervised the project, collected the data used to calculate the volume of stickleback eggs and, along with Lisa Chakrabarti, contributed to the planning and editing of the manuscript.

This chapter is the accepted version of the journal paper that is published in PLOS ONE 2024, 19: e0295485; https://doi.org/10.1371/journal.pone.0295485.

Published 18 July 2024.

2.2 Abstract

The three-spined stickleback (*Gasterosteus aculeatus*) is a teleost fish and a model organism in evolutionary ecology, useful for both laboratory and natural experiments. It is especially valued for the substantial intraspecific variation in morphology, behaviour and genetics. Classic work of Swarup (1958) has described the development in the laboratory of embryos from a single freshwater population, but this was carried out at higher temperature than many stickleback would encounter in the wild and variation between populations was not addressed. Here we describe the development of embryos from two sympatric, saltwater ecotypes of stickleback from

North Uist, Scotland raised at 14°C, the approximate temperature of North Uist lochs in the breeding season. The two ecotypes were (a) a large, migratory form in which the adults are completely plated with bony armour and (b) a smaller, low-plated form that is resident year-round in saltwater lagoons. By monitoring embryos every 24-hours post fertilisation, important characteristics of development were observed and photographed to provide a reference for North Uist ecotypes at this temperature. Hatching success was greater than 85% and did not differ between resident and migratory stickleback, but migratory eggs hatched significantly earlier than the resident ecotype. Our work provides a framework that can now be used to compare stickleback populations that may also grow in distinct environmental conditions, to help understand the breadth of normal developmental features and to characterise abnormal development.

2.3 Introduction

The three-spined stickleback (*Gasterosteus aculeatus*) has been increasingly studied and raised in aquaria (Reid et al., 2021). The repeated adaptation of oceanic stickleback to fresh water make it an attractive model to investigate parallel evolution (Jones et al., 2012). As such, the three-spined stickleback has become an important model in evolutionary genomics, with both laboratory and natural experiments widely reported. Despite much recent research on variation in the morphology, behaviour and genomics of stickleback, there is a paucity of work describing variation in the development of stickleback from fertilisation to hatching. Swarup 1958 described in detail the key stages in development of the three-spined stickleback, building upon Vrat, 1949 and Kuntz & Radcliffe, 1917. However, Swarup's embryos developed in the lab at 18–19°C, a relatively high temperature for stickleback, and did not consider the possibility of variation between populations.

Temperature is known to greatly influence development time in fish (Martell et al., 2006; Melendez and Mueller, 2021; Pauly and Pullin, 1988), so it is likely that at a colder, more physiologically relevant temperature for many stickleback populations, development time will be increased but this has not been quantified in the stickleback. A large amount of stickleback research is conducted on populations from North Uist (Western Isles, Scotland) (Colosimo et al., 2005a; Dean et al., 2019a; Haenel et al., 2019). Water temperatures in the island's lagoons have been recorded as between 13.1 and 15.0°C during the breeding season (May 2022 and 2023), a considerably lower temperature than stickleback development has previously been assessed at

(Swarup, 1958). Optimum growth for the stickleback has been recorded at 21°C (Lefébure et al., 2011). It is therefore likely that the colder temperatures experienced by stickleback in more northern regions, such as on North Uist, will alter both growth and development. Given the wide distribution of stickleback across the Northern Hemisphere encompassing large variation in environmental variables and therefore stickleback morphology, it is useful to quantify development of the stickleback at lower temperatures, and to compare contrasting ecotypes.

On North Uist, there are two morphologically distinct ecotypes that occur sympatrically in salt water: migratory and lagoon resident (Dean et al., 2019a). Migratory stickleback are large and completely plated, spending most of their lives at sea but migrating to brackish water to spawn, whereas smaller, low plated lagoon resident fish live permanently in coastal lagoons. Resident stickleback lay smaller clutches than migratory (Karve et al., 2013) and as previous work hints at a negative relationship between clutch size and egg volume (Elgar, 1990), migratory fish likely lay smaller eggs. High levels of reproductive isolation are maintained between the ecotypes, with an estimated hybridisation rate of ~1% (Dean et al., 2019a). Migratory and lagoon resident ecotypes vary in both morphology and genetics (Dean et al., 2019a), so there are likely also differences in egg size and developmental timing, as found between Arctic charr morphs (Beck et al., 2022).

Here, we compare the development of migratory and resident stickleback from North Uist at a temperature naturally experienced by these populations, and provide reference photographs for future work.

2.4 Methods

To compare development in sympatric stickleback ecotypes at a physiologically relevant temperature (14°C) and provide a photographic resource for future studies, we monitored the development of lagoon resident and migratory stickleback from North Uist, starting at fertilisation through to hatching. Coloured photographs of resident stickleback were taken to record the key stages and any differences between these and the migratory embryos were assessed. Hatching success and time to hatching were also recorded for both ecotypes. All work was carried out according to UK Home Office regulations (the Animal Scientific Procedures Act 1986 and ensuing legislation), under Project Licence (PP5421721) held by Andrew MacColl. This was approved by the University of Nottingham Animal Welfare and Ethics Review Board.

Fieldwork was conducted on North Uist between 30th April and 19th May 2023. To collect breeding wild stickleback of both sexes and ecotypes, mesh traps were left in Loch an Duin (57.64245, -7.209207), a saltwater lagoon in the North-East of the island, for 24-hours. Migratory and lagoon resident crosses were made, following standard procedures (Hatfield, 1997), by squeezing eggs from gravid, euthanised females into small petri dishes and mixing them with testes from euthanised reproductive males. Fish were euthanised with an overdose of tricaine methanesulfonate (400mg/L) followed by destruction of the brain in accordance with Schedule One of UK Home Office regulations. After fertilisation, eggs were covered in sterile water which was the media used throughout egg development. Egg number per clutch was kept between 20 and 30 where possible. Six crosses per ecotype were made using different males and females for each cross, and each was raised in a separate petri dish. Embryos were maintained at 14°C, the approximate water temperature of North Uist lochs in April, in an incubator (ICT-P Falc, portable mini incubator) where air could fully circulate. Every ~24-hours post-fertilisation, petri dishes were briefly taken out of the incubator and media carefully removed with a Pasteur pipette and then replaced with fresh, temperature-matched media. Other than changing the media and any turning of the eggs as a consequence of viewing them under the microscope, no additional egg care was implemented. Each dish was observed under a dissecting microscope (Olympus SZ61), key features of developing embryos noted and photographs taken. Embryo development was also scored based on Swarup 1958. The same person (MB) scored each cross throughout the experiment. This was repeated daily, until two days after the first hatched stickleback larvae was observed in each clutch.

Hatching success was calculated for each clutch of migratory and lagoon resident ecotypes separately as percentage of successfully hatched larvae. The number of days until the first appearance of a fully hatched stickleback and the number of days until 50% of the clutch had hatched was noted. Hatching success was compared between ecotypes using a binomial GLM with logit link. In one migratory clutch, 17 unfertilised eggs were observed 48-hours post-fertilisation; this was likely due to hardening of the eggs in the female reproductive tract which can be common in stickleback (Dean et al., 2019b). In this case hatching success was recalculated as the number of successfully hatched stickleback per total number of fertilised eggs, and this value was used in the model. Time to hatch (days) was compared between migratory and lagoon resident stickleback using two-sample Wilcoxon rank sum tests.

To assess differences in development between migratory and lagoon resident stickleback, the score based on Swarup's 1958 taxonomy was plotted at each 24-hour timepoint for both ecotypes. We tested for differences between ecotypes in the development score over multiple days using two-sample Wilcoxon rank sum tests, and used the false discovery rate (FDR) method to control for type 1 errors (Benjamini and Hochberg, 1995). Considering the small number of tests and clutches used in this analysis, we set a relatively relaxed FDR threshold of 0.1, which allowed for 10% of significant results to be false positives. As days to 50% hatched and observable differences in development were also assessed between ecotypes, we could be confident that differences in hatching time between migratory and resident stickleback was not a type I error.

As egg size could in part explain any differences in hatching success or days to hatch between migratory and resident stickleback, we have included measurements of egg volume for the two ecotypes found on North Uist, from two different lochs sampled in 2007 and 2011. Migratory and resident stickleback were collected from the saltwater lochs Ob nan Stearnain (57.601667, -7.172778) and Fairy Knoll (57.635278, -7.215000). Eggs were assumed to be ellipsoid and were measured using a dissecting microscope with an eyepiece graticule. Length (largest dimension when viewed from above) was measured and the measurement perpendicular to this was assumed to be the diameter at the widest point. These measurements were halved to get corresponding half-axis measurements, a and b respectively. These values were used to calculate volume for between 5 and 10 eggs per mature female, as $4/3\pi ab^2$. A mean egg volume was then calculated for each female and this was compared between ecotypes using a linear mixed effects model with ecotype as a fixed effect and loch as a random effect.

All analyses were done using the R language and performed in R Studio (R Core Team, 2021) and an alpha value of 0.05 used for statistical tests.

2.5 Results

The number of eggs selected per clutch averaged 23.6, with means of 27.0 and 20.2 eggs for migratory and resident clutches respectively (in total, clutches are larger than this, especially for migratory fish). There was no difference in hatching success between ecotypes (Wald $X^2_1 = 0.673$, $P = 0.412$; **Table 2.1**, **Figure 2.1a**), with hatching success averaging 85.0% in migratory stickleback and 92.7% in lagoon resident fish (**Figure 2.1a**). The number of days until appearance of the first hatched

larvae and the number of days until 50% of the clutch had hatched were significantly earlier in migratory than lagoon resident stickleback (Wilcoxon rank sum test: First larvae: p = 0.00300; 50% hatched: p = 0.00488; **Table 2.1**, **Figure 2.1b**). The first migratory fish hatched after 11.7 days on average and 50% of the clutch hatched after 12.2 days (clutches hatched on days 11 or 12) and the first resident fish hatched after 13.2 days, with 50% of the clutch having hatched after 13.7 days (clutches hatched on day 13 or 14). Resident stickleback had significantly larger eggs than migratory (χ^2 = 3.84, df = 1, p = 0.0499; **Table 2.1**, **Figure 2.2**).

Table 2.1: Hatching success, days to hatch and egg volume.

	Migratory	**Resident**
Hatching Success (%): mean +/- SD	85.0 +/- 21.6	92.7 +/- 6.7
Day to first hatched stickleback: mean +/- SD	11.7 +/- 0.5	13.2 +/- 0.5
Day to 50% hatched stickleback: mean +/- SD	12.2 +/- 0.4	13.7 +/- 0.4
Egg Volume (mm^3): mean +/- SD	1.97 +/- 0.34	2.20 +/- 0.27

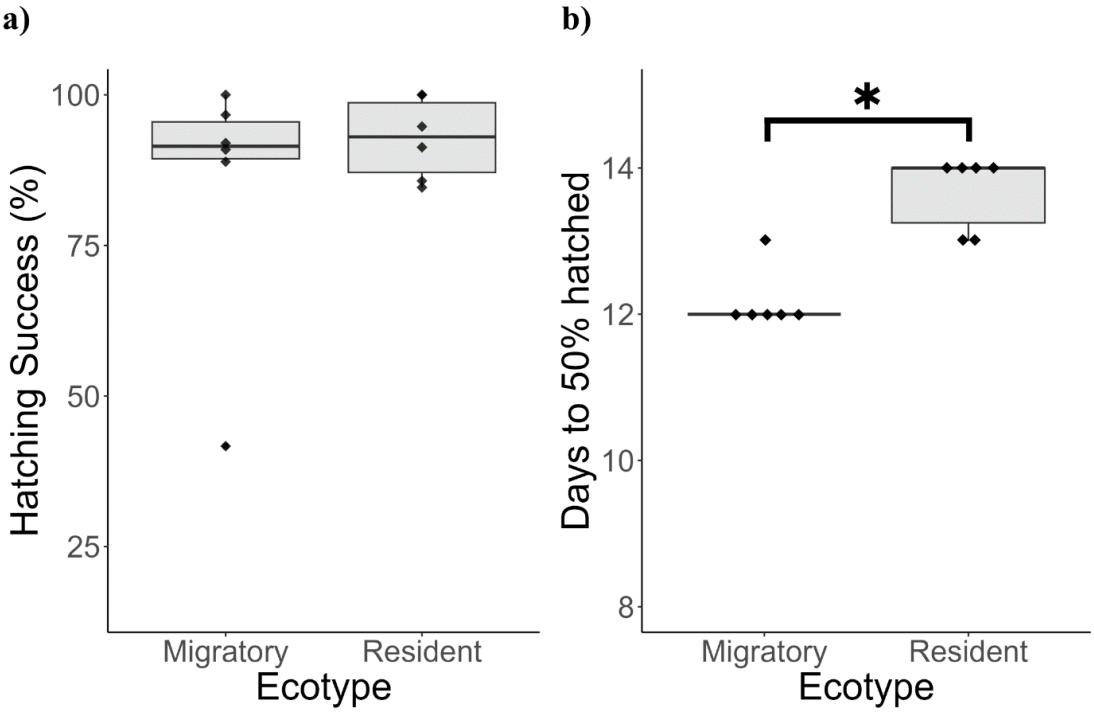

Figure 2.1: Hatching success (a) and days to 50% hatched (b) for migratory and resident three-spined stickleback incubated at 14°C. Hatching success was calculated per clutch as number of successfully hatched larvae divided by initial number of eggs. Days to hatch is calculated from fertilisation (day 0) until 50% of the clutch had hatched. Boxplot shows median and interquartile range and all data values

are displayed as points. n = 6 clutches per ecotype. Significant differences, $p < 0.05$, marked with an asterisk.

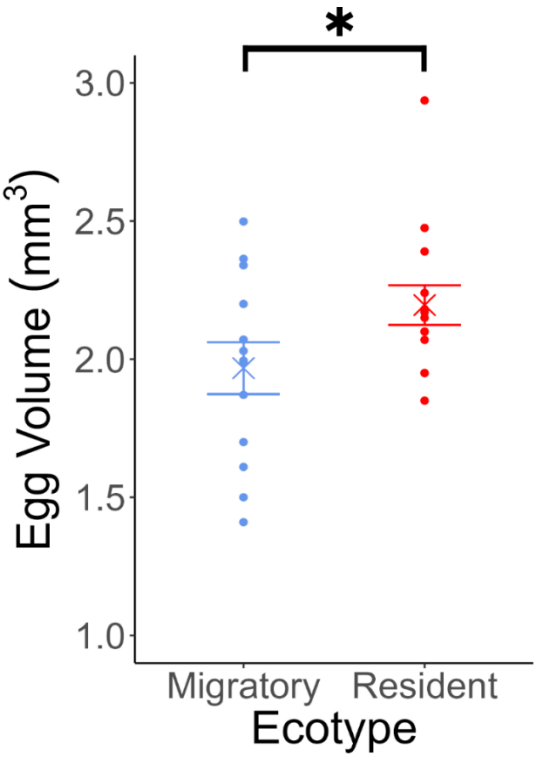

Figure 2.2: Egg volume for migratory and resident three-spined stickleback. Mean value for each ecotype is shown with a cross and error bars show standard error. Mean egg volumes for each female are displayed as points; n = 27. Significant differences, $p < 0.05$, marked with an asterisk.

Although there were quantitative differences in developmental stage between the ecotypes at days 2 and 12 (see below), our observations of the clutches revealed that development was very similar in migratory and resident clutches. Therefore, we only describe the development of lagoon resident clutches in detail, at each 24 hour interval. Day 0 is the day of fertilisation, day 1 refers to 24-hours post fertilisation, and so on. **Figure 2.3** and **Figure 2.4** show a photo time-series of development which gives a clearer impression than the line drawings that were previously available.

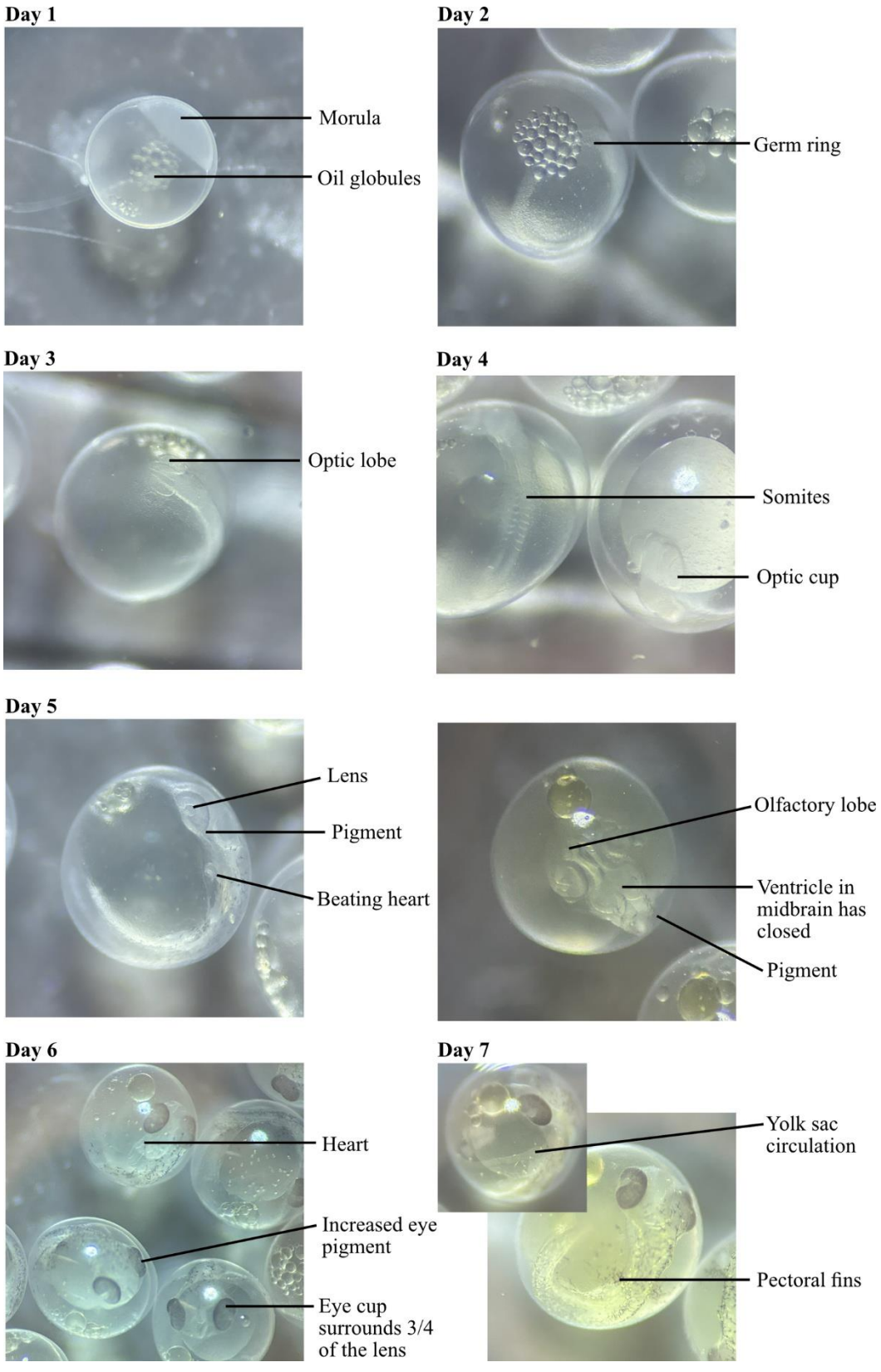

Figure 2.3: Three-spined stickleback development from day 1 (24-hours post fertilisation) to day 7. Images taken using a dissection microscope with a dark background on the stage, for contrast. Key features are labelled.

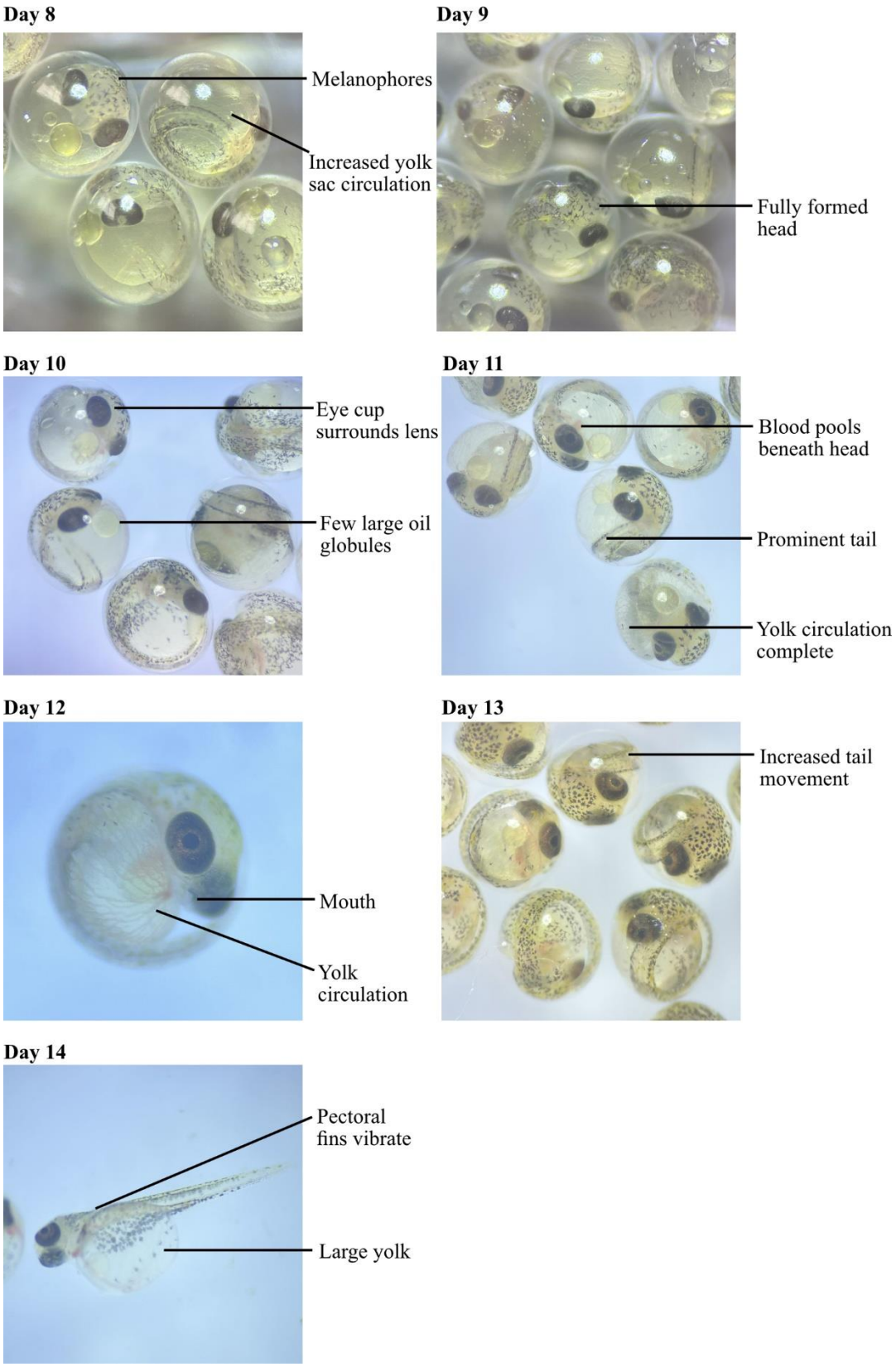

Figure 2.4: Three-spined stickleback development from day 8 up until hatching. Images taken using a dissection microscope with either a dark or light background on the stage, for contrast. Key features are labelled.

Day 1: By 24-hours post fertilisation, the egg had gone through the 2, 4, 8, 16 and 32-cell stage, reaching stage 9 in the Swarup series. The cells divided further, becoming smaller; these form the morula which sits on the yolk. Oil globules were visible in the yolk.

Day 2: Gastrulation had begun. A germ ring formed. The more opaque ring of cells seen in Swarup stage 12 were often not visible until the eggs were gently rotated, as the germ ring was usually on the ventral side. A dark background aided visualisation of features early in development.

Day 3: Optic lobes had formed either side of the forebrain (Swarup stage 16). The embryo protruded from the surface of the yolk sac.

Day 4: Somites appeared in the middle of the embryo. Rather than from the side of the embryo, as shown in Swarup 1958 stage 17, somites were best seen by gradually focusing through the yolk sac to the opposite side (**Figure 2.3**, day 4). Around six or seven pairs were clear in most cases, although occasionally there were more. The head had differentiated so that the optic lobes became optic vesicles where central cavities were visible, and then optic cups as lenses formed. The brain developed further so that separation between the mid- and hindbrain was clear.

Day 5: The heartbeat was apparent on the left side of the embryo (Swarup stage 19). This was most clear to see when looking at the embryo from the side, where only one eye is visible (**Figure 2.3**, day 5). Some pigment began to appear, starting on the outer margins of the eye and some scattered areas on the body. Ventricles in the midbrain had closed. Some gentle rotation of the eggs was necessary to see both the heartbeat and the features of the head, hence two images are provided for day 5 in **Figure 2.3**.

Day 6: More eye and body pigment was present so that most of the eye cup was dark in colour and this now surrounded almost all of the lens except for the lower portion. The tail occasionally moved, although at this point it was infrequent and difficult to capture. The split in the hindbrain could no longer be seen. The heart was larger and the three chambers were visible.

Day 7: Yolk sac circulation could be seen on the left of the embryo; often gently rotating the embryo was necessary to identify this. Pectoral fins started to develop. There was more pigment, including on the yolk sac. The head of the embryo became shorter and broader (Swarup stage 22).

Day 8: More melanophores were visible on the head. The yolk sac circulation increased in area; at this stage this was difficult to see as the colour is similar to the yolk sac so switching between a dark and light background helped distinguish this. Tail movement became more frequent and the eye pigment was darker throughout the eye cup. The split in the forebrain was still visible.

Day 9: The ventricle of the forebrain closed so the head was fully formed. The yolk sac circulation was almost complete (Swarup stage 23).

Day 10: The eye cup now completely surrounded the lens, which became dark in colour. The eye cup surrounding the lens happened at an earlier stage than in Swarup's descriptions as here this occurs prior to the completion of the yolk sac circulation and formation of the mouth, whereas this is noted at stage 24 of Swarup's descriptions where the embryo is almost ready to hatch (the final stage, approx. 24 hours prior to hatching). There were only a few larger oil globules and these were situated in front of the head. Blood also collected in front of the head. A change to a lighter background at this point in development was found to increase contrast between the pigmented features and the background, making identification easier.

Day 11: The blood collecting in front of the head became more apparent as the yolk circulation was complete and its red colour is clear, especially on a light background. The mouth formed and the tail became more prominent. To observe the mouth, gently moving the embryos was necessary to position the head of the embryo in the best light to capture the mouth; it was best observed looking at the front of the embryo (as in **Figure 2.4**, day 12).

Day 12: The amount of pigment on the body increased further. Tail movement was more frequent and the pectoral fins vibrated. The embryos displayed all key features described in stage 24 of Swarup's taxonomy and were ready for hatching.

Day 13 or 14: At day 13 or 14 hatching commenced. The head of the embryo pushed against the shell of the egg and broke free. Tail movement then freed the rest of the embryo. The hatched embryo was transparent and lay on its side as the yolk is large. The head remained curved around the edge of the yolk.

There were differences in development between lagoon resident and migratory stickleback: comparing development each day, migratory clutches were at a significantly higher score than residents at days 2, 4, 6 and 12 (**Figure 2.5**, **Table 2.2**), but after correcting for multiple testing only differences at days 2 and 12

remained significant (**Table 2.2**). Differences were therefore early in development when migratory clutches had a higher score and were therefore more developed than residents, and late in development (day 12) when the eggs of residents took longer to hatch than migratory clutches after reaching the final stage (24) in Swarup's scoring (**Figure 2.5**).

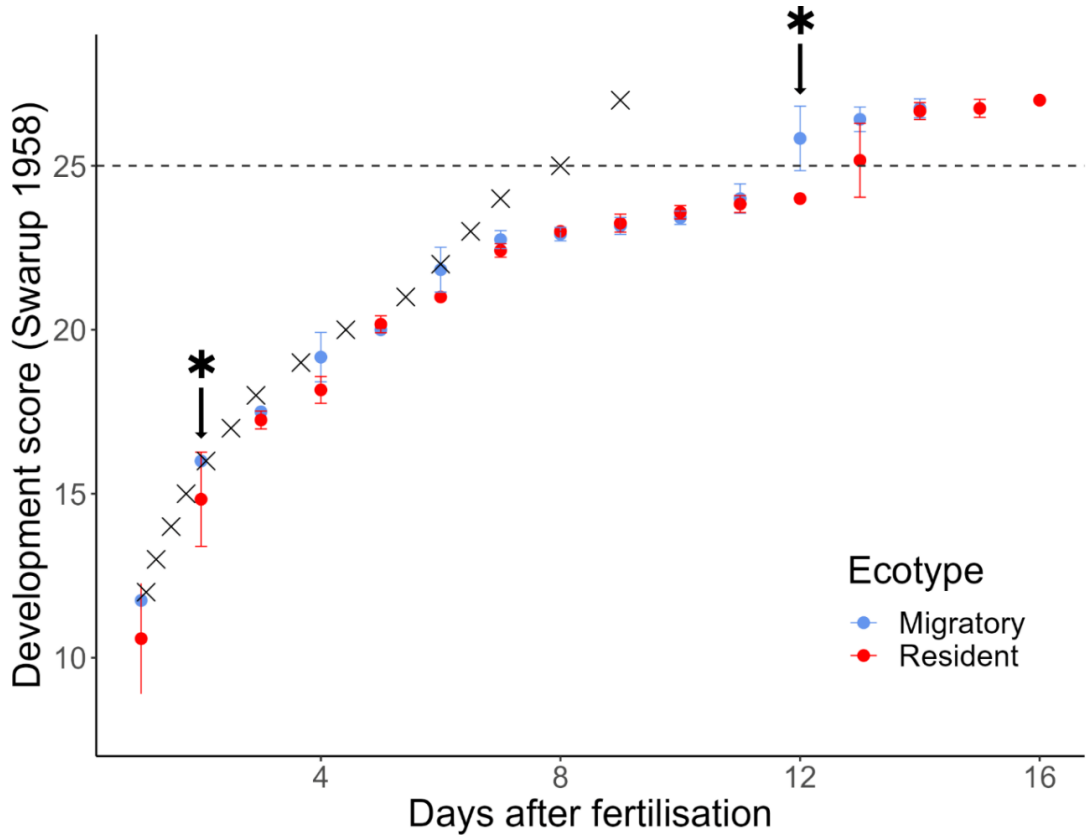

Figure 2.5: Development of stickleback embryos through time (days after fertilisation) estimated as the Swarup (1958) score. Migratory stickleback clutches are shown in blue and residents in red with error bars showing standard deviation. Clutches were raised at 14°C. Grey crosses show the development score from Swarup 1958 for comparison, where stickleback were raised at 18–19°C. Dotted line shows when stickleback have hatched. Asterisk shows days where there was a significant difference ($p < 0.05$) between migratory and resident scores (two-sample Wilcoxon rank sum tests) that remained significant after correcting for multiple comparisons using the FDR method: FDR = 0.10.

Table 2.2: Wilcoxon rank sum test results for comparisons between migratory and resident stickleback development scores at each day ranked in order of increasing p value, with multiple comparisons testing of results. FDR set to 0.10.

Day Tested	P-Value (Wilcoxon Rank Sum Test)	Rank	Benjamini-Hochberg significance
12	0.008113	1	Significant
2	0.00931	2	Significant
6	0.02766	3	Not significant
4	0.02889	4	Not significant
7	0.05429	5	Not significant
3	0.07053	6	Not significant
13	0.07955	7	Not significant
5	0.1739	8	Not significant
10	0.2184	9	Not significant
1	0.2361	10	Not significant
8	0.4047	11	Not significant
11	0.5407	12	Not significant
9	0.6404	13	Not significant
14	0.7077	14	Not significant

Progression of development in our clutches of migratory and resident stickleback (raised at 14°C) also differed strongly from those of Swarup raised at 18–19°C. Early in development (days 1 to 6) there is only a small difference, with those raised at 18–19°C having, in general, a slightly higher development score (**Figure 2.5**). However, by day 7 there is a large difference in score, with Swarup's having reached stage 24, the final stage before hatching, but both resident and migratory clutches raised at 14°C averaging a score of 22.6 (migratory mean was 22.8 and resident 22.4). Those raised at the higher temperatures hatch (stage 25) at days 6 to 8, while clutches raised at the lower temperature remain at the later stages of development (stages 22 to 24) for a longer time, before hatching between days 11 and 14.

2.6 Discussion

We describe visual features of development in the embryos of two contrasting ecotypes of three-spined stickleback, every 24 hours post-fertilisation, with key structures highlighted in photographs to increase the ease of identification of important features. This builds upon the work of Swarup (1958), where stages were named after key morphological characteristics and described in detail in stickleback embryos raised at 18 to 19°C. However, as stickleback development is strongly influenced by temperature, this work assessed these key features daily in stickleback developing at a lower, physiologically relevant temperature for where these populations would be found naturally, and to compare the two ecotypes. The hatching success of both ecotypes was high, with no differences between them. We have presented only coloured images of resident stickleback because, aside from the difference in hatching time, qualitatively we did not observe any differences in development between ecotypes. As we viewed embryos every 24 hours it remains possible that finer differences in detail exist but could not be observed here.

Migratory clutches tended to be further developed than residents from days 1 to 7, although this only reached significance at day 2. From day 8, no difference in development stage was observed between ecotypes, so resident clutches had 'caught up' with migratory, and both ecotypes had reached stage 24 at the same time. Migratory clutches then hatched on day 11 or 12 while residents remained at the last stage prior to hatching. The eggs of resident stickleback therefore hatched on average 1.5 days later than those of migratory fish. As embryos were checked every 24-hours, the hatch day was recorded as the day where 50% or more of the clutch had hatched. This could therefore be slightly longer than actual time to hatching (as stickleback may have hatched sometime within the day prior), but this should not cause a systematic bias between the ecotypes. Indeed, the difference between ecotypes was large, with little overlap in hatch day between groups.

The migratory and resident forms are known to vary greatly in morphology and genetics, so a difference in development is not unexpected (Dean et al., 2019a), and diverged Arctic charr morphs have been found to vary in egg size, development timing and size at hatching (Beck et al., 2022). Migratory stickleback have larger clutches than resident (Karve et al., 2013) and there is a trade-off between clutch size and egg size (Elgar, 1990; Karve et al., 2013), suggesting that the eggs of migratory fish are likely smaller than those of residents. Indeed, we show quantitatively that this is the

case for North Uist populations, with resident eggs having a larger volume than migratory eggs. The decreased yolk size and therefore nutrients for migratory embryos may explain the reduced time to hatch, as well as additional differences in the egg or membrane itself. The finding that migratory clutches with smaller eggs hatched earlier than residents with larger eggs agrees with previous work compiling development times from 84 species of teleost fish; they found that smaller eggs developed faster than larger eggs when all other factors, including temperature, were controlled (Pauly and Pullin, 1988). Further studies on the egg of both ecotypes would be required to fully understand these findings. Temperature, pH and dissolved oxygen have also previously been implicated in stickleback growth and development (Candolin et al., 2022; Lefébure et al., 2011; Wanzenböck et al., 2022) but as rearing conditions were consistent here, these cannot explain the differences in development between ecotypes.

In addition to the ecotype differences observed, by comparing resident and migratory stickleback raised at 14°C to stickleback raised at 18–19°C by Swarup (1958), the effect of incubation temperature can be explored, although this is limited as Swarup provides only an estimate for the time to reach each stage. All stickleback were raised in fresh water but different populations were used between studies, so additional population effects can also not be ruled out. Time to hatch was greater than 3 days longer at 14°C than Swarup found at the warmer temperature of 18–19°C. This reduced hatching time at increased temperatures has been reported across many fish species (Melendez and Mueller, 2021; Pauly and Pullin, 1988), with hatching time often inversely proportional to incubation temperature, for example in Haddock (*Melanogrammus aeglefinus*) (Martell et al., 2006). As differences between temperatures were not apparent until seven days post fertilisation, temperature has limited influence early on in stickleback development, up until yolk sac circulation, but warmer temperatures then induce hatching earlier. Similar findings have been made in the zebrafish (*Danio rerio*), where the same rate of early development was observed at a wide range of temperatures (Schirone and Gross, 1968). In the three-spined stickleback, temperature greatly effects paternal care behaviour, reproductive success and growth rate post-hatching (Hopkins et al., 2011; Lefébure et al., 2011), but effects on embryo development have rarely been studied.

This study has revisualised the key characteristics in three-spined stickleback development up until hatching, following the landmark work of Swarup (1958). Using North Uist lagoon resident and migratory populations that live in sympatry during the

breeding season provides further information on how different ecotypes develop at a temperature they would naturally experience. It provides a set of features that are clear at each day post fertilisation to allow comparison between future treatments, particularly important if we want to discover how stickleback embryos will cope with the increasing water temperature and carbon dioxide levels that may be experienced. These stages also provide a baseline for any abnormalities in development to be compared to. A high yet consistent hatching success between both ecotypes has also been shown and that migratory stickleback hatch at least a day earlier on average than resident stickleback from the same loch. Further investigation into this in natural populations, and studies of migratory and resident stickleback eggs, would be necessary to explain this pattern. However, as this species is often raised in aquaria at the temperature used here, this information adds to our knowledge of how long stickleback incubation lasts before hatching.

2.7 Acknowledgements

We are grateful to Laura Dean, Ann Lowe and Henry Lewis for their help and advice with this project during fieldwork.

2.8 References

Beck, S. V., Räsänen, K., Kristjánsson, B.K., Skúlason, S., Jónsson, Z.O., Tsinganis, M., Leblanc, C.A., 2022. Variation in egg size and offspring phenotype among and within seven Arctic charr morphs. *Ecol. Evol.* **12**, e9427. https://doi.org/10.1002/ece3.9427

Benjamini, Y., Hochberg, Y., 1995. Controlling the False Discovery Rate: A Practical and Powerful Approach to Multiple Testing. *J. R. Stat. Soc. Ser. B. Methodol.* **57**, 289–300. https://doi.org/10.1111/J.2517-6161.1995.TB02031.X

Candolin, U., Goncalves, S., Pant, P., 2022. Delayed early life effects in the threespine stickleback. *Proc. R. Soc. B.* **289**, 20220554. https://doi.org/10.1098/RSPB.2022.0554

Colosimo, P.F., Hosemann, K.E., Balabhadra, S., Villarreal, G., Dickson, H., Grimwood, J., Schmutz, J., Myers, R.M., Schluter, D., Kingsley, D.M., 2005. Widespread parallel evolution in sticklebacks by repeated fixation of ectodysplasin alleles. *Science* **307**, 1928–1933. https://doi.org/10.1126/science.1107239

Dean, L.L., Magalhaes, I.S., Foote, A., D'Agostino, D., McGowan, S., MacColl, A.D.C., 2019a. Admixture between Ancient Lineages, Selection, and the Formation of Sympatric Stickleback Species-Pairs. *Mol. Biol. Evol.* **36**, 2481–2497. https://doi.org/10.1093/MOLBEV/MSZ161

Dean, L.L., Robertson, S., Mahmud, M., MacColl, A.D.C., 2019b. Internal embryonic development in a non-copulatory, egg-laying teleost, the three-spined stickleback, *Gasterosteus aculeatus*. *Sci. Rep.* **9**, 2395. https://doi.org/10.1038/s41598-019-38584-w

Elgar, M.A., 1990. Evolutionary Compromise between a Few Large and Many Small Eggs: Comparative Evidence in Teleost Fish. *Oikos*. **59**, 283-287. https://doi.org/10.2307/3545546

Guidance on the operation of the Animals (Scientific Procedures) Act 1986 (ASPA) - GOV.UK. 2017 URL https://www.gov.uk/guidance/guidance-on-the-operation-of-the-animals-scientific-procedures-act-1986 (accessed 18.3.24).

Haenel, Q., Roesti, M., Moser, D., MacColl, A.D.C., Berner, D., 2019. Predictable genome-wide sorting of standing genetic variation during parallel adaptation to basic versus acidic environments in stickleback fish. *Evol. Lett.* **3**, 28-42. https://doi.org/10.1002/EVL3.99

Hatfield, T., 1997. Fluctuating asymmetry and reproductive isolation between two sticklebacks, *Environ. Biol. Fishes*. **49**, 63-69.

Hopkins, K., Moss, B.R., Gill, A.B., 2011. Increased ambient temperature alters the parental care behaviour and reproductive success of the three-spined stickleback (*Gasterosteus aculeatus*). *Environ. Biol. Fish.* **90**, 121–129. https://doi.org/10.1007/s10641-010-9724-8

Jones, F.C., Grabherr, M.G., Chan, Y.F., Russell, P., Mauceli, E., Johnson, J., Swofford, R., Pirun, M., Zody, M.C., White, S., Birney, E., Searle, S., Schmutz, J., Grimwood, J., Dickson, M.C., Myers, R.M., Miller, C.T., Summers, B.R., Knecht, A.K., Brady, S.D., Zhang, H., Pollen, A.A., Howes, T., Amemiya, C., Baldwin, J., Bloom, T., Jaffe, D.B., Nicol, R., Wilkinson, J., Lander, E.S., Di Palma, F., Lindblad-Toh, K., Kingsley, D.M., 2012. The genomic basis of adaptive evolution in threespine sticklebacks. *Nature.* **484**, 55–61. https://doi.org/10.1038/nature10944

Karve, A.D., Baker, J.A., Von Hippel, F.A., 2013. Female life-history traits of a species pair of threespine stickleback in Mud Lake, Alaska. *Evol. Ecol. Res.* **15**, 171-187.

Kuntz, A., Radcliffe, L., 1917. Notes on the Embryology and Larval Development of Twelve Teleostean Fishes. *NOAA Fisheries.* **35**.

Lefébure, R., Larsson, S., Byström, P., 2011. A temperature-dependent growth model for the three-spined stickleback *Gasterosteus aculeatus*. *J. Fish. Biol.* **79**, 1815–1827. https://doi.org/10.1111/j.1095-8649.2011.03121.x

Martell, D.J., Kieffer, J.D., Trippel, E.A., 2006. Effects of the embryonic thermal environment on haddock (*Melanogrammus aeglefinus*) developmental trajectories through exogenous feeding stages. *Mar. Biol.* **149**, 177–187. https://doi.org/10.1007/s00227-005-0190-3

Melendez, C.L., Mueller, C.A., 2021. Effect of increased embryonic temperature during developmental windows on survival, morphology and oxygen consumption of rainbow trout (*Oncorhynchus mykiss*). *Comp. Biochem. Physiol. A. Mol. Integr. Physiol.* **252**, 110834. https://doi.org/10.1016/j.cbpa.2020.110834

Pauly, D., Pullin, R.S. V, 1988. Hatching time in spherical, pelagic, marine fish eggs in response to temperature and egg size. *Environ. Biol. Fish*. **22**, 261-271. https://doi.org/10.1007/BF00004892

R Core Team, 2021. R: A language and environment for statistical computing. R foundation for Statistical Computing, Vienna, Austria. URL https://www.R-project.org/.

Reid, K., Bell, M.A., Veeramah, K.R., 2021. Threespine Stickleback: A Model System For Evolutionary Genomics. *Annu. Rev. Genomics. Hum. Genet.* **22**, 357-383. https://doi.org/10.1146/ANNUREV-GENOM-111720-081402

Schirone, R.C., Gross, L., 1968. Effect of temperature on early embryological development of the zebra fish, *Brachydanio rerio*. *J. Exp. Zool.* **169**, 43–52. https://doi.org/10.1002/jez.1401690106

Swarup, H., 1958. Stages in the Development of the Stickleback *Gasterosteus aculeatus* (L.). *Development*. **6**, 373–383. https://doi.org/10.1242/DEV.6.3.373

Vrat, V., 1949. Reproductive Behavior and Development of Eggs of the Three-Spined Stickleback (*Gasterosteus aculeatus*) of California **15**, 252–260. https://doi.org/10.2307/1438375

Wanzenböck, S., Fuxjäger, L., Ringler, E., Ahnelt, H., Shama, L.N.S., 2022. Temperature-Dependent Reproductive Success of Stickleback Lateral Plate Morphs: Implications for Population Polymorphism and Range Shifts Under Ocean Warming. *Front. Mar. Sci.* **9**. https://doi.org/10.3389/fmars.2022.759450

Chapter 3: A Common Anaesthetic, MS-222, Alters Measurements Made Using High-Resolution Respirometry in the Three-Spined Stickleback (*Gasterosteus aculeatus*)

Megan Barnes[1], Brad Ebanks[2], Andrew D.C. MacColl[1], Lisa Chakrabarti[2,3]

[1] School of Life Sciences, University of Nottingham, Nottingham NG7 2RD, UK.

[2] School of Veterinary Medicine and Science, Sutton Bonington Campus, University of Nottingham, Loughborough LE12 5RD, UK.

[3] Medical Research Council Versus Arthritis Centre for Musculoskeletal Ageing Research, Nottingham NG7 2RD, UK.

3.1 Statement of contribution

I planned the project, collected and analysed the data, prepared the figures and tables, and wrote and compiled the manuscript. Lisa Chakrabarti and Andrew MacColl supervised the project and contributed to the planning and editing of the manuscript. Brad Ebanks helped to develop the methodology and advised during the project.

This chapter is the accepted version of the journal paper that is published in *Fishes* 2023, 8, 42; https://doi.org/10.3390/fishes8010042.

Published 7 January 2023.

3.2 Abstract

Submersion in the anaesthetic MS-222 is a well-established and effective method used during the euthanasia of fish, but the consequences of treatment with this anaesthetic for mitochondrial respiration are yet to be established. This is important to evaluate, as an increasing amount of research is conducting high-resolution respirometry to measure respiration across multiple species of fish, including looking

at thermal sensitivity and mitochondrial responses to the warmer temperatures faced with climate change. Analysis often occurs after euthanasia with MS-222 without knowledge of how MS-222 itself affects any measured parameters of mitochondrial respiration, leaving potential for a misinterpretation of results. Here, high-resolution respirometry was conducted to explore how MS-222 affects oxidative phosphorylation in the brain and skeletal muscle of the three-spined stickleback, *Gasterosteus aculeatus*, which is a model species in evolutionary ecology. In the brain, differences in respiration were observed between three-spined sticklebacks euthanised with MS-222 and those where no anaesthetic was implemented. No differences between treatments were observed in the skeletal muscle, although variation between individuals was high and oxygen flux was lower than in the brain. Overall, this study highlights the need for a consistent method of euthanasia when conducting high-resolution respirometry in fish, as MS-222 may alter measures of oxidative phosphorylation.

Keywords: mitochondria; high-resolution respirometry; stickleback; *Gasterosteus aculeatus*; MS-222; anaesthetic

3.3 Introduction

MS-222, also known as tricaine methane sulphonate, tricaine mesylate and TMS, is commonly used in both the anaesthesia and euthanasia of some species of fish. As an agent for euthanasia, standard protocols involve immersion in a neutral solution of MS-222 followed by a secondary physical method such as pithing, where a metal spike is used to destroy the brain (Close et al., 1997). Being structurally close to other local anaesthetics including benzocaine, MS-222 works via a similar mechanism, altering the properties of voltage gated sodium channels to depress the central nervous system. The use of MS-222 is well established and effective (Collymore et al., 2014; Matthews and Varga, 2012), although it is not the only method of euthanasia approved and used in fish.

The side effects of MS-222 as an anaesthetic have been well studied (Collymore et al., 2014) and can include the induction of apoptosis and oxidative stress in fish gills (Wang et al., 2020), effects on the cardiovascular system (Hill et al., 2002), and reduced membrane fluidity and mitochondrial functionality in the sperm of the zebrafish (Zanin et al., 2021). However, any physiological effects of using MS-222 for fish euthanasia have not yet been characterised. With a growing body of work assessing mitochondrial respiration in fish, including studies of thermal sensitivity and

in particular mitochondrial responses to increased temperatures and altered environments due to climate change (Chung et al., 2018; Leo et al., 2018; Thoral et al., 2021), it is vital to take into account the consequences of using a prior overdose of anaesthetic such as MS-222. Knowing how MS-222 alters mitochondrial respiration in fish would ensure that any observed changes to respiration are in fact a consequence of the study conditions being assessed and not due to the anaesthetic itself, and they would allow more inciteful comparison of studies implementing different methods of euthanasia.

High-resolution respirometry (HRR) measures respiration in mitochondrial preparations, allowing analysis of the mitochondrial respiratory pathways. Respiration states including LEAK, OXPHOS and ET capacity can be measured and compared between treatment groups to give an overview of how MS-222 affects mitochondrial respiration. LEAK state is the non-phosphorylating resting state where oxygen flux is maintained only to compensate for the proton leak back across the inner mitochondrial membrane, which does not contribute to ATP generation. In the mitochondrion, electron transfer is coupled to the phosphorylation of ADP to ATP, so with ADP present, the respiratory capacity of mitochondria in the oxidative phosphorylation (OXPHOS) state can be measured. ET capacity, the electron-transfer capacity of mitochondria, is the maximum capacity of the non-coupled electron-transfer system, which is reached when ADP phosphorylation is uncoupled from electron transfer by the addition of a protonopore. These states can be attained experimentally by the addition of different substrate, inhibitor and uncoupler combinations.

In order to assess whether MS-222 has any effect on mitochondrial respiration, we conducted HRR on the brain and skeletal muscle of the three-spined stickleback (*Gasterosteus aculeatus*), which is a model organism in evolutionary ecology. We found that LEAK state respiration was reduced in the brain of fish euthanized with MS-222 in comparison to those without use of any anaesthetic. As MS-222 is altering some parameters of respiration, we conclude that the method used for euthanasia is an important factor to be considered when conducting HRR in fish.

3.4 Materials and methods

To assess the effect of MS-222 anaesthetic, which is commonly used in the euthanasia of fish species, on mitochondrial respiration, respiration states were compared between three-spined sticklebacks culled with MS-222 (n = 9) and those

culled without the use of any anaesthetic (n = 8). The Oroboros Oxygraph-2k Respirometer (O2k; Oroboros® Instruments, Innsbruck, Austria) was used for HRR, which allows an analysis of bioenergetics and oxidative phosphorylation in small amounts of biological samples, such as tissue homogenates which were used here (Devaux et al., 2019; Salin et al., 2019; Thoral et al., 2021).

3.4.1 Fish husbandry

Three-spined sticklebacks (*Gasterosteus aculeatus*) were raised in the aquarium. Fish of the same backcross from populations on the Scottish island of North Uist, hatched between 20th and 25th July 2018, were used for analysis (Dean et al., 2019a; Magalhaes et al., 2016). A balanced experiment was set up: two fish from the same tank were analysed; one fish was culled by submersion in MS-222 (400 mg/L) followed by pithing, and the other was killed by severing the spinal cord (here in referred to as decapitation) under UK Home Office project licence PP5421721. Fish were weighed and placed immediately on ice.

3.4.2 Dissection

Immediately prior to respirometry analysis with an Oroboros O2k, the brain of each stickleback was removed and weighed. The brain was then homogenised in ice cold MiRO5 buffer (Oroboros Instruments GmbH; 0.5 mM EGTA, 3 mM $MgCl_2$, 60 mM Lactobionic acid, 20 mM Taurine, 10 mM KH2PO4, 20 mM HEPES, 110 mM D-Sucrose, 1g/L BSA) using 20 crushes with an Eppendorf and micropestle (200 uL buffer per 3.5 mg of brain). Then, 3.5 mg of homogenised brain was added per 2 mL chamber of the O2k.

Analysis of muscle was always conducted in sequence after the brain. Tail skeletal muscle was taken from the left side of the fish, and the skin was carefully removed. Muscle was cut into fine pieces (<1 mm) and homogenised using a scalpel before a subsample was weighed and homogenised with 25 crushes using an Eppendorf and micropestle in ice-cold MiRO5 buffer (200 uL per 5 mg muscle). Then, 5 mg of muscle was added per 2 mL volume chamber. Where possible, technical replicates were conducted for both muscle and brain samples.

3.4.3 High-resolution respirometry

The O2k has two chambers, so two samples can be run simultaneously. In most cases, experimental design allowed one MS-222 sample and one decapitated sample to be analysed at the same time for direct comparison of fish from the same

tank/family. HRR was conducted using an O2k (Oroboros® Instruments, Innsbruck, Austria). Electrodes were calibrated at the start of each day. Analysis was conducted at 14 °C, as this is the approximate body temperature of the stickleback raised in the aquarium. Then, 2 mL MiRO5 was added to each O2k chamber prior to the brain or muscle sample.

A substrate–uncoupler–inhibitor–titration (SUIT) protocol ideal for assessing oxidative phosphorylation with NADH-linked substrates (complex I) and S-pathway substrates (complex II) was used (SUIT-004, Doerrier & Gnaiger). This allowed analysis of LEAK state respiration, oxidative phosphorylation (OXPHOS) and ET capacity. This protocol was selected as the substrates tested resulted in altered oxygen flux in tissue homogenates used, the protocol gave a good overview of many parameters of respiration including complex I and complex II respiration, and it was relatively short (<1 h), so it prevented sample deterioration. All substrate and inhibitor concentrations were optimized for fish tissue homogenate used in this study with final concentrations in parenthesis below. After the addition of a substrate or inhibitor, oxygen flux was allowed to reach equilibrium before marking the value and moving onto the next stage (**Figure 3.1**). All chemical reagents were supplied by Sigma-Aldrich (Merck, Darmstadt, Germany) except ADP which was supplied by Calbiochem (Merck, Darmstadt, Germany).

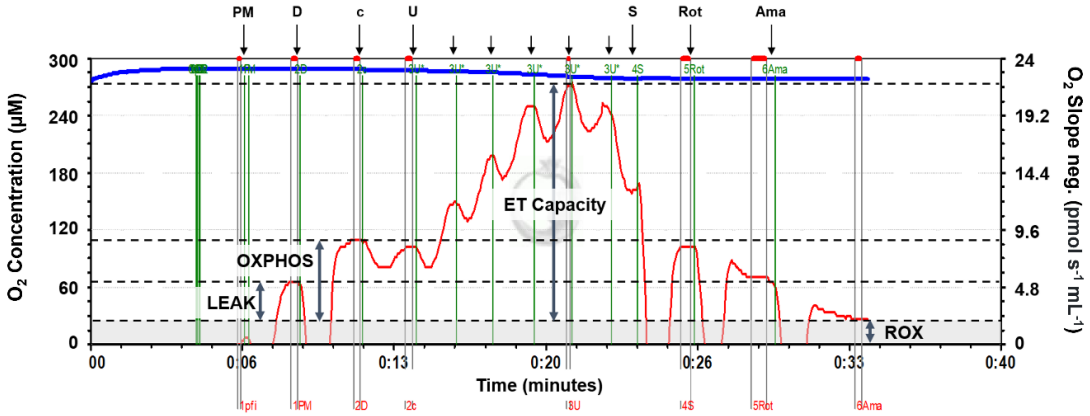

Figure 3.1: Annotated O2k Oxygraph. Example trace from the brain of a stickleback, following protocol described above. Blue line shows oxygen concentration, red line shows the oxygen flux. ROX, LEAK, OXPHOS and ET capacity respiration states labelled with double headed arrows. The point when each substrate/inhibitor was added is shown by arrows above the trace, and where oxygen flux reached equilibrium is shown in red below. PM = Pyruvate and Malate; D = ADP;

c = Cytochrome c; U = Uncoupler (CCCP), added repeatedly at each shorter arrow until a max. value was reached; S = Succinate; Rot = Rotenone; Ama = Antimycin A.

LEAK state was attained and measured by addition of the complex I substrates pyruvate (5 mM) and malate (2 mM) in the absence of ADP. In the mitochondria, pyruvate is converted to acetyl-CoA by pyruvate-dehydrogenase, and acetyl-CoA enters the TCA cycle where electrons are donated to NAD+, producing NADH. Malate is oxidized to oxaloacetate in the TCA cycle, also forming NADH. NADH enters the electron transport system (ETS) at complex I, and electron transfer to oxygen then occurs via the ETS enzyme complexes. However, without ADP addition, no phosphorylation of ADP can occur.

OXPHOS state respiration was measured by the addition of ADP (7.5 mM). To check the mitochondrial outer membrane integrity, cytochrome c (0.01 mM) was added. If the membrane had been damaged during prior tissue preparation, cytochrome c, which is part of the electron transport system, would have been lost from the membrane, so the addition of cytochrome c would increase the respiration rate. Experimental runs where a percentage increase of greater than 20% was observed were excluded from analysis.

ET capacity was measured by the stepwise addition of an uncoupler (carbonyl cyanide m-chlorophenyl hydrazone (CCCP), a protonophore, added in 1 µL increments of a 1 mM stock solution) to reach maximum oxygen flux. To test combined complex I and II respiration, succinate (10 mM) was added to allow the measurement of ET capacity with complex I and II reducing substrates. Succinate is converted to fumarate by complex II and succinate dehydrogenase while reducing FAD to $FADH_2$. To measure the contribution of complex II alone, a complex I inhibiter (rotenone; 0.5 uM) was added, which prevents electron transfer through complex I. Finally, complex III inhibitor antimycin A (2.5 uM) prevents electron transfer to give a measure of background oxygen flux (ROX) due to any oxidative side reactions.

3.4.4 Data Analysis

Raw data outputs for each stage were obtained from DatLab (DatLab v7, Oroboros, Innsbruck, Austria). Background corrected oxygen flux was calculated by subtracting ROX from the oxygen flux measured at each stage. Oxygen flux is expressed per 3.5 or 5 milligrams of tissue homogenate used for brain and muscle, respectively. Although the amount of brain or muscle tissue was kept constant between samples, the number of mitochondria may vary between samples; to account for this, an

internal normalization was conducted by calculating the Flux Control Ratio (FCR), which expresses respiratory control independent of mitochondrial content (Doerrier et al., 2018; Gnaiger, 2020). FCRs normalise each sample to the maximum oxygen flux reached by that sample, allowing comparison between samples from different individuals (Gnaiger, 2020). For samples with technical replicates, mean values were calculated, and these were used in further analysis, which was completed using R (R Core Team 2022, v4.2.2). Unpaired *t*-tests were conducted to determine if there were any differences in mean oxygen flux and FCRs with each substrate combination tested between decapitated and MS-222 treated fish.

Mean weights of the two treatment groups were 2.12 ± 0.59 grams for MS-222 treated and 2.14 ± 0.64 grams for decapitated. These did not differ significantly (Unpaired Student's *t*-test: $t_{df} = 15 = 0.0647$, $p = 0.949$). As fish were from different crosses, each raised in a separate tank, a one-way ANOVA was conducted to determine any effects on mitochondrial function: the cross/tank had no effect at any mitochondrial stage. To analyse all data together, a linear mixed model was fitted with oxygen flux as the dependent variable, the euthanasia method and respiration state nested within tissue type as fixed effects, and the cross/tank as a random effect (**Table S3.1**). This revealed that the tissue type and respiration state affected oxygen flux as expected; however, the euthanasia method did not, therefore not providing additional information on the consequences of MS-222 on the different parameters of mitochondrial respiration.

3.5 Results

3.5.1 Stickleback treated with MS-222 had altered respiration in the brain

With complex I substrates, treatment with MS-222 significantly reduced LEAK state respiration with pyruvate and malate as substrates (**Figure 3.2**) in the brain of the three-spined stickleback (FCR: $t_{df=15} = 2.392$, $p = 0.030$, **Figure 3.2**, **Table 3.1**). Note, however, that the oxygen flux did not differ significantly between groups (Oxygen Flux:: $t_{df=15} = 1.754$, $p = 0.100$, **Figure 3.2**, **Table 3.1**). There were no significant differences between OXPHOS state and ET capacity when comparing fish treated with MS-222 to those without, with any substrate combination (OXPHOS: Oxygen flux: $t_{df=15} = 0.085$, $p = 0.933$, FCR: $t_{df=15} = 0.954$, $p = 0.355$; ET Capacity: Oxygen flux: $t_{df=15} = -0.682$, $p = 0.506$, **Table 3.1**). With complex II substrates (succinate) in combination with complex I (pyruvate and malate), and in complex II substrates alone (in the presence of complex I inhibitor rotenone), there were no differences in oxygen

flux or FCRs between groups (**Table 3.1**). Although there were no significant differences between treatment groups, other than in the LEAK state, FCR values did tend to be lower for MS-222 than for decapitated fish.

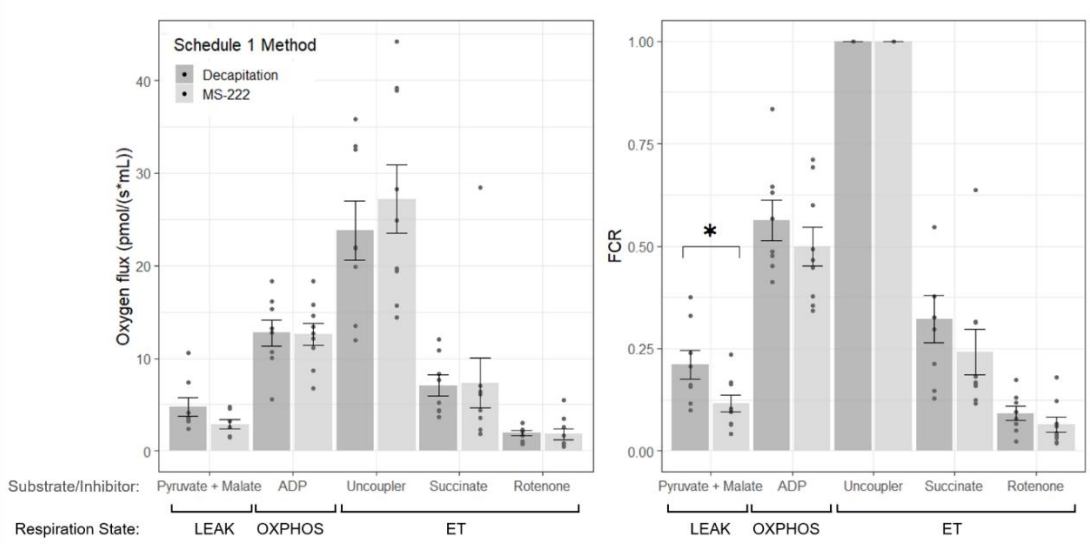

Figure 3.2: Mean oxygen flux and flux control ratios at LEAK, OXPHOS and ET respiration states in the brain of the stickleback with complex I substrates (pyruvate and malate) and complex II substrate (succinate). Average values per sample shown by points, n = 8 for decapitation (darker grey), n = 9 for MS-222 treated (lighter grey). Error bars show standard error. Significant differences ($p < 0.05$) depicted by a star (*) (unpaired Student's *t*-test).

Table 3.1: Oxygen flux and flux control ration values in the brain and muscle of three-spined stickleback treated with or without MS-222. Unpaired Student's *t*-test, significant differences ($p < 0.05$) between groups depicted by a star (*).

Respiration State and Substrates		Brain			Muscle		
		MS-222	Decapitated	P-Value	MS-222	Decapitated	P-Value
LEAK State (Complex I substrates)	Oxygen Flux (pmol s^{-1} mL^{-1}): Mean (s.e.)	2.872 (0.487)	4.739 (0.991)	0.100	2.130 (0.664)	1.819 (0.392)	0.684
	FCR: Mean (s.e)	0.116 (0.021)	0.210 (0.035)	**0.030***	0.332 (0.131)	0.262 (0.058)	0.618
OXPHOS State (Complex I substrates)	Oxygen Flux (pmol s^{-1} mL^{-1}): Mean (s.e.)	12.612 (1.174)	12.767 (1.415)	0.933	6.353 (1.063)	5.891 (1.204)	0.783
	FCR: Mean (s.e)	0.499 (0.047)	0.563 (0.049)	0.355	0.776 (0.061)	0.750 (0.048)	0.734
ET Capacity (Complex I substrates)	Oxygen Flux (pmol s^{-1} mL^{-1}): Mean (s.e.)	27.193 (3.708)	23.808 (3.203)	0.506	8.064 (1.317)	7.423 (1.321)	0.739
ET Capacity (Complex I and II substrates)	Oxygen Flux (pmol s^{-1} mL^{-1}): Mean (s.e.)	7.356 (2.705)	7.058 (1.123)	0.924	3.917 (0.834)	3.392 (0.664)	0.628
	FCR: Mean (s.e)	0.242 (0.055)	0.323 (0.057)	0.326	0.475 (0.043)	0.442 (0.041)	0.587
ET Capacity (Complex II substrates)	Oxygen Flux (pmol s^{-1} mL^{-1}): Mean (s.e.)	1.830 (0.581)	1.951 (0.270)	0.859	1.317 (0.279)	1.230 (0.162)	0.786
	FCR: Mean (s.e)	0.065 (0.018)	0.092 (0.017)	0.285	0.175 (0.042)	0.171 (0.015)	0.929

3.5.2 MS-222 had no effect on respiration in the skeletal tail muscle of the stickleback

In stickleback skeletal muscle, there was no difference between MS-222 treated and decapitated fish in any respiration state with any substrate combination (**Figure 3.3**, **Table 3.1**). With cytochrome c addition, however, there was an increase in oxygen flux of greater than 20% in four samples which were subsequently excluded from analysis, as this indicates mitochondrial membrane damage had occurred during tissue preparation. Oxygen flux was lower in the muscle compared to the brain and in general displayed more variation between individuals.

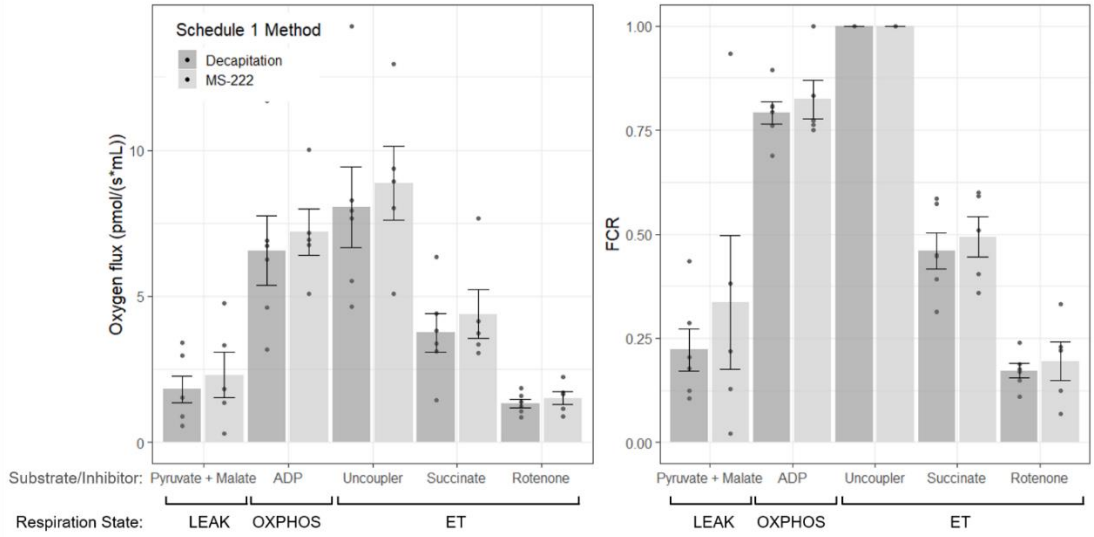

Figure 3.3: Mean oxygen flux and flux control ratios at LEAK, OXPHOS and ET respiration states in the skeletal tail muscle of the stickleback with complex I substrates (pyruvate and malate) and complex II substrates (succinate). Average values per sample shown by points, n = 7 for decapitation (darker grey), n = 6 for MS-222 treated (lighter grey), excluding those where significant membrane damage was detected. Error bars show standard error. No significant differences (p < 0.05) were found between treatment groups in either the oxygen flux or FCRs (unpaired Student's *t*-test).

3.6 Discussion

The effects of MS-222 as an agent for euthanasia on mitochondrial respiration in the three-spined stickleback have not been quantified previously. This study has shown that euthanasia with MS-222 can alter mitochondrial respiration in the brain of the stickleback, generally reducing respiration in comparison to in fish where no MS-222

was used. In particular, treatment with MS-222 caused a significant reduction of LEAK state respiration with complex I substrates pyruvate and malate. In the muscle, there were no differences between MS-222 treated and decapitated fish, which was perhaps due to the lower overall oxygen flux in muscle compared to brain. The smaller LEAK state oxygen flux (although note that this is not significantly different between groups) and FCR in the MS-222 treated group suggests that MS-222 can reduce the amount of proton leak across the membrane and decrease the contribution of this non-phosphorylating state to respiration. In the decapitated group, on average, LEAK respiration contributes to 21.0% of maximum respiration. This is in agreement with previous studies where approx. 20–25% of respiration has been found to drive mitochondrial proton leak in mammalian hepatocytes (Brand, 2000). With MS-222 treatment, this was reduced to 11.6% (**Table 3.1**) in the present study. As no significant differences in OXPHOS and ET states were found between treatment groups, MS-222 may specifically alter LEAK state respiration with pyruvate and malate as substrates. As proton leak is mainly a function of the inner mitochondrial membrane and is dependent on protonmotive force (Jastroch et al., 2010), the anaesthetic may alter mitochondrial membrane properties and reduce proton leak into the mitochondrial matrix (Sahlin et al., 2004). Further examination of mitochondrial respiration and membrane potential with different substrate combinations would be required to provide further information on the effect of MS-222 specifically on LEAK state respiration.

Although no significant differences were observed between the OXPHOS state and ET capacity with the substrate combinations tested, in the brain, FCR values for the MS-222 treatment group tended to be lower than the decapitated group. This suggests that mitochondrial respiration may be reduced when MS-222 is used during euthanasia. To confirm this, HRR measurements with additional individuals and alternative substrate combinations would be required, and further work could determine the precise mechanism of action of MS-222 on the ETS. The focus of the present study, however, was to determine whether MS-222 altered measurements made with HRR in fish to inform future work, and the findings here provide evidence that MS-222 may have an effect on respiration in mitochondria in the brain.

This study also provides a comparison of mitochondrial respiration between tissue types in the three-spined stickleback, which have not often been compared in species of fish. Oxygen flux was consistently higher in the brain compared to the muscle (**Figure 3.2**, **Figure 3.3**), despite larger amounts of skeletal muscle used for analysis.

The maximum ET capacity was higher in the brain, indicating higher maximum respiration rates. Each tissue has differing metabolic demands due to their function or conditions; the heart has previously been found to have the highest oxidative phosphorylation capacity (la Monaca & Fodale, 2012). In agreement with previous work using cytochrome c oxidase activity in rats as a measure of the OXPHOS system (la Monaca & Fodale, 2012), the brain showed increased specific oxidative phosphorylation activity in comparison to the muscle. Although the ease of homogenisation of the brain tissue likely in part explains this finding in the present study, the increase in energy requirement in the brain may also contribute to this difference.

As mitochondrial respiration has scarcely been measured in fish homogenised tissue compared to other model organisms, this study provides an overview of coupling efficiency in the three-spined stickleback. In the brain, FCRs for OXPHOS state (the coupled respiratory capacity with saturating ADP) with complex I substrates were 0.499 and 0.563 (**Table 3.1**) for the MS-222 and decapitated samples, respectively, agreeing with previous work on the cerebellum of two species of shark: *Hemiscyllium ocellatum* and *Chiloscyllium punctatum* (Devaux et al., 2019). A higher value indicates increased capacity of the phosphorylation system. In the muscle, these values were 0.776 and 0.750, respectively, indicating better coupled oxidative phosphorylation in the muscle compared to the brain, which was perhaps due to the high ATP demand in muscle for swimming. It should also be noted that in four skeletal tail muscle samples, there was an increase in oxygen consumption of greater than 20% with the addition of cytochrome c, indicating some membrane damage had occurred. This is likely due to tissue preparation, as the homogenisation of muscle required more time than homogenisation of the brain.

The deleterious effects of MS-222 as an anaesthetic on fish physiology have previously been studied, including altering blood haemostasis in zebrafish (*Danio rerio)* (Deebani et al., 2019), damaging morphological structure, altering osmoregulation and inducing apoptosis in the gills of the Chinese sea bass (*Lateolabrax maculatus)* (Wang et al., 2020), and altering antioxidant status in Gilthead sea bream (*Sparus aurata)* (Teles et al., 2019). Although any effect of MS-222 on mitochondrial respiration in fish has not previously been tested, these findings hint that MS-222 may alter mitochondrial physiology, including mitochondrial respiration, which was found here. This study therefore adds to the growing body of work highlighting the impact of MS-222 and other anaesthetics on fish physiology.

Overall, we have identified the effects of MS-222 on mitochondrial respiration in the three-spined stickleback, concluding that MS-222 used during euthanasia may alter HRR measurements made on the brain. Importantly, this highlights the need to consider the method of euthanasia used in combination with analysis of the brain with the O2k; this will ensure that any observed differences are due to differing treatments and not a consequence of any anaesthetic used, and they will allow a more inciteful comparison of studies of mitochondrial respirometry in fish. A consistent method of euthanasia and, where possible, avoiding anaesthetics such as MS-222 would prevent any disruption of findings. Despite no differences being observed in the muscle, effects of MS-222 may be smaller and harder to detect due to the overall lower oxygen flux, so caution should still be taken.

3.7 Acknowledgements

Thank you to all members of Lisa Chakrabarti's lab for their guidance in high-resolution respirometry and to the MacColl lab for their valuable advice and discussions.

3.8 References

Brand, M. D. 2000. Uncoupling to survive? The role of mitochondrial inefficiency in ageing. *Experimental Gerontology*, **35**, 811–820. https://doi.org/10.1016/S0531-5565(00)00135-2

Chung, D. J., Sparagna, G. C., Chicco, A. J., & Schulte, P. M. 2018. Patterns of mitochondrial membrane remodeling parallel functional adaptations to thermal stress. *J. Exp. Biol.* **221**. jeb174458. https://doi.org/10.1242/JEB.174458

Close, B., Banister, K., Baumans, V., Bernoth, E.-M., Bromage, N., Bunyan, J., Wolff Erhardt, P., Paul Flecknell, P., Gregory, N., Hansjoachim Hackbarth, P., David Morton, P., Clifford Warwick, M., Close, B., Croft, B., Lane, B., & Knoll, B. 1997. Recommendations for euthanasia of experimental animals: Part 2. *Lab Anim.*, **31**, 1–32. https://doi.org/10.1258/002367797780600297

Collymore, C., Tolwani, A., Lieggi, C., & Rasmussen, S. 2014. Efficacy and Safety of 5 Anesthetics in Adult Zebrafish (*Danio rerio*). *J. Am. Assoc. Lab. Anim. Sci.* **53**, 198-203. PMID: 24602548

Dean, L.L., Magalhaes, I.S., Foote, A., D'Agostino, D., McGowan, S., & MacColl, A.D.C. 2019. Admixture between Ancient Lineages, Selection, and the Formation of

Sympatric Stickleback Species-Pairs. *Mol. Biol. Evol.* **36**, 2481–2497. https://doi.org/10.1093/MOLBEV/MSZ161

Deebani, A., Iyer, N., Raman, R., & Jagadeeswaran, P. 2019. Effect of MS222 on Hemostasis in Zebrafish. *J. Am. Assoc. Lab. Anim. Sci.* **58**, 390-396. https://doi.org/10.30802/AALAS-JAALAS-18-000069

Devaux, J. B. L., Hickey, A. J. R., & Renshaw, G. M. C. 2019. Mitochondrial plasticity in the cerebellum of two anoxia-tolerant sharks: Contrasting responses to anoxia/re-oxygenation. *J. Exp. Biol.* **222**. jeb191353. https://doi.org/10.1242/jeb.191353

Doerrier, C., Garcia-Souza, L. F., Krumschnabel, G., Wohlfarter, Y., Mészáros, A. T., & Gnaiger, E. 2018. High-resolution fluorespirometry and oxphos protocols for human cells, permeabilized fibers from small biopsies of muscle, and isolated mitochondria. *Methods in Molecular Biology*. **1782**, 31–70. https://doi.org/10.1007/978-1-4939-7831-1_3

Doerrier, C., & Gnaiger, E. SUIT-004 - Bioblast. Retrieved August 22, 2022, from https://www.bioblast.at/index.php/SUIT-004

Gnaiger, E. 2020. Mitochondrial Pathways and Respiratory Control. An Introduction to OXPHOS Analysis. 5th ed. *Bioenerg. Commun.* **2**. https://doi.org/10.26124/bec:2020-0002

Hill, J. V., Davison, W., & Forster, M. E. 2002. The effects of fish anaesthetics (MS222, metomidate and AQUI-S) on heart ventricle, the cardiac vagus and branchial vessels from Chinook salmon (*Oncorhynchus tshawytscha*). *Fish Physiol. Biochem.* **27**, 19–28. https://doi.org/10.1023/B:FISH.0000021742.30567.2D

Jastroch, M., Divakaruni, A. S., Mookerjee, S., Treberg, J. R., & Brand, M. D. 2010. Mitochondrial proton and electron leaks. *Essays Biochem.* **47**, 53-67. https://doi.org/10.1042/BSE0470053

Leo, E., Dahlke, F. T., Storch, D., Pörtner, H. O., & Mark, F. C. 2018. Impact of Ocean Acidification and Warming on the bioenergetics of developing eggs of Atlantic herring *Clupea harengus*. *Conserv. Physiol.* **6**, coy050. https://doi.org/10.1093/CONPHYS/COY050

Magalhaes, I. S., D'Agostino, D., Hohenlohe, P. A., & MacColl, A. D. C. 2016. The ecology of an adaptive radiation of three-spined stickleback from North Uist, Scotland. *Mol. Ecol.* **25**, 4319–4336. https://doi.org/10.1111/MEC.13746

Matthews, M., & Varga, Z. M. 2012. Anesthesia and Euthanasia in Zebrafish. *ILAR Journal*, **53**, 192–204. https://doi.org/10.1093/ILAR.53.2.192

la Monaca, E., & Fodale, V. 2012. Effects of Anesthetics on Mitochondrial Signaling and Function. *Curr. Drug Saf.* **7**, 126–139. https://doi.org/10.2174/157488612802715681

Sahlin, K., Tonkonogi, M., & Fernström, M. 2004. The leaky mitochondrion. *Physiology News*. **56**, 27–28. https://doi.org/10.36866/PN.56.27

Salin, K., Villasevil, E. M., Anderson, G. J., Lamarre, S. G., Melanson, C. A., McCarthy, I., Selman, C., & Metcalfe, N. B. 2019. Differences in mitochondrial efficiency explain individual variation in growth performance. *Proc. R. Soc. B.* **286**, 20191466. https://doi.org/10.1098/RSPB.2019.1466

Teles, M., Oliveira, M., Jerez-Cepa, I., Franco-Martínez, L., Tvarijonaviciute, A., Tort, L., & Mancera, J. M. 2019. Transport and recovery of gilthead sea bream (*Sparus aurata* L.) sedated with clove oil and MS222: Effects on oxidative stress status. *Front. Physiol.* **10**. https://doi.org/ 10.3389/fphys.2019.00523

Thoral, E., Roussel, D., Chinopoulos, C., Teulier, L., Salin, K., & Thoral, E. 2021. Low oxygen levels can help to prevent the detrimental effect of acute warming on mitochondrial efficiency in fish. *Biol. Lett.* **17**, 20200759. https://doi.org/10.1098/RSBL.2020.0759

Wang, W., Dong, H., Sun, Y., Sun, C., Duan, Y., Gu, Q., Li, Y., Xie, M., & Zhang, J. 2020. Immune and physiological responses of juvenile Chinese sea bass (*Lateolabrax maculatus*) to eugenol and tricaine methanesulfonate (MS-222) in gills. *Aquac. Rep*. **18**, 100554. https://doi.org/10.1016/J.AQREP.2020.100554

Zanin, M., Varela Junior, A. S., Acosta, I. B., Gheller, S. M. M., Zimermann, E., Froes, C. N., Gehrcke, M. I., & Corcini, C. D. 2021. Tricaine methanesulfonate (MS-222) on the spermatic quality of zebrafish, *Danio rerio*. *Aquaculture*. **533**, 736090. https://doi.org/10.1016/J.AQUACULTURE.2020.736090

3.9 Supplementary material

Table S3.1: Results of linear mixed model (estimated using REML) on 140 observations with oxygen flux as the dependent variable, euthanasia method (decapitation, MS-222) and respiration state (PM, D, U, S, Rot) nested within tissue type (brain, muscle) as fixed effects, and cross/tank as a random effect. P values were calculated using a Wald t-distribution approximation. Significant values (P < 0.05) are depicted by a *. These results show the significant effect of tissue type and respiration state on oxygen flux, but no overall effect of euthanasia method, and therefore do not provide information on the effect of MS-222 on different parameters of mitochondrial respiration.

Fixed Effects	**Estimate**	**Standard Error**	**t value**	**p value**
Intercept	4.0896	1.3857	2.951	0.004*
MS-222	0.5368	0.7212	0.744	0.458
Muscle	-1.8202	1.6128	-1.129	0.261
Brain:D	8.8225	1.6128	5.47	< 0.001*
Muscle:D	4.3742	1.6128	2.712	0.008
Brain:U	23.1364	1.6128	14.346	< 0.001*
Muscle:U	5.8007	1.6128	3.597	< 0.001*
Brain:S	3.4593	1.6128	2.145	0.034*
Muscle:S	1.7938	1.6128	1.112	0.268
Brain:Rot	-1.8911	1.6128	-1.173	0.243
Muscle:Rot	-0.7593	1.6128	-0.471	0.639

Random Effects	**Name**	**Variance**	**Standard Deviation**
Cross	Intercept	1.864	1.365
Residual	Residual	18.207	4.267

Chapter 4: Repeated Association of Mitochondrial Lineage with Habitat in Atlantic Three-spined Stickleback.

4.1 Abstract

Genetic sequences from the mitochondrial genome have long been used as neutral markers of population structure, often without consideration of their adaptive significance. In the Atlantic, two mitochondrial lineages of the three-spined stickleback diverged in separate refugia during the last glaciation and have since recolonised the northern Atlantic. Here we reveal that not only is phylogeographic history important, but mitochondrial lineages in Atlantic stickleback are associated with adaptive potential: fish residing permanently in fresh water were predominantly one lineage, whereas completely plated fish living at least some of their lives in salt water, and therefore likely migratory fish, were a mix of the two lineages, with mitochondrial lineage also associated with maximum sea surface temperature in saltwater populations. We found sex-specific differences in standard length between mitochondrial lineages in mixed, freely interbreeding populations, linking mtDNA variation to life-history traits independent to the nuclear genome. Given these associations with habitat and phenotype, our results suggest that mitochondrial sequences are unlikely to make good neutral markers and highlights the Atlantic three-spined stickleback as an exciting natural model for further investigations into both the physiological and evolutionary consequences of mtDNA variation.

4.2 Introduction

Genetic sequences from the mitochondrial genome have long been used as neutral markers of population structure (Avise et al., 1987). Although accumulating evidence makes a presumption of neutrality untenable (Ballard and Kreitman, 1995; Ballard and Whitlock, 2004), many studies of phylogeography continue to use mitochondrial sequences without considering their putative adaptive significance (Kang et al., 2022; Yonezawa et al., 2024) and this may mislead inferences about phylogeographic history, for example if particular mitochondrial sequences are associated with particular habitats or adaptive traits. This does not necessarily mean that the mitochondrial sequences are themselves adaptive, although that might be the case,

but rather that they may be in linkage disequilibrium with adaptive alleles elsewhere in the genome. Such an association with adaptation could easily arise where different clades evolve in allopatry for some period before coming back into secondary contact.

Glaciations during the Pleistocene influenced the geographic distribution of many species. Large areas were covered in ice sheets which caused extinctions, dispersal, or species survived in southern refugia until they could expand once again into more northern areas following glacial retreat (Hewitt, 2000). Post-glacially colonised regions generally have lower genetic diversity (Hewitt, 2000), but with range expansions comes selection and adaptation to new environments (Hewitt, 1996). Mitochondrial markers were extensively used to reveal the histories of recolonisation of temperate latitudes by terrestrial and freshwater organisms following the last glacial period (Hewitt, 2000, 2004) and mitochondrial DNA (mtDNA) was favoured as a neutral marker for such genetic studies (Hewitt, 2000; Santucci et al., 1998). This allowed the inference of where refugia have been and the patterns of recolonisation (Hewitt, 2000). Although post-glacial recolonisation of terrestrial and freshwater species has been well studied (Hewitt, 2000, 2004), patterns in the oceans are less well recognised (but see Gagnaire et al., 2015; Gérard et al., 2008).

Repeated colonisation of freshwater environments post-glaciation has influenced the evolution of multiple fish species, including the three-spined stickleback ('stickleback', *Gasterosteus aculeatus*). The stickleback is a small teleost fish widely distributed throughout coastal marine, brackish and freshwater habitats in the Northern Hemisphere. At the end of the last ice age, ancestrally marine stickleback repeatedly colonised freshwater habitats leading to extensive phenotypic diversification (Bell and Foster, 1995; Jones et al., 2012), making the stickleback an important model in evolutionary ecology. Freshwater and marine stickleback display large morphological differences (Peichel and Marques, 2017), including in armour plating controlled by the Eda gene (Colosimo et al., 2005); resident freshwater or saltwater stickleback are low-plated while migratory marine stickleback are completely plated with a row of 32 to 36 armour plates. The divergence of key adaptive traits have been well-studied in the stickleback (Barrett et al., 2008; Chan et al., 2010; Cresko et al., 2004).

It is well established that there are two main mitochondrial clades present in stickleback in the northern Atlantic (Mäkinen and Merilä, 2008), with colonisation of the Atlantic a result of invasion from the Pacific via the Arctic Ocean (Fang et al., 2018; Mäkinen and Merilä, 2008; Orti et al., 1994). The European ('*Eu*') lineage is

widespread in Europe, but the trans-Atlantic (‘*At*’) lineage is found predominantly on the East Coast of North America as well as in a few populations in western and northern Europe (Mäkinen and Merilä, 2008). Estimates of their divergence time range from 128,000 to 58,000 years before present (Dean et al., 2019a; Mäkinen and Merilä, 2008; Ravinet et al., 2013). Here, we hypothesise that the two clades diverged in separate refugia on opposite sides of the Atlantic, during the Pleistocene. The *Eu* lineage is well documented to have survived in southern European refugia (Defaveri et al., 2012; Mäkinen and Merilä, 2008a; Sanz et al., 2015) and as the *At* mtDNA is found predominantly in eastern North America (Mäkinen and Merilä, 2008), we predict that the *At* refugium was on the East Coast of North America in regions free from ice during the last glaciation. Since the melting of the ice sheets both lineages have been able to recolonise previously glaciated regions, spreading North and across the Atlantic resulting in multiple places of secondary contact including Greenland (Liu et al., 2016), Ireland (Ravinet et al., 2013) and Scotland (Dean et al., 2019a).

One place of known secondary contact is North Uist in the Western Isles of Scotland, which was colonised by marine stickleback after the last glaciation approximately 8,000 years ago. Sequencing part of the cytochrome b (CYTB) and control region of the mtDNA revealed differences in the proportions of each lineage between the ecotypes present on North Uist; the freshwater and lagoon resident populations were found to be predominantly the *Eu* lineage (greater than 94%), whereas anadromous populations which live in the sea but migrate to brackish or fresh water during the breeding season were an equal mix of the two lineages (Dean et al., 2019a). This hints that the *Eu* lineage may be better adapted to permanently colonising fresh and brackish lochs, but this pattern could also be explained by multiple colonisation events by the two diverged lineages. No widescale studies of stickleback across the Atlantic have tested whether mitochondrial clades associate with adaptive phenotypes and therefore whether mitochondrial sequences are good neutral markers, as they are so often used. Whether the pattern of freshwater stickleback being predominantly *Eu* persists with additional North Uist sampling locations and across the Atlantic would aid explanation of whether the history or differing adaptive potential of the two mitochondrial lineages has influenced the current distribution of the stickleback.

Here we will present further understanding of the phylogenetic structure of stickleback in the Atlantic using mtDNA. We will present evidence in support of the hypothesis that stickleback mitochondrial clades originated in separate refugia on opposite sides of the Atlantic as we reveal a cline in the lineages’ distribution with distance from the

predicted *At* refugium. We will describe in detail the distribution, habitat and phenotype associations of the two lineages to show that they have different adaptive propensities that make an assumption of neutrality unlikely.

4.3 Methods

4.3.1 Sample collection

Stickleback were sampled from 15 freshwater and 4 brackish lochs on North Uist in the Western Isles of Scotland during May 2022 and a further 3 freshwater locations in May 2023 (see **Figure 4.1** and **Table S4.1** for North Uist sampling locations). Lochs were selected in order to provide an overview of the geographic distribution of mitochondrial lineages across North Uist. Traps were set at regular intervals along the shoreline and left overnight. Approximately 10 stickleback were collected from each population at random (although we ensured that no young of the year were included). Stickleback were euthanised with an overdose of MS-222 (400mg/L) followed by pithing. Fish were weighed, standard length measurements taken and then the left side of the specimen was photographed. Caudal and pectoral fins were clipped and stored in ethanol for later DNA extraction. Each individual was assigned a unique identification number. We also obtained additional samples from Canada (Nova Scotia; Newfoundland; Quebec), Maine (Lubec), Iceland and Portugal to expand the survey area (**Table S4.1**). Qiagen 96-well DNeasy blood and tissue extraction kit was used to extract DNA from Uist, Iceland and Portugal stickleback fin clips. NEB Monarch genomic DNA purification kit was used for all other samples.

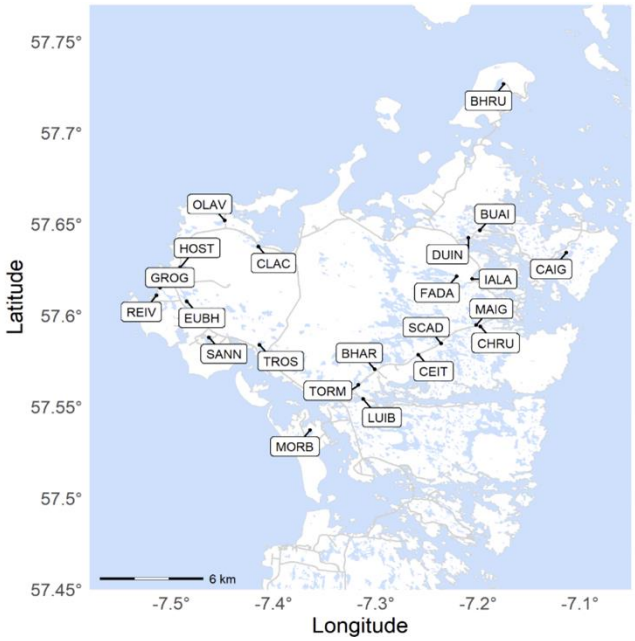

Figure 4.1: Sampling locations on North Uist, Western Isles of Scotland. DUIN, LUIB, CLAC and MORB are brackish lochs; all other locations are freshwater. Migratory stickleback were also caught in lochs GROG, OLAV, CLAC, BHRU, DUIN, and LUIB, and assigned the population names GROM, OLAM, CLAM, BHRM, DUIM and LUIM, respectively. See **Table S4.1** for further information.

4.3.2 Mitochondrial lineages

4.3.2.1 Assay design

To investigate the distribution of the two ancient mitochondrial lineages in the Atlantic, we designed a polymerase chain reaction (PCR) and restriction fragment length polymorphism (RFLP)-based assay to distinguish *Eu* and *At* stickleback. Whole genomes were sequenced (Illumina) and NOVOPlasty (Dierckxsens et al., 2017) used to assemble mitochondrial genomes from North Uist stickleback. Sequences were aligned to the reference mitochondrial genome, accession number MH205729 (Jiang et al., 2018) using Bioedit (Hall, 1999) and trimmed to 15,662bp. jModelTest (Posada, 2008) was used to find the best fitting nucleotide substitution model and a maximum likelihood phylogenetic tree constructed with RAxML (GTR + Gamma IX) (Stamatakis, 2014). See **Figure S4.1** for phylogeny. This was used to assign mitochondrial sequences to either the *Eu* or *At* lineage. We then identified sites that consistently differed between the two lineages. SNP2CAPS (Thiel et al., 2004) was used to identify restriction sites that would result in *Eu* and *At* mtDNA being cut differently by specific restriction enzymes (**Figure S4.2**). Once potential sites were

identified, these were checked manually and primers targeting an approx. 600bp region around the SNP were designed using Primer3 (Untergasser et al., 2012). See **Table 4.1** for primer information. To be confident that the assay was reliable, two sites were chosen: one in ND4 and one in ND5, where a specific restriction enzyme would cut one lineage only (**Figure S4.2**). If an individual is *Eu*, the amplified region of ND4 will be cut by Hind*III* but ND5 will not be cut by Pst*I.* If *At*, the reverse is true: the amplified region of ND5 will be cut by Pst*I* but ND4 will not be cut by Hind*III.* This ensures that the assay is reliable by providing a positive result for both lineages.

Table 4.1: Primers and restriction enzymes used in the PCR-RFLP based assay to determine mitochondrial lineage of the three-spined stickleback.

Primer	Forward Sequence	Reverse Sequence	Enzyme	Cuts	*Eu* size (bases)	*At* size (bases)
ND4	TCTCGTTGCC CTCCTTCTAC	TCCAAGGTTG CAAGGCTTG	Hind*III*	*Eu*	183; 442	625
ND5	CGGACTAAAC CAACCACACC	GTGATGTGGG GTTAAGCGAG	Pst*I*	*At*	616	219; 397

4.3.2.2 PCR conditions

The regions of interest were amplified by PCR with specific primers (**Table 4.1**) in a 20µl reaction volume. Each reaction included 1µl DNA, 10µl of PCR master mix (Quanta Bio Accustart), 1µl forward primer, 1µl reverse primer (Sigma) and 7µl nucleotide free water. PCR was performed in a thermocycler (G-Storm GS1). PCR reaction conditions were as follows: initial denaturation at 94°C for 3 minutes followed by 36 cycles: denaturation at 94°C, 30 seconds; annealing at 60°C, 30 seconds; extension at 72°C, 1 minute. Then a final extension at 72°C for 5 minutes. To confirm successful amplification of the target region, 4µl of each PCR product were separated on a 1.5% agarose gel at 100 Volts for 30-40 minutes alongside a 100bp ladder (NEB) and then visualised using UV-illumination (iBright CL750 Imaging System, ThermoFisher Scientific).

4.3.2.3 Restriction enzyme digest

0.8µl of appropriate restriction enzyme (see **Table 4.1**) and 1.5µl of 10X restriction enzyme buffer were added to the remaining PCR products and incubated at 37°C for 1 hour in a thermocycler. 4µl of the product was separated on a 2% agarose gel at 100V for 40-50 minutes and then visualised as before. From the gels, the number and

size of the bands (**Table 4.1**, **Figure S4.2**) were used to determine the mitochondrial lineage of each individual.

4.3.2.4 Confirmation of assigned lineages

To confirm the assay was reliable, ND4 and ND5 genes were amplified from a subset of individuals using the same primers (**Table 4.1**) and PCR conditions. ExoSAP-IT PCR product clean-up reagent (Thermo Fisher Scientific) was used before PCR products were sequenced (Source Genomics). ND4 and ND5 sequences were used to confirm that SNPs to distinguish lineages matched results from restriction enzyme digest. To confirm that the PCR-RFLP-based assay would be reliable across all Atlantic samples, mitochondrial sequences of stickleback from Nova Scotia, Iceland and Portugal were assembled using NOVOPlasty and aligned to North Uist sequences, as above. A new phylogenetic tree was constructed from mitogenomes to confirm the mitochondrial lineage of these samples, which were 100% consistent with the ND4 and ND5 assay.

4.3.3 Mitochondrial lineages from the literature

To combine the results of the present study with existing findings, an extensive literature search was conducted (**Table 4.2**). Relevant papers were extracted from a Web of Science search for mitochondria* and stickleback* which resulted in 80 publications. These were manually searched for mentions of the *Eu* and *At* lineage, and sampling location, mitochondrial lineage, and any additional phenotypic or environmental data was collected for each individual sampled. A NCBI Genbank search for the three-spined stickleback CYTB gene revealed 30 population set results. Datasets and corresponding publications were manually filtered for those from the Atlantic Ocean. CYTB sequences from these were aligned using Bioedit (Hall, 1999) and a maximum likelihood phylogenetic tree constructed using MEGA11 (TN93 + G) (Tamura et al., 2021). From this, mitochondrial lineage could be assigned. All data were combined for analysis.

Table 4.2: Literature assessing mitochondrial lineages of the three-spined stickleback in the Atlantic compiled in the present study.

Authors	Journal	Year	Region	Continent	DOI	CYTB Accession Number (GenBank)
Artamonova et al.	Water	2022	White Sea	Europe	10.3390/w14162484	OK482598 – OK482649
Laakkonen et al.	Journal of Evolutionary Biology	2020	Newfoundland	North America	10.1111/jeb.13674	MT736717 – MT736720
Dean et al.	Molecular Biology & Evolution	2019	North Uist	Europe	10.1093/molbev/msz161	MG602878 – MG602914
Vila et al.	PLoS ONE	2017	Ibero-balaeric	Europe	10.1371/journal.pone.0170685	KX910738 – KX910761
Rahn et al.	Infection, Genetics & Evolution	2016	North Uist	Europe	10.1016/j.meegid.2016.07.011	KT971072 – KT971072
Liu et al.	Molecular Ecology	2016	Greenland	Europe	10.1111/mec.13827	ENA ERP016886
Sanz et al.	Freshwater Biology	2015	Iberian Peninsula	Europe	10.1111/fwb.12611	KJ201010 – KJ201015
Wang et al.	Journal of Biogeography	2015	Baltic Sea	Europe	10.1111/jbi.12591	KJ628012
Ravinet et al.	Ecology & Evolution	2013	Ireland	Europe	10.1002/ece3.853	KC478175 – KC478281
De Faveri et al.	Marine Biology	2012	Baltic Sea	Europe	10.1007/s00227-012-1951-4	JQ983161 – JQ983255
Lucek et al.	Molecular Ecology	2010	Switzerland	Europe	10.1111/j.1365-294X_2010.04781.x	HM590665 – HM590669
Mäkinen & Merilä	Molecular Phylogenetics & Evolution	2008	Europe	Europe	10.1016/j.ympev.2007.06.011	EF525391 – EF525476
Wilson et al.	Journal of Heredity	2001	Hudson River	North America	10.1093/jhered/92.2.159	AF356079

4.3.4 Phylogeographic analyses

We first assessed the distribution of stickleback mitochondrial lineages across populations and ecotypes on North Uist, before combining this with results from across the North Atlantic to determine whether mitochondrial lineage was associated with geography, habitat and phenotype. 'Distance from North America' was calculated following predicted Atlantic Ocean currents as the great circle distance from a specified point (40, -70) close to the most western point in the dataset (41.52099, -70.9814) using the function 'distHaversine' in the geosphere package in RStudio (**Figure S4.3**). We then used a generalised linear model with binomial error distribution and logit link to model the number of *At* fish per population (successes) as a function of the following variables: i) Distance from North America. ii) Salinity: whether the population lived in salt water during its lifetime (1) or resided permanently in fresh water (0). iii) Plate morphology: the proportion of completely plated fish per population (see **Figure S4.4** for complete and low plated stickleback examples). This was collated from the searched literature, obtained from collaborators, or taken from North Uist samples collected in the present study. Using a binomial generalised mixed model accounted for the total number of samples per population.

To test whether temperature could explain the distribution of *Eu* and *At* stickleback, the nearest minimum, maximum and variation in sea surface temperature (SST) to each saltwater population in the dataset were included in a separate generalised linear model with binomial error distribution and logit link. Gridded daily SST values were available from the National Oceanic and Atmospheric Administration (NOAA) database (ERDDAP version 2.25.1, dataset ID: noaa_aoml_381e_5d49_f14b, available at https://upwell.pfeg.noaa.gov/erddap/griddap). For each available year (2021 to 2023), the six lowest winter temperatures and the six maximum summer temperatures per grid location were extracted and then averaged to get an average minimum and maximum temperature for each location. The variation in SST for each point was then calculated by subtracting the minimum SST from the maximum SST. The nearest SST datapoint to each stickleback population was added to the dataset. Each temperature variable was included separately in the model, and model comparisons conducted to find the variable that explained the most variation. The best fitting model was selected according to Akaike Information Criterion (AIC).

To check that results were not biased by the incorporation of large numbers of populations from our main study site, North Uist, all analyses were then repeated without North Uist populations. These analyses are presented in the supplementary

material as findings generally did not differ between the full dataset and that without North Uist. Any differences are highlighted below.

4.3.5 Morphological information

4.3.5.1 Standard length

Standard length (SL) measurements were taken using a calliper immediately after euthanasia of stickleback samples. We also sampled further migratory North Uist stickleback in April and May 2024 from LUIM and CLAM (**Figure 4.1**), as well as sampling three further populations: FAIM (57.636023, -7.2164260), OBSM (57.60167, -7.17278), and GROM (57.615827, -7.513195). Data from both years were combined for analysis. As female stickleback are larger than males (Aguirre et al., 2008, Kitano et al., 2007), we analysed SL separately for males and females. SL was compared between mitochondrial lineages using a linear mixed effects model with mitochondrial lineage as a fixed effect and population as a random effect.

4.3.5.2 Armour

Fish caught on North Uist in May 2022 were bleached and stained with alizarin red in order to visualise bony 'armour'. A standard protocol was followed (Peichel et al., 2001). Briefly, fish were rehydrated, fixed in 10% buffered neutral formalin and washed before maceration, bleaching and bone staining in alizarin red. The left sides of the fish were photographed using a tripod mounted digital camera with flash. ImageJ (Schneider et al., 2012) was used to scale images and counts of lateral plate number and measurements of armour were made, including first and second dorsal length spine, longest plate length, pelvis height and length, and pelvic spine length (**Figure S4.4**). As all continuous armour measurements, excluding lateral plate number, were significantly correlated with standard length, these were size standardised by taking the residuals of a regression against standard length. A PCA was carried out to visualise the axis of greatest variation.

4.3.5.3 Otolith measurements

To ensure that there was no bias in age between *Eu* and *At* stickleback which could explain any morphological differences, we dissected the otoliths from a subset of fish using previously described methods (Jones and Hynes, 1950; Singkam and MacColl, 2018), as reading the annual otolith rings is a well-established method to determine age in fish (Jones and Hynes, 1950). The sagitta (largest otolith) was extracted under a dissection microscope (Leica KL200 LED) and cleaned using fine forceps before being mounted onto a microscope slide using Sigma Aldrich DPX. Slides were viewed and photographed under a microscope (Nikon Phase Contrast-2) at x100

magnification using a dark background. The number and type of seasonal rings were recorded and measurements of the diameter at the widest point taken using ImageJ (Schneider et al., 2012). Whether otolith diameter was influenced by SL, sex, or mitochondrial lineage was determined by fitting a linear model. The proportion of each otolith score was calculated for each lineage and Fisher's Exact Test used to determine whether there was an association between lineage and the scores.

4.3.6 Genetic differences between migratory stickleback

Populations selected for morphological analysis were generally an almost equal mix of *Eu* and *At* fish, reducing any nuclear genetic differences between lineages. To confirm this, we looked for any nuclear genetic divergence between *Eu* and *At* stickleback by calculating F_{ST}, assigning the two mitochondrial lineages as independent populations. We constructed a SNP dataset from short read sequences (Illumina) including migratory individuals from four populations (CLAM, BHRM, OLAM, LUIM), using BCFtools v.1.18 to call variant sites and VCFtools v.0.1.16 to calculate F_{ST} statistics with a window size of 20kb. We also assessed the mitochondrial sequence differences using the mitogenomes of migratory stickleback from North Uist that were assembled in section **4.3.2**, to determine whether there were any fixed synonymous or non-synonymous substitutions.

4.4 Results

4.4.1 North Uist

We identified 35 fixed nucleotide differences between *Eu* and *At* stickleback mitogenomes from North Uist (analysis included 180 individuals from either resident or migratory populations) and used two of these to design a diagnostic assay to distinguish the two mitochondrial lineages in the Atlantic. The mitochondrial lineages of 358 North Uist individuals were successfully determined using the PCR and RFLP-based assay. The six migratory populations (**Figure 4.2**) were an almost equal mix of the two mitochondrial lineages, except for one population on the east of the island that was predominantly *At*. Both lagoon and saltwater resident populations were predominantly *Eu* (**Figure 4.2**). Where we identified *At* lineage stickleback in fresh water, these tended to be on the west coast of North Uist or to the north. CAIG, the most easternly population, was also predominantly *At* (**Figure 4.2**), but not all individuals were low plated like other North Uist freshwater populations and this loch has a recent and direct connection to the sea unlike most freshwater lochs sampled, making it slightly saline.

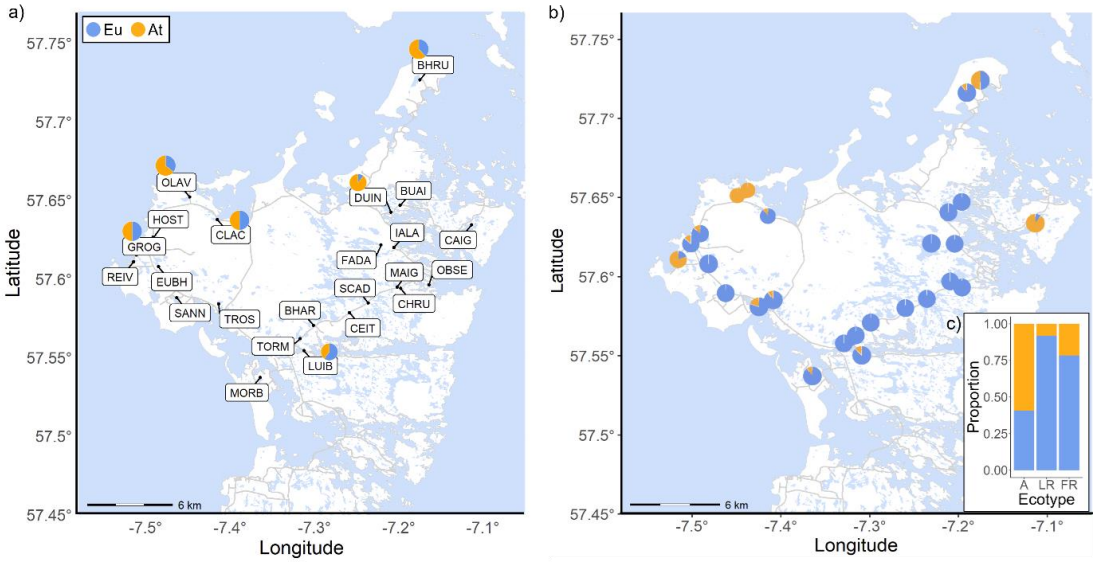

Figure 4.2: Mitochondrial lineages on North Uist. Pie charts show the proportion of *Eu* and *At* stickleback for (a) anadromous (migratory stickleback that spend most of their lives in the sea but breed in saltwater or freshwater lochs) or (b) resident populations on North Uist. Results of sampling in the present study only. Blue = *Eu*, orange = *At*. In b) resident populations from BHRU, OLAV, TORM and TROS were sampled in the loch and in a stream connected to the loch so include both results; loch result furthest right. See **Table S4.1** for population details. c) Total proportion of *Eu* and *At* stickleback per ecotype. A = Anadromous; LR = Lagoon Resident; FR = Freshwater Resident. n = 88, 38, and 232 for A, LR and FR respectively.

4.4.2 Evidence for two refugia

The mitochondrial lineage of 733 individuals from 67 populations including those from North Uist, Iceland, Portugal and North America were successfully determined using the diagnostic assay. These samples were combined with information collated from the literature. The geographical distribution of lineages is shown in **Figure 4.3**. Populations in Europe were predominantly the *Eu* lineage while in North America populations were a more equal mix of *Eu* and *At* (**Figure 4.3**). There were many locations across the Atlantic where both lineages co-occurred including Nova Scotia, Newfoundland, Greenland, Iceland, Ireland and Scotland, suggesting that both have spread across the Atlantic Ocean. The proportion of *At* fish in populations decreased with increasing distance from North America, particularly in samples spending at least part of their lives in salt water (**Figure 4.4**, **Table 4.3**).

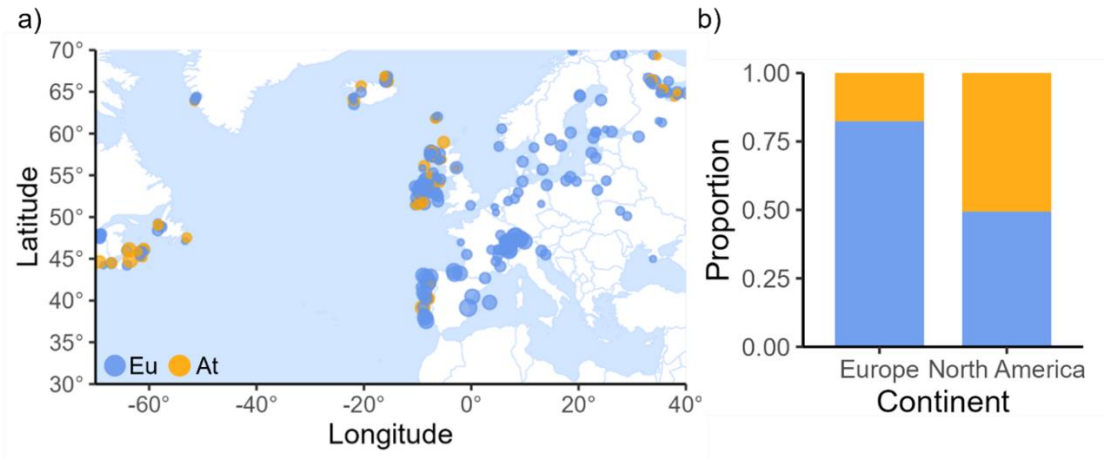

Figure 4.3: **Stickleback mitochondrial lineages in the Atlantic.** a) Map of the northern Atlantic with points showing the distribution of *Eu* (blue) and *At* (orange) stickleback. The size of points shows the number of samples per population. b) The proportion of *Eu* and *At* stickleback in Europe and North America (n = 1887 and 160 individuals respectively); see **Figure S4.1** for classification of regions into Europe or North America.

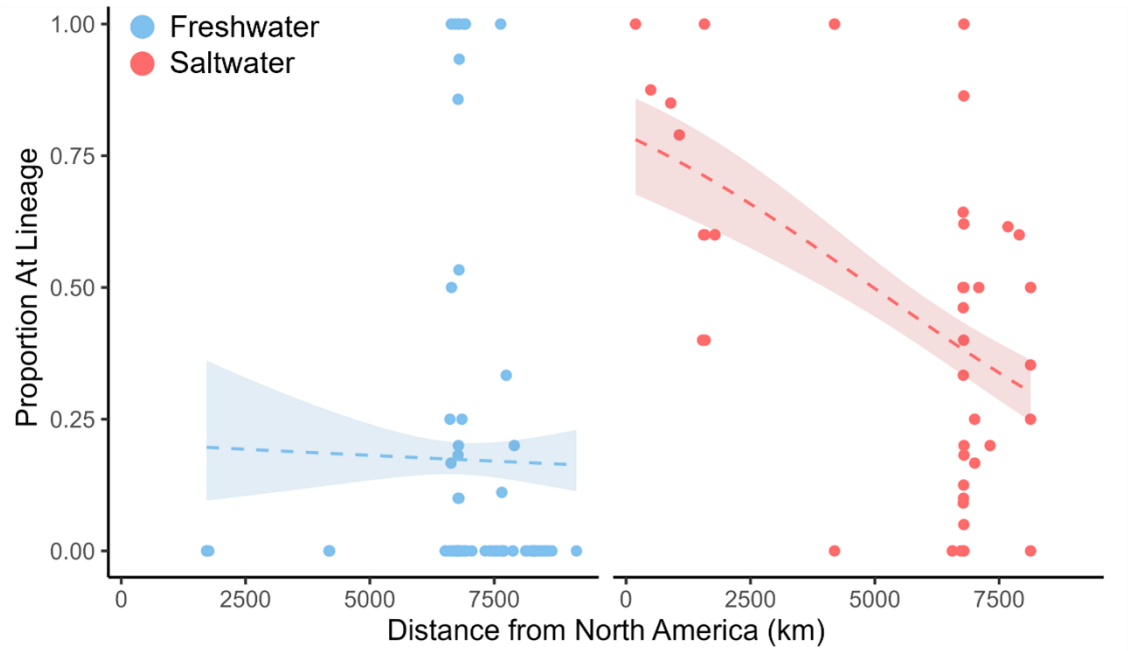

Figure 4.4: Change in the proportion of *At* stickleback with distance from North America in freshwater and saltwater populations. Each point is a freshwater (light blue) or saltwater (red) population. Dashed line shows binomial generalised linear model with the proportion of *At* stickleback per population as a function of distance from North America. Shading shows standard error. Including samples where plate

morphology is also known. n = 125 and 47 freshwater and saltwater populations respectively.

Table 4.3: Factors affecting the proportion of stickleback with the *At* mitochondrial haplotype in populations across the North Atlantic. Results are from a binomial generalised linear model with logit link modelling the number of *At* fish per population (successes) with the distance from North America, plate morphology, salinity, and the interaction of plate morphology and salinity as predictors. 172 populations were included in the model. Values in bold are significant at the 5% significance level.

Predictor	Wald F	d.f	P-value
Distance	8.000	1,168	**0.005**
Plating	3.554	1,168	0.061
Salinity	4.425	1,168	**0.037**
Plating x Salinity	34.843	1,168	**<0.001**

4.4.3 Mitochondrial lineage associated with habitat and phenotype

Salinity and plate morph information was available for 1550 individuals from 172 populations. Most freshwater stickleback belonged to the *Eu* lineage, irrespective of distance from North America or their plate morph. Low plated fish in salt water were also predominantly *Eu*, but completely plated fish were a more equal mix of *Eu* and *At* (**Figure 4.5**). This resulted in a significant interaction between plate morph and salinity in addition to distance influencing the proportion of *At* fish (**Table 4.3**). When excluding North Uist, the overall pattern of freshwater and low plated saltwater fish being predominantly *Eu* persisted (**Figure S4.5**, **Figure S4.6**), but we found no significant association of mitochondrial lineage with plate morphology (**Table S4.2**) which differs to the full dataset. This is likely due to the reduced information known about plate morph in regions other than our study site North Uist, especially as no low plated stickleback were sampled in North America (the low plate morph is almost entirely absent in North American freshwater populations, with complete and partially plated individuals often dominating (Haines, 2022)).

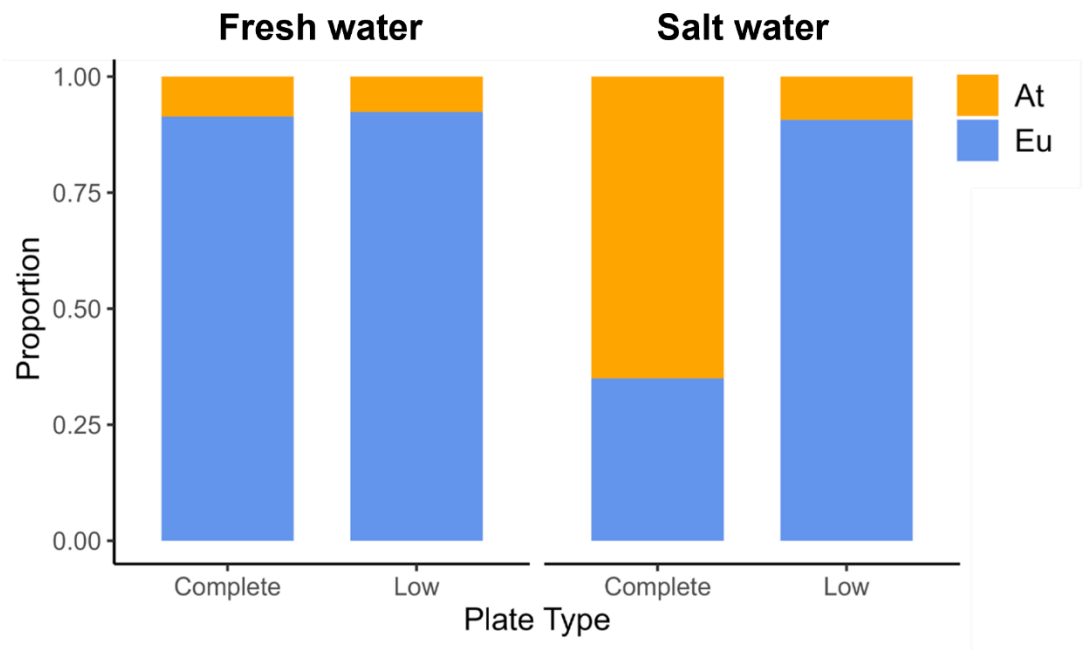

Figure 4.5: The proportion of *Eu* and *At* lineage stickleback that were complete or low plated in fresh water and salt water. n = 1118 and 438 individuals (125 and 47 populations) for fresh water and salt water respectively. Saltwater fish are defined as those that spend some or all of their lives in salt water. Freshwater fish reside permanently in fresh water.

4.4.4 Temperature

To determine whether temperature had influenced the distribution of stickleback mitochondrial haplotypes in the Atlantic, we tested whether the maximum, minimum, or variation in SST influenced the proportion of *At* stickleback in saltwater populations. SST was not included in analysis of the whole dataset as we had no information about the temperature of freshwater sampling sites, which likely vary greatly dependant on their location, accessibility to the sea, and depth for example. In this analysis we also included populations where plate morphology was unknown to increase the size of the dataset (77 saltwater populations), so we were unable to test for an association with plate morphology. The best fitting model according to AIC and BIC in both the full dataset and without North Uist included distance and the average maximum SST as predictors (Wald's $F_{1,75} = 24.546$, $p < 0.001$ for maximum SST; $F_{1,75} = 77.037$, $p < 0.001$ for distance from North America, **Table 4.4**; see **Table S4.3** for results without North Uist). There was no interaction between maximum SST and distance ($F_{1,74} = 1.381$, $p = 0.244$). When including more than one SST parameter in the model, only maximum SST was significant. When accounting for distance, there were fewer *At* stickleback where maximum SST was higher (**Figure 4.6**).

Table 4.4: SST parameters affecting the proportion of stickleback with the *At* mitochondrial haplotype in saltwater populations across the North Atlantic. Results of the generalised linear models assessing the effects of distance and three SST parameters (maximum, minimum and variation in SST) on the proportion of *At* stickleback per saltwater population. All models were compared to a generalised linear model with only distance as a predictor. d.f = degrees of freedom. Values in bold are significant at $p < 0.05$.

Predictor	AIC	BIC	Wald F	d.f	P-value
Maximum SST	279.444	286.476	24.546	1,75	**<0.001**
Minimum SST	307.207	314.238	2.043	1,75	0.157
Variation in SST	294.494	301.526	12.889	1,75	**<0.001**

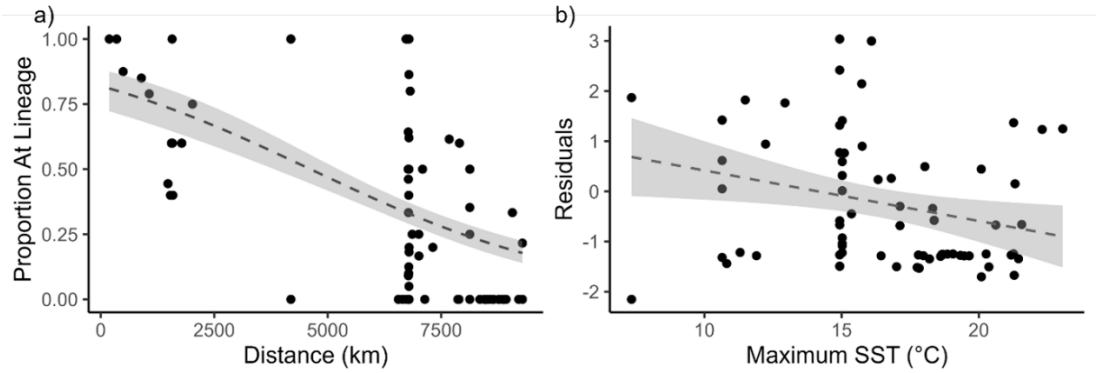

Figure 4.6: Change in the proportion of *At* lineage stickleback with sea surface temperature. a) The change in the proportion of *At* stickleback with distance from North America in salt water, including populations with unknown plate morphology. Dashed line shows the binomial generalised linear model with the proportion of *At* stickleback per population as a function of distance from North America. b) The average maximum SST plotted against the residuals of a) to account for distance, with the dashed line showing the linear regression ($F_{1,75} = 6.0247$, $p = 0.016$). n = 77 populations.

4.4.5 Morphology

4.4.5.1 Standard length and armour

We compared the SL of six anadromous stickleback populations from North Uist (see **Figure S4.7** for populations) as these populations were generally an almost equal mix of *Eu* and *At* fish, reducing any effect of both population and nuclear genetic differences. We found that female *At* stickleback had a larger SL than female *Eu* fish (**Figure 4.7**, $\chi^2_1 = 4.151$, $p = 0.0416$). This pattern was found in four of the six

populations assessed and was unlikely to be a consequence of SL variation between populations, although sample sizes did vary between populations (**Figure S4.7**). We found no difference in SL between lineages in males (**Figure 4.7**, χ^2_1 = 0.003, p = 0.958). After size standardisation, there were no differences in armour measurements between lineages (**Figure 4.7)**.

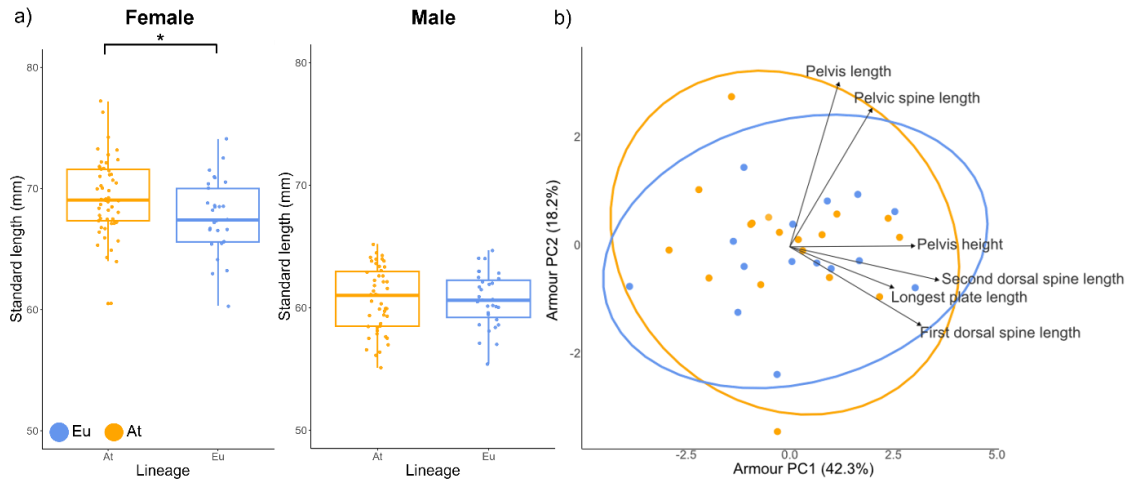

Figure 4.7: Morphological differences between *Eu* and *At* anadromous stickleback from North Uist. a) SL differences between mitochondrial lineages in female and male stickleback. n = 83 and 78 individuals for females and males respectively (six populations, see **Figure S4.7** for population differences). Boxplot shows median and interquartile range, points show individual data points. Significant differences ($p < 0.05$) in SL between lineages is shown with an asterisk. b) Armour differences between lineages. n = 34 individuals from three populations.

4.4.5.2 Otoliths measurements

At least one otolith was successfully dissected and measured from 46 individuals (**Figure 4.8**). Otolith diameter correlated with SL (**Figure 4.8**, $F_{1,40}$ = 6.560, p = 0.014) but there was no difference in otolith diameter between *Eu* and *At* stickleback ($F_{1,40}$ = 0.877, p = 0.355) or between females and males ($F_{1,40}$ = 0.416, p = 0.522). 40 out of the 46 otoliths dissected were clear, while six were unreadable. All otoliths had a transparent edge consistent with stickleback being sampled from North Uist lochs in April (Singkam and MacColl, 2018). Out of 40 individuals with at least one readable otolith, 85.7% of *Eu* and 88.5% of *At* samples were 2S (**Figure 4.8b**, two sets of seasonal rings), with the remainder being 3S (**Figure 4.8c**, three sets of seasonal rings). The proportions of 2S and 3S otoliths did not significantly differ between *Eu* and *At* stickleback (**Figure 4.8d**, Fisher's Exact Test, p-value = 1). According to the Jones & Hynes (1950) method, 2S and 3S otoliths imply that stickleback were 2 or 3

years old, respectively. In the western Atlantic, anadromous stickleback are estimated to live for only a year (Able and Fahay, 2010), so the pattern of seasonal otolith annuli in anadromous stickleback likely differs to that of freshwater fish that have previously been reported (Jones and Hynes, 1950; Singkam and MacColl, 2018). Despite this, there was no difference in otolith size or score between mitochondrial lineages (**Figure 4.8**) and as assessing the otolith rings is a well-established method to determine age in fish, age was unlikely to differ between the *Eu* and *At* fish sampled, so did not influence morphological findings.

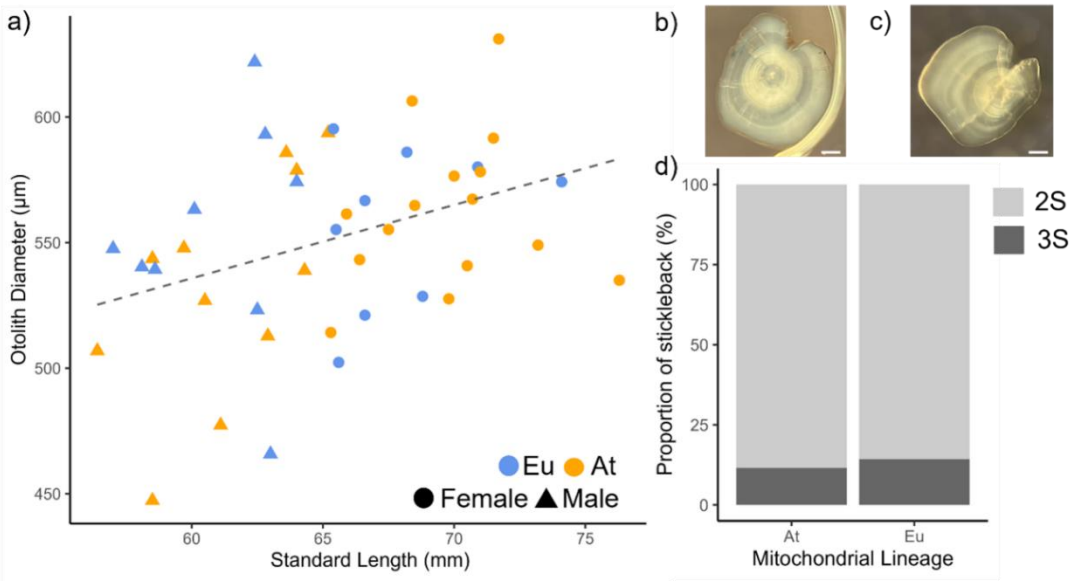

Figure 4.8: Comparison of otoliths from anadromous North Uist stickleback. a) Otolith diameter was correlated with standard length of the stickleback ($F_{1,42}$ = 6.673, p = 0.014, dashed line) but there was no effect of sex (circle = female, square = male) or mitochondrial lineage (blue = *Eu*, orange = *At*). Each point represents an individual stickleback. n = 46. b) Example of 2S otolith. Two sets of growth rings. c) Example of 3S otolith. Three sets of growth rings. In b) and c) scale bar is 100µm. d) Otolith scores based on Jones & Hynes (1950) method for *At* and *Eu* stickleback. n = 40.

4.4.6 Genetic differences between migratory stickleback

Comparisons of the nuclear genomes between *Eu* and *At* stickleback revealed no regions of high divergence (**Figure 4.9**) and an average mean F_{ST} value of -0.000282. The nuclear genomes of the two mitochondrial lineages are well mixed in migratory North Uist populations, suggesting that these are a single undifferentiated migratory population segregating only by the mtDNA. We can therefore assume that morphological differences between lineages are most likely a result of mitochondrial rather than nuclear differences.

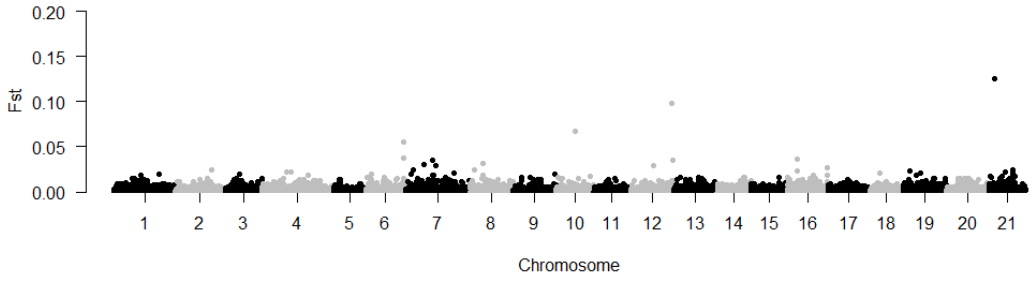

Figure 4.9: No evidence of nuclear genetic differences between mitochondrial lineages in migratory populations from North Uist. Genome-wide F_{ST} estimates for 6,061,748 SNPs calculated using VCFtools with a window size of 20kb. Four North Uist migratory populations included: CLAM, BHRM, OLAM, LUIM, n = 56.

There were 37 fixed nucleotide differences between *Eu* and *At* migratory stickleback from North Uist (analysis included 30 individuals from four migratory populations) in the mitochondrial protein coding genes, including four non-synonymous substitutions in ATP6, COX1 and ND5. There was one fixed difference in tRNA Tyrosine (**Figure 4.10**).

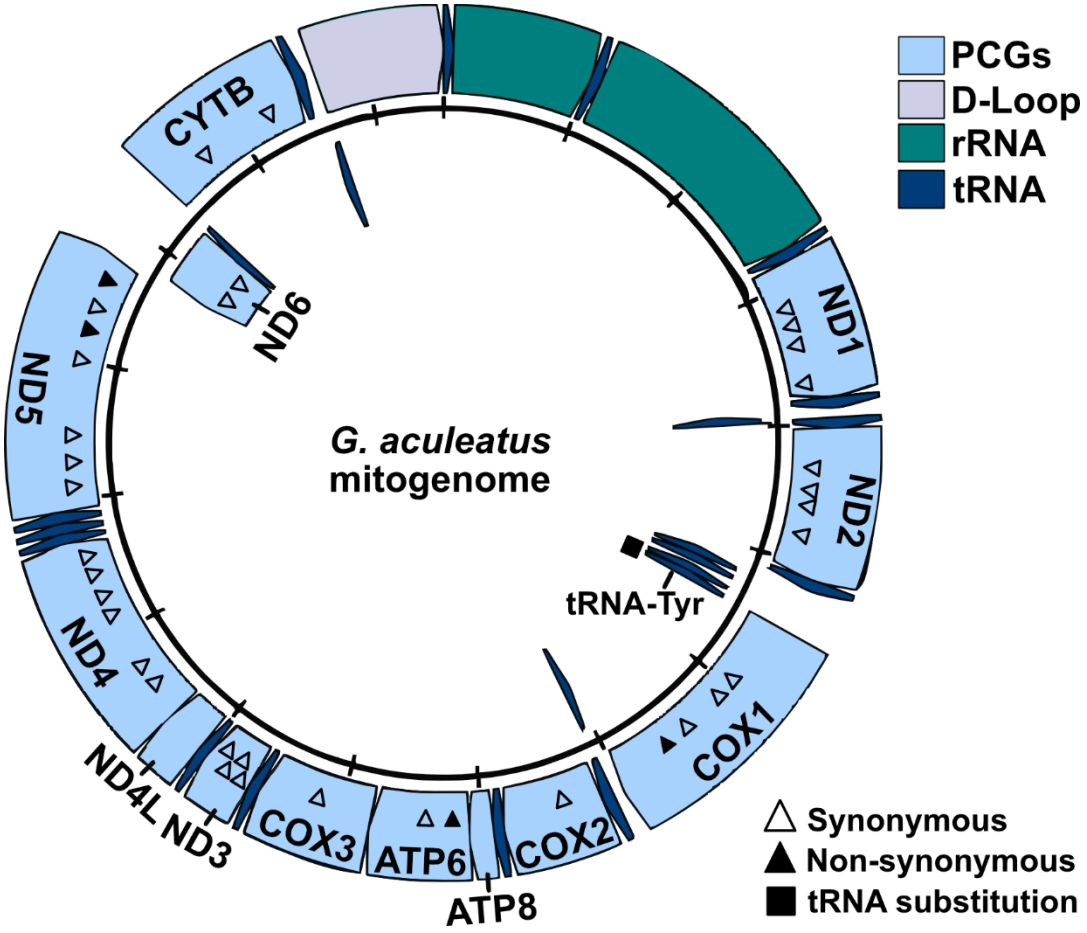

Figure 4.10: Locations of fixed nucleotide differences in the mitogenome between *Eu* and *At* migratory stickleback from North Uist. Image edited from circularMT (Goodman and Carr, 2024) using the stickleback reference mitogenome (Jiang et al., 2018) as the input. Fixed synonymous (open triangles) and non-synonymous (filled triangles) differences between *Eu* and *At* mitochondrial PCGs and tRNAs (filled squares). Four populations: LUIM, BHRM, CLAM and OLAM (n = 30).

4.5 Discussion

Here we provide evidence that Atlantic stickleback mitochondrial lineages originated in refugia on opposite sides of the Atlantic Ocean and have since spread and come into secondary contact at multiple locations. Our analyses suggest that Atlantic stickleback mitochondrial lineages are associated with adaptive potential: fish residing permanently in fresh water were predominantly the *Eu* lineage (even in North America), whereas completely plated fish living at least some of their lives in salt water (therefore likely migratory fish) were a mix of the two lineages. As the stickleback is originally a marine species, this suggests that the ocean is now a

panmictic population of the two mitochondrial lineages, but there may have been selection for the *Eu* lineage in fresh water. Given that non-migratory fish living in salt water were also predominantly the *Eu* lineage, this may be due to differences in migratory behaviour and habitat associations, although it is difficult to be certain because most published studies do not record whether the fish they sampled were migratory.

On North Uist, our own study area, non-migratory, saltwater ('lagoon resident') and freshwater ('freshwater resident') stickleback were predominantly *Eu* and low-plated. These populations are confined to low-energy lagoon or freshwater environments. Migratory fish, which were approximately 50% *At*, were completely plated, which may help them to escape high predation in the sea. The different proportions of *Eu* and *At* stickleback between ecotypes has previously been discussed (Dean et al., 2019a), and can be explained by both colonisation history and differences in adaptive potential between the lineages. We show that the *At* lineage was found in fresh water predominantly on the west side of the island, consistent with the *At* lineage originating in North America and spreading across the Atlantic Ocean. One population in the east is the only exception to this pattern, but this loch differs to other sampling sites on North Uist in numerous parameters including accessibility to the sea, salinity, and stickleback plate morphs, so may require further assessment. The finding that *At* fish are mainly in the western populations could suggest that the *Eu* lineage colonised North Uist first, establishing the resident populations, followed by a second wave of colonisation from the *At* lineage from the west which rarely succeeded in colonising fresh water and lagoons, but introgressed into the migratory populations. As we have found no evidence to date of any barriers to gene flow between the lineages, this is likely due to stickleback with the *Eu* mtDNA being better adapted to the resident lifestyle or habitat, such as differences in temperature or diet that can alter metabolic requirements. This is supported further by our finding that this pattern persisted across the Atlantic.

Given the associations with habitat and adaptive phenotypes, our results suggest that mitochondrial sequences are unlikely to make good neutral markers of population history and geography. This might occur because the mitochondrial sequences themselves confer differences in adaptive potential (Camus and Inwongwan, 2023; Li et al., 2018; Pegan et al., 2024; Zhao et al., 2022), but might also arise because the mitochondrial sequences are in linkage disequilibrium with other sources of adaptive differences that arose in allopatry in the respective refugia. Our preliminary data (Chapter 6) do suggest that there may be temperature related differences in

mitochondrial function between *Eu* and *At* individuals, irrespective of nuclear genomic differences, and older work also hints at wider adaptive differences between the two refugial lineages (Heuts, 1947; Münzing, 1963), which differ in morphology and habitat preferences.

The *Eu* and *At* lineages have greatly diverged mtDNA (Dean et al., 2019a; Mäkinen and Merilä, 2008) with at least thirty fixed nucleotide substitutions, so the mitochondrial sequences themselves may have different adaptive potential. Sequence differences in the mitochondrial genome can greatly influence fitness as the mtDNA encodes components of the electron transfer system (ETS) in the mitochondrial inner membrane that is responsible for oxidative phosphorylation and energy generation. As the mtDNA is involved in such a fundamental process, variation in sequence may have functional consequences and be selected for in certain habitats that differ in metabolic demands. Signatures of positive selection have been identified in the mitochondrial genome of some species (James et al., 2016) and this has been linked to adaptation to a particular environment including high-altitude (Cheviron et al., 2012; Lui et al., 2015; Wang et al., 2016), latitudinal clines (Foote et al., 2011a; Garvin et al., 2011) and diet (Aw et al., 2018). We also identified a fixed difference in tRNA-Tyrosine between *Eu* and *At* migratory stickleback from North Uist; whether this could influence mitochondrial function requires further investigation. Our preliminary results (Chapter 6) suggest that there are temperature-dependent differences in mitochondrial respiration between *Eu* and *At* stickleback, which could result in different adaptive propensities between lineages, but this has not been explicitly tested. As energy generation also relies on the cooperation of mitochondrial and nuclear encoded components, coevolution of the two genomes is important (Barreto et al., 2018), which may have resulted in diverged nuclear genes, as well as mitochondrial, when lineages evolved in allopatry, and could also result in adaptive differences between stickleback mitochondrial lineages. From our comparison of the nuclear genomes of North Uist migratory stickleback using short read sequences, we found no evidence of any regions of high divergence between the mitochondrial lineages. This makes it unlikely that the nuclear genome explains the differences between *Eu* and *At* stickleback, although we cannot rule out with complete certainty that there are not differences that we have been unable to detect in this analysis. We did identify a small number of regions across the nuclear genome that had a higher F_{ST} value than expected, suggesting that there is a small amount of genetic differentiation between *Eu* and *At* stickleback. These regions are likely being maintained despite gene flow, so may warrant further investigation.

As we found that non-migratory populations were predominantly the *Eu* lineage, stickleback with the *Eu* mtDNA may be better adapted to residing permanently in fresh or saltwater habitats. Selective agents influencing energy requirements within these environments may include one or more of the following: (i) Temperature: lakes and streams are heavily influenced by climate compared to the Atlantic Ocean so are more variable and may reach increased temperature extremes which could influence mitochondrial respiratory enzymes and oxidative phosphorylation (Chouinard-Boisvert et al., 2024; Pichaud et al., 2010). Any variation in mtDNA sequence that increased mitochondrial efficiency at high or low temperatures could be selected for and provide an advantage in colonising fresh water. Our findings show that there were less *At* stickleback at higher maximum SSTs, suggesting that *At* fish may be less well-adapted to warm waters. This is consistent with present day observations of migratory stickleback at the southern edge of their range in eastern North America (New Jersey), which are likely to be largely or entirely of the *At* lineage, breeding very early in the year (February or March) when coastal sea surface temperatures are low (less than 6°C), and the resulting juveniles then migrate northwards, following cold oceanic water (Able and Fahay, 2010). These temperatures are much lower than those experienced by breeding stickleback on the eastern side of the Atlantic.

(ii) Nutrient availability: resident fish must adapt to lower nutrient availability than in the ocean, including reduced availability of long chain polyunsaturated fatty acids (Ishikawa et al., 2021) which can alter mitochondrial membranes and mitochondrial efficiency (Salin et al., 2021). Mitochondrial variants that provide the most efficient ATP production with limited or specific resources may be advantageous in fresh water and lagoons. Alternatively, resident stickleback do not migrate, so may require less energy than anadromous stickleback, meaning that selection for efficient ATP production may be relaxed in resident stickleback, allowing the biosynthesis of other key molecules from the Krebs cycle (Martínez-Reyes and Chandel, 2020) that may be less available from freshwater diets.

(iii) Salinity: stickleback are ancestrally marine and have repeatedly colonised lower salinity environments. Shifting between different salinity habitats involves increased energy expenditure and altered mitochondrial efficiency (Sebastian et al., 2022). However, as resident fish in both fresh and brackish water were primarily *Eu,* and observations from fish raised in aquaria suggest that both lineages do well long-term in both salt and fresh water, mitochondrial sequence variation is unlikely to be associated with salinity alone.

Our data provide evidence that the *Eu* and *At* lineages originated in separate refugia in the eastern and western Atlantic respectively (Makinen & Merila 2008), as at increasing distances from the predicted North American refugium the proportion of *At* stickleback decreased. The almost complete absence of the *At* lineage in continental western Europe suggests that the *Eu* lineage originated in a refugium somewhere in Europe. Our analyses show that since the melting of the ice sheets, *Eu* and *At* lineages have spread north and across the Atlantic Ocean to meet at multiple locations including Nova Scotia, Newfoundland, Greenland, Ireland and Scotland, in agreement with previous work (Dean et al., 2019; Liu et al., 2016; Ravinet et al., 2013). We describe the distribution of the two main mitochondrial clades in the Atlantic, with the *Eu* lineage predominant in Europe and the *At* on the East Coast of North America and some northern European populations, which is in agreement with previous mtDNA-based studies (Makinen & Merila, 2008; DeFaveri et al., 2012; Sanz et al., 2015). Unlike previous work (Makinen & Merila, 2008; Fang et al., 2018), we identified stickleback of the *Eu* lineage, as well as *At*, in North America, indicating that the *Eu* clade has spread across the Atlantic from refugia in southern Europe. Freshwater populations in eastern North America were rare in our study, but were entirely *Eu*, adding to the evidence that stickleback with the *Eu* mtDNA may be better adapted to colonising fresh water. Individuals from these populations were also completely plated unlike the majority of freshwater stickleback in Europe and the Pacific (Haines, 2022). Using nuclear SNP data, Fang et al. (2018) suggest that the ancestral area for the *At* clade was in the English Channel, which is not consistent with our results as we report the highest proportion of *At* stickleback in North America, with very few individuals of the *At* lineage in populations closest to the English Channel. The finding that *At* stickleback in the eastern Atlantic were predominantly on the west coast of both North Uist and Ireland (Ravinet et al., 2013) also supports the *At* lineage originating in the western Atlantic.

We identified differences in standard length between mitochondrial lineages in North Uist migratory stickleback: *At* females were on average 2 to 3mm longer than *Eu* females. Given the strong positive relationship between length and clutch size in stickleback (Dean et al., 2019b), as in most teleost fishes, this suggests that *At* stickleback are likely to be more fecund than *Eu* stickleback. This analysis was conducted on wild-caught stickleback but is consistent with preliminary data comparing the growth rate of the two mitochondrial lineages between weeks 5 and 12 in aquaria, where *At* fish had a higher growth rate than *Eu* when fed the same diet (Lewis et al. unpublished). Assuming that North Uist migratory populations segregate

by mtDNA but are otherwise panmictic (Haenel et al., 2022) limiting any nuclear genetic differences, which is supported by our F_{ST} analysis, it is most likely that the difference in size between *Eu* and *At* stickleback is a side effect of metabolic differences due to the mtDNA variation, potentially including the four non-synonymous differences we identified between *Eu* and *At* migratory stickleback. When assessing the otoliths of migratory stickleback from North Uist, we found no difference in otolith size or the pattern of rings between *Eu* and *At* individuals. As otoliths are well-established method to determine age in fish (Jones and Hynes, 1950; Singkam and MacColl, 2018), this makes it very unlikely that age explains any variation in morphology between the two mitochondrial lineages. However, we also highlight that the pattern of the seasonal rings of otoliths from North Uist migratory stickleback may differ to other stickleback populations as previous findings suggest that migratory stickleback live to only one year old (Able and Fahay, 2010; our own observations from North Uist), yet we scored otoliths as 2S or 3S which implies 2- or 3-year-old fish. Reading annual otolith rings to estimate age relies on differing growth patterns in poor versus good growth conditions (most likely related to food availability and temperature) which result in opaque rings during faster growth and translucent rings during slow growth. Previous work has focussed on freshwater stickleback (Jones and Hynes, 1950; Singkam and MacColl, 2018), but growth conditions experienced by migratory fish may differ to that of freshwater fish as migratory stickleback will spend most of their lives at sea but come into fresh water or lagoons during the breeding season. How this influences the formation of otolith annual rings has not been investigated to our knowledge, but this may be an important direction of future research.

Previous work in *Drosophila* has shown that mtDNA variation alone can influence fitness traits (Christie et al., 2011; Dowling and Wolff, 2023), but very few studies in wild, natural populations confirm the fitness impacts of mtDNA variation (Dobelmann et al., 2019; Schwartz et al., 2015) and it is even rarer to have a natural study system that allows the assessment of the fitness consequences of mtDNA variation alone (i.e. in the same nuclear genetic background). If variation in the mtDNA sequence improves the efficiency of oxidative phosphorylation and energy generation in particular environments, this could allow the increased growth of migratory *At* fish. As mitochondria are maternally inherited, natural selection on mitogenome variation would only occur where variants provide an advantage for females, consistent with differences in SL only being in North Uist females. However, why differences in mtDNA sequence alone would only impact the SL of females and not males remains

unclear and warrants further investigation. One possible explanation could include differences in mitochondrial content and function between sexes, as found in other organisms (Gaignard et al., 2015; Junker et al., 2022; Rodnick et al., 2014), but this has not been assessed in the stickleback to our knowledge. Studies in *Drosophila* found that mitochondrial haplotype affected mtDNA copy number and mitochondrial gene expression dependent on sex, and this could be linked to sex-specific life-history traits (Camus et al., 2015), so whether there are differences in mtDNA content between sexes and mitochondrial lineages in the stickleback that could influence growth should be explored further.

An alternative explanation for the differences in SL we observed may be that the mtDNA evolved alongside changes in morphology, such as SL, as the lineages diverged in allopatry. Selection may have then acted on SL differences that provided an advantage in particular environments (Dean et al., 2019b; Kraak and Bakker, 1998). However, when these lineages came into secondary contact on North Uist, introgression of the mtDNA should have masked these associations if *Eu* and *At* fish were freely interbreeding. As we observed size differences in North Uist populations, it remains possible, although seems very unlikely, that there is some degree of reproductive isolation between the lineages, perhaps due to mitonuclear coadaptation and subsequent incompatibilities when lineages come back into contact (Ellison and Burton, 2008, 2006; Hill, 2020), although we have found no evidence of this to date and we found no nuclear genetic differences between mitochondrial lineages. We also cannot rule out the smaller size of *Eu* females providing an additional advantage in freshwater colonisation, as resident stickleback are smaller than migratory fish (Dean et al., 2019a), giving them an advantage against many freshwater predators, although we found no differences in armour traits between lineages. Slower growth may also be an advantage when inhabiting environments with restricted nutrient availability (Dupont-Prinet et al., 2010), such as the lochs and lagoons on North Uist.

Here we show that there is a cline in the mitochondrial lineage of Atlantic stickleback with distance from North America, evidencing that the history of the two clades has influenced the phylogeographic structure. Mitochondrial lineages in Atlantic stickleback were associated with adaptive potential: fish residing permanently in fresh water were predominantly the *Eu* lineage, whereas completely plated fish living at least some of their lives in salt water, and therefore likely migratory fish, were a mix of the *Eu* and *At* lineages. Given these associations with habitat and phenotype, our results suggest that mitochondrial sequences are unlikely to make good neutral markers. This likely occurs because the mitochondrial sequences themselves have

different adaptive potential, but we cannot rule out with complete certainty that differences in adaptive potential between lineages has arisen because the mitochondrial sequences are in linkage disequilibrium with adaptive alleles elsewhere in the genome, a result of clades evolving in allopatry. Further work would be necessary to decipher whether any combination of environmental variables result in selection for the *Eu* mtDNA and to identify whether there are any signatures of natural selection across the mitochondrial genome. Our study is one of only a few that has linked mtDNA variation to life-history traits in natural populations, making the Atlantic three-spined stickleback an exciting model for further investigations into both the physiological and evolutionary consequences of mtDNA variation.

4.6 References

Able, K.W., Fahay, M.P., 2010. Ecology of Estuarine Fishes: Temperate waters of the North Atlantic. The John Hopkins University Press. Baltimore.

Aguirre, W.E., Ellis, K.E., Kusenda, M., Bell, M.A., 2008. Phenotypic variation and sexual dimorphism in anadromous threespine stickleback: implications for postglacial adaptive radiation. *Biol. J. Linn. Soc.* **95**, 465-478. https://doi.org/10.1111/j.1095-8312.2008.01075.x

Artamonova, V.S., Bardukov, N. V., Aksenova, O. V., Ivanova, T.S., Ivanov, M. V., Kirillova, E.A., Koulish, A. V., Lajus, D.L., Malyutina, A.M., Pashkov, A.N., Reshetnikov, S.I., Makhrov, A.A., 2022. Round-the-World Voyage of the Threespine Stickleback (*Gasterosteus aculeatus*): Phylogeographic Data Covering the Entire Species Range. *Water* **14**, 2484. https://doi.org/10.3390/W14162484/S1

Avise, J.C., Arnold, J., Martin Bal, R., Bermingham, E., Lamb, T., Neigel, J.E., Reeb, C.A., Saunders, N.C., 1987. Intraspecific phylogeography: The Mitochondrial DNA Bridge Between Population Genetics and Systematics. *Ann. Rev. Ecol. Sys.* **18**, 489–522. https://doi.org/10.1146/annurev.es.18.110187.002421

Aw, W.C., Towarnicki, S.G., Melvin, R.G., Youngson, N.A., Garvin, M.R., Hu, Y., Nielsen, S., Thomas, T., Pickford, R., Bustamante, S., Vila-Sanjurjo, A., Smyth, G.K., Ballard, J.W.O., 2018. Genotype to phenotype: Diet-by-mitochondrial DNA haplotype interactions drive metabolic flexibility and organismal fitness. *PLoS Genet* **14**. https://doi.org/10.1371/JOURNAL.PGEN.1007735

Ballard, J.W.O., Kreitman, M., 1995. Is mitochondrial DNA a strictly neutral marker? *Trends in Ecology & Evolution*, **10**, 485-488. https://doi.org/10.1016/S0169-5347(00)89195-8

Ballard, J.W.O., Whitlock, M.C., 2004. The incomplete natural history of mitochondria. *Mol. Ecol.* **13**, 729-744. https://doi.org/10.1046/j.1365-294X.2003.02063.x

Barreto, F.S., Watson, E.T., Lima, T.G., Willett, C.S., Edmands, S., Li, W., Burton, R.S., 2018. Genomic signatures of mitonuclear coevolution across populations of *Tigriopus californicus. Nat. Ecol. Evol.* **2**, 1250–1257. https://doi.org/10.1038/s41559-018-0588-1

Barrett, R.D.H., Rogers, S.M., Schluter, D., 2008. Natural selection on a major armor gene in threespine stickleback. *Science* **322**, 255–257. https://doi.org/10.1126/SCIENCE.1159978

Bell, M.A., Foster, S.A., 1995. The Evolutionary Biology of the Threespine Stickleback. *J. Anim. Ecol.* **64**, 418. https://doi.org/10.2307/5902

Camus, M.F., Inwongwan, S., 2023. Mitonuclear interactions modulate nutritional preference*. Biol. Lett.* **19**. https://doi.org/10.1098/rsbl.2023.0375

Camus, M.F., Wolf, J.B.W., Morrow, E.H., Dowling, D.K., 2015. Single Nucleotides in the mtDNA Sequence Modify Mitochondrial Molecular Function and Are Associated with Sex-Specific Effects on Fertility and Aging. *Curr. Biol.* **25**, 2717–2722. https://doi.org/10.1016/J.CUB.2015.09.012

Chan, Y.F., Marks, M.E., Jones, F.C., Villarreal, G., Shapiro, M.D., Brady, S.D., Southwick, A.M., Absher, D.M., Grimwood, J., Schmutz, J., Myers, R.M., Petrov, D., Jónsson, B., Schluter, D., Bell, M.A., Kingsley, D.M., 2010. Adaptive evolution of pelvic reduction in sticklebacks by recurrent deletion of a Pitx1 enhancer. *Science* **327**, 302. https://doi.org/10.1126/SCIENCE.1182213

Cheviron, Z.A., Bachman, G.C., Connaty, A.D., McClelland, G.B., Storz, J.F., 2012. Regulatory changes contribute to the adaptive enhancement of thermogenic capacity in high-altitude deer mice. *PNAS.* **109**, 8635–8640. https://doi.org/10.1073/PNAS.1120523109

Chouinard-Boisvert, S., Ghinter, L., St-Pierre, A., Mortz, M., Desrosiers, V., Dufresne, F., Tardif, J.-C., Huard, J., Sirois, P., Fortin, S., Blier, P.U., 2024. Mitochondrial functions and fatty acid profiles in fish heart: an insight into physiological limitations linked with thermal tolerance and age. *J. Exp. Biol*. **227**, jeb247502. https://doi.org/10.1242/JEB.247502

Christie, J.S., Picornell, A., Moya, A., Ramon, M.M., Castro, J.A., 2011. Mitochondrial DNA effects on fitness in *Drosophila subobscura*. *Heredity* **107**, 239–245. https://doi.org/10.1038/hdy.2011.8

Colosimo, P.F., Hosemann, K.E., Balabhadra, S., Villarreal, G., Dickson, H., Grimwood, J., Schmutz, J., Myers, R.M., Schluter, D., Kingsley, D.M., 2005. Widespread parallel evolution in sticklebacks by repeated fixation of ectodysplasin alleles. *Science* **307**, 1928–1933. https://doi.org/10.1126/SCIENCE.1107239

Cresko, W.A., Amores, A., Wilson, C., Murphy, J., Currey, M., Phillips, P., Bell, M.A., Kimmel, C.B., Postlethwait, J.H., 2004. Parallel genetic basis for repeated evolution of armor loss in Alaskan threespine stickleback populations. *Proc. Natl. Acad. Sci.* **101**, 6050-6055. https://doi.org/10.1073/pnas.0308479101

Dean, L.L., Magalhaes, I.S., Foote, A., D'Agostino, D., McGowan, S., MacColl, A.D.C., 2019a. Admixture between Ancient Lineages, Selection, and the Formation of Sympatric Stickleback Species-Pairs. *Mol. Biol. Evol.* **36**, 2481–2497. https://doi.org/10.1093/MOLBEV/MSZ161

Dean, L.L., Robertson, S., Mahmud., M, MacColl, A.D.C., 2019b. Internal embryonic development in a non-copulatory, egg-laying teleost, the three-spined stickleback, *Gasterosteus aculeatus*. *Sci. Rep*. **9**, 2395. https://doi.org/10.1038/s41598-019-38584-w

Defaveri, J., Zanella, L.N., Zanella, D., Mrakovčić, M., Merilä, J., 2012. Phylogeography of isolated freshwater three-spined stickleback *Gasterosteus aculeatus* populations in the Adriatic Sea basin. *J. Fish. Biol.* **80**, 61–85. https://doi.org/10.1111/J.1095-8649.2011.03147.X

Dierckxsens, N., Mardulyn, P., Smits, G., 2017. NOVOPlasty: de novo assembly of organelle genomes from whole genome data. *Nucleic Acids Res.* **45**, e18. https://doi.org/10.1093/NAR/GKW955

Dobelmann, J., Alexander, A., Baty, J.W., Gemmell, N.J., Gruber, M.A.M., Quinn, O., Wenseleers, T., Lester, P.J., 2019. The association between mitochondrial genetic variation and reduced colony fitness in an invasive wasp. *Mol. Ecol.* **28**, 3324–3338. https://doi.org/10.1111/MEC.15159

Dowling, D.K., Wolff, J.N., 2023. Evolutionary genetics of the mitochondrial genome: insights from *Drosophila*. *Genetics*. **224**, iyad036. https://doi.org/10.1093/GENETICS/IYAD036

Dupont-Prinet, A., Chatain, B., Grima, L., Vandeputte, M., Claireaux, G., McKenzie, D.J., 2010. Physiological mechanisms underlying a trade-off between growth rate and tolerance of feed deprivation in the European sea bass (*Dicentrarchus labrax*). *J. Exp. Biol.* **213**, 1143–1152. https://doi.org/10.1242/JEB.037812

Ellison, C.K., Burton, R.S., 2008. Interpopulation hybrid breakdown maps to the mitochondrial genome. *Evolution*. **62**, 631–638. https://doi.org/10.1111/j.1558-5646.2007.00305.x

Ellison, C.K., Burton, R.S., 2006. Disruption of Mitochondrial Function in Interpopulation Hybrids of *Tigriopus californicus*. *Evolution.* **60**, 1382. https://doi.org/10.1554/06-210.1

Fang, B., Merilä, J., Ribeiro, F., Alexandre, C.M., Momigliano, P., 2018. Worldwide phylogeny of three-spined sticklebacks. *Mol. Phylogenet. Evol.* **127**, 613–625. https://doi.org/10.1016/J.YMPEV.2018.06.008

Foote, A.D., Morin, P.A., Durban, J.W., Pitman, R.L., Wade, P., Willerslev, E., Gilbert, M.T.P., Fonseca, R.R.D., 2011. Positive selection on the killer whale mitogenome. *Biol. Lett.* **7**, 116–118. https://doi.org/10.1098/rsbl.2010.0638

Gagnaire, P.A., Broquet, T., Aurelle, D., Viard, F., Souissi, A., Bonhomme, F., Arnaud-Haond, S., Bierne, N., 2015. Using neutral, selected, and hitchhiker loci to assess connectivity of marine populations in the genomic era. *Evol. Appl.* **8**, 769–786. https://doi.org/10.1111/EVA.12288

Gaignard, P., Savouroux, S., Liere, P., Pianos, A., Thérond, P., Schumacher, M., Slama, A., Guennoun, R., 2015. Effect of Sex Differences on Brain Mitochondrial Function and Its Suppression by Ovariectomy and in Aged Mice. *Endocrinology*. **156**, 2893–2904. https://doi.org/10.1210/EN.2014-1913

Garvin, M.R., Bielawski, J.P., Gharrett, A.J., 2011. Positive Darwinian Selection in the Piston That Powers Proton Pumps in Complex I of the Mitochondria of Pacific Salmon. *PLoS One* **6**, e24127. https://doi.org/10.1371/JOURNAL.PONE.0024127

Gérard, K., Bierne, N., Borsa, P., Chenuil, A., Féral, J.P., 2008. Pleistocene separation of mitochondrial lineages of Mytilus spp. mussels from Northern and Southern Hemispheres and strong genetic differentiation among southern populations. *Mol. Phylogenet. Evol.* **49**, 84–91. https://doi.org/10.1016/J.YMPEV.2008.07.006

Goodman, S.J., Carr, I.M., 2024. Drawing mitochondrial genomes with circularMT. *Bioinformatics*. **40**, btae450. https://doi.org/10.1093/bioinformatics/btae450

Haenel, Q., Guerard, L., MacColl, A.D.C., Berner, D., 2022. The maintenance of standing genetic variation: Gene flow vs. selective neutrality in Atlantic stickleback fish. *Mol. Ecol.* **31**, 811–821. https://doi.org/10.1111/MEC.16269

Haines, G.E., 2022. Intraspecific diversity of threespine stickleback (*Gasterosteus aculeatus*) populations in eastern Canada. *Environ. Biol. Fishes.* **106**, 1177–1194. https://doi.org/10.1007/S10641-022-01362-1

Hall, T.A., 1999. Bioedit: A user-friendly biological sequence alignment editor and analysis program for windows 95/98/NT. *Nucleic. Acids Symp. Ser.* **41**, 95-98.

Heuts, M.J., 1947. Experimental studies on adaptive evolution in *Gasterosteus aculeatus* L. *Evolution* **1**, 89–102. https://doi.org/10.1111/J.1558-5646.1947.TB02717.X

Hewitt, G., 2000. The genetic legacy of the Quaternary ice ages. *Nature* **405**, 907-913. https://doi.org/10.1038/35016000

Hewitt, G.M., 2004. Genetic consequences of climatic oscillations in the Quaternary. *Phil. Trans. R. Soc. B.* **359,** 183–195. https://doi.org/10.1098/rstb.2003.1388

Hewitt, G.M., 1996. Some genetic consequences of ice ages, and their role in divergence and speciation. *Biological Journal of the Linnean Society* **58**, 247–276. https://doi.org/10.1111/J.1095-8312.1996.TB01434.X

Hill, G.E., 2020. Mitonuclear Compensatory Coevolution. *Trends in Genetics* **36**, 403–414. https://doi.org/10.1016/j.tig.2020.03.002

James, J.E., Piganeau, G., Eyre-Walker, A., 2016. The rate of adaptive evolution in animal mitochondria. *Mol. Ecol.* **25**, 67–78. https://doi.org/10.1111/mec.13475

Jiang, J.Q., Wang, Q.X., Liu, J.W., Liu, C.Z., 2018. Characterization of the complete mitochondrial genome of three-spined stickleback, *Gasterosteus aculeatus*. *Mitochondrial DNA B Resour.* **3**, 1133-1134. https://doi.org/10.1080/23802359.2018.1473732

Jones, F.C., Grabherr, M.G., Chan, Y.F., Russell, P., Mauceli, E., Johnson, J., Swofford, R., Pirun, M., Zody, M.C., White, S., Birney, E., Searle, S., Schmutz, J., Grimwood, J., Dickson, M.C., Myers, R.M., Miller, C.T., Summers, B.R., Knecht, A.K., Brady, S.D., Zhang, H., Pollen, A.A., Howes, T., Amemiya, C., Baldwin, J.,

Bloom, T., Jaffe, D.B., Nicol, R., Wilkinson, J., Lander, E.S., Di Palma, F., Lindblad-Toh, K., Kingsley, D.M., 2012. The genomic basis of adaptive evolution in threespine sticklebacks. *Nature* **484**, 55–61. https://doi.org/10.1038/nature10944

Jones, J.W., Hynes, H.B.N., 1950. The Age and Growth of *Gasterosteus aculeatus*, *Pygosteus pungitius* and *Spinachia vulgaris*, as Shown by their Otoliths. *J. Anim. Ecol.* **19**, 59. https://doi.org/10.2307/1571

Junker, A., Wang, J., Gouspillou, G., Ehinger, J.K., Elmér, E., Sjövall, F., Fisher-Wellman, K.H., Neufer, P.D., Molina, A.J.A., Ferrucci, L., Picard, M., 2022. Human studies of mitochondrial biology demonstrate an overall lack of binary sex differences: A multivariate meta-analysis. *FASEB J* **36**, e22146. https://doi.org/10.1096/FJ.202101628R

Kang, B., Hsu, K.C., Wu, J.H., Chiu, Y.W., Lin, H. Du, Ju, Y.M., 2022. Population genetic diversity and structure of *Rhinogobius candidianus* (Gobiidae) in Taiwan: Translocation and release. *Ecol. Evol.* **12**. https://doi.org/10.1002/ece3.9154

Kitano, J., Mori, S., Peichel, C.L., 2007. Sexual dimorphism in the external morphology of the threespine stickleback (*Gasterosteus aculeatus*). *Copeia*, **2**, 336-349. https://doi.org/10.1643/0045-8511(2007)7[336:SDITEM]2.0.CO;2

Kraak, S.B.M., Bakker, T.C.M., 1998. Mutual mate choice in sticklebacks: attractive males choose big females, which lay big eggs. *Anim. Behav.* **56**, 859–866. https://doi.org/10.1006/ANBE.1998.0822

Laakkonen, H.M., Hardman, M., Strelkov, P., Väinölä, R., 2021. Cycles of trans-Arctic dispersal and vicariance, and diversification of the amphi-boreal marine fauna. *J. Evol. Biol.* **34**, 73–96. https://doi.org/10.1111/JEB.13674

Li, X.D., Jiang, G.F., Yan, L.Y., Li, R., Mu, Y., Deng, W.A., 2018. Positive Selection Drove the Adaptation of Mitochondrial Genes to the Demands of Flight and High-Altitude Environments in Grasshoppers. *Front. Genet.* **9**, 1–12. https://doi.org/10.3389/fgene.2018.00605

Liu, S., Hansen, M.M., Jacobsen, M.W., 2016. Region-wide and ecotype-specific differences in demographic histories of threespine stickleback populations, estimated from whole genome sequences. *Mol. Ecol*. **25**, 5187–5202. https://doi.org/10.1111/MEC.13827

Lucek, K., Roy, D., Bezault, E., Sivasundar, A., Seehausen, O., 2010. Hybridization between distant lineages increases adaptive variation during a biological invasion:

stickleback in Switzerland. *Mol. Ecol.* **19**, 3995–4011. https://doi.org/10.1111/J.1365-294X.2010.04781.X

Lui, M.A., Mahalingam, S., Patel, P., Connaty, A.D., Ivy, C.M., Cheviron, Z.A., Storz, J.F., McClelland, G.B., Scott, G.R., 2015. High-altitude ancestry and hypoxia acclimation have distinct effects on exercise capacity and muscle phenotype in deer mice. *Am. J. Physiol. Regul. Integr. Comp. Physiol.* **308**, R779. https://doi.org/10.1152/AJPREGU.00362.2014

Mäkinen, H.S., Merilä, J., 2008. Mitochondrial DNA phylogeography of the three-spined stickleback (*Gasterosteus aculeatus*) in Europe-Evidence for multiple glacial refugia. *Mol. Phylogenet. Evol.* **46**, 167–182. https://doi.org/10.1016/j.ympev.2007.06.011

Martínez-Reyes, I., Chandel, N.S., 2020. Mitochondrial TCA cycle metabolites control physiology and disease. *Nat. Commun.* **11**, 102. https://doi.org/10.1038/s41467-019-13668-3

Münzing, J., 1963. The evolution of variation and distributional patterns in European populations of the three-spined stickleback, *Gasterosteus aculeatus*. *Evolution* **17**, 320–332. https://doi.org/10.1111/j.1558-5646.1963.tb03285.x

Orti, G., Bell, M.A., Reimchen, T.E., Meyer, A., 1994. Global survey of mitochondrial DNA sequences in the threespine stickleback: evidence for recent migrations. *Evolution* **48**, 608–622. https://doi.org/10.1111/J.1558-5646.1994.TB01348.X

Pegan, T.M., Berv, J.S., Gulson-Castillo, E.R., Kimmitt, A.A., Winger, B.M., 2024. The pace of mitochondrial molecular evolution varies with seasonal migration distance. *Evolution* **78**, 160–173. https://doi.org/10.1093/evolut/qpad200

Peichel, C.L., Marques, D.A., 2017. The genetic and molecular architecture of phenotypic divergence in sticklebacks. *Phil. Trans. R. Soc. B.* **372**. 20150486 https://doi.org/10.1098/RSTB.2015.0486

Peichel, C.L., Nereng, K.S., Ohgi, K.A., Cole, B.L.E., Colosimo, P.F., Buerklet, C.A., Schluter, D., Kingsley, D.M., 2001. The genetic architecture of divergence between threespine stickleback species. *Nature* **414**, 901–905. https://doi.org/10.1038/414901a

Pichaud, N., Chatelain, E.H., Ballard, J.W.O., Tanguay, R., Morrow, G., Blier, P.U., 2010. Thermal sensitivity of mitochondrial metabolism in two distinct mitotypes of

Drosophila simulans: evaluation of mitochondrial plasticity. *J. Exp. Biol.* **213**, 1665–1675. https://doi.org/10.1242/JEB.040261

Posada, D., 2008. jModelTest: Phylogenetic Model Averaging. *Mol. Biol. Evol.* **25**, 1253–1256. https://doi.org/10.1093/MOLBEV/MSN083

Rahn, A.K., Krassmann, J., Tsobanidis, K., MacColl, A.D.C., Bakker, T.C.M., 2016. Strong neutral genetic differentiation in a host, but not in its parasite. *Infect. Genet. Evol.* **44**, 261–271. https://doi.org/10.1016/J.MEEGID.2016.07.011

Ravinet, M., Harrod, C., Eizaguirre, C., Prod, P.A., Paulo Prod, C.A., 2013. Unique mitochondrial DNA lineages in Irish stickleback populations: cryptic refugium or rapid recolonization? *Ecol. Evol.* **4**, 2488–2504. https://doi.org/10.1002/ece3.853

Rodnick, K.J., Gamperl, A.K., Nash, G.W., Syme, D.A., 2014. Temperature and sex dependent effects on cardiac mitochondrial metabolism in Atlantic cod (*Gadus morhua L.*). *J. Therm. Biol.* **44**, 110–118. https://doi.org/10.1016/J.JTHERBIO.2014.02.012

Salin, K., Mathieu-Resuge, M., Graziano, N., Dubillot, E., Le Grand, F., Soudant, P., Vagner, M., 2021. The relationship between membrane fatty acid content and mitochondrial efficiency differs within- and between- omega-3 dietary treatments. *Mar. Environ. Res.* **163**, 105205. https://doi.org/10.1016/J.MARENVRES.2020.105205

Santucci, F., Emerson, B.C., Hewitt, G.M., 1998. Mitochondrial DNA phylogeography of European hedgehogs. *Mol. Ecol.* **7**, 1163–1172. https://doi.org/10.1046/j.1365-294x.1998.00436.x

Sanz, N., Araguas, R.M., Vidal, O., Viñas, J., 2015. Glacial refuges for three-spined stickleback in the Iberian Peninsula: mitochondrial DNA phylogeography. *Freshw. Biol.* **60**, 1794–1809. https://doi.org/10.1111/FWB.12611

Schneider, C.A., Rasband, W.S., Eliceiri, K.W., 2012. NIH Image to ImageJ: 25 years of image analysis. *Nat. Methods.* **9,** 671–675. https://doi.org/10.1038/nmeth.2089

Schwartz, T.S., Arendsee, Z.W., Bronikowski, A.M., 2015. Mitochondrial divergence between slow- and fast-aging garter snakes. *Exp. Gerontol.* **71**, 135–146. https://doi.org/10.1016/J.EXGER.2015.09.004

Sebastian, W., Sukumaran, S., Gopalakrishnan, A., 2022. Comparative mitogenomics of Clupeoid fish provides insights into the adaptive evolution of mitochondrial oxidative phosphorylation (OXPHOS) genes and codon usage in the heterogeneous habitats. *Heredity.* **128**, 236-249. https://doi.org/10.1038/s41437-022-00519-z

Singkam, A.R., MacColl, A.D.C., 2018. Otolith development in wild populations of stickleback: Jones & Hynes method does not apply to most populations. *J. Fish Biol.* **93**, 272–281. https://doi.org/10.1111/JFB.13687

Stamatakis, A., 2014. RAxML version 8: a tool for phylogenetic analysis and post-analysis of large phylogenies. *Bioinformatics.* **30**, 1312–1313. https://doi.org/10.1093/BIOINFORMATICS/BTU033

Tamura, K., Stecher, G., Kumar, S., 2021. MEGA11: Molecular Evolutionary Genetics Analysis Version 11. *Mol. Biol. Evol.* **38**, 3022–3027. https://doi.org/10.1093/MOLBEV/MSAB120

Thiel, T., Kota, R., Grosse, I., Stein, N., Graner, A., 2004. SNP2CAPS: a SNP and INDEL analysis tool for CAPS marker development. *Nucleic Acids Res.* **32**, e5. https://doi.org/10.1093/NAR/GNH006

Untergasser, A., Cutcutache, I., Koressaar, T., Ye, J., Faircloth, B.C., Remm, M., Rozen, S.G., 2012. Primer3—new capabilities and interfaces. *Nucleic Acids Res.* **40**, e115. https://doi.org/10.1093/NAR/GKS596

Vila, M., Hermida, M., Fernández, C., Perea, S., Doadrio, I., Amaro, R., Miguel, E.S., 2017. Phylogeography and Conservation Genetics of the Ibero-Balearic Three-Spined Stickleback (*Gasterosteus aculeatus*). *PLoS One.* **12**, e0170685. https://doi.org/10.1371/JOURNAL.PONE.0170685

Wang, C., Shikano, T., Persat, H., Merilä, J., 2015. Mitochondrial phylogeography and cryptic divergence in the stickleback genus *Pungitius*. *J. Biogeogr.* **42**, 2334–2348. https://doi.org/10.1111/JBI.12591

Wang, Y., Shen, Y., Feng, C., Zhao, K., Song, Z., Zhang, Y., Yang, L., He, S., 2016. Mitogenomic perspectives on the origin of Tibetan loaches and their adaptation to high altitude. *Sci. Rep.* **6**, 29690. https://doi.org/10.1038/srep29690

Wilson, A.B., Vincent, A., Ahnesjö, I., Meyer, A., 2001. Male Pregnancy in Seahorses and Pipefishes (Family Syngnathidae): Rapid Diversification of Paternal

Brood Pouch Morphology Inferred From a Molecular Phylogeny. *Heredity.* **92**, 159–166. https://doi.org/10.1093/JHERED/92.2.159

Yonezawa, T., Mannen, H., Honma, K., Matsunaga, M., Rakotondraparany, F., Ratsoavina, F.M., Wu, J., Nishibori, M., Yamamoto, Y., 2024. Origin and spatial population structure of Malagasy native chickens based on mitochondrial DNA. *Sci. Rep.* **14**, 569. https://doi.org/10.1038/s41598-023-50708-x

Zhao, D., Guo, Y., Gao, Y., 2022. Natural selection drives the evolution of mitogenomes in Acrossocheilus. *PLoS One* **17**: e0276056. https://doi.org/10.1371/journal.pone.0276056

4.7 Supplementary Material

Table S4.1: Latitude, longitude and the number of samples per population. Stickleback were either sampled for the present study (North Uist, Portugal, Iceland), sent from collaborators (Newfoundland, Nova Scotia, Quebec), or were compiled from the literature (see **Table 4.2** for original papers). N.A = North America.

Population	Region	Continent	Latitude	Longitude	n
F_S1	France	Europe	47.491390	6.770830	1
Antela	Ibero-Balearic	Europe	42.115660	-7.683950	9
Asma	Ibero-Balearic	Europe	42.834410	-8.574940	5
Castanos	Ibero-Balearic	Europe	43.317000	-3.009100	1
Gobelas	Ibero-Balearic	Europe	43.319020	-2.994590	1
Guisande	Ibero-Balearic	Europe	42.840160	-8.680410	5
Majorca	Ibero-Balearic	Europe	39.802590	3.120570	3
Mira	Ibero-Balearic	Europe	37.607220	-8.658310	2
Mondego	Ibero-Balearic	Europe	40.371900	-8.071130	3
Penyscola	Ibero-Balearic	Europe	40.350920	0.375440	3
Rato	Ibero-Balearic	Europe	42.535630	-7.832780	4
Sado	Ibero-Balearic	Europe	38.004520	-8.387930	3
Salas	Ibero-Balearic	Europe	41.921770	-8.013190	1
Tagus	Ibero-Balearic	Europe	39.024190	-8.829920	3
Txingudi	Ibero-Balearic	Europe	43.363770	-1.780960	1
Valencia	Ibero-Balearic	Europe	39.412240	-0.384940	3
Vouga	Ibero-Balearic	Europe	40.663170	-8.561490	8
Egg1	Iceland	Europe	66.485820	-15.931577	4
Egg2	Iceland	Europe	66.485559	-15.930343	6
Egg3	Iceland	Europe	66.485538	-15.929624	4
Herd	Iceland	Europe	63.866801	-21.818869	13
Hrin	Iceland	Europe	66.506888	-15.975552	16
MIDF	Iceland	Europe	65.324212	-20.895125	5
MIDF_M	Iceland	Europe	65.343095	-20.906488	5
Nes1	Iceland	Europe	66.481013	-15.926585	4
Nes2	Iceland	Europe	66.481026	-15.925622	17
URRI	Iceland	Europe	64.068169	-21.909467	1
VIFC	Iceland	Europe	64.079367	-21.877461	1
VIFR	Iceland	Europe	64.079367	-21.877461	1
AIB	Ireland	Europe	53.293900	-9.542100	4
ANN	Ireland	Europe	53.556900	-10.09300	4
BAN	Ireland	Europe	53.182300	-7.998100	4
BON	Ireland	Europe	54.265700	-8.216700	4
BUR	Ireland	Europe	52.744000	-6.813800	2
BWL	Ireland	Europe	52.675600	-8.577300	2
CAM	Ireland	Europe	53.286300	-9.559400	5
CCO	Ireland	Europe	53.447600	-8.858700	1
CRN	Ireland	Europe	51.817000	-10.115000	4

CUR	Ireland	Europe	51.895900	-8.545900	2
DER	Ireland	Europe	51.888500	-10.033000	1
FEE	Ireland	Europe	53.929800	-9.574500	3
FER	Ireland	Europe	55.009100	-7.347100	4
FUR	Ireland	Europe	53.905500	-9.578100	5
GCR	Ireland	Europe	54.337900	-8.387300	5
GIL	Ireland	Europe	52.259900	-10.035000	4
GLC	Ireland	Europe	53.662100	-9.772400	3
GLN	Ireland	Europe	54.588300	-6.240600	2
GMO	Ireland	Europe	54.243200	-9.700800	1
LEN	Ireland	Europe	53.661300	-7.230300	4
LIL	Ireland	Europe	52.202900	-6.393300	6
LWR	Ireland	Europe	53.471400	-9.101000	4
NAM	Ireland	Europe	51.878600	-10.032000	5
ROB	Ireland	Europe	52.596100	-9.065600	6
SFD	Ireland	Europe	54.463600	-5.608500	6
TAC	Ireland	Europe	52.197500	-6.459900	4
TAL	Ireland	Europe	54.076600	-8.918400	3
TUL	Ireland	Europe	53.134500	-6.905700	5
TYS	Ireland	Europe	52.339800	-9.819600	4
UBD	Ireland	Europe	51.742400	-8.819900	2
LAMH	Mainland Scotland	Europe	56.894405	-5.868758	1
LANO	Mainland Scotland	Europe	56.994805	-5.806989	1
LMOR	Mainland Scotland	Europe	56.961656	-5.793240	1
LNEA	Mainland Scotland	Europe	56.906266	-5.832262	1
MEA	Mainland Scotland	Europe	57.605390	-6.176790	4
RCAL	Mainland Scotland	Europe	56.865705	-5.418379	1
SHEL	Mainland Scotland	Europe	56.757787	-5.744810	1
TYNE	Mainland Scotland	Europe	55.989227	-2.634747	5
TYNE_M	Mainland Scotland	Europe	56.004868	-2.603196	5
10GEA	North Uist	Europe	57.642780	-7.421670	4
11MGB	North Uist	Europe	57.601670	-7.410000	2
19EIL	North Uist	Europe	57.573330	-7.258330	2
ACHA	North Uist	Europe	57.595830	-7.395000	3
ARDH	North Uist	Europe	57.580000	-7.413330	6
AROI	North Uist	Europe	57.595000	-7.430000	2
BHAR	North Uist	Europe	57.570513	-7.301183	13
BHRU/BHRM[1]	North Uist	Europe	57.726658	-7.174834	15/29
BHRUST[3]	North Uist	Europe	57.714761	-7.190764	10
BUAI	North Uist	Europe	57.646698	-7.198228	11
CAIG/CAIM[1]	North Uist	Europe	57.634399	-7.113622	15/3
CEIT	North Uist	Europe	57.578464	-7.258303	10
CHRU	North Uist	Europe	57.594060	-7.197733	11
CLAC/CLAM[1]	North Uist	Europe	57.637635	-7.414877	11/26
DAIM	North Uist	Europe	57.593060	-7.209720	3
DUBH	North Uist	Europe	57.581670	-7.403330	4
DUIN/DUIM[1]	North Uist	Europe	57.643060	-7.211110	20/22

EUBH	North Uist	Europe	57.618330	-7.495000	11
FADA	North Uist	Europe	57.621483	-7.220838	8
FAIK/FAIM[1]	North Uist	Europe	57.635280	-7.215000	17/14
GROG/GROM[1]	North Uist	Europe	57.615186	-7.510884	11/6
HOST	North Uist	Europe	57.626333	-7.491277	30
IALA	North Uist	Europe	57.620006	-7.205617	10
LUIB/LUIM[1]	North Uist	Europe	57.554330	-7.312329	8/10
MAGA	North Uist	Europe	57.602780	-7.481670	4
MAIG	North Uist	Europe	57.595000	-7.201670	11
MORA	North Uist	Europe	57.575000	-7.271670	2
MORB	North Uist	Europe	57.537269	-7.364290	10
OBSE/OBSM[1]	North Uist	Europe	57.601670	-7.172780	11/10
OLAV/OLAM[1]	North Uist	Europe	57.652038	-7.447717	22/14
OLST[3]	North Uist	Europe	57.653439	-7.440187	10
REIV	North Uist	Europe	57.611328	-7.514678	21
SANN	North Uist	Europe	57.587980	-7.463170	13
SCAD	North Uist	Europe	57.585000	-7.236110	13
STRA	North Uist	Europe	57.610000	-7.183610	2
STRM	North Uist	Europe	57.610000	-7.183610	5
TORM	North Uist	Europe	57.562500	-7.316940	15
TOST[3]	North Uist	Europe	57.559890	-7.320791	9
TROS	North Uist	Europe	57.583967	-7.413632	10
TRST[3]	North Uist	Europe	57.582787	-7.418870	10
TRUF/TRUM[1]	North Uist	Europe	57.652500	-7.243060	10/6
ALM2	Portugal	Europe	39.504722	-8.615028	5
ANC1	Portugal	Europe	41.810194	-8.861222	5
ANSO	Portugal	Europe	39.978750	-8.573028	5
CAPE	Portugal	Europe	37.645889	-8.568861	5
CORU	Portugal	Europe	40.371472	-8.712028	5
RIMA	Portugal	Europe	38.594139	-8.646722	5
Torgal	Portugal	Europe	37.640000	8.610000	1
AGS1	Switzerland	Europe	47.577780	7.838060	1
AGS2	Switzerland	Europe	47.405830	8.083610	1
AGS3	Switzerland	Europe	47.586670	8.228610	4
BEL1	Switzerland	Europe	46.966390	7.352220	4
BEL2	Switzerland	Europe	46.967500	7.396940	4
BEL3	Switzerland	Europe	47.082500	7.199720	4
BEP1	Switzerland	Europe	46.956940	7.389170	4
BES1	Switzerland	Europe	47.084170	7.409440	2
BES2	Switzerland	Europe	46.983060	7.253060	4
BES3	Switzerland	Europe	46.961390	7.379440	3
BLP1	Switzerland	Europe	47.451390	7.928330	3
GES1	Switzerland	Europe	46.179720	6.008890	2
SGL1	Switzerland	Europe	47.483890	9.559720	3
SGP1	Switzerland	Europe	47.478610	9.558330	3
SGS1	Switzerland	Europe	47.325830	9.575280	3
VDL1	Switzerland	Europe	46.777780	6.641670	5

VDL2	Switzerland	Europe	46.517220	6.578060	3
VDS2	Switzerland	Europe	46.778610	6.626670	5
VSS1	Switzerland	Europe	46.213890	7.314720	4
VSS2	Switzerland	Europe	46.384720	6.853610	3
ZHS1	Switzerland	Europe	47.442780	8.468330	3
Kob_L31	Greenland	N.A	64.131047	-51.371717	1
Kob_L32	Greenland	N.A	64.131047	-51.371717	1
Kob_L33	Greenland	N.A	64.131047	-51.371717	1
Kob_M26	Greenland	N.A	64.137992	-51.390978	1
Kob_M27	Greenland	N.A	64.137992	-51.390978	1
Kob_M28	Greenland	N.A	64.137992	-51.390978	1
Qar_L31	Greenland	N.A	63.991000	-51.446000	1
Qar_L33	Greenland	N.A	63.991000	-51.446000	1
Qar_L35	Greenland	N.A	63.991000	-51.446000	1
BPNF	Newfoundland	N.A	48.782569	-58.082483	5
CBNF	Newfoundland	N.A	48.971542	-58.066864	5
HANF	Newfoundland	N.A	49.011414	-58.134500	5
ANNS	Nova Scotia	N.A	45.631092	-61.960575	5
Baddeck[2]	Nova Scotia	N.A	46.095856	-61.088890	10
Blues Cove	Nova Scotia	N.A	45.900598	-61.088890	10
Canal Lake 2019[2]	Nova Scotia	N.A	44.497959	-63.901367	20
Cherry Burton 2019	Nova Scotia	N.A	46.029800	-64.103064	19
PLNS	Nova Scotia	N.A	45.624031	-61.839383	5
PPNS	Nova Scotia	N.A	45.440244	-61.320600	5
MAI	Penebscot bay	N.A	44.366700	-68.900000	8
a Foin	Quebec	N.A	47.764600	-61.088890	6
Croche	Quebec	N.A	47.777400	-61.088890	6
Rond	Quebec	N.A	47.749500	-61.088890	5
Temiscouata	Quebec	N.A	47.687700	-61.088890	5
LLYD	USA	N.A	41.520986	-70.981427	1

[1] North Uist sympatric species pairs, population name ending in ‘M’ refers to anadromous stickleback.

[2] White stickleback from Nova Scotia.

[3] Stream populations from North Uist.

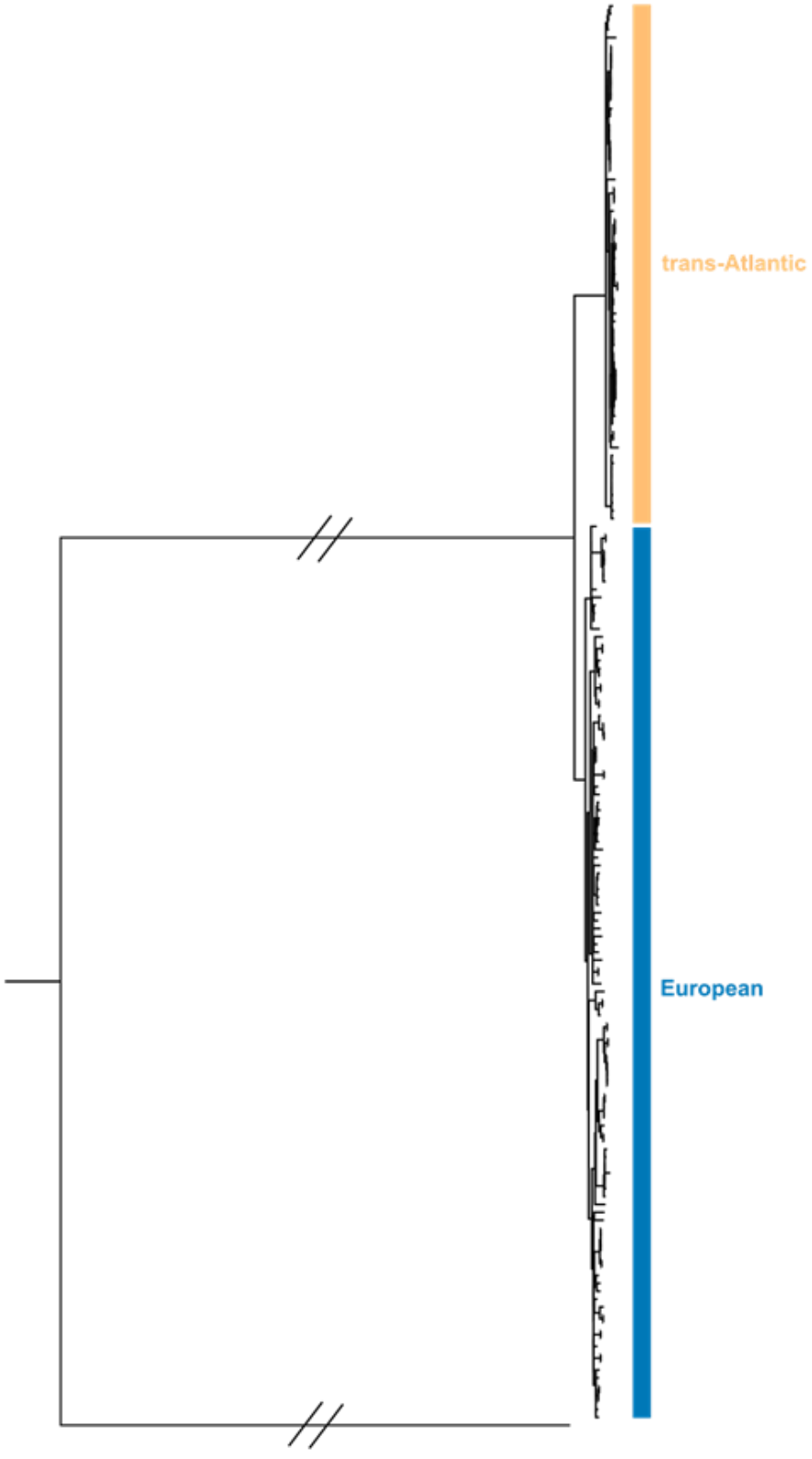

Figure S4.1: Maximum likelihood phylogenetic tree. Constructed using RAxML from the mitogenomes of 180 North Uist stickleback with *G. wheatlandi* as an outgroup. Two main clades are labelled.

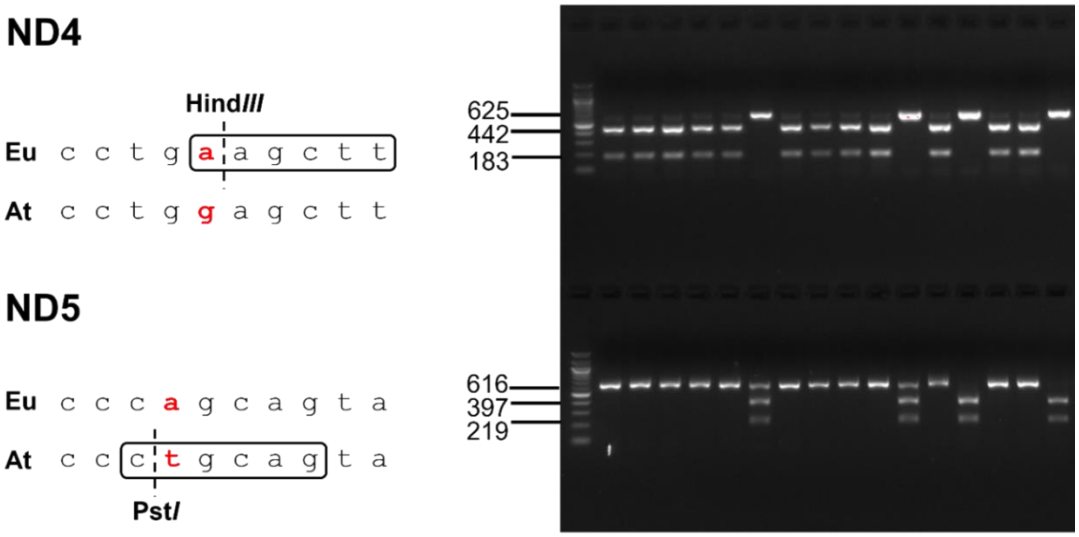

Figure S4.2: DNA sequences and example gel used to distinguish mitochondrial lineages. Regions of ND4 and ND5 have a fixed difference between *Eu* and *At* mtDNA (left, shown in red). The restriction site recognised by Hind*III* or Pst*I* is circled and the restriction enzyme cut site is shown by the dashed line. *Eu* ND4 is cut by Hind*III* and *At* ND5 is cut by Pst*I.* ND4 and ND5 were first amplified using specific primers (see **Table 4.1**) resulting in 625bp and 616bp DNA fragments, respectively. These were digested with the appropriate restriction enzyme and run on a 2% agarose gel (right). 100bp ladder (NEB) in the left lane followed by 16 stickleback samples from Luib or LuiM, North Uist (see **Figure 4.1** and **Table S4.1** for location). The same samples are aligned in the top and bottom sections of the gel. Top section shows ND4 PCR followed by restriction enzyme digest with Hind*III* which results in one band (625bp) for *At* mtDNA and two bands (442 and 183bp) for *Eu* mtDNA. Bottom sections shows ND5 PCR and restriction enzyme digest with Pst*I,* with one band (616bp) for *Eu* mtDNA and two bands for *At* mtDNA (397 and 219bp). Results were used when both the ND4 and ND5 assay gave consistent results.

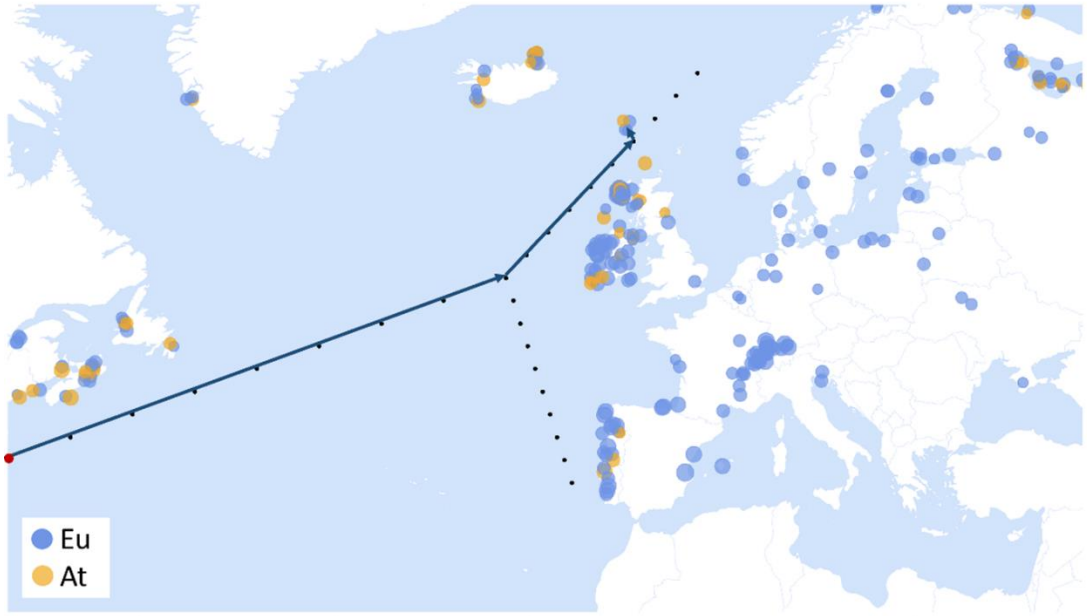

Figure S4.3: Map of the Atlantic showing locations of *Eu* (blue) and *At* (orange) stickleback. Black points show the predicted ocean currents in the Atlantic and were used to calculate distance from most western point in North America, shown in red. Example of distance calculation shown by arrows: distance from North America (red point) to the nearest point on the path to the sampling location + direct distance from sampling location to nearest point on the path = total distance from North America. All distances are great circle distances and all calculations were conducted in R.

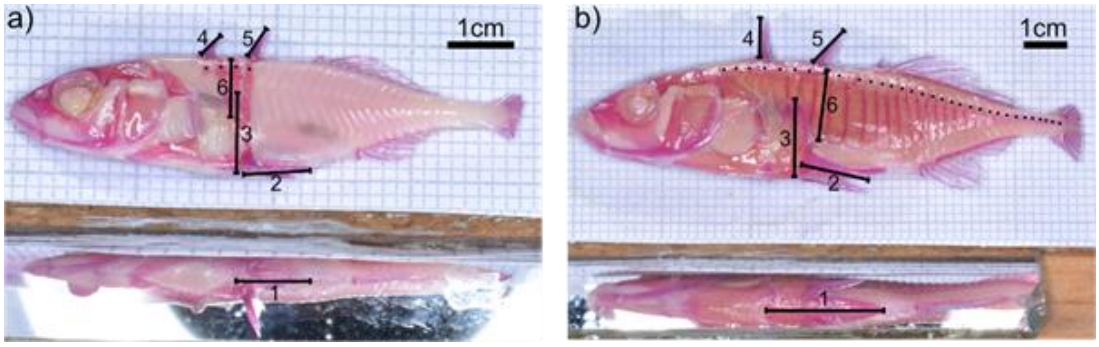

Figure S4.4: Armour measurements from low (a) and completely (b) plated stickleback stained with alizarin red. Measurements were made using ImageJ. 1. Pelvis length. 2. Pelvic spine length. 3. Pelvis height. 4. First dorsal spine length. 5. Second dorsal spine length. 6. Longest plate length. Each individual plate is marked with a dot.

Table S4.2: Factors affecting the proportion of stickleback with the *At* mitochondrial haplotype in populations across the North Atlantic, excluding North Uist. Results are from a binomial generalised linear model with logit link modelling the number of *At* fish per population (successes) with the distance from North America, salinity, and the interaction of distance and salinity as predictors. 204 populations were included in the model. Values in bold are significant at the 5% significance level.

Predictor	Wald F	d.f	P-value
Distance	1.602	1,201	0.207
Salinity	34.004	1,201	**< 0.001**
Distance x Salinity	6.8197	1,201	**0.010**

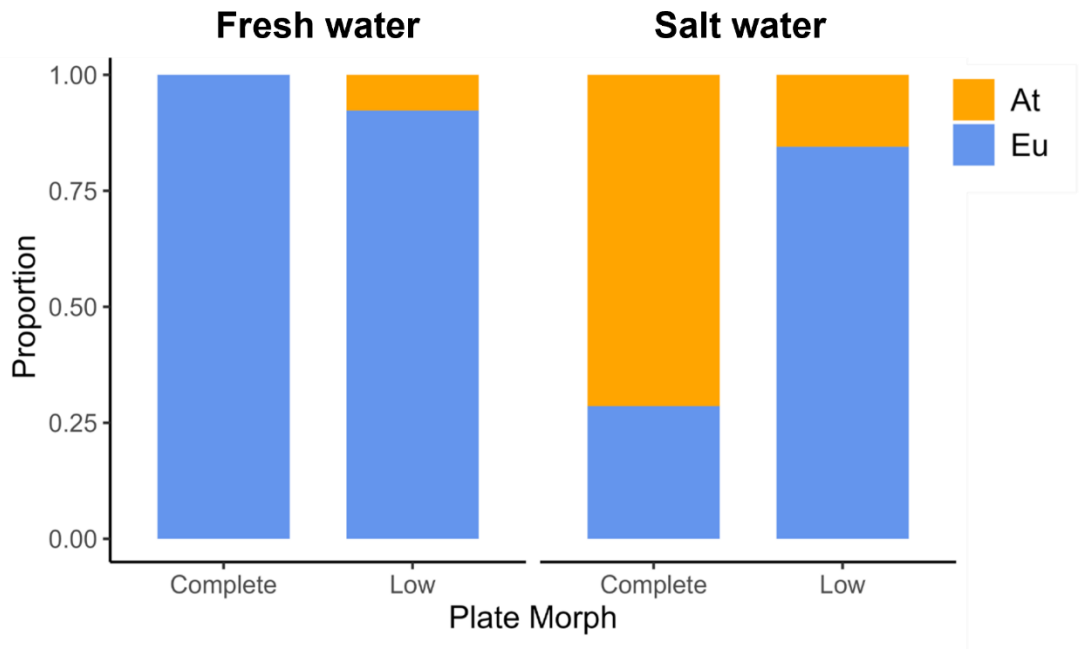

Figure S4.5: The proportion of *Eu* and *At* lineage stickleback that were complete or low plated in fresh water and salt water, excluding samples from North Uist. n = 779 and 191 individuals for fresh water and salt water respectively. Saltwater fish are defined as those that spend some or all of their lives in salt water. Freshwater fish reside permanently in fresh water.

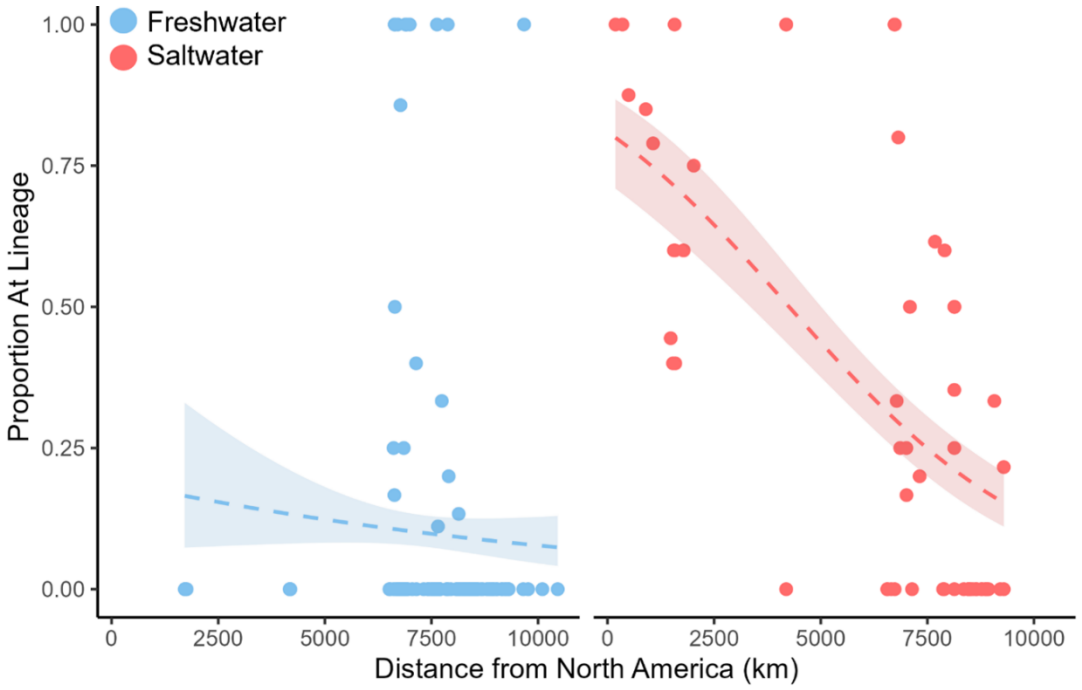

Figure S4.6: Change in the proportion of *At* stickleback with distance from North America in freshwater and saltwater populations, excluding North Uist. Each point is a freshwater (light blue) or saltwater (red) population. Dashed line shows binomial generalised linear model with the proportion of *At* stickleback per population as a function of distance from North America. Shading shows standard error. n = 145 and 59 freshwater and saltwater populations respectively.

Table S4.3: SST parameters affecting the proportion of stickleback with the *At* mitochondrial haplotype in saltwater populations across the North Atlantic, excluding North Uist. Results of the generalised linear models assessing the effects of distance and three SST parameters (maximum, minimum and variation in SST) on the proportion of *At* stickleback per saltwater population. All models were compared to a generalised linear model with only distance as a predictor. d.f = degrees of freedom. Values in bold are significant at $p < 0.05$. n = 59 populations.

Predictor	AIC	BIC	Wald F	d.f	P-value
Maximum SST	146.151	152.383	23.326	1,57	**< 0.001**
Minimum SST	173.382	179.615	0.112	1,57	0.7392
Variation in SST	159.869	166.102	12.368	1,57	**< 0.001**

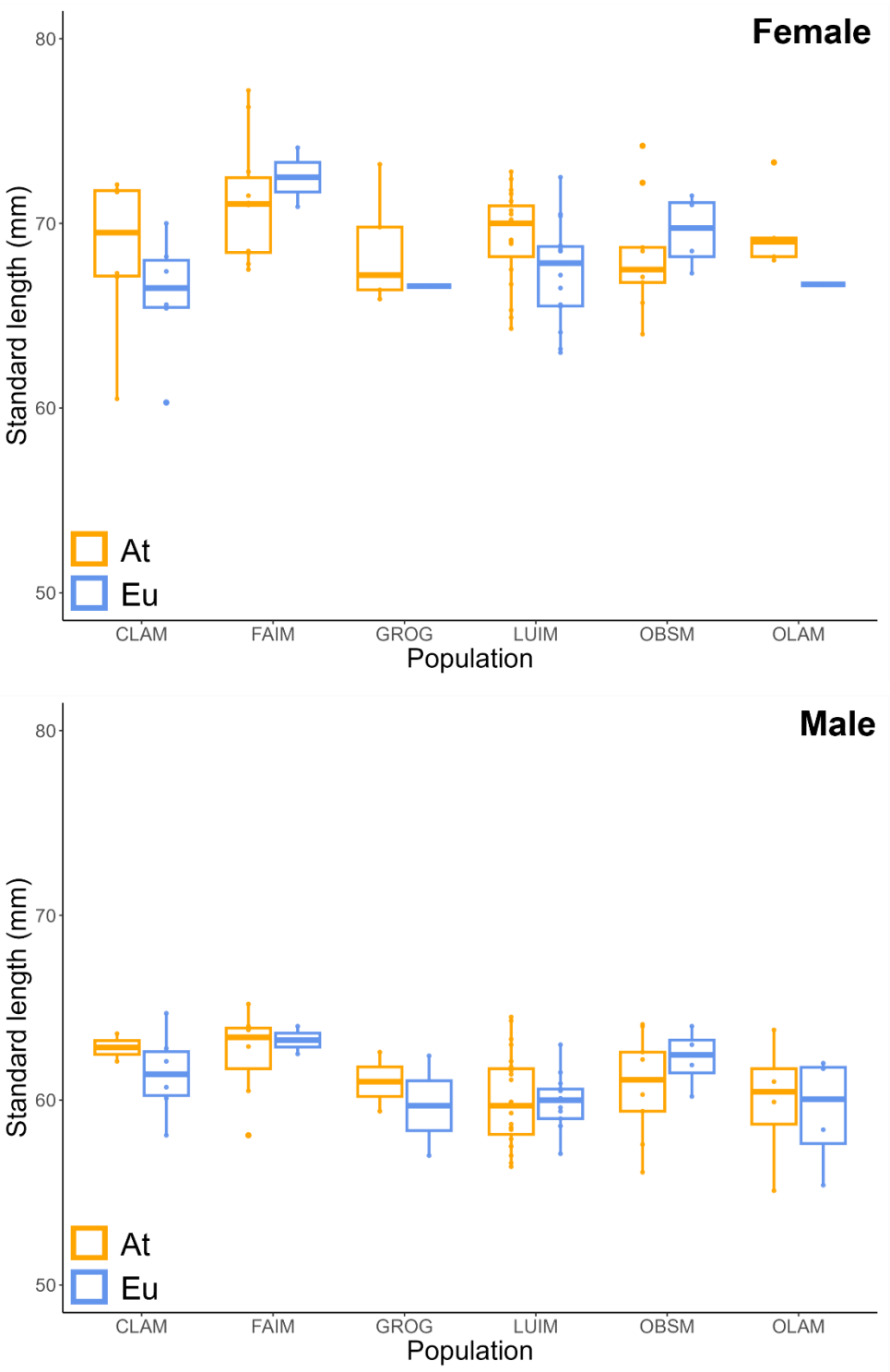

Figure S4.7: Standard length differences between *Eu* and *At* anadromous stickleback from six North Uist populations. Populations with an approximately equal mix of individuals of the *Eu* and *At* lineages were used for this comparison. Boxplot shows median and interquartile range, points show individual data points. n = 83 and 78 individuals for females and males respectively. See **Figure 4.1** and **Table S4.1** for sampling locations.

Chapter 5: Positive Selection in the Mitochondrial Protein Coding Genes of the Three-spined Stickleback

5.1 Abstract

Mitochondrial sequences were once considered neutral markers but increasing evidence suggests that they are adaptive, and mtDNA variation has been associated with climate, altitude and diet. As the mitochondrial genes encode components of the oxidative phosphorylation pathway in the mitochondrial inner membrane which is responsible for the majority of a cells aerobic energy production, any changes in sequence have the potential to alter mitochondrial function, and environments with differing metabolic requirements may drive how selection acts on the mtDNA. There are two well studied mitochondrial lineages of the three-spined stickleback in the Atlantic which differ in frequency between migratory and freshwater resident populations. To test whether the evolution of stickleback mitochondrial lineages and freshwater colonisation was accompanied by selection acting on mitochondrial function, we assembled and analysed stickleback mitogenomes. Using multiple phylogenetic selection analyses to test for signatures of positive selection across the protein-coding mitochondrial genes, we identified candidate sites in the complex I genes with evidence of long-term selection that were predicted to alter protein structure, and found sites specific to one lineage evolving under selection that may have accompanied their adaptation to fresh water. This not only adds to the increasing evidence that mitochondrial sequences are non-neutral, but demonstrates the potential role of the mitochondria in adaptive processes.

5.2 Introduction

The mitochondrial genome has long been used as a neutral marker of population structure (Avise et al., 1987; Moritz et al., 1987), becoming a useful tool in population genetics due to its maternal inheritance (Giles et al., 1980), lack of recombination (Ladoukakis and Zouros, 2017), elevated mutation rates (Sigurdardóttir et al., 2000) and multiple copies per cell (Smeitink et al., 2001). The mitochondrial DNA was considered selectively neutral (Avise et al., 1987), but this assumption is no longer widely accepted (Ballard and Kreitman, 1995) and increasing evidence suggests that it may be adaptive (da Fonseca et al., 2008; Li et al., 2018; Zhao et al., 2022). Given

the functional importance of the mitochondrially encoded proteins, it is necessary to understand the evolution of mtDNA, including how natural selection may promote sequence variation. Mitochondria are responsible for greater than 95% of a cells energy production in the form of adenosine triphosphate (ATP) via the process of oxidative phosphorylation (OXPHOS) (Nguyen et al., 2019), which depends on the cooperation of the 13 mitochondrially encoded peptides with at least 70 more nuclear encoded peptides (Smeitink et al., 2001). Variation in mtDNA sequence can therefore have important functional consequences for fitness, and environments with differing metabolic requirements may drive how selection acts on the mtDNA and mitochondrial function.

Purifying selection is the main driver of mtDNA evolution (Popadin et al., 2013) but variation in mtDNA sequence has often been linked to the environment (Baris et al., 2016; Camus et al., 2017; Scott et al., 2011), suggesting that it may be adaptive. Evidence of positive selection has been identified in the mitochondrial protein coding genes (PCGs) and has been associated with high-altitude adaptation (Cheviron et al., 2012; Lui et al., 2015; Wang et al., 2016; Yu et al., 2011; Zhou et al., 2014), latitudinal clines (Foote et al., 2011b; Garvin et al., 2011) and diet (Aw et al., 2018; Ballard and Youngson, 2015; Towarnicki and Ballard, 2018). Such studies have often compared populations from two contrasting environments and identified sites with evidence of positive selection by calculating ω, the ratio of non-synonymous to synonymous mutations, using codon-based or maximum likelihood approaches, or by assessing the physiochemical properties of amino acid substitutions. Inferring the mechanism by which the positively selected sites may impact mitochondrial function is more difficult, although this has been assessed in more recent cases (Zhang et al., 2024) as the structure of the respiratory complexes become better resolved, for example in Pacific salmon (genus *Oncorhynchus*) (Garvin et al., 2011) where multiple sites in the piston arm of complex I were found to evolve under positive selection and were hypothesised to be involved in proton pumping (Garvin et al., 2011). No study of the functional consequences of these amino acid substitutions has been conducted, and as species with diverse phenotypes were assessed (Garvin et al., 2011), the nuclear genome will also influence mitochondrial function (Hill, 2020). Ideal models to be able to identify positively selected sites in the mitochondrial genome and then determine the physiological impacts of these include populations where mtDNA variants segregate within otherwise panmictic populations, minimising differences in the nuclear genetic background (Baris et al., 2016).

The three-spined stickleback (*Gasterosteus aculeatus,* 'stickleback') is widely distributed over the Northern Hemisphere where it has repeatedly adapted to colonise freshwater environments (Bell and Foster, 1995; Jones et al., 2012). There are two well-studied stickleback mitochondrial clades: the Trans-North Pacific (TNP) or 'Japanese' clade which is found predominantly in the western Pacific, and the Euro-North American (ENA) clade which is found throughout Europe and along both the west and east coast of North America (Beck et al., 2022; Johnson and Taylor, 2004; Ortl et al., 1994; Taylor et al., 1999). Here, we assess the phylogenetic structure within the ENA clade, including two lineages from the Pacific Ocean that we term the Pacific South (*PS*) and Pacific North (*PN*), and two well-studied lineages in the Atlantic: the European (*Eu*) and trans-Atlantic (*At*) (Mäkinen and Merilä, 2008). Divergence times have been previously estimated (Dean et al., 2019; Fang et al., 2018; Mäkinen and Merilä, 2008; Ravinet et al., 2013) suggesting that the Atlantic Ocean was colonised from the Pacific via the Arctic Ocean (Fang et al., 2018; Orti et al., 1994). During the Pleistocene, repeated glaciations influenced the distribution of aquatic species, including the stickleback. In the Atlantic, it is likely that the *Eu* and *At* lineages evolved in allopatry, and evidence suggests that *Eu* stickleback survived in refugia in Southern Europe (Defaveri et al., 2012; Fang et al., 2018; Mäkinen and Merilä, 2008; Sanz et al., 2015), but less is known about the origin of the *At* lineage. As the *At* lineage has predominantly been found in North America (Mäkinen and Merilä, 2008), we have previously hypothesised and provided evidence for a refugium where *At* stickleback diverged along the East Coast of North America (Chapter 4). This has resulted in two highly diverged mitochondrial lineages in the Atlantic (*Eu* and *At*) which have since spread (Dean et al., 2019; Liu et al., 2016; Mäkinen and Merilä, 2008; Ravinet et al., 2013).

The frequencies of Atlantic stickleback mitochondrial lineages differ between migratory and resident populations in North Uist, Scottish Western Isles (Dean et al., 2019), and this persists across the Atlantic (Chapter 4). Migratory populations contain fish with either the *Eu* or *At* mtDNA (Dean et al., 2019) but are otherwise panmictic (Haenel et al., 2022), but it is predominantly the *Eu* lineage that resides permanently in fresh water and brackish lagoons (Chapter 4, Dean et al., 2019a). Migratory and resident lifestyles differ in energy requirements, and the Atlantic Ocean and fresh or brackish water differ greatly in many environmental parameters including temperature and food sources that may also alter metabolic requirements. Shallow freshwater lakes and streams are influenced greatly by climate and will fluctuate in temperature more than the Atlantic Ocean, likely resulting in selection promoting amino acid

variants that allow the metabolic machinery to be efficient at a large range of temperatures. Food sources also differ between environments; in fresh water, diets are often lower in key nutrients than in the sea (Ishikawa et al., 2021; Twining et al., 2021) which may alter how substrates are utilised in the mitochondria to produce energy, while starvation has been shown to increase the coupling efficiency of mitochondria in birds (Monternier et al., 2015, 2014). Low food availability may therefore result in selection for mitochondrial genome variation that provides the most efficient ATP production with limited or specific resources.

As it is predominantly the *Eu* lineage that has colonised fresh water and brackish lagoons (Chapter 4, Dean et al., 2019), and the two lineages have different histories, it is likely that *Eu* and *At* stickleback have evolved under different selective pressures. The two mitochondrial lineages likely evolved in allopatry on opposite sides of the Atlantic Ocean (Chapter 4, Mäkinen and Merilä, 2008) where they will have experienced different environmental conditions. During the last glacial maximum (LGM) in Europe, the ice sheets covered most of the UK and Scandinavia but did not reach Southern England and mainland Europe (Svendsen et al., 2004), providing opportunity for *Eu* stickleback to get into fresh water. In comparison, a large proportion of the East Coast of North America was covered by ice (Dyke and Prest, 1987), presumably severely restricting the potential distribution of *At* stickleback in fresh water. Natural selection may have acted on mitochondrial sequence variation during this period of allopatry. The *At* lineage is descendent from stickleback that have crossed the Atlantic Ocean where they may have experienced prolonged colder temperatures, while the *Eu* lineage has likely spent more of its history as resident populations (Dean et al., 2019a; Mäkinen and Merilä, 2008). This may have resulted in different selective agents driving mitogenome divergence between the lineages. As a result, the *Eu* lineage may be better adapted to reside permanently in freshwater and brackish environments, while the *At* lineage is more suited to a migratory lifestyle. If positive selection was acting on mitochondrial PCGs when the lineages were in allopatry, we would expect to find evidence of long-term positive selection or selection along the branches near to the *Eu* and *At* split that have resulted in sites with almost fixed differences between *Eu* and *At* fish. In addition, as it is predominantly the *Eu* lineage that has colonised fresh and brackish water, we hypothesised that there may be evidence of natural selection specific to the *Eu* lineage, where beneficial genotypes and phenotypes for the colonisation of fresh water and adaptation to the local environment would be selected for.

To test whether the evolution of stickleback mitochondrial lineages and freshwater colonisation was accompanied by selection acting on mitochondrial function, we assembled and analysed the mitogenomes of stickleback from four known mitochondrial lineages: *PN*, *PS*, *Eu* and *At*. We used different approaches including those based on the ratio of non-synonymous to synonymous mutations (dN/dS) and those using the physiochemical properties of amino acids to test for signatures of positive selection across the protein-coding mitochondrial genome. We identified sites in the complex I genes with evidence of long-term selection that are predicted to alter protein structure, as well as finding sites specific to the *Eu* lineage evolving under natural selection that may have accompanied their adaptation to fresh water. This not only adds to the increasing evidence that mitochondrial sequences are non-neutral, but demonstrates the potential role of the mitochondria in adaptive processes.

5.3 Methods

5.3.1 Sample collection and DNA extraction

We were able to assemble mitogenomes from samples previously obtained for other projects. Briefly, three-spined stickleback were sampled from multiple lochs on North Uist in the Western Isles of Scotland in May 2022 by setting mesh traps along the perimeter (see **Figure 5.1** and **Table S5.1** for sampling locations). After 24 hours, approximately 10 stickleback per population were collected and euthanised via an overdose of tricaine methanesulfonate (400mg/L) followed by the destruction of the brain according with Schedule One of UK Home Office regulations. Caudal and pectoral fin clips were taken and stored in ethanol for later DNA extraction. We also received additional samples from Canada (Nova Scotia and Quebec), Maine (Lubec), Iceland and Portugal (**Table S5.1**). Sampling included both resident and migratory stickleback. Qiagen 96-well DNeasy blood and tissue extraction kit was used to extract DNA from North Uist, Iceland and Portugal samples; NEB Monarch genomic DNA purification kit was used for all other samples. Samples were sequenced using Illumina sequencing technology.

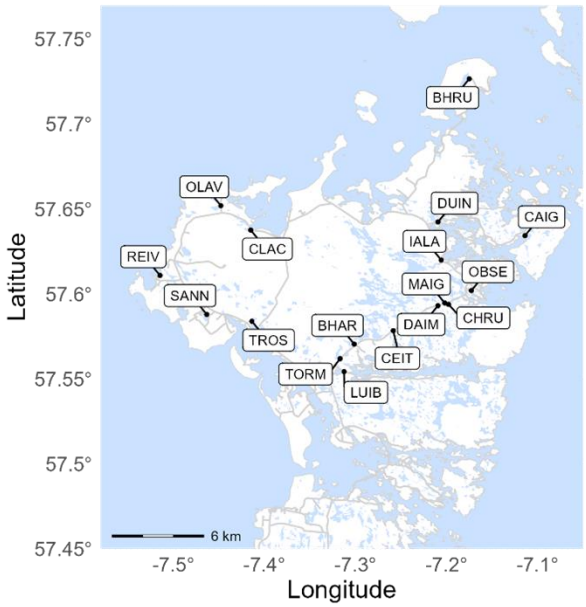

Figure 5.1: Sampling location in North Uist, Scottish Western Isles. See **Table S5.1** for specific coordinates.

5.3.2 Mitogenomes

We assembled the mitogenomes of 253 samples covering a wide range of the stickleback's distribution in the Atlantic (*Eu* and *At* lineages), as well as 27 samples from the Pacific, including the *PN* and *PS* lineages and the Japan Sea stickleback (*Gasterosteus nipponicus*). Mitochondrial reads were assembled using NOVOPlasty (Dierckxsens et al., 2017) which assembles mitogenomes from whole genome sequencing data. Protein coding nucleotide sequences were aligned using MAFFT (Katoh et al., 2019) and translated into amino acid sequences using MEGA11 (Tamura et al., 2021). DnaSPv6 (Rozas et al., 2017) was used to calculate the nucleotide diversity of each gene and the ratio of non-synonymous to synonymous mutations (dN/dS) was calculated using PAML model M0, which assumes one dN/dS across branches and sites (Álvarez-Carretero et al., 2023; Yang, 2007). A subset of 99 sequences was randomly selected for phylogenetic reconstruction and detection of positive selection. We first confirmed that there was no evidence of recombination in the mtDNA sequences using GARD (Pond et al., 2006), implemented in the datamonkey interface (Weaver et al., 2018).

5.3.3 Phylogenetic analysis

PCGs were concatenated using PhyKIT (Steenwyk et al., 2021) with a total length of 11,415bp excluding stop codons, and the best partitioning of the concatenated sequences was obtained according to IQTREE (Minh et al., 2020) with the optimal

evolutionary model for each partition (Chernomor et al., 2016; Kalyaanamoorthy et al., 2017) selected using Bayesian information criterion (BIC). We used IQTREE to implement a maximum likelihood method to assess phylogenetic relationships with *G. nipponicus* as an outgroup.

5.3.4 Detection of positive selection

Selection analysis was performed using the 13-protein coding mitochondrial genes. We utilised methods based on the ratio of non-synonymous to synonymous substitutions (dN/dS), first using the CODEML package implemented in PAML (Yang, 2007).

5.3.4.1 CODEML branch models

To test whether stickleback lineages evolved under different selective pressures, we first implemented branch models in CODEML. We compared the branch model which allows ω (dN/dS) to vary between branches to the null model M0 which assumes the same ω for all branches using a likelihood ratio test (LRT), which is twice the difference in log-likelihood between null and alternative hypotheses, compared with the χ^2 distribution. To test whether ω varied between mitochondrial genes, we fitted branch models for each gene individually as well as to the concatenated PCGs. We first defined the Atlantic lineages (*Eu* and *At*) as the foreground to test whether selective pressures differed between the Atlantic and Pacific. Then, to assess whether ω differed between lineages in the Atlantic, we defined either the *Eu* or *At* lineage as the foreground.

5.3.4.2 RELAX

As an increase in ω can suggest relaxed selection as well as positive selection (Zwonitzer et al., 2023), we used the RELAX package (Wertheim et al., 2015) implemented in HyPhy (Kosakovsky Pond et al., 2005) to predict whether selection in the foreground ('test') lineage was intensified or relaxed compared to the rest of the phylogeny. If selection is intensified, some sites experience strong positive selection (ω much greater than 1) while other sites are under strong purifying selection (ω much less than 1), so the distribution of ω diverges. When selection is relaxed, ω converges towards 1. RELAX compares the distribution of ω across sites in the test lineage to the reference, determining the selection intensity parameter k. This is compared to a model where there is a single distribution of ω across all branches (k = 1) using a LRT. When introducing k significantly improves the model fit, selection on the test lineage is either intensified (k > 1) or relaxed (k < 1) compared to the reference. As with CODEML branch models, we conducted RELAX analysis on each mitochondrial

gene individually and on the concatenated PCGs, first defining both the *Eu* and *At* as the test branches with the rest of the phylogeny as the reference, and then the *Eu* and *At* lineages separately.

5.3.4.3 CODEML site models

We then ran a series of models to test whether there was selection acting on particular sites, irrespective of the phylogenetic branch. Site models assume that ω remains the same across all branches of the phylogeny but can vary between codons. We first compared model M0 (one ratio) with M1a (nearly neutral) to test for variability of selective pressure among the amino acid sites (Álvarez-Carretero et al., 2023). If model M1a was a significantly better fit than model M0, we then compared model M1a (nearly neutral) with M2a (positive selection) and M7 (neutral model) with M8 (positive selection) to test for positive selection. Model comparisons were conducted using LRTs. Comparisons that reached significance at the 5% level suggested the presence of sites under positive selection.

5.3.4.4 FUBAR

We also tested for evidence of positive selection using Fast Unconstrained Bayesian AppRoximation (FUBAR) (Murrell et al., 2013) which infers dN and dS, again assuming that selection on each site is constant throughout the phylogeny. We implemented this using the Hyphy package (Kosakovsky Pond et al., 2005). FUBAR infers a posterior probability (pp) of each site belonging to either a diversifying or purifying selection class, and we took a pp > 0.9 as evidence of selection.

5.3.4.5 CODEML branch-site models

As selection may only be acting on particular sites within specific branches of the phylogeny, which may be masked when assuming ω is the same for all sites or all branches, we implemented branch-site model A in CODEML, where ω can vary between both sites and branches. This identifies sites within a predefined lineage that may be under selection. We looked for evidence of selection in particular branches of the phylogeny, first defining the Atlantic lineages (*Eu* and *At*) as the foreground. We then assigned each lineage (*PS, PN, Eu* or *At*) independently as the foreground lineage. To test whether there was evidence of positive selection in the foreground lineage, we compared model A to a null model where $\omega_0 = 1$ using the LRT. For both site and branch-site models, the Bayes Empirical Bayes (BEB) method in CODEML was used to identify codons under positive selection; those with a pp > 0.9 were considered candidate sites.

5.3.4.6 TreeSAAP

As the previous methods are based on dN/dS, we also tested for positive selection using TreeSAAP (Woolley et al., 2003) which utilises the structural and biochemical properties of amino acid replacements. The program assigns each change in amino acid a magnitude category from 1 to 8, with 1 being the most conservative substitutions and 8 the most radical. We considered sites in categories 6 to 8 which also had high support ($p < 0.001$) as candidate positively selected sites. Where we identified sites that differed between the majority of individuals from the *Eu* and *At* lineages, this region within the alignment was visualised using JalView (Waterhouse et al., 2009) and the physiochemical properties of the amino acids labelled.

5.3.5 Structural location of positively selected sites

To predict the potential functional consequences of positively selected amino acids, we made 3D protein structures from the genes of interest using the structure prediction tool I-TASSER (Roy et al., 2010) and visualised these using Mol* Viewer (Sehnal et al., 2021). Positively selected sites were identified using Mol* Viewer and manually labelled. All 3D models were constructed from an *Eu* sequence.

5.4 Results

5.4.1 Mitogenomes

In total, 253 mitogenomes were assembled using NOVOPlasty (Dierckxsens et al., 2017). We found low levels of nucleotide diversity in the PCGs with the highest diversity in ND1, ND3 and ND2, while lowest nucleotide diversity was in COX2, ND4L and COX3 (**Table 5.1**). All genes produced unique haplotypes for the four major lineages. We calculated the number of synonymous and non-synonymous mutations in the *Eu* and *At* lineage (**Figure 5.2**). In both lineages, ND5 and ND2 had a higher number of non-synonymous mutations than expected and COX1 and ND6 had fewer non-synonymous mutations. As we were interested in any major differences between *Eu* and *At* stickleback that could have facilitated adaptation, we took a random subset of 99 samples including those from the *Eu*, *At*, *PN* and *PS* lineages. This increased the speed of further analysis without compromising the reliability of findings. GARD found no evidence of recombination, as expected for mtDNA. We calculated dN/dS values for each gene in this subset using the PAML site model M0. All genes had dN/dS ratios less than one (**Table 5.1**) suggesting genes evolved predominantly under purifying selection. ATP8, ND5 and ND2 had the highest dN/dS.

Table 5.1: Diversity of the mitochondrial PCGs. All values calculated from full sequence set (253 individuals), except for dN/dS which was calculated from the random subset of 99 sequences using CODEML site model M0.

Gene	Size (bp)	Number of haplotypes	Polymorphic sites	Nucleotide diversity	Peptides after translating	dN/dS
ATP6	681	61	73	0.00459	19	0.0466
ATP8	165	19	19	0.00548	8	0.3648
COX1	1557	93	132	0.00367	13	0.0227
COX2	690	38	45	0.00094	13	0.0712
COX3	783	54	67	0.00239	19	0.0788
CYTB	1140	92	124	0.00380	34	0.1172
ND1	978	90	131	0.00638	32	0.1028
ND2	1044	115	151	0.00584	53	0.1501
ND3	348	33	35	0.00596	8	0.0634
ND4	1380	110	168	0.00521	50	0.1031
ND4L	294	22	27	0.00221	5	0.0477
ND5	1836	154	267	0.00571	95	0.1569
ND6	519	58	63	0.00471	7	0.0774

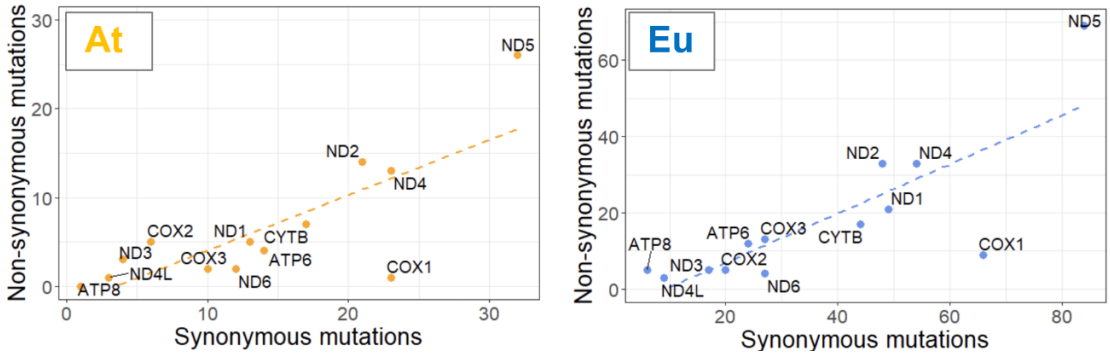

Figure 5.2: Synonymous and non-synonymous nucleotide substitutions in the mitochondrial PCGs. *At* (left) and *Eu* (right).

5.4.2 Phylogeny

Concatenated PCGs resulted in a 11,415bp sequence. The best partition scheme produced 4 subsets, and the corresponding substitution model was estimated (**Table 5.2**). A maximum likelihood phylogenetic tree was constructed from the concatenated nucleotide sequences (**Figure 5.3**). The topology was similar to previous studies, with the Atlantic lineages evolving from the Pacific. To assess only non-synonymous

substitutions, a phylogenetic tree was also constructed in IQTREE using the translated sequences (**Figure S5.1**).

Table 5.2: Partition scheme of 13 concatenated PCGs. Numbers after the gene name refer to codon positions.

Partition	Best Model	Number of Sites	Partition Scheme
1	HKY+F+I	3025	ATP6_1; ATP8_2; COX2_3; CYTB_1; ND1_1; ND2_1; ND3_1; ND4_1; ND4L_1; ND5_1; ND6_1
2	TIM+F+I	4815	ATP6_2; ATP8_1; COX1_1; COX1_2; COX2_1; COX2_2; COX3_1; COX3_2; CYTB_2; ND1_2; ND2_2; ND3_2; ND4_2; ND4L_2; ND5_2; ND6_2
3	TN+F+G4	3402	ATP6_3; ATP8_3; COX1_3; COX3_3; CYTB_3; ND1_3; ND2_3; ND3_3; ND4_3; ND4L_3; ND5_2
4	HKY+F+G4	173	ND6_3

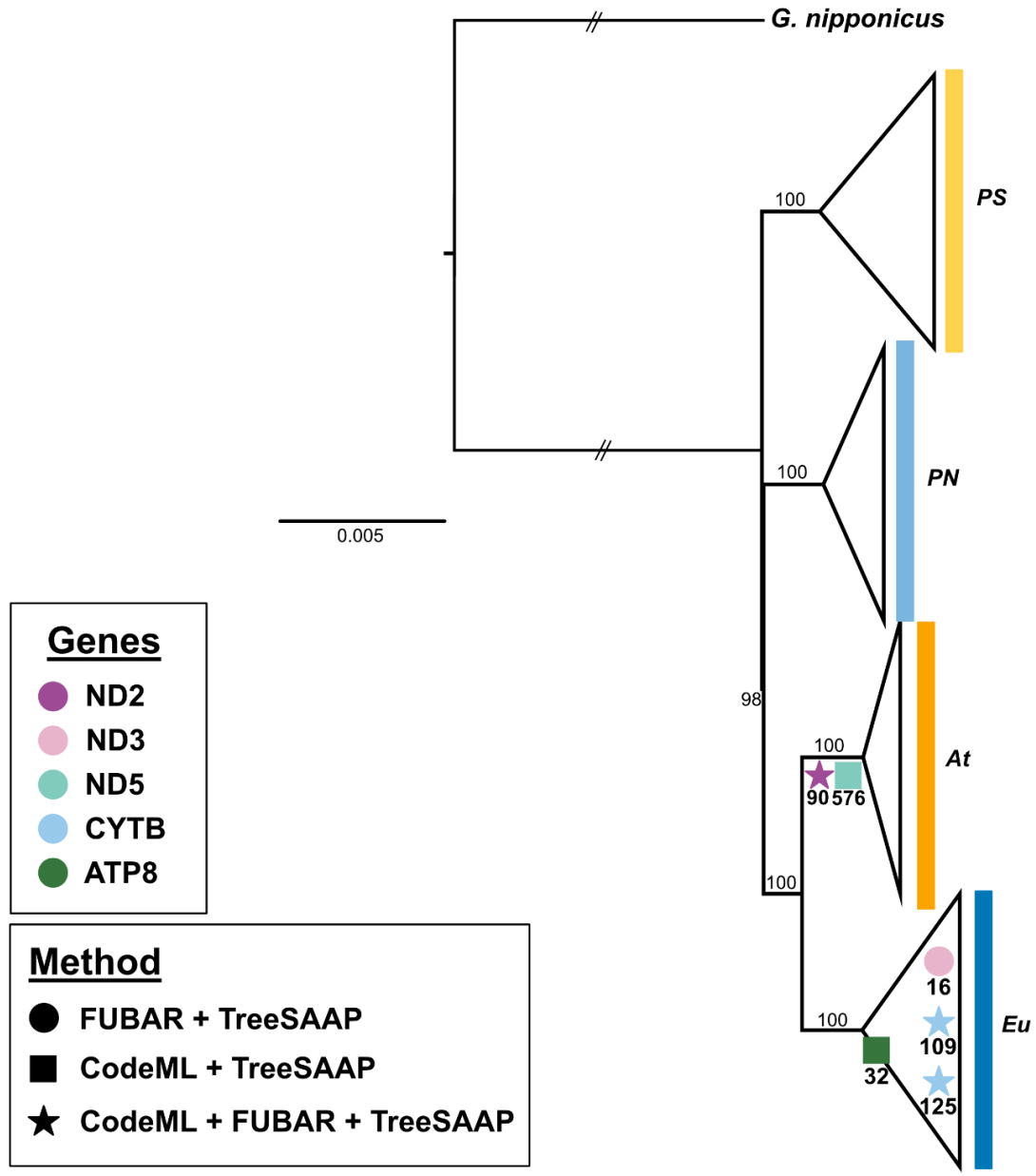

Figure 5.3: Maximum likelihood phylogenetic tree, showing locations with strong evidence of selection. Constructed from partitions of 13 mitochondrial PCGs (11,415bp) using IQTREE with *G. nipponicus* as an outgroup. Main nodes were supported with bootstrap values > 95% (1000 ultrafast bootstrap replicates in IQTREE). Circles represent codons under selection identified using FUBAR and TreeSAAP; squares represent codons identified by CODEML and TreeSAAP, stars represent sites identified by FUBAR, CODEML and TreeSAAP. Position in the phylogeny indicates the approximate location where selection was detected (i.e. positive selection was identified at CYTB site 125 recently within the *Eu* lineage, near to tips of the phylogeny). Using TreeSAAP, radical amino acid substitutions were

identified in the *At* lineage within ND2 and ND5, but CODEML site models identified long-term positive selection at these same sites.

5.4.3 Evidence of positive selection

As the Atlantic Ocean was colonised from the Pacific, we first tested for selection specific to the Atlantic lineages across each mitochondrial PCG using CODEML branch models. We then tested the *Eu* and *At* lineages independently as these likely evolved in separate refugia on opposite sides of the Atlantic. Since spreading, the *Eu* lineage, but rarely the *At* lineage, has colonised fresh water, suggesting that the lineages may have evolved under different selective pressures. As selection may have only been acting on specific sites, we used CODEML site models and FUBAR to assess whether there was evidence of long-term selection in any codons across the whole phylogeny, before using CODEML branch-site models to determine if there was selection in sites specific to any one lineage. We finally used TreeSAAP to detect any radical changes in the physiochemical properties of amino acids. Results from all site-specific tests are presented in **Table 5.3**.

Table 5.3: Codons in the mitochondrial PCGs identified as being under positive selection. Multiple methods were used: FUBAR (pp > 0.9), CODEML site models (models M2a and/or M8 significant at the 5% level and sites had pp > 0.9 using BEB), branch-site models (model A was significantly better fitting than the null model at the 5% significance level and sites had pp > 0.9 using BEB) and TreeSAAP (sites in magnitude categories 6 to 8, significant at p < 0.001). Sites highlighted and in **bold** were identified by TreeSAAP plus at least one method based on dN/dS. * pp > 0.95, ** pp > 0.99, n.s = not significant (method did not identify evidence of positive selection at the site). αm = power to be at the middle of an α-helix; α = α-helical tendencies; EC = equilibrium constant; PC = power to be at the C-terminal; IP = isoelectric point; SARR = solvent accessible reduction ratio; Bd = buriedness; Comp = composition; Hp = hydropathy. ↑ or ↓ refers to an increase or decrease in amino acid property, respectively.

Gene	Codon	FUBAR (pp)	CODEML site models (pp)		CODEML branch-site model A		TreeSAAP						
			M2a	M8	Lineage	pp	Lineage	From	To	Property	↑↓	Category	Notes
ND1	7	n.s	n.s	n.s	n.s	n.s	*At*	Thr	Ala	α	↑	6	One At
	93	n.s	n.s	n.s	n.s	n.s	*Eu*	Ala	Thr	α	↓	6	One *Eu*
	98	n.s	n.s	n.s	n.s	n.s	*Eu*	Ala	Thr	α	↓	6	One *Eu*
	107	0.908	n.s	n.s	n.s	n.s	n.s	n.s	n.s	n.s	n.s	n.s	n.s
	179	n.s	n.s	n.s	n.s	n.s	*PN*	Ala	Thr	α	↓	6	One *PN*
	193	n.s	n.s	n.s	n.s	n.s	*Eu*	Ala	Thr	α	↓	6	One *Eu*
	247	n.s	n.s	n.s	n.s	n.s	*PN*	Thr	Ala	α	↑	6	One *PN*
	274	n.s	n.s	n.s	n.s	n.s	*Eu*	Ala	Thr	α	↓	6	One *Eu*
	310	n.s	n.s	n.s	n.s	n.s	*Eu*	Ala	Thr	α	↓	6	Two *Eu*
ND2	**90**	**0.958***	**0.778**	**0.960***	**n.s**	**n.s**	***At***	**Thr**	**Ala**	**α**	↑	**6**	**Most *At*, some *PN***
	276	n.s	n.s	n.s	n.s	n.s	*PS*	Ala	Thr	α	↓	6	One *PS*
	300	n.s	n.s		n.s	n.s	*PN*	Ala	Thr	α	↓	6	Three *PN*
	310	n.s	n.s	n.s	n.s	n.s	*Eu*	Thr	Ala	α	↑	6	One *Eu*
	311	n.s	n.s	n.s	n.s	n.s	*PS*	Thr	Met	α	↑	6	One *PS*

Gene	Codon	FUBAR (pp)	CODEML site models (pp)		CODEML branch-site model A		TreeSAAP						
			M2a	M8	Lineage	pp	Lineage	From	To	Property	↑↓	Category	Notes
	339	n.s	n.s	n.s	n.s	n.s	*PN, PS*	Ala	Thr	α	↓	6	One *PN* and one *PS*
	342	n.s	n.s	n.s	n.s	n.s	*Eu*	Ala	Thr	α	↓	6	One *Eu*
ND3	**16**	**0.921**	**n.s**	**n.s**	**n.s**	**n.s**	***Eu, PN***	**Val**	**Ile**	**EC**	↓	**8**	**Two *Eu*, two *PN***
ND5	11	n.s	0.839	0.982*	n.s	n.s	n.s	n.s	n.s	n.s	n.s	n.s	n.s
	64	n.s	0.704	0.908	Atlantic	0.943	n.s	n.s	n.s	n.s	n.s	n.s	n.s
	275	n.s	0.792	0.965*	Eu	0.989*	n.s	n.s	n.s	n.s	n.s	n.s	n.s
					Atlantic	0.976*							
	355	n.s	n.s	n.s	Eu	0.916	n.s	n.s	n.s	n.s	n.s	n.s	n.s
	501	n.s	n.s	n.s	Eu	0.908	n.s	n.s	n.s	n.s	n.s	n.s	n.s
	554	n.s	0.702	0.907	n.s	n.s	n.s	n.s	n.s	n.s	n.s	n.s	n.s
	555	0.908	n.s	n.s	n.s	n.s	n.s	n.s	n.s	n.s	n.s	n.s	n.s
	576	**n.s**	**0.717**	**0.916**	**Atlantic**	**0.945**	***At***	**His**	**Tyr**	**αm**	↓	**7**	**Most *At***
ND6	46	n.s	n.s	n.s	n.s	n.s	*At*	His	Tyr	αm	↓	7	One *At*
	167	n.s	n.s	n.s	n.s	n.s	*Eu*	Arg	Cys	Bd, IP, Comp, Hp	↑↓↑↑	8,8,8,7	One *Eu*
CYTB	**109**	**0.965***	**0.801**	**0.968***	**Atlantic**	**0.976***	***Eu***	**Tyr**	**His**	**αm**	↑	**7**	**Two *Eu***
	118	n.s	n.s	n.s	n.s	n.s	*PN*	Ile	Val	EC	↑	8	Six *PN*
	125	**0.927**	**0.782**	**0.961***	**Eu**	**0.990***	***Eu***	**Met**	**Ile**	**EC**	↓	**8**	**One *Eu***
					Atlantic	**0.977***							
	153	n.s	n.s	n.s	n.s	n.s	*Eu*	Val	Ile	EC	↓	8	One *Eu*
	156	n.s	n.s	n.s	n.s	n.s	*PN*	Val	Ile	EC	↓	8	One *PN*
	188	n.s	n.s	n.s	n.s	n.s	*Eu*	Val	Ile	EC	↓	8	One *Eu*
	237	n.s	n.s	n.s	n.s	n.s	*PS*	Ile	Val	EC	↑	8	One *PS*
	353	n.s	n.s	n.s	n.s	n.s	*PN*	Val	Ile	EC	↓	8	Three *PN*

Gene	Codon	FUBAR (pp)	CODEML site models (pp)		CODEML branch-site model A		TreeSAAP						
			M2a	M8	Lineage	pp	Lineage	From	To	Property	↑↓	Category	Notes
	364	n.s	n.s	n.s	n.s	n.s	*Eu*	Val	Ile	EC	↓	8	One *Eu*
COX1	489	n.s	n.s	n.s	n.s	n.s	*Eu*	Glu	Lys	IP	↑	8	One *Eu*
COX2	120	n.s	n.s	n.s	n.s	n.s	*PN*	Ala	Thr	Pα	↓	6	One *PN*
	129	n.s	n.s	n.s	n.s	n.s	*PS*	Ala	Thr	Pα	↓	6	One *PS*
COX3	155	n.s	n.s	n.s	Eu	0.911	n.s	n.s	n.s	n.s	n.s	n.s	n.s
	219	n.s	n.s	n.s	Eu	0.907	n.s	n.s	n.s	n.s	n.s	n.s	n.s
ATP6	13	n.s	n.s	n.s	n.s	n.s	*At*	Val	Ile	EC	↓	8	Most *At*
	17	n.s	n.s	n.s	n.s	n.s	*Eu*	Val	Ile	EC	↓	8	One *Eu*
	29	n.s	n.s	n.s	n.s	n.s	*PN*	Val	Ile	EC	↓	8	Two *PN*
	227	n.s	n.s	n.s	n.s	n.s	*PN*	Val	Ile	EC	↓	8	One *PN*
ATP8	**32**	**n.s**	**n.s**	**n.s**	**Eu**	**0.908**	***Eu***	**Ile**	**Thr**	**SARR**	↓	**8**	**Most *Eu***
	40	n.s	n.s	n.s	n.s	n.s	*Eu*	Gln	Arg	IP	↑	7	One *Eu*
	48	n.s	n.s	n.s	n.s	n.s	*PS*	Asp	Asn	PC	↓	6	One *PS*

5.4.3.1 CODEML branch models and RELAX analysis

We first implemented CODEML branch models to test whether there was evidence of selection in the Atlantic lineages. Across the concatenated PCGs, the Atlantic lineages had a significantly higher ω than the Pacific inferring that selection had acted on the mitochondrial genome (**Figure 5.4**, **Table S5.2**). Assessing ω of each gene independently, we found that COX3, CYTB, ND1, ND2, ND4 and ND5 had a higher ω in the Atlantic lineages than the rest of the phylogeny (**Figure 5.4**, **Table S5.2**). We then used RELAX to determine whether this increase in ω was likely due to intensified or relaxed selection. This revealed that it was predominantly relaxed selection acting on the Atlantic stickleback mitochondrial PCGs, with the concatenated sequences, ND1 and ND4 having a selection intensity parameter (k) less than 1 that significantly improved the model fit (**Figure 5.4**, **Table S5.3**). COX3 also had a value of k less than 1 but this did not quite reach significance (p = 0.096). The selection intensity parameters of CYTB, ND2 and ND5 were greater than 1 (1.50, 1.46 and 1.69) suggesting that there may be positive, rather than relaxed, selection in these genes in the Atlantic lineages, but these did not significantly improve the model fit to those where k was fixed at 1 (p = 0.160, 0.343, 0.198 respectively).

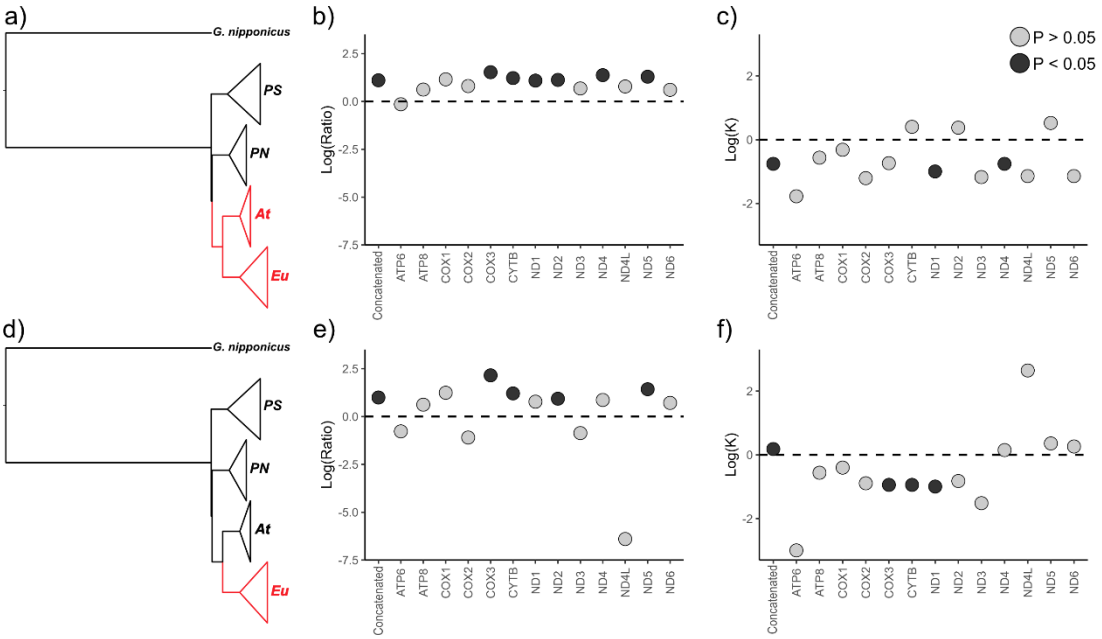

Figure 5.4: CODEML branch model results and RELAX analysis. Atlantic lineages (a-c) or the *Eu* lineage (d-f) as the test branches. Test branches labelled in red and reference in black on the phylogeny (a and d). CODEML branch tests (b and e) were conducted on the concatenated PCGs and each individual gene with the $\log_{10}$ of the ratio of ω for the test lineage to ω of the reference lineages presented as points. Points above the dashed line have a higher value of ω in the test lineage than the

rest of the phylogeny. RELAX analysis was conducted in HyPhy (c and f) with $\log_{10}$ of the selection intensity parameter k presented as points for concatenated PCGs and each individual gene. Points above the dashed line suggest intensified selection compared to the reference, points below the line suggest relaxed selection. Significant results ($p < 0.05$) are filled in black, non-significant points in grey.

We then reanalysed the phylogeny using CODEML branch models with only the *Eu* lineage as the foreground to test whether there may be selection specific to the *Eu* lineage. This showed that the mitochondrial PCGs were largely under selection (**Figure 5.4**, **Table S5.2**) as the concatenated PCGs of the *Eu* lineage had a significantly higher ω than the rest of the phylogeny, and when assessing individual genes COX3, CYTB, ND2 and ND5 also had evidence of selection (**Figure 5.4**, **Table S5.2**). Analyses using RELAX suggested that the *Eu* sequences were predominantly evolving under intensified selection compared to the rest of the phylogeny as the selection intensity parameter was greater than 1 in the concatenated sequences (**Figure 5.4, Table S5.3**), although this pattern was not apparent in individual genes. RELAX only identified three genes where the model with k as a free parameter significantly improved the fit: COX3, CYTB and ND1 were under relaxed selection (**Figure 5.4**, **Table S5.3**). ND5 was predicted to be under intensified selection with k = 1.43 but this did not quite reach significance ($p = 0.053$). With the *At* lineage as the test, only the concatenated sequences and COX2 had evidence of selection using CODEML branch models (**Table S5.2**) and RELAX did not find evidence of relaxed or intensified selection in the concatenated PCGs or in any gene individually (**Table S5.3**).

5.4.3.2 CODEML site models

To test whether there was evidence of selection in particular codons across the whole phylogeny which may be masked by overwhelming signals of purifying selection in gene-wide analyses, we implemented CODEML site models (**Table 5.3**, **Table S5.4, Table S5.5**). Both models M2a and M8 were significantly better fits than models M1a and M7, respectively, indicating the presence of a small number of sites evolving under positive selection. BEB analysis under model M8 revealed sites with posterior probabilities greater than 0.9: two sites in CTYB (site 109, pp = 0.968 and site 125, pp = 0.961), one site in ND2 (site 90, pp = 0.960) and five sites in ND5 (11, pp =

0.982; 64, pp = 0.908; 275, pp = 0.965; 554, pp = 0.907; 576, pp = 0.916) had evidence of long-term positive selection (**Table 5.3**, **Table S5.4**).

5.4.3.3 FUBAR

We confirmed findings using FUBAR which detected CYTB sites 109 and 125 and ND2 site 90, but also identified additional sites in ND1, ND3 and ND5 (**Table 5.4**). Using FUBAR, we found 728 codons under purifying selection (**Table 5.5**), suggesting that the main driver of mtDNA evolution is purifying selection, with ND1 and ND6 having the highest percentage of sites.

Table 5.4: Six sites identified as likely under positive selection by FUBAR. Posterior probabilities greater than 0.9 are shown. Sites in **bold** were also candidates identified by CODEML site or branch-site models.

Gene	Site	α	β	β-α	Prob [α>β]	Prob [α<β]	Bayes Factor [α<β]
ND1	107	1.533	10.724	9.192	0.053	0.908	39.272
ND2	**90**	**1.513**	**17.119**	**15.606**	**0.015**	**0.958**	**90.2**
ND3	**16**	**1.493**	**12.415**	**10.923**	**0.044**	**0.921**	**46.114**
ND5	555	1.541	10.713	9.172	0.053	0.908	39.032
CYTB	**109**	**1.725**	**23.205**	**21.48**	**0.011**	**0.965**	**110.484**
CYTB	**125**	**2.402**	**17.467**	**15.065**	**0.032**	**0.927**	**50.191**

Table 5.5: Number and percentage of sites per mitochondrial PCG identified as being under purifying selection using FUBAR.

Gene	Length	Number of Sites	Percentage of Sites (%)
ATP6	227	47	20.7
ATP8	55	7	12.7
COX1	519	89	17.1
COX2	230	26	11.3
COX3	261	36	13.8
CYTB	380	76	20.2
ND1	326	75	22.8
ND2	348	75	21.6
ND3	116	18	15.5
ND4	460	94	20.4
ND4L	98	20	20.4

ND5	612	127	20.8
ND6	173	38	22.0

5.4.3.4 CODEML branch-site models

We implemented CODEML branch-site models (**Figure 5.3**, **Table 5.3**, **Table S5.6**, **Table S5.7**) to test if there was evidence of selection in sites within any one lineage. In the Atlantic lineages we found evidence of selection in CYTB and ND5 with BEB analysis identifying two sites in CYTB (109 and 125) and three sites in ND5 (64, 275, 576). We found evidence of positive selection in the *Eu* lineage in ND5, CYTB, COX3 and ATP8. BEB analysis revealed three sites in ND5 (275, pp = 0.989; 355, pp = 0.916; 501, pp = 0.908), one site in CYTB (125, pp = 0.990), two sites in COX3 (155, pp = 0.0.911; 219, pp = 0.907) and one site in ATP8 (32, pp = 0.908). With the *At, PN, or PS* lineage as the foreground branch, there was no evidence of positive selection (**Table S5.6**).

5.4.3.5 TreeSAAP

Using TreeSAAP, we were able to identify multiple sites under positive selection with radical amino acid substitutions (magnitude categories 6 to 8). Properties altered by amino acid changes included α-helical tendencies, the equilibrium constant, the power to be at the middle of an α-helix, the isoelectric point, the power to be at the C-terminal and the solvent accessible reduction ratio (**Table 5.3**). 38 sites were identified as having evidence of positive selection (**Table 5.3**), with 19 sites in the complex I genes and nine sites in complex III (CYTB). Selection in most sites was identified in more recent nodes of the phylogeny with only a few samples having radical amino acid replacements, but in a few cases positive selection was identified by TreeSAAP in sites that differed between a large number of individuals or between lineages (**Table 5.3**). A change from Threonine (Thr) to Alanine (Ala) was found at ND2 site 90 (**Figure S5.2**) in the *At* and *PS* lineages. This substitution decreases the α-helical tendencies of the protein. A substitution from Histidine (His) to Tyrosine (Tyr) in the *At* lineage at ND5 site 576 (**Figure S5.2**) was predicted to be under selection by TreeSAAP, decreasing the power to be at the middle of an α-helix. This site is located in the piston arm of complex I, within an α-helix. ATP8 site 32 was also a candidate for selection

using TreeSAAP, with a substitution from Isoleucine (Ile) to Thr in most *Eu* individuals (**Figure S5.2**), which reduces the solvent accessible reduction ratio.

5.4.4 Candidate sites

We considered sites to have strong evidence of positive selection if they were identified by at least two methods including one based on dN/dS as well as TreeSAAP (**Figure 5.3**, **Table 5.3**, **Figure S5.1**). This included six sites: ND2 90; ND3 16; ND5 576; CYTB 109 and 125; ATP8 32. Sites in ND2 and CYTB were identified by all methods, ND3 site 16 was identified by FUBAR and TreeSAAP, and ND5 576 and ATP8 site 32 were candidates according to CODEML and TreeSAAP. Substitutions at these sites were predicted to alter protein function as amino acid changes result in different properties which can be selected for, and these sites have a high amount of non-synonymous substitutions compared to synonymous, all of which indicate that they likely evolved under positive selection.

5.4.5 Structural location of positively selected sites

The three-dimensional structures of ND2 and ND5 were predicted using I-TASSER (Roy et al., 2010). Positively selected sites were mapped onto the predicted protein structures (**Figure 5.5**). ND2 site 90 was adjacent to a transmembrane helix and ND5 site 576 was located in the C-terminal piston pump.

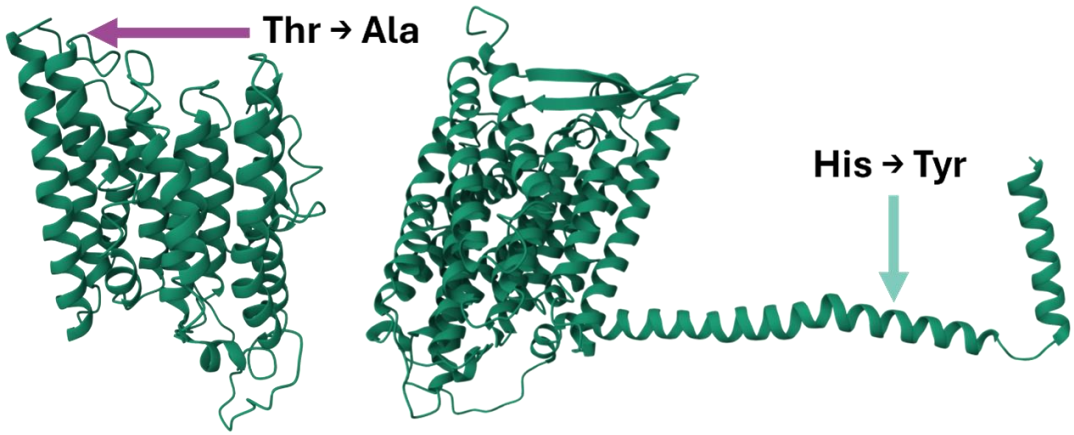

Figure 5.5: **Structures of ND2 (left) and ND5 (right) with locations of the candidate positively selected sites labelled.** Positive selection was detected at ND2 site 90 and ND5 site 576. Structures were created using I-TASSER (Roy et al., 2010) and viewed in Mol* Viewer (Sehnal et al., 2021). Thr = Threonine; Ala = Alanine; His = Histidine; Tyr = Tyrosine.

5.5 Discussion

We examined the potential role of natural selection acting on mitochondrial genome evolution. We found that selection had been acting primarily on complex I of the electron transport system (ETS), with a higher rate of non-synonymous to synonymous mutations in both the *Eu* and *At* lineages, and evidence of selection within ND2 and ND5 across the phylogeny. As the *At* lineage differed in sequence to most *Eu* fish at one positively selected site in both of these genes, selection on the mitochondrial PCGs was likely experienced as the *Eu* and *At* fish evolved in allopatry, due to the lineages experiencing different environmental conditions and metabolic demands during this time. When assessing positive selection that may occur only in certain branches of the phylogeny (i.e. episodic positive selection), we identified selection in multiple sites within the *Eu* lineage, including in ATP8, ND3 and CYTB, but there was no evidence of selection specific to the *At, PN,* or *PS* lineages. As the *Eu* lineage has been more successful at colonising fresh water than the *At* lineage in the Atlantic, these findings suggest that there has been selection for mitochondrial variants that provide an advantage for freshwater adaptation within the *Eu* lineage. Together, these findings add to the increasing evidence that mitochondrial sequences are non-neutral, and show that mitochondria can be involved in adaptive processes.

Although an elevated dN/dS has often been assumed to indicate positive selection, relaxed purifying selection can also increase dN/dS (Zwonitzer et al., 2023). By utilising the package RELAX, we were able to show that the increased rates of dN/dS in the mitochondrial PCGs in the Atlantic were likely due to relaxed selection. This may occur as stickleback were able to spread into new niches as they colonised the Atlantic, relaxing previous selective constraints. Alternatively, a reduction in population size as stickleback colonised the Atlantic Ocean (if only a small number of individuals established the Atlantic populations) could have also reduced the strength of selection (Wertheim et al., 2015). Only CYTB, ND2 and ND5 had some evidence of positive selection but this did not reach significance. Candidate sites from CODEML branch-site tests included those in CYTB and ND5, so although we did not find evidence of positive selection across whole genes, some sites within these may have experienced positive selection.

Eu and *At* stickleback likely evolved in allopatry on opposite sides of the Atlantic where they may have experienced differences in climate, potentially resulting in selection for different amino acid variants in the mitochondrial PCGs. Species adapting to new environments may face different energy requirements and be subject

to different selective agents, including temperature. Biochemical reactions in the mitochondria are influenced by temperature (Hunter-Manseau et al., 2019; Sokolova, 2023), so mitochondrial function may be limited at temperature extremes, which is particularly important for ectotherms (Chung and Schulte, 2020), including the stickleback, as body temperature reflects their environment. Selection on mtDNA variation has previously been associated with temperature (Foote et al., 2011; Garvin et al., 2011; Sebastian et al., 2020; Silva et al., 2014) and experimental evidence has shown that mtDNA haplotype frequencies change dependent on temperature in both the seed beetle (*Callosobruchus maculatus*) (Immonen et al., 2020) and the fruit fly (*Drosophila melanogaster)* (Lajbner et al., 2018), highlighting the important role of temperature in mitogenome evolution. Mitochondrial genes, in particular complex I, are suggested to be involved in adaptation to the cold in Atlantic salmon (Consuegra et al., 2015) and gentoo penguins (Noll et al., 2022). Likewise, we identified a key role of mitochondrial complex I in the evolution of mtDNA, finding long-term positive selection within ND2 and ND5 using CODEML site models; at these sites the amino acid sequence in the *At* lineage differed to most of the *Eu* lineage as well as most *PN* and *PS* samples. These substitutions were predicted to alter the structure or function of the protein so we hypothesise that there was selection in complex I of the *At* lineage for mitochondrial variants which may improve function in the cold, while *Eu* stickleback have maintained complex I function across a larger temperature range, consistent with the histories of *Eu* and *At* stickleback in the Atlantic.

Stickleback entered the Atlantic from the Pacific, via the Arctic Ocean (Fang et al., 2018; Mäkinen and Merilä, 2008b), and during the last glacial period were forced southwards; the *At* lineage is predicted to have originated in a refugium along the East Coast of North America (Chapter 4, Mäkinen and Merilä, 2008), so likely spent a larger portion of its history in colder Arctic waters than the *Eu* lineage, which diverged in warmer Southern European refugia (Defaveri et al., 2012; Fang et al., 2018; Mäkinen and Merilä, 2008; Sanz et al., 2015). Due to the extent of the ice sheets in North America (Dyke and Prest, 1987), which covered a large proportion of where stickleback currently inhabit (Mäkinen and Merilä, 2008), the distribution of *At* fish, and therefore the range of environmental conditions experienced, was potentially restricted during the LGM (Dyke and Prest, 1987; Mäkinen and Merilä, 2008; Svendsen et al., 2004). As the *Eu* lineage was less restrained by the ice sheets in Europe (Svendsen et al., 2004), *Eu* stickleback would have had increased opportunity to colonise new environments, including fresh water, so mitochondrial variants that sustained function across a whole suite of environmental conditions, including

fluctuations in temperature, would have been advantageous to the *Eu* lineage. Substitutions in the mitochondrial PCGs that were beneficial for mitochondrial function in cold temperatures may have been selected for in the *At* lineage, consistent with present day migratory stickleback at the southern edge of their range in eastern North America (which are likely largely the *At* lineage) breeding early in the year when temperatures are low, but juveniles migrating northwards to remain in cold oceanic water (Able and Fahay, 2010). These temperatures are much lower than those experienced by breeding stickleback on the eastern side of the Atlantic. We identified long-term selection in sites within ND2 and ND5 across the stickleback phylogeny, suggesting that advantageous genetic variants have spread across both the *Eu* and *At* lineages. When assessing the candidate sites in ND2 and ND5, we found almost fixed differences in mitochondrial sequence between *Eu* and *At* fish, hinting that a different amino acid at these sites may have been beneficial for each lineage.

Positive selection was predominantly in complex I, with sites in ND2 and ND5 identified by both dN/dS and amino acid property-based methods; these are almost fixed differences in sequence between the *Eu* and *At* lineages. Selection in the mitochondrial PCGs, particularly complex I, has been identified in numerous other marine organisms where it has been associated with temperature (Baltazar-Soares et al., 2021; Silva et al., 2014; Wilson et al., 2020) and deep-sea environments (Shen et al., 2019; Yang et al., 2021; Zhang et al., 2017). Complex I plays a central role in energy production, being the largest complex of the ETS with 14 central subunits (Carroll et al., 2006; Efremov et al., 2010; Wirth et al., 2016a), and contributes to the formation of reactive oxygen species (ROS) (Wirth et al., 2016a). The crystal structure of complex I from the bacterium *Thermus thermophilus* has been resolved (Baradaran et al., 2013), providing a wealth of information about the highly conserved core subunits; ND2, ND5 and ND4 are the proton pumps, transporting protons from the mitochondrial matrix to the intermembrane space to create the electrochemical gradient required for ATP generation.

ND5 site 576 (as well as sites 554 and 555 which were identified by at least one test for positive selection; **Table 5.3**) is located in the piston arm of ND5 which links the proton pumps (Baradaran et al., 2013; Garvin et al., 2011) and is predicted to facilitate coordination in proton pumping (Hunte et al., 2010). The location of ND5 site 576 along this helix suggests that it may interact with ND4. Previous studies have also identified positive selection and radical amino acid property substitutions in the C-terminal region of ND5 including in some teleost fish lineages (Mukundan et al., 2022), mammals (da Fonseca et al., 2008) and toads of the genus *Bombina* (Pabijan

et al., 2008). Multiple sites in the C-terminal region, including site 576 which was also a candidate in the present study, had evidence of positive selection in Pacific salmon (genus *Oncorhynchus*) (Garvin et al., 2011). Taken together, these findings implicate the C-terminal piston arm of ND5 in adaptive evolution across a large number of organisms, warranting further investigation into its function. We found that *At* stickleback had an amino acid substitution from His to Tyr at ND5 site 576, which is located in an α-helix. His is a positively charged amino acid while Tyr is hydrophobic and neutral, and TreeSAAP predicted that this radical substitution decreased the power of the amino acid to be in the middle of an α-helix. This replacement may therefore have functional effects for mitochondria, although additional experiments would need to test this explicitly: protein stability, function or ROS production could be affected and may depend on the specific environmental conditions. The black-spotted stickleback (*Gasterosteus wheatlandi),* a closely related species to the three-spined stickleback, has the same codon in ND5 (nucleotide positions 1726-8; amino acid site 576) as the *At* lineage (Kawahara et al., 2009*,* GenBank accession: AB445129.1). As the distribution of *G. wheatlandi* is restricted to salt or brackish water in the Western Atlantic (GBIF 2023), similar to the predicted distribution of the *At* lineage during the LGM, this supports this variant being advantageous for functioning in cold waters with little temperature variation.

We also detected selection in ND2 site 90 using multiple methods. Positive selection in ND2 was previously detected in association with high-altitude (Yu et al., 2011; Zhou et al., 2014), temperature (Teacher et al., 2012) and flight (Li et al., 2018), suggesting that ND2 can play a role in adaptation to new environments with differing metabolic requirements. As ND2 is another proton pumping subunit of mitochondrial complex I (Baradaran et al., 2013; Efremov et al., 2010), mutations have the potential to alter the movement of H^+ across the membrane and in turn effect mitochondrial function, including ATP production. Site 90 is predicted to be at the start of a transmembrane helix and a change from Thr to Ala in most of the *At* and *PS* lineages was suggested to increase α-helical tendencies. As this site is located just outside of an α-helix, this could suggest that the start of the helix may differ between Atlantic stickleback lineages which may have functional consequences, but again, the physiological consequences of complex I amino acid substitutions would need to be experimentally confirmed.

Although the almost fixed differences in mitochondrial complex I genes between lineages likely evolved in allopatry approximately 100,000 years ago (Dean et al., 2019), they could be influencing the present-day distribution of stickleback in the

Atlantic. The *At* lineage is rare in resident populations in fresh and brackish water. Resident populations experience fluctuating temperatures and likely much higher temperatures than stickleback in the Atlantic Ocean, so the changes in the sequence of complex I genes that may improve mitochondrial function in the cold could be detrimental in warmer environments. In contrast, the *Eu* lineage has had to maintain complex I function across a wider variety of temperatures, so is well suited to survive at high as well as low temperatures. In support of this, we have previously shown that the proportion of *At* stickleback within populations decreased with increasing maximum sea surface temperatures (Chapter 4), suggesting that *At* fish are less well-adapted to warm temperatures. Preexisting mutations in complex I could therefore have restricted *At* fish from colonising fresh water.

The finding that there was evidence of episodic positive selection in the *Eu* lineage only is quite striking. This suggests the presence of sites in the *Eu* mitochondrial PCGs that are adaptive, but none were identified in the *At, PN or PS* lineages (although the smaller sample size of Pacific stickleback may make identifying selection specific to these lineages more challenging). This finding coincides with the observation that it is predominantly the *Eu* lineage, compared to the *At*, that is found in resident populations in the Atlantic. *Eu* stickleback have been exposed to a larger range of environmental conditions (temperatures, salinities, diets) which in turn alter their metabolic demands; small changes to mitochondrial function, including energy production, could be beneficial and selected for in these habitats. We therefore hypothesised that there would be evidence of positive selection specific to the *Eu* lineage and as predicted, the *Eu* lineage had elevated dN/dS ratios in the majority of the mitochondrial PCGs and we identified episodic selection in codons within ATP8, ND3 and CYTB using multiple phylogenetic methods. Most *Eu* fish had an Ile to Thr substitution in ATP8 which was predicted to decrease the solvent accessible reduction ratio, likely influencing protein structure and/or function. ATP8 is a subunit of ATP synthase (complex V) which produces ATP from ADP and inorganic phosphate. ATP8, along with ATP6, functions as part of the F_0 component of ATP synthase, moving protons from the inner mitochondrial membrane into the mitochondrial matrix (Dimroth, 1999); this drives the catalytic function of the F_1 component. The N-terminal region of ATP8 has a transmembrane α-helix and the C-terminal region extends into the peripheral stalk (He et al., 2018) so ATP8 is important in the assembly and stability of the complex (Devenish et al., 1992; He et al., 2018). The substitution in ATP8 observed in *Eu* stickleback could be beneficial for the colonisation of fresh and brackish water as metabolic demands in these habitats differ to the Atlantic Ocean.

Selective agents could include i) temperature: temperature influences mitochondrial function (Hunter-Manseau et al., 2019; Sokolova, 2023) and previous evidence suggests that *Eu* fish are better suited to high maximum sea surface temperatures than *At* (Chapter 4), ii) diet: the diet of freshwater, and most likely lagoon resident, stickleback is often lower in key nutrients than in the sea (Ishikawa et al., 2021; Twining et al., 2021) which could require slight modifications to the ETS to increase mitochondrial efficiency in poor diet conditions, and iii) salinity: changes in salinity require efficient osmoregulation which is energy dependent so may benefit from changes in mitochondrial function. Although changes in salinity may be driving the selection of beneficial mtDNA variants within the *Eu* lineage, as resident fish in both fresh and brackish water are primarily *Eu,* and observations from fish raised in aquaria suggest that both lineages do well long-term in both salt and fresh water, almost fixed differences in mtDNA between the lineages (e.g. in complex I) are unlikely to be involved in adaptation to lower salinities alone.

We also found evidence of positive selection in ND3 and CYTB within a few branches of the *Eu* lineage. A change from Valine (Val) to Ile at ND3 site 16 was identified in samples from Portugal and North Uist, and similarly, a substitution from Tyr to His at CYTB site 109 was found in a sample from Quebec and North Uist. As selection was detected at the same sites in multiple branches of the phylogeny and across different geographic locations, variation in these sites may be important in adaptation to common environmental conditions and may be advantageous for freshwater colonisation as all individuals with the alternative amino acid were freshwater resident stickleback. Selection in CYTB has previously been identified (Sebastian et al., 2022b), and linked to temperature adaptation in fish (Baltazar-Soares et al., 2021; Silva et al., 2014). Although rarer, evidence of positive selection has previously been found in ND3, for example in Atlantic Salmon (Consuegra et al., 2015), but could not be correlated to any environmental parameters. Amino acid variation in these genes could therefore be advantageous in adapting to the local environment where there are small differences in metabolic requirements. Alternatively, as we found some evidence of relaxed selection in these genes, and samples with amino acid substitutions were all non-migratory freshwater fish, purifying selection may have been relaxed as ATP production does not need to be so efficient for migration, which would also increase dN/dS.

Although the evidence presented infers a role of selection in mitochondrial PCG evolution and we have used phylogenetic selection analyses to start to distinguish positive selection from relaxed purifying selection, we cannot rule out the involvement

of genetic drift in the diversification of stickleback mtDNA. However, during the divergence of Atlantic stickleback lineages in allopatry, population sizes were unlikely to be small enough for these mutations to become almost fixed by chance, and the same positively selected sites and amino acid substitutions have been highlighted in multiple *Eu* branches which makes it unlikely that these have occurred randomly. TreeSAAP analysis revealed positively selected sites where amino acid substitutions result in changes in physiochemical properties which accompanied elevated dN/dS, further adding to the evidence that positive selection has shaped the evolution of stickleback mitochondrial PCGs. Further tests of the functional consequences of these substitutions could help confirm this. We have also previously identified an association between stickleback mitochondrial lineages and sea surface temperature in the Atlantic (Chapter 4) which provides evidence that variation in mitochondrial sequences between lineages does have adaptive consequences, suggesting a role of natural selection. The non-random frequencies of mitochondrial lineages in migratory versus resident populations (Dean et al., 2019a) also hints at a role of natural selection in mitogenome evolution.

Results from this study highlight the importance of mitochondria in adaptive processes, further demonstrating that the mitochondrial sequences are non-neutral. We found evidence of long-term positive selection in the mitochondrial PCGs, particularly in ND2 and ND5 of complex I, where amino acids that differ between most *Eu* and *At* stickleback were predicted to have functional consequences for complex I, which could be associated with temperature. We also found episodic positive selection specific to the *Eu* lineage that may have accompanied their adaptation to the resident stickleback lifestyle, including exposure to extremes in temperature and reduced nutritional availability. It would be interesting to compare mitochondrial sequences of stickleback inhabiting isolated freshwater locations that are known to experience different temperatures across the Atlantic. Although we identified mutations that were predicted to have a functional effect for mitochondria, the next steps would be experimentally proving that changes in sequence observed between *Eu* and *At* stickleback do change mitochondrial function in particular conditions and could therefore be selected for. Atlantic stickleback populations are a good model to test this as many migratory populations that segregate by mtDNA are otherwise panmictic, so nuclear differences between mitochondrial lineages are unlikely (Chapter 4). This provides a unique opportunity to test for differences in oxidative phosphorylation, ROS production, and additional measures of mitochondrial capacity that would only reflect differences in the mtDNA sequence.

5.6 References

Able, K.W., Fahay, M.P., 2010. Ecology of Estuarine Fishes: Temperate waters of the North Atlantic. The John Hopkins University Press. Baltimore.

Álvarez-Carretero, S., Kapli, P., Yang, Z., 2023. Beginner's Guide on the Use of PAML to Detect Positive Selection. *Mol. Biol. Evol.* **40**, msad041. https://doi.org/10.1093/molbev/msad041

Avise, J.C., Arnold, J., Martin Bal, R., Bermingham, E., Lamb, T., Neigel, J.E., Reeb, C.A., Saunders, N.C., 1987. Intraspecific Phylogeography: The Mitochondrial DNA Bridge Between Population Genetics and Systematics. *Ann. Rev. Ecol. Syst.* **18**, 489–522. https://doi.org/10.1146/annurev.es.18.110187.002421

Aw, W.C., Towarnicki, S.G., Melvin, R.G., Youngson, N.A., Garvin, M.R., Hu, Y., Nielsen, S., Thomas, T., Pickford, R., Bustamante, S., Vila-Sanjurjo, A., Smyth, G.K., Ballard, J.W.O., 2018. Genotype to phenotype: Diet-by-mitochondrial DNA haplotype interactions drive metabolic flexibility and organismal fitness. *PLoS Genet.* **14**, e1007735. https://doi.org/10.1371/JOURNAL.PGEN.1007735

Ballard, J.W.O., Youngson, N.A., 2015. Review: can diet influence the selective advantage of mitochondrial DNA haplotypes? *Biosci. Rep.* **35**, e00277. https://doi.org/10.1042/BSR20150232

Ballard, J.W.O., Kreitman, M., 1995. Is mitochondrial DNA a strictly neutral marker? *TREE.* **10**, 485-488. https://doi.org/10.1016/S0169-5347(00)89195-8

Baltazar-Soares, M., Lima, A.R. de A., Silva, G., 2021. Targeted sequencing of mitochondrial genes reveals signatures of molecular adaptation in a nearly panmictic small pelagic fish species. *Genes.* **12**, 91. https://doi.org/10.3390/genes12010091

Baradaran, R., Berrisford, J.M., Minhas, G.S., Sazanov, L.A., 2013. Crystal structure of the entire respiratory complex I. *Nature* **494**, 443–448. https://doi.org/10.1038/nature11871

Baris, T.Z., Blier, P.U., Pichaud, N., Crawford, D.L., Oleksiak, M.F., 2016. Gene by environmental interactions affecting oxidative phosphorylation and thermal sensitivity. *Am. J. Physiol. Regul. Integr. Comp. Physiol.* **311**, R157–R165. https://doi.org/10.1152/ajpregu.00008.2016

Beck, E.A., Bassham, S., Cresko, W.A., 2022. Extreme intraspecific divergence in mitochondrial haplotypes makes the threespine stickleback fish an emerging evolutionary mutant model for mito-nuclear interactions. *Front. Genet.* **13**. https://doi.org/10.3389/fgene.2022.925786

Bell, M.A., Foster, S.A., 1995. The Evolutionary Biology of the Threespine Stickleback. *J. Anim. Ecol.* **64**, 418-419. https://doi.org/10.2307/5902

Camus, M.F., Wolff, J.N., Sgrò, C.M., Dowling, D.K., 2017. Experimental Support That Natural Selection Has Shaped the Latitudinal Distribution of Mitochondrial Haplotypes in Australian *Drosophila melanogaster*. *Mol. Biol. Evol.* **34**, 2600–2612. https://doi.org/10.1093/MOLBEV/MSX184

Carroll, J., Fearnley, I.M., Skehel, J.M., Shannon, R.J., Hirst, J., Walker, J.E., 2006. Bovine complex I is a complex of 45 different subunits. *J. Biol. Chem.* **281**, 32724–32727. https://doi.org/10.1074/JBC.M607135200

Chernomor, O., Von Haeseler, A., Minh, B.Q., 2016. Terrace Aware Data Structure for Phylogenomic Inference from Supermatrices. *Syst. Biol.* **65**, 997–1008. https://doi.org/10.1093/SYSBIO/SYW037

Cheviron, Z.A., Bachman, G.C., Connaty, A.D., McClelland, G.B., Storz, J.F., 2012. Regulatory changes contribute to the adaptive enhancement of thermogenic capacity in high-altitude deer mice. *PNAS.* **109**, 8635–8640. https://doi.org/10.1073/PNAS.1120523109

Chung, D.J., Schulte, P.M., 2020. Mitochondria and the thermal limits of ectotherms. *J. Exp. Biol.* **223**, jeb227801. https://doi.org/10.1242/JEB.227801

Consuegra, S., John, E., Verspoor, E., De Leaniz, C.G., 2015. Patterns of natural selection acting on the mitochondrial genome of a locally adapted fish species. *Genet. Sel. Evol.* **47**, 58. https://doi.org/10.1186/S12711-015-0138-0

da Fonseca, R.R., Johnson, W.E., O'Brien, S.J., Ramos, M.J., Antunes, A., 2008. The adaptive evolution of the mammalian mitochondrial genome. *BMC Genomics.* **9**, 119. https://doi.org/10.1186/1471-2164-9-119

Dean, L.L., Magalhaes, I.S., Foote, A., D'Agostino, D., McGowan, S., MacColl, A.D.C., 2019. Admixture between Ancient Lineages, Selection, and the Formation of Sympatric Stickleback Species-Pairs. *Mol. Biol. Evol.* **36**, 2481–2497. https://doi.org/10.1093/MOLBEV/MSZ161

Defaveri, J., Zanella, L.N., Zanella, D., Mrakovčić, M., Merilä, J., 2012. Phylogeography of isolated freshwater three-spined stickleback *Gasterosteus aculeatus* populations in the Adriatic Sea basin. *J. Fish Biol.* **80**, 61–85. https://doi.org/10.1111/J.1095-8649.2011.03147.X

Devenish, R.J., Papakonstantinou, T., Galanis, M., Law, R.H.P., Linnane, A.W., Nagley, P., 1992. Structure/Function Analysis of Yeast Mitochondrial ATP Synthase Subunit 8. *Ann. N. Y. Acad. Sci.* **671**, 403–414. https://doi.org/10.1111/j.1749-6632.1992.tb43814.x

Dierckxsens, N., Mardulyn, P., Smits, G., 2017. NOVOPlasty: de novo assembly of organelle genomes from whole genome data. *Nucleic Acids Res.* **45**, e18. https://doi.org/10.1093/NAR/GKW955

Dimroth, P., 1999. Operation of the F_0 motor of the ATP synthase. *Bioenergetics.* **1458**, 374-386. https://doi.org/https://doi.org/10.1016/S0005-2728(00)00088-8

Dyke, A.S., Prest, V.K., 1987. Late Wisconsinan and Holocene history of the Laurentide Ice Sheet. *Geographie Physique et Quaternaire* **41**, 237–263. https://doi.org/10.7202/032681ar

Efremov, R.G., Baradaran, R., Sazanov, L.A., 2010. The architecture of respiratory complex I. *Nature*. **465**, 441–445. https://doi.org/10.1038/nature09066

Fang, B., Merilä, J., Ribeiro, F., Alexandre, C.M., Momigliano, P., 2018. Worldwide phylogeny of three-spined sticklebacks. *Mol. Phylogenet. Evol.* **127**, 613–625. https://doi.org/10.1016/J.YMPEV.2018.06.008

Foote, A.D., Morin, P.A., Durban, J.W., Pitman, R.L., Wade, P., Willerslev, E., Gilbert, M.T.P., Fonseca, R.R.D., 2011. Positive selection on the killer whale mitogenome. *Biol. Lett.* **7**, 116–118. https://doi.org/10.1098/rsbl.2010.0638

Garvin, M.R., Bielawski, J.P., Gharrett, A.J., 2011. Positive Darwinian Selection in the Piston That Powers Proton Pumps in Complex I of the Mitochondria of Pacific Salmon. *PLoS One.* **6**, e24127. https://doi.org/10.1371/JOURNAL.PONE.0024127

Giles, R.E., Blanc, H., Cann, H.M., Wallace, D.C., 1980. Maternal inheritance of human mitochondrial DNA. *PNAS*. **77**, 6715–6719. https://doi.org/10.1073/pnas.77.11.6715

Haenel, Q., Guerard, L., MacColl, A.D.C., Berner, D., 2022. The maintenance of standing genetic variation: Gene flow vs. selective neutrality in Atlantic stickleback fish. *Mol. Ecol.* **31**, 811–821. https://doi.org/10.1111/MEC.16269

He, J., Ford, H.C., Carroll, J., Douglas, C., Gonzales, E., Ding, S., Fearnley, I.M., Walker, J.E., 2018. Assembly of the membrane domain of ATP synthase in human mitochondria. *PNAS*. **115**, 2988–2993. https://doi.org/10.1073/pnas.1722086115

Hill, G.E., 2020. Mitonuclear Compensatory Coevolution. *Trends in Genetics.* **36**, 403–414. https://doi.org/10.1016/j.tig.2020.03.002

Hunte, C., Zickermann, V., Brandt, U., 2010. Functional modules and structural basis of conformational coupling basis of conformational coupling in mitochondrial complex I. *Science.* **329**, 448–451. https://doi.org/10.1126/SCIENCE.1191046

Hunter-Manseau, F., Desrosiers, V., Le François, N.R., Dufresne, F., Detrich, H.W., Nozais, C., Blier, P.U., 2019. From Africa to Antarctica: Exploring the Metabolism of Fish Heart Mitochondria Across a Wide Thermal Range. *Front. Physiol.* **10**, 451138. https://doi.org/10.3389/FPHYS.2019.01220

Immonen, E., Berger, D., Sayadi, A., Liljestrand-Rönn, J., Arnqvist, G., 2020. An experimental test of temperature-dependent selection on mitochondrial haplotypes in *Callosobruchus* maculatus seed beetles. *Ecol. Evol.* **10**, 11387–11398. https://doi.org/10.1002/ece3.6775

Ishikawa, A., Stuart, Y.E., Bolnick, D.I., Kitano, J., 2021. Copy number variation of a fatty acid desaturase gene Fads2 associated with ecological divergence in freshwater stickleback populations. *Biol. Lett.* **17**, 20210204. https://doi.org/10.1098/RSBL.2021.0204

Johnson, L.S., Taylor, E.B., 2004. The distribution of divergent mitochondrial DNA lineages of threespine stickleback (*Gasterosteus aculeatus*) in the northeastern Pacific Basin: post-glacial dispersal and lake accessibility, *J. Biogeogr*. **7**, 1073-1083. https://doi.org/10.1111/j.1365-2699.2004.01078.x ·

Jones, F.C., Grabherr, M.G., Chan, Y.F., Russell, P., Mauceli, E., Johnson, J., Swofford, R., Pirun, M., Zody, M.C., White, S., Birney, E., Searle, S., Schmutz, J., Grimwood, J., Dickson, M.C., Myers, R.M., Miller, C.T., Summers, B.R., Knecht, A.K., Brady, S.D., Zhang, H., Pollen, A.A., Howes, T., Amemiya, C., Baldwin, J., Bloom, T., Jaffe, D.B., Nicol, R., Wilkinson, J., Lander, E.S., Di Palma, F., Lindblad-

Toh, K., Kingsley, D.M., 2012. The genomic basis of adaptive evolution in threespine sticklebacks. *Nature*. **484**, 55–61. https://doi.org/10.1038/nature10944

Kalyaanamoorthy, S., Minh, B.Q., Wong, T.K.F., Von Haeseler, A., Jermiin, L.S., 2017. ModelFinder: fast model selection for accurate phylogenetic estimates. *Nat. Methods.* **14**, 587–589. https://doi.org/10.1038/nmeth.4285

Katoh, K., Rozewicki, J., Yamada, K.D., 2019. MAFFT online service: multiple sequence alignment, interactive sequence choice and visualization. *Brief. Bioinform.* **20**, 1160–1166. https://doi.org/10.1093/BIB/BBX108

Kawahara, R., Miya, M., Mabuchi, K., Near, T.J., Nishida, M., 2009. Stickleback phylogenies resolved: Evidence from mitochondrial genomes and 11 nuclear genes. *Mol. Phylogenet. Evol.* **50**, 401–404. https://doi.org/10.1016/J.YMPEV.2008.10.014

Kosakovsky Pond, S.L., Frost, S.D.W., Muse, S. V., 2005. HyPhy: hypothesis testing using phylogenies*. Bioinformatics.* **21**, 676–679. https://doi.org/10.1093/BIOINFORMATICS/BTI079

Ladoukakis, E.D., Zouros, E., 2017. Evolution and inheritance of animal mitochondrial DNA: Rules and exceptions. *J. Biol. Res. Thessaloniki.* **24**, 2. https://doi.org/10.1186/s40709-017-0060-4

Lajbner, Z., Pnini, R., Camus, M.F., Miller, J., Dowling, D.K., 2018. Experimental evidence that thermal selection shapes mitochondrial genome evolution. *Sci. Rep.* **8**, 9500. https://doi.org/10.1038/s41598-018-27805-3

Li, X.D., Jiang, G.F., Yan, L.Y., Li, R., Mu, Y., Deng, W.A., 2018. Positive Selection Drove the Adaptation of Mitochondrial Genes to the Demands of Flight and High-Altitude Environments in Grasshoppers. *Front. Genet.* **9**. https://doi.org/10.3389/fgene.2018.00605

Liu, S., Hansen, M.M., Jacobsen, M.W., 2016. Region-wide and ecotype-specific differences in demographic histories of threespine stickleback populations, estimated from whole genome sequences. *Mol. Ecol.* **25**, 5187–5202. https://doi.org/10.1111/MEC.13827

Lui, M.A., Mahalingam, S., Patel, P., Connaty, A.D., Ivy, C.M., Cheviron, Z.A., Storz, J.F., McClelland, G.B., Scott, G.R., 2015. High-altitude ancestry and hypoxia acclimation have distinct effects on exercise capacity and muscle phenotype in deer mice. *Am. J. Physiol. Regul. Integr. Comp. Physiol.* **308**, R779-R791. https://doi.org/10.1152/AJPREGU.00362.2014

Mäkinen, H.S., Merilä, J., 2008. Mitochondrial DNA phylogeography of the three-spined stickleback (*Gasterosteus aculeatus*) in Europe-evidence for multiple glacial refugia. *Mol. Phylogenet. Evol.* **46**, 167–182. https://doi.org/10.1016/J.YMPEV.2007.06.011

Minh, B.Q., Schmidt, H.A., Chernomor, O., Schrempf, D., Woodhams, M.D., Von Haeseler, A., Lanfear, R., Teeling, E., 2020. IQ-TREE 2: New Models and Efficient Methods for Phylogenetic Inference in the Genomic Era. *Mol. Biol. Evol.* **37**, 1530–1534. https://doi.org/10.1093/MOLBEV/MSAA015

Monternier, P.A., Fongy, A., Hervant, F., Drai, J., Collin-Chavagnac, D., Rouanet, J.L., Roussel, D., 2015. Skeletal muscle phenotype affects fasting-induced mitochondrial oxidative phosphorylation flexibility in cold-acclimated ducklings. *J. Exp. Biol.* **218**, 2427–2434. https://doi.org/10.1242/jeb.122671

Monternier, P.A., Marmillot, V., Rouanet, J.L., Roussel, D., 2014. Mitochondrial phenotypic flexibility enhances energy savings during winter fast in king penguin chicks. *J. Exp. Biol.* **217**, 2691–2697. https://doi.org/10.1242/jeb.104505

Moritz, C., Dowling, T.E., Brown, W.M., 1987. Evolution of animal mitochondrial DNA: Relevance for population biology and systematics. *Ann. Rev. Ecol. Syst.* **18**, 269-292. https://doi.org/10.1146/annurev.es.18.110187.001413

Mukundan, L.P., Sukumaran, S., Raj, N., Jose, A., Gopalakrishnan, A., 2022. Positive selection in the mitochondrial protein coding genes of teleost regional endotherms: Evidence for adaptive evolution. *J. Mar. Biol. Ass. India.* **64**, 1. https://doi.org/10.6024/jmbai.2022.64.1.2320-02

Murrell, B., Moola, S., Mabona, A., Weighill, T., Sheward, D., Kosakovsky Pond, S.L., Scheffler, K., 2013. FUBAR: A Fast, Unconstrained Bayesian AppRoximation for Inferring Selection. *Mol. Biol. Evol.* **30**, 1196–1205. https://doi.org/10.1093/MOLBEV/MST030

Nguyen, B.Y., Ruiz-Velasco, A., Bui, T., Collins, L., Wang, X., Liu, W., 2019. Mitochondrial function in the heart: the insight into mechanisms and therapeutic potentials. *Br. J. Pharmacol.* **176**, 4302-4318. https://doi.org/10.1111/BPH.14431

Noll, D., Leon, F., Brandt, D., Pistorius, P., Le Bohec, C., Bonadonna, F., Trathan, P.N., Barbosa, A., Rey, A.R., Dantas, G.P.M., Bowie, R.C.K., Poulin, E., Vianna, J.A., 2022. Positive selection over the mitochondrial genome and its role in the

diversification of gentoo penguins in response to adaptation in isolation. *Sci. Rep*. **12**, 3767. https://doi.org/10.1038/s41598-022-07562-0

Orti, G., Bell, M.A., Reimchen, T.E., Meyer, A., 1994. Global survey of mitochondrial DNA sequences in the threespine stickleback: evidence for recent migrations. *Evolution*. **48**, 608–622. https://doi.org/10.1111/J.1558-5646.1994.TB01348.X

Pabijan, M., Spolsky, C., Uzzell, T., Szymura, J.M., 2008. Comparative analysis of mitochondrial genomes in *Bombina* (Anura; Bombinatoridae). *J. Mol. Evol.* **67**, 246–256. https://doi.org/10.1007/S00239-008-9123-3

Pond, S.L.K., Posada, D., Gravenor, M.B., Woelk, C.H., Frost, S.D.W., 2006. Automated phylogenetic detection of recombination using a genetic algorithm. *Mol. Biol. Evol.* **23**, 1891–1901. https://doi.org/10.1093/molbev/msl051

Popadin, K.Y., Nikolaev, S.I., Junier, T., Baranova, M., Antonarakis, S.E., 2013. Purifying selection in mammalian mitochondrial protein-coding genes is highly effective and congruent with evolution of nuclear genes. *Mol. Biol. Evol.* **30**, 347–355. https://doi.org/10.1093/molbev/mss219

Ravinet, M., Harrod, C., Eizaguirre, C., Prod, P.A., Paulo Prod, C.A., 2013. Unique mitochondrial DNA lineages in Irish stickleback populations: cryptic refugium or rapid recolonization? *Ecol. Evol*. **4**, 2488–2504. https://doi.org/10.1002/ece3.853

Roy, A., Kucukural, A., Zhang, Y., 2010. I-TASSER: a unified platform for automated protein structure and function prediction. *Nat. Protoc.* **5**, 725–738. https://doi.org/10.1038/nprot.2010.5

Rozas, J., Ferrer-Mata, A., Sanchez-DelBarrio, J.C., Guirao-Rico, S., Librado, P., Ramos-Onsins, S.E., Sanchez-Gracia, A., 2017. DnaSP 6: DNA Sequence Polymorphism Analysis of Large Data Sets. *Mol. Biol. Evol.* **34**, 3299–3302. https://doi.org/10.1093/MOLBEV/MSX248

Sanz, N., Araguas, R.M., Vidal, O., Viñas, J., 2015. Glacial refuges for three-spined stickleback in the Iberian Peninsula: mitochondrial DNA phylogeography. *Freshw. Biol.* **60**, 1794–1809. https://doi.org/10.1111/FWB.12611

Scott, G.R., Schulte, P.M., Egginton, S., Scott, A.L.M., Richards, J.G., Milsom, W.K., 2011. Molecular Evolution of Cytochrome c Oxidase Underlies High-Altitude Adaptation in the Bar-Headed Goose. *Mol. Biol. Evol.* **28**, 351–363. https://doi.org/10.1093/MOLBEV/MSQ205

Sebastian, W., Sukumaran, S., Gopalakrishnan, A., 2022. Comparative mitogenomics of Clupeoid fish provides insights into the adaptive evolution of mitochondrial oxidative phosphorylation (OXPHOS) genes and codon usage in the heterogeneous habitats. *Heredity.* **128**, 236–249. https://doi.org/10.1038/s41437-022-00519-z

Sebastian, W., Sukumaran, S., Zacharia, P.U., Muraleedharan, K.R., Dinesh Kumar, P.K., Gopalakrishnan, A., 2020. Signals of selection in the mitogenome provide insights into adaptation mechanisms in heterogeneous habitats in a widely distributed pelagic fish. *Sci. Rep.* **10**, 9081. https://doi.org/10.1038/s41598-020-65905-1

Sehnal, D., Bittrich, S., Deshpande, M., Svobodová, R., Berka, K., Bazgier, V., Velankar, S., Burley, S.K., Koča, J., Rose, A.S., 2021. Mol* Viewer: modern web app for 3D visualization and analysis of large biomolecular structures. *Nucleic Acids Res.* **49**, W431–W437. https://doi.org/10.1093/NAR/GKAB314

Shen, X., Pu, Z., Chen, X., Murphy, R.W., Shen, Y., 2019. Convergent Evolution of Mitochondrial Genes in Deep-Sea Fishes. *Front. Genet.* **10**. https://doi.org/10.3389/FGENE.2019.00925

Sigurdardóttir, S., Helgason, A., Gulcher, J.R., Stefansson, K., Donnelly, P., 2000. The Mutation Rate in the Human mtDNA Control Region. *AJHG.* **66**, 1599–1609. https://doi.org/10.1086/302902

Silva, G., Lima, F.P., Martel, P., Castilho, R., 2014. Thermal adaptation and clinal mitochondrial DNA variation of European anchovy. *Proc. R. Soc. B.* **281**, 20141093. https://doi.org/10.1098/rspb.2014.1093

Smeitink, J., van den Heuvel, L., DiMauro, S., 2001. The genetics and pathology of oxidative phosphorylation. *Nat. Rev. Genet.* **2**, 342-352. https://doi.org/10.1038/35072063

Sokolova, I.M., 2023. Ectotherm mitochondrial economy and responses to global warming. *Acta. Physiologica*. **237**, e13950. https://doi.org/10.1111/apha.13950

Steenwyk, J.L., Buida, T.J., Labella, A.L., Li, Y., Shen, X.X., Rokas, A., 2021. PhyKIT: a broadly applicable UNIX shell toolkit for processing and analyzing phylogenomic data. *Bioinformatics*. **37**, 2325–2331. https://doi.org/10.1093/BIOINFORMATICS/BTAB096

Svendsen, J.I., Alexanderson, H., Astakhov, V.I., Demidov, I., Dowdeswell, J.A., Funder, S., Gataullin, V., Henriksen, M., Hjort, C., Houmark-Nielsen, M., Hubberten, H.W., Ingólfsson, Ó., Jakobsson, M., Kjær, K.H., Larsen, E., Lokrantz, H., Lunkka, J.P., Lysså, A., Mangerud, J., Matiouchkov, A., Murray, A., Möller, P., Niessen, F., Nikolskaya, O., Polyak, L., Saarnisto, M., Siegert, C., Siegert, M.J., Spielhagen, R.F., Stein, R., 2004. Late Quaternary ice sheet history of northern Eurasia. *Quat. Sci. Rev*. **23**, 1229–1271. https://doi.org/10.1016/j.quascirev.2003.12.008

Tamura, K., Stecher, G., Kumar, S., 2021. MEGA11: Molecular Evolutionary Genetics Analysis Version 11. *Mol. Biol. Evol.* **38**, 3022–3027. https://doi.org/10.1093/MOLBEV/MSAB120

Taylor, Eric B, Mcphail, J.D., Taylor, E B, 1999. Evolutionary history of an adaptive radiation in species pairs of threespine sticklebacks (*Gasterosteus*): insights from mitochondrial DNA. *Biol. J. Linn. Soc*. **66**, 271-291.

Teacher, A.G., André, C., Merilä, J., Wheat, C.W., 2012. Whole mitochondrial genome scan for population structure and selection in the Atlantic herring. *BMC. Evol. Biol.* **12**, 248. https://doi.org/10.1186/1471-2148-12-248

Towarnicki, S.G., Ballard, J.W.O., 2018. Mitotype Interacts With Diet to Influence Longevity, Fitness, and Mitochondrial Functions in Adult Female *Drosophila*. *Front. Genet*. **9**. https://doi.org/10.3389/FGENE.2018.00593

Twining, C.W., Bernhardt, J.R., Derry, A.M., Hudson, C.M., Ishikawa, A., Kabeya, N., Kainz, M.J., Kitano, J., Kowarik, C., Ladd, S.N., Leal, M.C., Scharnweber, K., Shipley, J.R., Matthews, B., 2021. The evolutionary ecology of fatty-acid variation: Implications for consumer adaptation and diversification. *Ecol. Lett.* **24**, 1709–1731. https://doi.org/10.1111/ele.13771

Wang, Y., Shen, Y., Feng, C., Zhao, K., Song, Z., Zhang, Y., Yang, L., He, S., 2016. Mitogenomic perspectives on the origin of Tibetan loaches and their adaptation to high altitude. *Sci. Rep.* **6**, 29690. https://doi.org/10.1038/srep29690

Waterhouse, A.M., Procter, J.B., Martin, D.M.A., Clamp, M., Barton, G.J., 2009. Jalview Version 2-A multiple sequence alignment editor and analysis workbench. *Bioinformatics*. **25**, 1189–1191. https://doi.org/10.1093/bioinformatics/btp033

Weaver, S., Shank, S.D., Spielman, S.J., Li, M., Muse, S. V., Kosakovsky Pond, S.L., 2018. Datamonkey 2.0: A Modern Web Application for Characterizing Selective

and Other Evolutionary Processes. *Mol. Biol. Evol.* **35**, 773–777. https://doi.org/10.1093/MOLBEV/MSX335

Wertheim, J.O., Murrell, B., Smith, M.D., Pond, S.L.K., Scheffler, K., 2015. RELAX: Detecting Relaxed Selection in a Phylogenetic Framework. *Mol. Biol. Evol.* **32**, 820–832. https://doi.org/10.1093/MOLBEV/MSU400

Wilson, R.E., Sonsthagen, S.A., Smé, N., Gharrett, A.J., Majewski, A.R., Wedemeyer, K., Nelson, R.J., Talbot, S.L., 2020. Mitochondrial genome diversity and population mitogenomics of polar cod (*Boreogadus saida*) and Arctic dwelling gadoids. *Polar Biol*. **43**, 979–994. https://doi.org/10.1007/S00300-020-02703-5

Wirth, C., Brandt, U., Hunte, C., Zickermann, V., 2016. Structure and function of mitochondrial complex I. *BBA Bioenergetics.* **1857**, 902–914. https://doi.org/10.1016/J.BBABIO.2016.02.013

Woolley, S., Johnson, J., Smith, M.J., Crandall, K.A., McClellan, D.A., 2003. TreeSAAP: Selection on Amino Acid Properties using phylogenetic trees. *Bioinformatics.* **19**, 671–672. https://doi.org/10.1093/BIOINFORMATICS/BTG043

Yang, M., Dong, D., Li, X., 2021. The complete mitogenome of *Phymorhynchus* sp. (Neogastropoda, Conoidea, Raphitomidae) provides insights into the deep-sea adaptive evolution of Conoidea. *Ecol. Evol*. **11**, 7518–7531. https://doi.org/10.1002/ECE3.7582

Yang, Z., 2007. PAML 4: Phylogenetic Analysis by Maximum Likelihood. *Mol. Biol. Evol.* **24**, 1586–1591. https://doi.org/10.1093/MOLBEV/MSM088

Yu, L., Wang, X., Ting, N., Zhang, Y., 2011. Mitogenomic analysis of Chinese snub-nosed monkeys: Evidence of positive selection in NADH dehydrogenase genes in high-altitude adaptation. *Mitochondrion*. **11**, 497–503. https://doi.org/10.1016/j.mito.2011.01.004

Zhang, B., Zhang, Y.H., Wang, X., Zhang, H.X., Lin, Q., 2017. The mitochondrial genome of a sea anemone *Bolocera* sp. exhibits novel genetic structures potentially involved in adaptation to the deep-sea environment. *Ecol. Evol.* **7**, 4951–4962. https://doi.org/10.1002/ECE3.3067

Zhang, J., Shu, L., Peng, Z., 2024. Adaptive evolution of mitochondrial genomes in *Triplophysa* cavefishes. *Gene*. **893**, 147947. https://doi.org/10.1016/j.gene.2023.147947

Zhao, D., Guo, Y., Gao, Y., 2022. Natural selection drives the evolution of mitogenomes in *Acrossocheilus*. *PLoS One* **17**, e0276056. https://doi.org/10.1371/journal.pone.0276056

Zhou, T., Shen, X., Irwin, D.M., Shen, Y., Zhang, Y., 2014. Mitogenomic analyses propose positive selection in mitochondrial genes for high-altitude adaptation in galliform birds. *Mitochondrion*. **18**, 70–75. https://doi.org/10.1016/j.mito.2014.07.012

Zwonitzer, K.D., Iverson, E.N.K., Sterling, J.E., Weaver, R.J., Maclaine, B.A., Havird, J.C., 2023. Disentangling Positive Selection from Relaxed Selection in Animal Mitochondrial Genomes. *Am. Nat.* **202**, E121–E129. https://doi.org/10.1086/725805

5.7 Supplementary Material

Table S5.1: Locations of the samples used for phylogenetic reconstruction and selection analysis.

Region	Atlantic/Pacific	Population	Latitude	Longitude
Iceland	Atlantic	Egg3	66.485538	-15.929624
Iceland	Atlantic	Nes2	66.481026	-15.925622
Iceland	Atlantic	Egg1	66.48582	-15.931577
Iceland	Atlantic	Hrau	66.5220642	-16.0409986
Iceland	Atlantic	Midf	65.324212	-20.895125
Iceland	Atlantic	Hrin	66.5068878	-15.9755517
Maine, US	Atlantic	Lubec	44.827921	-61.08889
North Uist, Scotland	Atlantic	Daim	57.593167	-7.209242
North Uist, Scotland	Atlantic	Olav/OlaM[1]	57.65204	-7.44771
North Uist, Scotland	Atlantic	Bhru	57.72666	-7.174834
North Uist, Scotland	Atlantic	Luib/LuiM[1]	57.55433	-7.312329
North Uist, Scotland	Atlantic	Tros	57.58397	-7.413632
North Uist, Scotland	Atlantic	Clac/ClaM[1]	57.63764	-7.414877
North Uist, Scotland	Atlantic	Obse	57.602046	-7.172522
North Uist, Scotland	Atlantic	Caig	57.6344	-7.113622
North Uist, Scotland	Atlantic	Reiv	57.61095	-7.514554
North Uist, Scotland	Atlantic	Iala	57.62001	-7.205617
North Uist, Scotland	Atlantic	Bhar	57.57051	-7.301183
North Uist, Scotland	Atlantic	Ceit	57.57846	-7.258303
North Uist, Scotland	Atlantic	Chru	57.59393	-7.197603
North Uist, Scotland	Atlantic	Torm	57.56198	-7.316751
North Uist, Scotland	Atlantic	Sann	57.58798	-7.46317
North Uist, Scotland	Atlantic	Maig	57.59478	-7.201768
North Uist, Scotland	Atlantic	Duin/DuiM[1]	57.64245	-7.209207
Nova Scotia	Atlantic	Cherry Burton	46.0298	-64.103064
Nova Scotia	Atlantic	Canal Lake[2]	44.497959	-63.901367
Nova Scotia	Atlantic	Baddeck[2]	46.09586	-61.0889
Portugal	Atlantic	Cape	37.645889	-8.568861
Portugal	Atlantic	Mara	38.569667	-8.736389
Portugal	Atlantic	Anc1	41.810194	-8.861222
Quebec, Canada	Atlantic	Temiscouata	47.6877	-68.8411
Quebec, Canada	Atlantic	Croche	47.7774	-68.7935
Mainland Scotland	Atlantic	Tyne	55.989227	-2.634747
Mainland Scotland	Atlantic	Lmor	56.961656	-5.79324
Mainland Scotland	Atlantic	Lano	56.994805	-5.806989
California, US	Pacific	Bigr	39.283852	-123.715522
California, US	Pacific	Sals	36.677925	-121.746117

Vancouver, US	Pacific	Bnma	48.892177	-123.685489
Vancouver, US	Pacific	Litc	49.013271	-122.746135
Vancouver, US	Pacific	Bnst	48.882214	-123.704321

[1]North Uist sympatric species pairs, population name ending in 'M' refers to anadromous stickleback.

[2]White stickleback from Nova Scotia.

Table S5.2: CODEML branch model results. Comparisons with model M0 (ω remains the same across branches) for each gene and concatenated PCGs using a LRT (twice the difference in log-likelihood (ℓ) between null and alternative hypotheses (2Δℓ), compared with the χ^2 distribution). The critical values are $\chi^2_{1,5\%} = 3.84$ (1 degree of freedom at 5% significance, *); $\chi^2_{1,1\%} = 6.63$ (1 degree of freedom at 1% significance, **), $\chi^2_{1,0.1\%} = 10.83$ (1 degree of freedom at 0.1% significance, ***). d.f = degrees of freedom. ω (dN/dS) is given for the test lineage and the background.

Test Lineage	Gene	ℓ M0	ℓ Branch Model	df	2Δℓ	P-Value	ω Test	ω Background
Atlantic	Concatenated	-22626.6	-22599.5	1	54.3101	0.000***	0.1705	0.0564
	ATP6	-1253.96	-1253.94	1	0.0358	0.850	0.0427	0.0494
	ATP8	-269.249	-269.092	1	0.3144	0.575	0.5229	0.2812
	COX1	-2614.63	-2613.72	1	1.8066	0.179	0.0391	0.0123
	COX2	-1085	-1084.61	1	0.7647	0.382	0.1003	0.0448
	COX3	-1321.39	-1319.06	1	4.6565	0.031*	0.1535	0.0333
	CYTB	-2193.05	-2183.18	1	19.7417	0.000***	0.2053	0.0605
	ND1	-1974.34	-1971.61	1	5.4495	0.020*	0.1756	0.0591
	ND2	-2131.55	-2127.55	1	7.9937	0.005**	0.2803	0.0909
	ND3	-557.541	-557.38	1	0.3226	0.570	0.0794	0.0402
	ND4	-2760.43	-2754.98	1	10.8942	0.001***	0.2015	0.051
	ND4L	-484.22	-484.084	1	0.2725	0.602	0.0755	0.0345
	ND5	-3832.77	-3829.25	1	7.0426	0.008**	0.2804	0.0769
	ND6	-973.656	-973.344	1	0.6246	0.429	0.1089	0.0593
Eu	Concatenated	-22626.6	-22606.2	1	40.8484	0.000***	0.1927	0.0711

	ATP6	-1253.96	-1253.67	1	0.5727	0.449	0.0247	0.0535
	ATP8	-269.249	-269.086	1	0.3248	0.569	0.5230	0.2809
	COX1	-2614.63	-2613.6	1	2.0468	0.123	0.0507	0.0146
	COX2	-1085	-1084.47	1	1.0500	0.306	0.0318	0.095
	COX3	-1321.39	-1316.85	1	9.0768	0.003**	0.2370	0.0275
	CYTB	-2193.05	-2183.21	1	19.6695	0.000***	0.2278	0.0679
	ND1	-1974.34	-1973.11	1	2.4435	0.118	0.1766	0.0812
	ND2	-2131.55	-2129.24	1	4.6034	0.032*	0.2932	0.1153
	ND3	-557.541	-557.244	1	0.5949	0.441	0.0452	0.1071
	ND4	-2760.43	-2758.66	1	3.5211	0.061	0.1971	0.0828
	ND4L	-484.22	-483.791	1	0.8583	0.354	0.0001	0.0601
	ND5	-3832.77	-3827.52	1	10.4864	0.001**	0.3862	0.0925
	ND6	-973.656	-972.883	1	1.5464	0.214	0.1270	0.0622
At	Concatenated	-22626.6	-22624.7	1	3.9270	0.0475*	0.1413	0.0928
	ATP6	-1253.96	-1253.83	1	0.0004	0.9840	0.0670	0.0422
	ATP8	-269.249	-269.248	1	0.0065	0.93571	128.6631	0.3649
	COX1	-2614.63	-2614.62	1	4.5871	0.0322*	0.0246	0.0224
	COX2	-1085	-1082.7	1	2.2694	0.1320	0.3536	0.0394
	COX3	-1321.39	-1320.25	1	0.1319	0.7165	0.0001	0.0889
	CYTB	-2193.05	-2186.20	1	13.6875	0.000***	0.0601	0.1185
	ND1	-1974.34	-1973.19	1	2.2947	0.1298	0.2103	0.0872
	ND2	-2131.55	-2130.71	1	1.6787	0.1951	0.2730	0.1343

ND3	-557.541	-557.514	1	0.0550	0.8146	0.0513	0.0687
ND4	-2760.43	-2758.74	1	3.3792	0.0660	0.2045	0.0845
ND4L	-484.22	-482.639	1	3.1633	0.0753	0.6182	0.0244
ND5	-3832.77	-3838.51	1	-11.4805	1.0000	0.1848	0.1545
ND6	-973.656	-973.656	1	0.0001	0.9934	0.0764	0.0776

Table S5.3: RELAX analysis results. Atlantic (*Eu* and *At*), *Eu*, or *At* lineages as the test and the rest of the phylogeny as the reference. P values calculated by comparing a model including k as a free parameter to a null model where k = 1 using a LRT and compared with the χ^2 distribution. Tests conducted for the concatenated PCGs and each gene individually. k > 1 infers intensified selection, k < 1 infers relaxed selection. * p < 0.05, ** p < 0.01, *** p < 0.001.

Gene	Test	k	P-Value
Concatenated	Atlantic	0.47	0.000***
	Eu	1.20	0.042*
	At	0.54	0.183
ATP6	Atlantic	0.17	0.525
	Eu	0.05	0.299
	At	0.70	0.678
ATP8	Atlantic	0.57	0.515
	Eu	0.57	0.515
	At	0.92	0.993
COX1	Atlantic	0.73	0.331
	Eu	0.67	0.245
	At	0.82	0.992
COX2	Atlantic	0.30	0.284
	Eu	0.41	0.074
	At	0.13	0.051
COX3	Atlantic	0.48	0.096
	Eu	0.39	0.012*
	At	0.69	0.340
CYTB	Atlantic	1.50	0.160
	Eu	0.39	0.018*
	At	0.47	0.261
ND1	Atlantic	0.37	0.002**
	Eu	0.37	0.002**
	At	1.08	0.794
ND2	Atlantic	1.46	0.343
	Eu	0.44	0.206
	At	1.08	0.857
ND3	Atlantic	0.31	0.406
	Eu	0.22	0.108
	At	4.29	0.353
ND4	Atlantic	0.47	0.041*
	Eu	1.16	0.638
	At	0.47	0.266
ND4L	Atlantic	0.32	0.609
	Eu	14.09	0.784
	At	5.34	0.145
ND5	Atlantic	1.69	0.198
	Eu	1.43	0.053
	At	0.54	0.123
ND6	Atlantic	0.32	0.705
	Eu	1.30	0.595

	*A*t	0.77	0.710

Table S5.4: CODEML site model results. Comparisons between M0 and M1a, M1a & M2a and M7 & M8 using a LRT (twice the difference in log-likelihood (ℓ) between null and alternative hypotheses (2Δℓ), compared with the χ^2 distribution). Degrees of freedom (df) is the difference in number of parameters (np) between models. The critical values are $\chi^2_{2,5\%}$ = 5.99 (2 degrees of freedom at 5% significance, *); $\chi^2_{2,1\%}$ = 9.21 (2 degrees of freedom at 1% significance, **); $\chi^2_{2,0.1\%}$ = 13.82 (2 degrees of freedom at 0.1% significance, ***). When model comparisons were found to be significant using the LRT, BEB was implemented in CODEML to identify codons under positive selection and posterior probabilities > 0.9 shown.

Model Comparison	Model	ℓ	np	df	2Δℓ	P-Value	Sites (posterior probability > 0.9)
M0 (one ratio) vs M1a (nearly neutral)	0	-22626.64	200	1	126.6	< 0.001 ***	n.a
	1a	-22563.34	201				
M1a (nearly neutral) vs M2a (positive selection)	1a	-22563.34	201	2	11.1	0.004 **	No sites with posterior probability > 0.9
	2a	-22557.77	203				
M7 (betal) vs M8 (beta & ω)	7	-22576.53	201	2	8.4	0.015 *	CYTB 109 (0.968); CYTB 125 (0.961); ND2 90 (0.960); ND5 11 (0.982); ND5 64 (0.908); ND5 275 (0.965); ND5 554 (0.907); ND5 576 (0.916)
	8	-22572.31	203				

Table S5.5: **Parameter estimates for CODEML site models.** Model M0: One ω across all sites and branches. Model M1a: p_0 = proportion of sites where $\omega_0 < 1$; p_1 = proportion of sites where $\omega_1 = 1$. Model M2a adds p_2 = proportion of sites where $\omega_2 > 1$. M7: Parameters p and q describe ω for sites where $0 < \omega < 1$. M8: p_0 = proportion of sites with ω from the beta distribution; p_1 = proportion of sites with $\omega > 1$.

Model	dN/dS	Parameters
M0 (one ratio)	0.0993	ω = 0.0993
M1a (nearly neutral)	0.0959	p_0 = 0.9401 (p_1 = 0.0599), ω_0 = 0.0383

M2a (positive selection)	0.1043	p_0 = 0.9623, p_1 = 0.0324 (p_2 = 0.0053), ω_0 = 0.0518
M7 (beta)	0.1033	p = 0.0277, q = 0.2026
M8 (beta&ω)	0.1634	p_0 = 0.8847 (p_1 = 0.1153), p = 0.0050, q = 1.8987, ω = 1.0000

Table S5.6: CODEML branch-site model results. Comparison with the Atlantic, *Eu, At, PN* or *PS* lineage defined as the foreground lineage. Null and alternative models compared with LRT (twice difference in log likelihood (ℓ) between models (2Δℓ), compared with the χ^2 distribution). df = degrees of freedom. n.s = not significant. The critical values are $\chi^2_{1,5\%}$ = 3.84 (1 degree of freedom at 5% significance, *); $\chi^2_{1,1\%}$ = 6.63 (1 degree of freedom at 1% significance, **). The Bayes Empirical Bayes (BEB) method was implemented in CODEML to identify sites under positive selection in the predefined lineage and posterior probabilities (pp) > 0.9 shown.

Foreground branch	ℓ Alternative	ℓ Null	df	2Δℓ	P-Value	Sites (posterior probability > 0.9)
Atlantic (*Eu* and *At*)	-22537.2	-22540.13	1	5.86	0.015 *	CYTB 109 (0.976); CYTB 125 (0.977); ND5 64 (0.943); ND5 275 (0.976); ND5 576 (0.945)
At	-22558.9	-22559.88	1	1.96	0.162	n.s
Eu	-22543.05	-22547.53	1	8.96	0.002 **	ATP8 32 (0.908); COX3 155 (0.911); COX3 219 (0.907); CYTB 125 (0.990); ND5 275 (0.989); ND5 355 (0.916); ND5 501 (0.908)
PN	-22561.8	-22561.8	1		1	n.s
PS	-22560.4	-22560.4	1		0.983	n.s

Table S5.7: Maximum likelihood estimates for CODEML branch-site models. Sites from class 0 are under purifying selection along all branches, class 1 are under neutral evolution, classes 2a and 2b allow positive selection along the foreground

branches but background branches are under purifying selection (2a) or neutral evolution (2b).

Foreground Lineage	Site Class	Proportion	Background ω	Foreground ω
Atlantic	0	0.9144	0.0267	0.0267
	1	0.0331	1.0000	1.0000
	2a	0.0507	0.0267	2.0252
	2b	0.0018	1.0000	2.0252
At	0	0.9305	0.0357	0.0357
	1	0.0542	1.0000	1.0000
	2a	0.0144	0.0357	3.5198
	2b	0.0008	1.0000	3.5198
Eu	0	0.9254	0.0316	0.0316
	1	0.0422	1.0000	1.0000
	2a	0.0310	0.0316	3.3427
	2b	0.0014	1.0000	3.3427
PN	0	0.9016	0.0343	0.0343
	1	0.0575	1.0000	1.0000
	2a	0.0385	0.0343	1.0000
	2b	0.0025	1.0000	1.0000
PS	0	0.8651	0.0347	0.0347
	1	0.0546	1.0000	1.0000
	2a	0.0755	0.0347	1.0000
	2b	0.0048	1.0000	1.0000

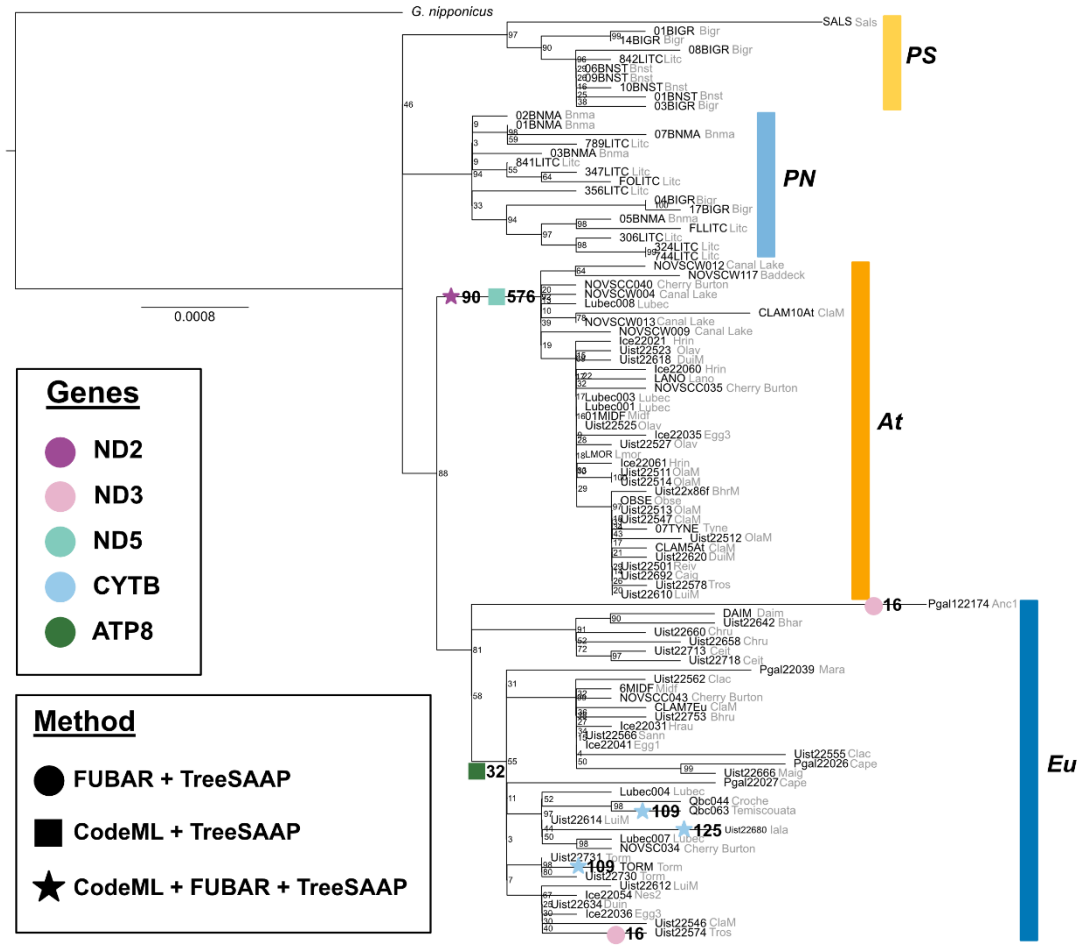

Figure S5.1: Maximum likelihood phylogenetic tree constructed from concatenated amino acid sequences of the 13 mitochondrial PCGs using IQTREE. 1000 ultrafast bootstrap replicates using IQTREE. All nodes are labelled with the sample name (black) and population (grey); populations refer to locations in **Figure 5.1** and **Table S5.1**. Colours and shapes represent genes under positive selection and the methods used to detect selection, respectively.

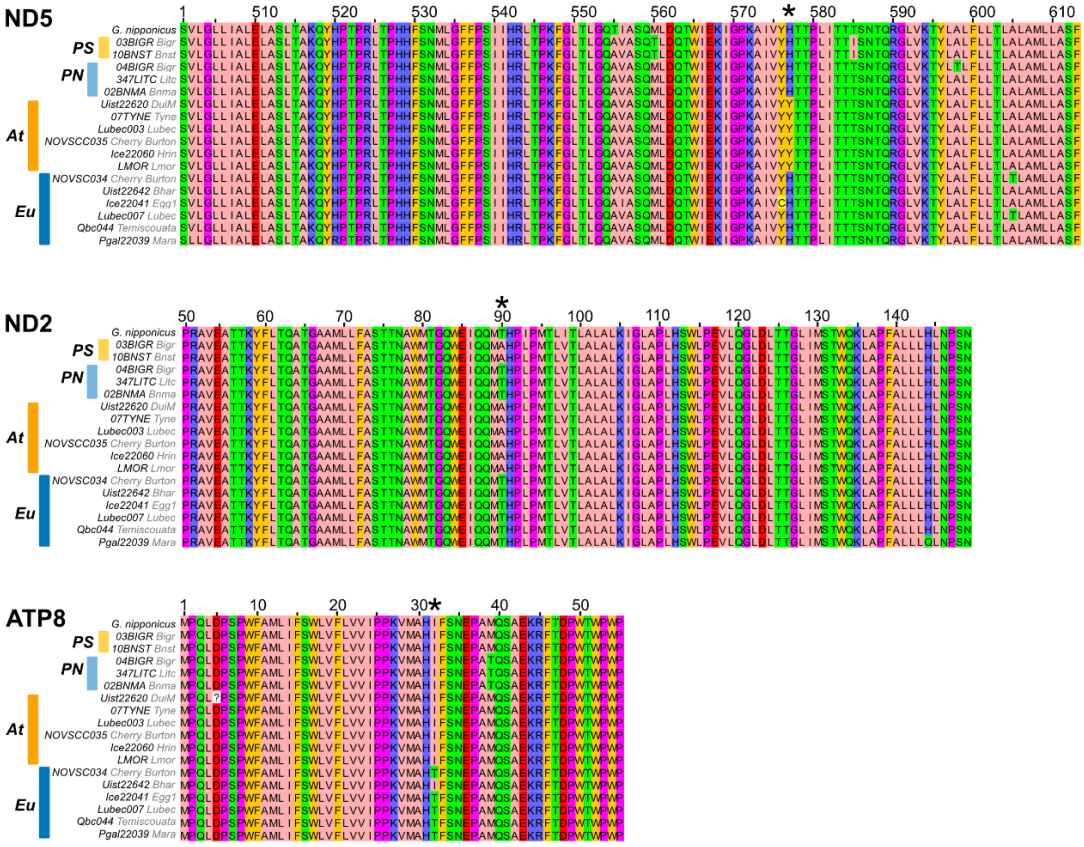

Figure S5.2: Amino acid sequences surrounding positively selected sites that differ between most *Eu* and *At* stickleback. Example sequences from each lineage. C-terminal region (sites 500 to 613) of ND5, sites 50 to 149 of ND2 and entire amino acid sequence of ATP8 displayed. Sites where positive selection was detected by multiple methods is shown with an asterisk. Amino acids are coloured by physiochemical property with zappo colour scheme in JalView (Waterhouse et al., 2009): Aliphatic/hydrophobic (I,L,V,A,M) = light pink; aromatic (FWY) = orange; positive (KRH) = blue; negative (DE) = red; hydrophilic (STNQ) = green; conformationally special (PG) = dark pink; cysteine (C) = yellow.

Chapter 6: Physiological Consequences of Mitochondrial DNA Variation in the Three-spined Stickleback

6.1 Abstract

Mitochondrial DNA (mtDNA) sequences have often been used as a neutral marker, but increasing evidence suggests that the mitochondrial genome is not neutral and may be involved in adaptive processes. Alongside numerous nuclear genes, the mitochondrial genome encodes components of the oxidative phosphorylation pathway in the inner mitochondrial membrane which is responsible for the majority of a cell's aerobic ATP production. mtDNA variation has previously been shown to alter mitochondrial function, which may play a role in environmental adaptation, but this has rarely been assessed independent of the nuclear genetic background. There are two well-studied mitochondrial lineages of the three-spined stickleback in the Atlantic with greatly diverged mitochondrial genomes, and the frequencies of these lineages differ between stickleback ecotypes. Utilising migratory populations that segregate by their mtDNA but are otherwise panmictic, making nuclear genetic differences unlikely, we were able to explicitly link mtDNA sequence variation to physiological mitochondrial variation. We performed high-resolution respirometry, identifying that at cold temperatures, one mitochondrial lineage had higher complex I respiration when electron transport was uncoupled from ADP phosphorylation. This adds to the accumulating evidence that the mitochondrial sequences are non-neutral and may be adaptive.

6.2 Introduction

Genetic sequences from the mitochondrial genome have long been used as neutral markers of population structure in molecular ecology and phylogeography (Avise et al., 1987), but accumulating evidence makes this assumption of neutrality unlikely (Ballard and Kreitman, 1995; Ballard and Whitlock, 2004; Hill, 2015). The bioenergetic consequences of mitochondrial DNA (mtDNA) mutations have been well studied in many models (Wallace, 1999), but the importance of mtDNA variation in natural populations for adaptation and speciation has often been overlooked.

Mitochondria play a key role in the production of ATP, heat and reactive oxygen species (ROS). The oxidative phosphorylation (OXPHOS) pathway is responsible for

the majority of a cell's ATP production when oxygen is available. This system has five enzyme complexes situated in the inner mitochondrial membrane: complexes I, III, IV and V have subunits encoded by both the nuclear and mitochondrial genomes whereas complex II (CII) is entirely encoded by the nuclear DNA. Electrons enter the electron transfer system (ETS) at complex I (CI) (Hirst, 2013) or CII (Cecchini, 2003) from the Krebs cycle or glycolysis and are passed through additional protein complexes in a series of redox reactions. Some of the energy produced from these reactions is dissipated as heat, but the rest is used to pump hydrogen ions from the mitochondrial matrix to the intermembrane space, creating a proton gradient which is utilised by ATP synthase to form ATP as protons flow down the gradient. As the mtDNA encodes peptides involved in this fundamental process, changes to mtDNA sequence could have consequences for mitochondrial function which may be beneficial to an organism in certain genetic backgrounds or specific environmental conditions, allowing organisms to adapt to new environments through natural selection on this genetic variation.

Metabolic demands differ between environments. Both climate and food availability can result in different metabolic requirements; these are important selective agents in natural populations. For example, in low temperatures efficient heat generation may be favoured, whereas low food availability or nutritional content may require more efficient ATP production. Variation in mtDNA sequences have been experimentally shown to alter mitochondrial function, which may have permitted adaptation to altitude (Cheviron et al., 2012; Lui et al., 2015; Scott et al., 2015, 2011), altered diets (Aw et al., 2018; Ballard and Youngson, 2015; Pichaud et al., 2013; Towarnicki and Ballard, 2020) and temperatures (Baris et al., 2016; Whitehead, 2009). Such studies provide evidence that mtDNA variation results in functional consequences for physiology and fitness and could therefore be adaptive, but this is often environment dependent and is conditional on the nuclear genetic background (Barreto et al., 2018; Ellison and Burton, 2008; Immonen et al., 2020b). Relatively few studies have explicitly linked mtDNA sequence variation to functional mitochondrial variation. Assessing the physiological consequences of mitochondrial genome variation independent of any nuclear effects has been accomplished utilising cybrid cell lines (Gómez-Durán et al., 2012, 2010; Kenney et al., 2014; Wilkins et al., 2014) and *Drosophila* as a model (Pichaud et al., 2012; Wolff et al., 2016). By comparing natural populations from two different environments, altered mitochondrial sequences and functions have been identified which likely impacted environmental adaptation (Cheviron et al., 2012; Lui et al., 2015; Scott et al., 2015, 2011), but these findings are dependent on the nuclear

genome (Hill, 2020). Ideal natural models utilise admixed populations containing two or more mitochondrial variants, minimising any nuclear genetic differences (Baris et al., 2016). The study of further natural populations is required to infer both the physiological and evolutionary consequences of mtDNA variation.

Repeated colonisation of freshwater environments post-glaciation has influenced the evolution of multiple fish species, including the three-spined stickleback (Bell and Foster, 1995; Jones et al., 2012) ('stickleback', *Gasterosteus aculeatus*). The stickleback is a small teleost fish widely distributed throughout coastal marine, brackish and freshwater habitats in the Northern Hemisphere. There are two highly diverged mitochondrial lineages in the Atlantic (Mäkinen and Merilä, 2008): the European ('*Eu*') and trans-Atlantic ('*At*'). There are at least thirty fixed nucleotide differences between these lineages and estimates of their divergence time range from 128,000 to 58,000 years before present, clearly pre-dating the last glacial maximum (Dean et al., 2019a; Mäkinen and Merilä, 2008a; Ravinet et al., 2013). Both lineages are found in coastal marine habitats across the Atlantic, including the East coast of North America, Greenland, Iceland, Ireland, Scotland and mainland Europe (Dean et al., 2019; Liu et al., 2016; Mäkinen and Merilä, 2008; Ravinet et al., 2013). However, we have previously found that the *Eu* lineage has often colonised fresh water and brackish lagoons across the Atlantic, but the *At* lineage has rarely done so (Chapter 4, Dean et al., 2019).

Metabolic requirements differ greatly between coastal marine and fresh or brackish environments: not only does moving from salt to fresh or brackish water require efficient osmoregulation which is an energy dependent process, but both the climate and food sources differ between the Atlantic Ocean and fresh/brackish habitats (Ishikawa et al., 2021b; Twining et al., 2021). Permanently inhabiting lakes, streams and lagoons also requires a shift from a migratory to resident lifestyle. Stickleback research has focused on the nuclear genetic basis of freshwater adaptation, including the Ectodysplasin (*Eda*) locus which controls armour plate loss (Colosimo et al., 2005a; Jones et al., 2012), and the evolution of duplications of fatty acid desaturase 2 (*Fads2*) that permits adaptation to freshwater environments where food sources have poor nutritional quality (Ishikawa et al., 2021b; Twining et al., 2021). However, as energy requirements differ between freshwater and marine environments, mitochondrial metabolic differences may play a key role in adaptation which has rarely been studied, although the modification of mitochondrial pathways has previously been associated with hydrogen sulphide adaptation in other fish (Greenway et al., 2020). Adapting to the local environment will favour small changes in metabolic

function, which may occur as a consequence of mtDNA differences between *Eu* and *At* stickleback. As the *Eu* and *At* haplotypes segregate within otherwise panmictic anadromous populations (Haenel et al., 2022) there are very unlikely to be nuclear genetic differences between lineages and no morphological differences have previously been recorded (but see Chapter 4). This makes the Atlantic stickleback a valuable model to determine whether mtDNA variation alone can have functional consequences for OXPHOS and therefore for adaptation.

Here we used the Oroboros Oxygraph-O2k (O2k; Oroboros® Instruments, Innsbruck, Austria) to measure mitochondrial respiratory function in the brain and heart of *Eu* and *At* stickleback across three assay temperatures. Mitochondrial respiration in the stickleback is known to be strongly affected by assay temperature (Chouinard-Boisvert et al., 2024), but no work to our knowledge has compared the major evolutionary lineages. We measured respiration rate at the temperature extremes that these stickleback populations may experience in the wild, as well as at 14°C, the temperature that the stickleback had been raised at in the University of Nottingham aquarium, as previous work comparing mitochondrial respiration between mitochondrial haplotypes suggested that differences may have only been apparent under stress or certain environmental conditions (Baris et al., 2016). We first identified temperature dependent differences in uncoupled respiration between *Eu* and *At* stickleback, before utilising frozen tissue and new frozen protocols to confirm that differences were in CI respiration, which has subunits encoded by the mtDNA.

6.3 Methods

To determine whether the diverged mitochondrial DNA sequences between *Eu* and *At* lineage stickleback have functional consequences for mitochondrial respiration, high-resolution respirometry (HRR) was performed using the Oroboros Oxygraph-O2k (Oroboros® Instruments, Innsbruck, Austria) to compare mitochondrial respiration in homogenised heart and brain samples from both lineages. We used two different tissues to find out if effects were organ specific. Migratory populations with a known mix of *Eu* and *At* stickleback (Chapter 4, Dean et al., 2019) were selected to ensure minimal nuclear genetic differences. We performed HRR at three assay temperatures. Additional HRR assays were then conducted on frozen tissue to confirm findings.

6.3.1 Fish husbandry

Migratory stickleback were collected from North Uist in the Western Isles of Scotland in May 2022 using mesh traps set along the perimeter of lochs. Traps were left for 24-

hours before stickleback in breeding condition were collected from Loch an Duin (57.64245, -7.209207) and Loch Bhrusda (57.726658, -7.174834). Crosses from two separate populations were made following standard procedures (Hatfield, 1997), by squeezing eggs from gravid, euthanised females into small petri dishes and mixing them with the testes from euthanised reproductive males. Fish were euthanised with an overdose of tricaine methanesulfonate (400mg/L) followed by destruction of the brain in accordance with Schedule One of UK Home Office regulations. Fin clips were taken from the mother, which were used to extract DNA and determine mitochondrial lineage as mitochondria are maternally inherited. Migratory populations were selected as on North Uist these populations have previously been identified as being an approximately equal mix of the two mitochondrial lineages (Chapter 4, Dean et al., 2019), therefore limiting variation in the nuclear genomes between lineages (Chapter 4), as both live alongside each other and interbreed. Fertilised clutches were transported to the University of Nottingham aquarium where they hatched and were raised at approximately 14°C and fed a combination of paramecium and brine shrimp until approximately 3 months old before being fed frozen blood worm once a day. At 9 to 10 months old, stickleback were large enough to extract tissues from and conduct HRR. They were then euthanised as above.

6.3.2 Determining mitochondrial lineage

DNA was extracted from the fin clips from each mother using Quanta Bio Extracta DNA prep for PCR. A polymerase chain reaction (PCR) and restriction fragment length polymorphism (RFLP)-based assay was used to distinguish lineages. Briefly, an approximately 600bp fragment of ND4 and ND5 was amplified from each sample using specific primers (**Table 6.1**). PCR was performed in a thermocycler (G-Storm GS1). PCR reaction conditions were as follows: initial denaturation at 94°C for 3 minutes followed by 36 cycles: denaturation at 94°C, 30 seconds; annealing at 60°C, 30 seconds; extension at 72°C, 1 minute. Then a final extension at 72°C for 5 minutes. The ND4 fragment was incubated with Hind*III* and ND5 with Pst*I*. If the sample was of the *Eu* lineage, the amplified region of ND4 was cut but ND5 was not, and vice versa if an individual was *At* (**Table 6.1**). 4µl of each product was separated on a 2% agarose gel at 100 Volts for 30-40 minutes alongside a 100bp ladder (NEB) and then visualised using UV-illumination (iBright CL750 Imaging System, ThermoFisher Scientific). Using both assays ensured a positive result for both lineages. The mitochondrial lineage of the offspring was therefore known and individuals from each mitochondrial lineage could be selected at random for HRR trials. However, to ensure

that the correct lineage had been assigned, fin clips were taken from the individual used for HRR and the assays above repeated.

Table 6.1: Primers, restriction enzymes and resulting DNA fragment sizes used to distinguish mitochondrial lineages.

Primer	Forward Sequence	Reverse Sequence	Enzyme	Cuts	*Eu* size (bases)	*At* size (bases)
ND4	TCTCGTTGCC CTCCTTCTAC	TCCAAGGTTG CAAGGCTTG	Hind*III*	*Eu*	183; 442	625
ND5	CGGACTAAAC CAACCACACC	GTGATGTGGG GTTAAGCGAG	Pst*I*	*At*	616	219; 397

6.3.3 Dissection and sample preparation

HRR experiments were conducted over a month in March and April 2023. Stickleback were euthanised by submersion in MS-222 followed by pithing. Although MS-222 has previously been found to alter some HRR measurements in the brain (Barnes et al., 2023), any effect would be equal for *Eu* and *At* stickleback so will not bias results. Samples were kept on ice. Immediately prior to HRR, the heart of each stickleback was removed, weighed, and homogenised in 200µl ice cold MiRO5 buffer (Oroboros Instruments GmbH; 0.5 mM EGTA, 3 mM $MgCl_2$, 60 mM Lactobionic acid, 20 mM Taurine, 10 mM KH_2PO_4, 20 mM HEPES, 110 mM D-Sucrose, 1g/L BSA) using 20 crushes with a micropestle. All of the heart homogenate was added to the 2ml chamber of the O2k. Analysis of the brain was always conducted after the heart. The brain of the same stickleback was dissected, weighed and homogenised as above. 5mg of brain homogenate was added per chamber and this was assayed at the same temperature as the heart.

6.3.4 High-Resolution Respirometry

Mitochondrial respiration was measured at three different assay temperatures with samples being randomly assigned a treatment. Assay temperatures were 14°C as this is the approximate temperature stickleback were raised at in the aquarium, and 6°C and 22°C as these are the approximate lower and upper limits that three-spined stickleback will experience in lochs on North Uist. O2k electrodes were calibrated at the correct temperature before each set of samples. A protocol to assess mitochondrial respiration with NADH-linked substrates (CI) and S-pathway substrates (CII) was used to get an overview of different parameters of respiration with different substrate combinations. Substrate concentrations had previously been optimised for use with stickleback tissue (Barnes et al., 2023). After substrate or inhibitor addition,

oxygen flux reached equilibrium which was subsequently marked before moving on to the next substrate addition.

MiRO5 was added to each O2k chamber, reaching a final volume of 2ml. Heart or brain homogenate was then added and allowed to reach equilibrium before the protocol commenced (**Figure 6.1**). Pyruvate (5mM) and malate (2mM) were first added which stimulate CI linked respiration. This measures LEAK state ($LEAK_{CI}$) as no ADP is present to be phosphorylated. In the mitochondria, pyruvate is converted to acetyl-CoA by pyruvate dehydrogenase. Acetyl CoA then enters the Krebs cycle where electrons are donated to NAD+, producing NADH. Also in the Krebs cycle, malate is oxidised to oxaloacetate producing NADH. NADH enters the ETS at CI and electrons are transported through the ETS enzyme complexes. However, without ADP, no phosphorylation can occur.

ADP (5mM) was then added in excess to stimulate OXPHOS ($OXPHOS_{CI}$). Succinate, a CII linked substrate, was added to get a measure of OXPHOS with both CI and CII substrates ($OXPHOS_{CI+CII}$). Succinate is converted to fumarate by succinate dehydrogenase, while reducing FAD to $FADH_2$. Membrane integrity was tested by adding cytochrome c (0.01mM). If any membrane damage had occurred, cytochrome c would have been lost from the membrane; addition of further cytochrome c would have therefore increased respiration rate. No experimental runs displayed more than a 15% increase in oxygen flux with cytochrome c addition, so membrane integrity was considered intact in all runs. Electron transfer (ET) capacity was measured as oxygen consumption when electron transfer and phosphorylation are uncoupled (electron transfer is no longer limited by the capabilities of the phosphorylation system), reached by titrating in carbonyl cyanide m-chlorophenyl hydrazone (CCCP; 0.5µM steps) until maximal rate of oxygen consumption was reached (**Figure 6.1**). This gives a measure of ET capacity with both CI and CII substrates ($ET\ capacity_{CI+CII}$), but to measure CII respiration alone ($ET\ capacity_{CII}$) the complex I inhibitor rotenone (0.5µM) was added. Antimycin A (2.5µM), which inhibits CIII and thus gives a measure of residual oxygen consumption (ROX) due to oxidative side reactions, was last to be added and used as the background measure to be subtracted from other values. Chemical reagents were supplied by Sigma-Aldrich, except for ADP with was supplied by Merck (Calbiochem).

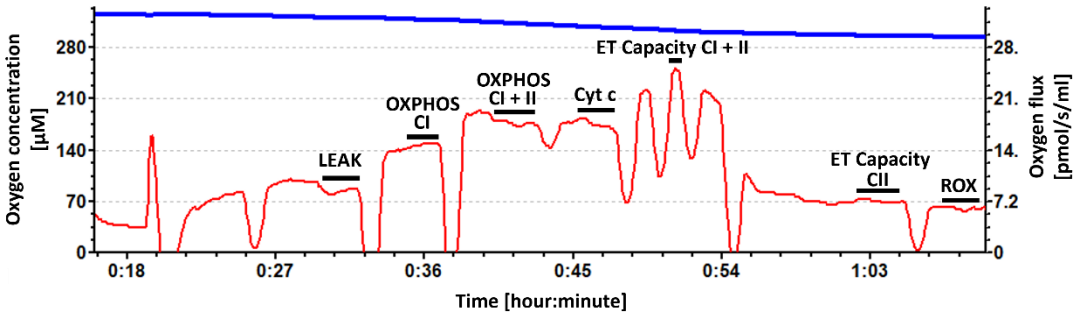

Figure 6.1: Annotated O2k Oxygraph. Example trace from the brain of the stickleback measured at 14°C following the described protocol. Blue line shows the oxygen concentration (µM) in the chamber, red line shows the rate of oxygen consumption (flux pmol/s/ml) per 5mg of tissue. Measured respiration states are shown by black bars.

6.3.5 HRR with frozen tissue

To follow up the initial HRR conducted on the brains and heart of *Eu* and *At* stickleback, two further protocols were conducted on frozen tissue with an assay temperature of 6°C. The use of frozen tissue allowed use of samples previously collected for other purposes, reducing the number of stickleback sacrifices necessary. Samples were collected in May 2023 and 2024 following the method described previously from three lochs on North Uist, where known mixed populations of *Eu* and *At* stickleback are found: Loch an Duin (57.64245, -7.209207), Loch nan Clachan (57.637635, -7.4148770) and Loch Grogarry (57.615827, -7.513195). These were euthanised (as in section **6.3.3**) and were frozen at -20°C during fieldwork before being transferred to -80°C in Nottingham no more than two weeks later. HRR was conducted in November 2023 or August 2024. Hearts were dissected and homogenised as in section **6.3.3** and 2.5mg tissue was added per chamber. In November 2023, the brains of the same stickleback were subsequently dissected and homogenised as in **6.3.3** and 4mg was added per chamber. Two protocols were conducted per sample.

When frozen, the Krebs cycle is inactivated and the mitochondrial outer membrane is compromised meaning that samples can only be assessed in the non-coupled state (Ebanks et al., 2023). Protocols were designed following Ebanks et al. 2023, modified to assess CI and CII separately. Protocol 1 measured CI linked respiration by the addition of NADH which is directly oxidised by CI, while Protocol 2 measured CII linked respiration (**Figure 6.2**) by the addition of succinate. Both protocols started with the addition of cytochrome c (0.01mM) and uncoupler (CCCP; 0.5µM) to ensure

mitochondria were fully uncoupled. In Protocol 1, CII was first inhibited by malonate (5mM) before addition of NADH (20mM) and the peak specific flux was marked. In Protocol 2, CI was inhibited with rotenone (0.5µM) and Succinate (1M) added before marking peak specific flux. Respiration was then inhibited by rotenone (0.5µM; Protocol 1) or malonate (5mM, Protocol 2) and antimycin A (2.5µM; Protocols 1 and 2) and this value was used for background correction.

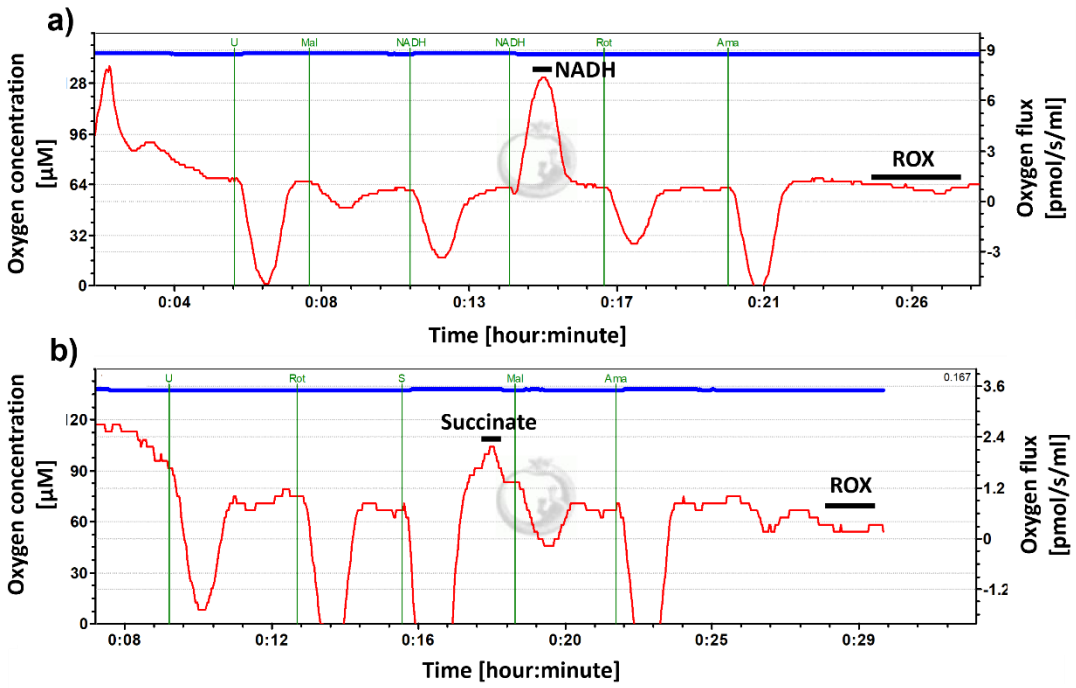

Figure 6.2: Example frozen tissue HRR protocol to measure CI (a) and CII (b) respiration in the stickleback heart. Blue line shows the oxygen concentration in the chamber; red line is the rate of oxygen consumption (flux) per 2.5mg tissue. Titration of NADH and succinate results in a peak of oxygen flux before decrease. Measured respiration states are shown by black bars.

6.3.6 Data analysis

Standard length and body mass were compared between lineages using t-tests as body size can influence metabolic physiology in fish (Luo et al., 2012). Raw HRR data for each stage were extracted from DatLab (DatLab v7, Oroboros, Innsbruck, Austria). Background correction calculations were conducted by subtracting ROX from each value (**Figure 6.1**), and we calculated the oxygen flux per milligram of tissue added to the O2k chamber. Flux control ratios (FCRs) were then calculated; these give the ratio of oxygen flux in each respiration state and substrate combination tested ($LEAK_{CI}$, $OXPHOS_{CI}$, $OXPHOS_{CI+CII}$), normalised to the maximum oxygen flux in ET state (ET $capacity_{CI+CII}$). This expresses respiratory control independent of

mitochondrial content and allows comparison between samples (Doerrier et al., 2018; Gnaiger, 2020). Values were calculated for each temperature and tissue separately. Further analysis was conducted in R (R Core Team 2021).

The proportion of respiration due to CI and CII was evaluated at ET capacity using HRR measurements. This was calculated as follows, using the background corrected values:

$$\text{CI contribution} = (\text{ET Capacity}_{\text{CI+II}} - \text{ET Capacity}_{\text{CII}}) / \text{ET Capacity}_{\text{CI+II}}$$

$$\text{CII contribution} = \text{ET Capacity}_{\text{CII}} / \text{ET Capacity}_{\text{CI+II}}$$

Only CI contribution is presented as values for CI and CII contribution add to one and therefore show the same results.

Linear models were fitted to three respiratory states (LEAK, $\text{OXPHOS}_{\text{CI}}$, $\text{OXPHOS}_{\text{CI+II}}$) and to CI contribution with temperature, mitochondrial lineage and an interaction between these as explanatory variables. Standard length, body mass, sex and population did not significantly affect FCRs in any state. As we fitted multiple linear models with four different response variables and two tissue types, we used the false discovery rate (FDR) method to control for type 1 errors (Benjamini and Hochberg, 1995; Mcdonald, 2014) with an FDR threshold of 0.1 which allowed for 10% of significant results to be false positives.

Maximum peak specific flux values for NADH and Succinate measured during HRR on frozen tissue were background corrected by subtracting the value for ROX (**Figure 6.2**) and are presented as oxygen consumption per 2.5mg heart tissue or per 4mg brain tissue. CI and CII respiration in both tissues were analysed separately. Background corrected respiration rates were log transformed and compared between lineages by conducting t-tests.

6.4 Results

6.4.1 Mitochondrial lineages

The mitochondrial lineage of all samples was successfully determined using the diagnostic assays. There was no difference in standard length (t-test: t = 0.983, df = 28.4, p-value = 0.334) or body mass (t-test: t = -0.465, df = 32.1, p-value = 0.645) between lineages. For final sample sizes see **Table 6.2**.

Table 6.2: Number of *Eu* and *At* samples used for HRR.

Tissue	Temperature (°C)	*Eu* number	*At* number
Brain	6	5	5
	14	4	8
	22	2	6
Heart	6	6	4
	14	2	7
	22	6	5

6.4.2 High-Resolution Respirometry

Three respirometry states were compared: LEAK with CI substrates ($LEAK_{CI}$); OXPHOS with CI substrates ($OXPHOS_{CI}$); OXPHOS with CI and CII substrates ($OXPHOS_{CI+II}$). These are presented as FCRs (**Figure 6.3**) which is the ratio of oxygen flux in each respiration state normalised to the maximum oxygen flux in ET state. This allows a comparison of respiration between mitochondrial lineages independent of mitochondrial content (Doerrier et al., 2018; Gnaiger, 2020). We also calculated and compared the contribution of CI to maximal respiration rate when mitochondria were uncoupled (ET capacity state) between *Eu* and *At* stickleback. We present only CI contribution as CI and CII contributions add to one and therefore show the same results.

In the heart, temperature influenced FCRs in $LEAK_{CI}$ and $OXPHOS_{CI+II}$ states (**Figure 6.3, Table 6.3, Table S6.1**), although in $LEAK_{CI}$ state this did not remain significant after correcting for multiple testing (**Table S6.2**). LEAK respiration was lowest at 14°C but increased at both temperature extremes, whereas with increasing temperatures respiration rate increased in $OXPHOS_{CI+II}$ state (**Figure 6.3**). $OXPHOS_{CI}$ was not significantly affected by temperature or lineage, however FCRs at 14 and 22°C tended to be higher than at 6°C. CI contribution was dependent on the mitochondrial lineage in the heart; CI contribution in the *Eu* lineage was largely unaffected by assay temperature, but in *At* stickleback CI contribution decreased with increasing temperature. This resulted in a large difference in CI contribution between *Eu* and *At* stickleback at 6°C.

In the brain, respiration rate increased with increasing temperatures in both LEAK and OXPHOS states (**Figure 6.3**, **Table 6.3**, **Table S6.1**). Mitochondrial lineage did not influence FCRs or CI contribution, although *At* stickleback FCRs tended to be

lower than *Eu*. FCRs in $OXPHOS_{CI}$ and $OXPHOS_{CI+CII}$ states were generally higher in the heart than the brain. In $LEAK_{CI}$, FCRs were similar in both tissues at 6°C but in the brain FCRs increased with temperature in contrast to the heart where FCRs decreased at the higher assay temperatures (although there was no significant effect of assay temperature after correction for multiple comparisons (**Table S6.2**)).

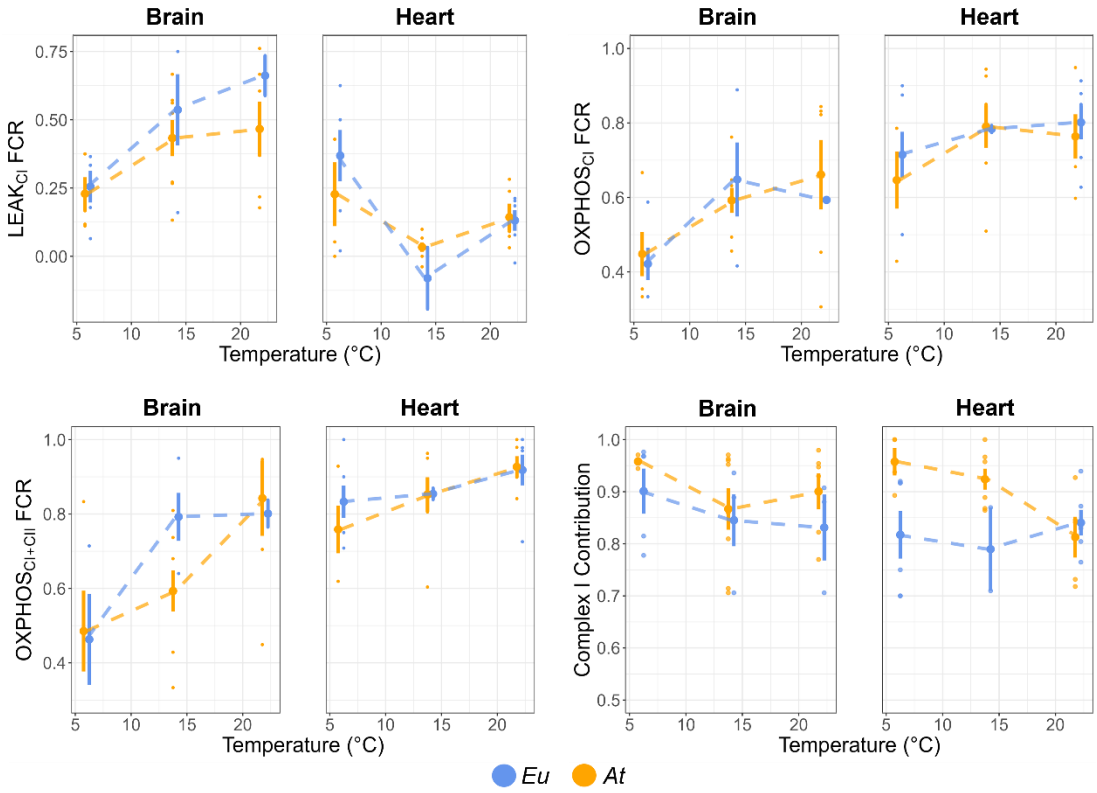

Figure 6.3: Comparison of mitochondrial respiration in the brain and heart of *Eu* and *At* stickleback conducted at three assay temperatures. Respiration rates are presented as FCRs in three respiratory states ($LEAK_{CI}$, $OXPHOS_{CI}$ and $OXPHOS_{CI+CII}$) to provide a normalised value to compare across samples. The contribution of CI to maximal respiration rate when mitochondrial were uncoupled is also presented (calculation shown in **6.3.6**). The *Eu* lineage is shown in blue and the *At* in orange. Each point shows an individual sample. Dashed lines join the mean values from the three assay temperatures. Error bars show standard error. See **Table 6.2** for final sample sizes.

Table 6.3: Results of linear models fitted to three respiratory states ($LEAK_{CI}$, $OXPHOS_{CI}$, $OXPHOS_{CI+II}$) and to CI contribution to maximum uncoupled respiration rate. Temperature, mitochondrial lineage and their interaction as

explanatory variables. Values where P < 0.05 shown in **bold**. Values in ***italics*** were no longer significant after correcting for multiple testing (see **Table S6.2**).

Tissue	Respiratory State	Treatment P Values		
		Assay Temperature	Mitochondrial Lineage	Assay temperature x Mitochondrial Lineage
Heart	LEAK	***0.039***	0.226	0.298
	$OXPHOS_{CI}$	0.119	0.707	0.856
	$OXPHOS_{CI+II}$	**0.012**	0.518	0.364
	CI contribution	0.181	**0.013**	**0.019**
Brain	LEAK	**0.004**	0.229	0.298
	$OXPHOS_{CI}$	**0.006**	0.921	0.943
	$OXPHOS_{CI+II}$	**0.001**	0.454	0.880
	CI contribution	0.187	0.158	0.556

6.4.3 HRR with frozen tissue

As mitochondrial lineage significantly affected CI contribution in the heart (**Figure 6.3**), in particular at 6°C, and this pattern, although not significant, was also present in the brain, we next aimed to determine whether it was the function of CI and/or CII in the ETS that differed between lineages. The *Eu* lineage had a lower CI contribution than *At* at 6°C in the heart; this could be due to a decrease in the function of CI and/or an increase in the function of CII. As the mtDNA encodes seven CI core subunits but CII is entirely encoded by the nuclear genome, we hypothesised that differences would be in CI respiration. We assessed the NADH-linked CI pathway and the Succinate-linked CII pathway separately to determine if either pathway differed between lineages. An assay temperature of 6°C was chosen as this is where the largest difference between *Eu* and *At* stickleback was identified (**Figure 6.3**). Frozen stickleback were used so the Krebs cycle was disrupted and the outer membrane ruptured, uncoupling the mitochondria (Ebanks et al., 2023). All HRR measurements would therefore be in ET Capacity state.

At stickleback had higher CI respiration with NADH than *Eu* in both the heart (**Figure 6.4**; $t_{12.3} = 2.619$, $p = 0.022$), and the brain ($t_{6.19} = 3.203$, $p = 0.018$) but CII respiration with Succinate did not differ between lineages in either tissue (**Figure 6.4**; Heart: $t_{15.271} = 0.558$, $p = 0.585$; Brain: $t_{6.99} = 0.693$, $p = 0.511$). As there was one CI and CII value much higher than the rest within the *At* lineage in the heart, the analysis was repeated

excluding these values, but this did not change overall findings in CI ($t_{9.04}$ = 2.392, p = 0.040) or CII ($t_{13.30}$ = 0.104, p = 0.919) respiration.

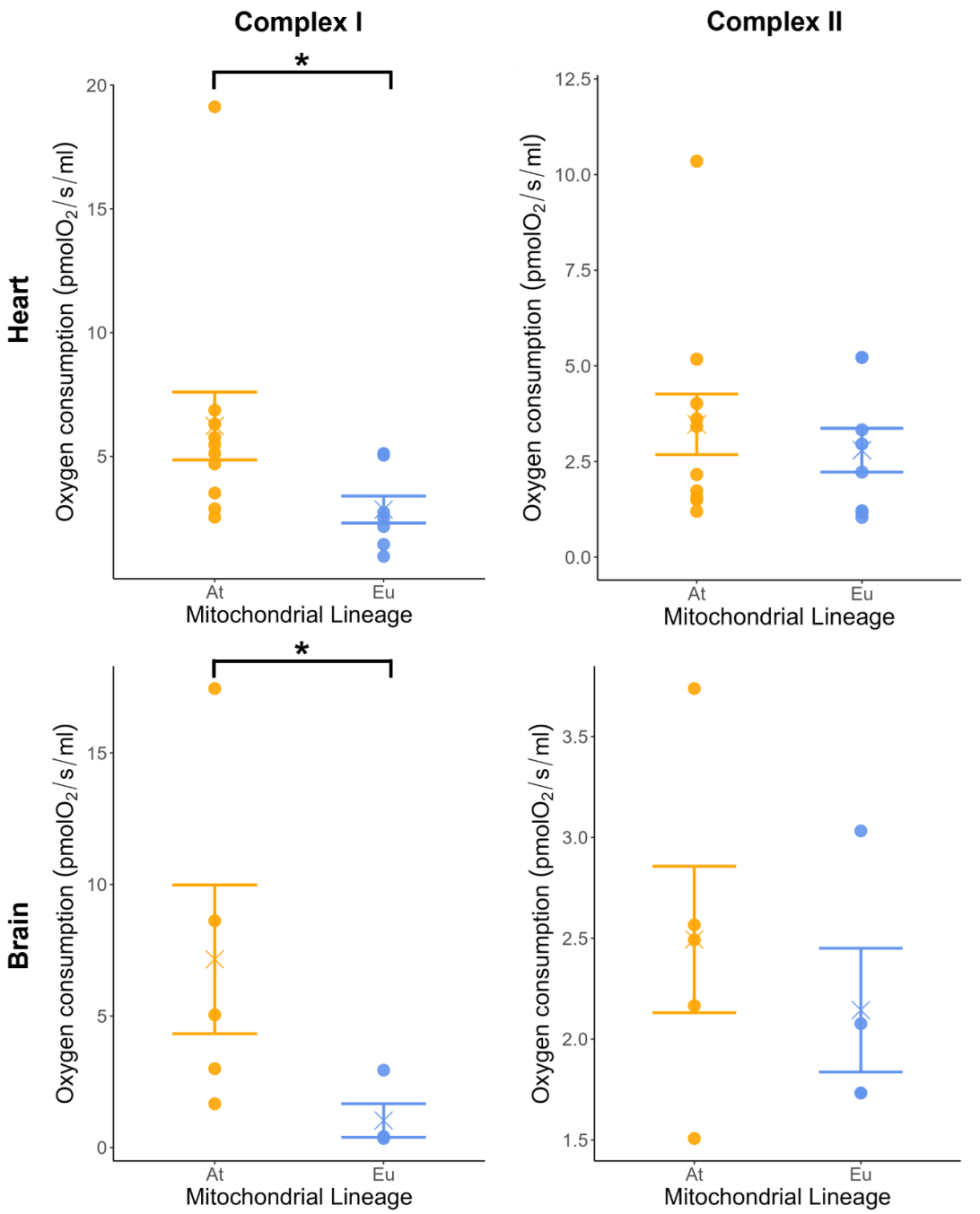

Figure 6.4: HRR using frozen *Eu* and *At* stickleback heart and brain. CI respiration measured by the addition of NADH; CII measured with succinate. *Eu* lineage in blue and *At* in orange with individual data points shown. Error bars show standard error. Peak rate of oxygen consumption presented per 2.5mg heart homogenate or 4mg brain homogenate. Significant differences between lineages at p < 0.05 labelled with asterisk. n = 20 and 9 for the heart and brain respectively.

6.5 Discussion

6.5.1 Variation in mitochondrial sequence had physiological consequences for CI respiration

We investigated how *Eu* and *At* mitochondrial lineages and temperature affected mitochondrial physiology in the heart and brain of *Eu* and *At* Atlantic three-spined stickleback with a common nuclear genetic background. Temperature affected multiple parameters of respiration, and CI contribution to uncoupled respiration differed between mitochondrial lineages in the heart, dependent on the assay temperature. Uncoupled mitochondria are not restrained by the phosphorylation system and allow measurement of the maximum capacity of the electron transfer system. This resulted in a large difference in complex contributions between *Eu* and *At* stickleback at 6°C, because while *Eu* stickleback maintained complex contributions across all assay temperatures, the *At* lineage decreased CI contribution with increasing temperature.

By conducting HRR using frozen tissue, we identified that the difference between mitochondrial lineages at cold temperatures was due to CI and not CII respiration. From these results it could be suggested that the differences in enzyme complex contribution to flux were due to alterations in respiration via CI with CII function remaining the same, although we cannot rule out with complete certainty that some of the differences we saw were due to interactions between CI and CII that were not measured. This is consistent with CI, but not CII, having mitochondrially encoded subunits. These findings suggest that variation in the mtDNA sequence between *Eu* and *At* stickleback has physiological consequences for CI function, particularly at cold temperatures.

6.5.2 CI respiration differed between lineages

By designing two HRR protocols to assess CI and CII respiration separately in frozen and therefore uncoupled tissue, we found that at 6°C *At* stickleback had a higher CI respiration rate than *Eu* in both the heart and brain but there were no differences in CII. Whether this difference holds true at the higher temperatures we assessed requires further investigation. Frozen tissue protocols have only recently been implemented on the O2k (Ebanks et al., 2023). Here we developed two assays to be conducted on homogenised frozen tissue to assess CI and CII linked respiration in two simultaneous runs with one protocol per O2k chamber. By measuring the peak specific flux with NADH (CI) or succinate (CII) in separate protocols, we were able to

assess each lineages maximal rate of oxygen consumption via CI or CII alone. Titration of NADH and succinate led to a rapid increase, followed by decrease, in oxygen consumption which was also found in other frozen tissue protocols (Ebanks et al., 2023). This decrease in oxygen consumption may be due to the freezing process inactivating the Krebs cycle, therefore preventing the cycling of substrates so that once used up respiration rate decreased. Peak specific flux was also lower with succinate than NADH, which agrees with the observation that CI contribution was higher than CII in fresh tissue.

Our findings suggest that differences in mitochondrial function between *Eu* and *At* stickleback are most likely in complex I and present at cold assay temperatures. Subunits of CI are encoded by both the mitochondrial and nuclear genomes but as we used freely interbreeding, naturally occurring admixed populations, nuclear genetic differences between lineages were unlikely (Chapter 4), suggesting that mtDNA variation can influence CI respiration independent of the nuclear genetic background. As we only identified differences in uncoupled respiration between mitochondrial lineages, whether differences could have further implications for mitochondrial function still requires research. For example, whether these CI differences observed at maximal respiration rate (attained when respiration is uncoupled) influence mitochondrial efficiency, ATP production or ROS generation could now be investigated.

We found that CI differences were dependent on the environment, in agreement with work in alternative models (Aw et al., 2018; Baris et al., 2016; Pichaud et al., 2013). CI is the largest enzyme complex of the ETS; it transfers electrons from NADH to ubiquinone and pumps protons from the mitochondrial matrix to the intermembrane space. CI contributes significantly to the formation of reactive oxygen species (ROS) (Wirth et al., 2016), which can cause oxidative damage and mitochondrial dysfunction (Guo et al., 2013). The observed differences in CI respiration between *Eu* and *At* stickleback could result in differences in ROS production which could have long-term consequences for fitness and survival, dependent on the environment, but this would need to be tested.

6.5.3 Temperature affected multiple respiratory parameters

The assay temperature also influenced the different respirometry parameters, as found in other fish species including the killifish (*Fundulus heteroclitus*) (Baris et al., 2016). We observed a decrease in OXPHOS respiration in both the brain and heart at cold temperatures, in agreement with previous work (Jørgensen et al., 2023; Menail

et al., 2022), including in the stickleback (Chouinard-Boisvert et al., 2024). Mitochondrial respiration was maintained even at 22°C, our predicted upper thermal limit of North Uist lochs, suggesting that stickleback mitochondria are well-adapted to these temperatures and might tolerate higher temperatures than they generally experience in their natural environment. Whether the temperature that the stickleback are acclimated to influences mitochondrial function could also now be tested.

6.5.4 Tissue-specific differences in respiratory parameters

FCRs were generally higher in the heart muscle than the brain, perhaps indicating increased efficiency in the heart. $LEAK_{CI}$ respiration, which is oxygen consumption, compensating for proton leak, that does not result in ATP production, differed between tissue types. In the brain we observed an increase in FCRs with temperature, in agreement with previous findings in the stickleback (Chouinard-Boisvert et al., 2024). In the heart, maximum $LEAK_{CI}$ was at the temperature extremes, in particular at 6°C, which was not tested previously, although after correcting for multiple testing we found no effect of temperature on $LEAK_{CI}$ in the heart. When measuring mitochondrial respiration using frozen tissue at 6°C, we found differences in CI and no differences in CII respiration rate in both tissues we assessed, so these findings were generally not tissue specific.

6.5.5 Ecological and evolutionary consequences

The frequencies of *Eu* and *At* fish differ between habitat types, with the Atlantic Ocean a mix of both lineages but stickleback with the *Eu* mtDNA dominating in fresh water and saltwater lagoons (Chapter 4, Dean et al., 2019). As metabolic requirements differ between freshwater and oceanic environments, we hypothesised that mtDNA variation that caused differences in mitochondrial function could result in different adaptive potential. Here we show measurable, temperature-dependent differences in CI respiration between Atlantic stickleback mitochondrial lineages that differ in mtDNA sequence. Complex contributions in the *Eu* stickleback were maintained across assay temperatures in contrast to the *At* lineage where CI contribution declined when assayed at higher temperatures. This suggests that *At* CI function may decline in warmer environments, but this would need to be tested further as the contribution of alternative substrates could compensate for the decline in CI (Menail et al., 2022), and we have not assessed the physiological consequences for mitochondria at temperatures above 22°C. This could at least in part explain why there are very few locations where we find *At* stickleback in freshwater (Chapter 4), as these likely reach higher temperatures than the Atlantic Ocean. This is consistent with our previous

results suggesting that there are fewer *At* stickleback in habitats that reach higher maximum sea surface temperatures (Chapter 4). Diet can also alter metabolic requirements between environments and mitochondrial physiology (Aw et al., 2018; Ballard and Youngson, 2015; Towarnicki and Ballard, 2020). The reduced nutritional quality of the freshwater diet (Twining et al., 2021) could favour small changes in metabolic function, although whether the differences in CI respiration we found between lineages could be beneficial under particular circumstances would need further exploration.

6.5.6 Conclusions

We have shown that the variation in mtDNA between stickleback mitochondrial lineages in the Atlantic had temperature-dependent physiological consequences, in particular uncoupled respiration via CI, where the *At* lineage had higher CI respiration at cold temperatures than the *Eu* lineage. As the populations studied were admixed, freely interbreeding *Eu* and *At* stickleback, nuclear genetic differences were minimal. So, although we cannot definitely rule out mitochondrial sequences being in linkage disequilibrium with adaptive alleles in the nuclear genome, differences in OXPHOS are most likely due to the mtDNA variation between lineages. This adds to the accumulating evidence that the mitochondrial sequences are non-neutral and may therefore be adaptive. Whether the observed differences in CI respiration have further implications for mitochondrial function or individual fitness should now be investigated.

6.6 References

Avise, J.C., Arnold, J., Martin Bal, R., Bermingham, E., Lamb, T., Neigel, J.E., Reeb, C.A., Saunders, N.C., 1987. Intraspecific phylogeography: The Mitochondrial DNA Bridge Between Population Genetics and Systematics. *Ann. Rev. Ecol. Sys.* **18**, 489–522. https://doi.org/10.1146/annurev.es.18.110187.002421

Aw, W.C., Towarnicki, S.G., Melvin, R.G., Youngson, N.A., Garvin, M.R., Hu, Y., Nielsen, S., Thomas, T., Pickford, R., Bustamante, S., Vila-Sanjurjo, A., Smyth, G.K., Ballard, J.W.O., 2018. Genotype to phenotype: Diet-by-mitochondrial DNA haplotype interactions drive metabolic flexibility and organismal fitness. *PLoS Genet* **14**, e1007735. https://doi.org/10.1371/JOURNAL.PGEN.1007735

Ballard, J.W.O., Youngson, N.A., 2015. Review: can diet influence the selective advantage of mitochondrial DNA haplotypes? *Biosci. Rep.* **35**, e00277. https://doi.org/10.1042/BSR20150232

Ballard, J.W.O., Kreitman, M., 1995. Is mitochondrial DNA a strictly neutral marker? *TREE.* **10**, 485-488. https://doi.org/10.1016/S0169-5347(00)89195-8

Ballard, J.W.O., Whitlock, M.C., 2004. The incomplete natural history of mitochondria. *Mol. Ecol.* **13**, 729-744. https://doi.org/10.1046/j.1365-294X.2003.02063.x

Baris, T.Z., Blier, P.U., Pichaud, N., Crawford, D.L., Oleksiak, M.F., 2016. Gene by environmental interactions affecting oxidative phosphorylation and thermal sensitivity. *Am. J. Physiol. Regul. Integr. Comp. Physiol.* **311**, R157–R165. https://doi.org/10.1152/ajpregu.00008.2016

Barnes, M., Ebanks, B., MacColl, A., Chakrabarti, L., 2023. A Common Anaesthetic, MS-222, Alters Measurements Made Using High-Resolution Respirometry in the Three-Spined Stickleback (*Gasterosteus aculeatus*). *Fishes* **8**, 42. https://doi.org/10.3390/fishes8010042

Barreto, F.S., Watson, E.T., Lima, T.G., Willett, C.S., Edmands, S., Li, W., Burton, R.S., 2018. Genomic signatures of mitonuclear coevolution across populations of *Tigriopus californicus*. *Nat. Ecol. Evol.* **2**, 1250–1257. https://doi.org/10.1038/s41559-018-0588-1

Bell, M.A., Foster, S.A., 1995. The Evolutionary Biology of the Threespine Stickleback. *J. Anim. Ecol*. **64**, 418-419. https://doi.org/10.2307/5902

Benjamini, Y., Hochberg, Y., 1995. Controlling the False Discovery Rate: A Practical and Powerful Approach to Multiple Testing. *J. R. Stat. Soc. Ser. B.* **57**, 289–300. https://doi.org/10.1111/J.2517-6161.1995.TB02031.X

Brijs, J., Sandblom, E., Sundh, H., Gräns, A., Hinchcliffe, J., Ekström, A., Sundell, K., Olsson, C., Axelsson, M., Pichaud, N., 2017. Increased mitochondrial coupling and anaerobic capacity minimizes aerobic costs of trout in the sea. *Sci. Rep.* **7**, 45778. https://doi.org/10.1038/srep45778

Cecchini, G., 2003. Function and structure of complex II of the respiratory chain. *Ann. Rev. Biochem.* **72**, 77–109. https://doi.org/10.1146/ANNUREV.BIOCHEM.72.121801.161700

Cheviron, Z.A., Bachman, G.C., Connaty, A.D., McClelland, G.B., Storz, J.F., 2012. Regulatory changes contribute to the adaptive enhancement of thermogenic capacity in high-altitude deer mice. *PNAS.* **109**, 8635–8640. https://doi.org/10.1073/PNAS.1120523109

Chouinard-Boisvert, S., Ghinter, L., St-Pierre, A., Mortz, M., Desrosiers, V., Dufresne, F., Tardif, J.-C., Huard, J., Sirois, P., Fortin, S., Blier, P.U., 2024. Mitochondrial functions and fatty acid profiles in fish heart: an insight into physiological limitations linked with thermal tolerance and age. *J. Exp. Biol*. **227**, jeb247502. https://doi.org/10.1242/JEB.247502

Colosimo, P.F., Hosemann, K.E., Balabhadra, S., Villarreal, G., Dickson, H., Grimwood, J., Schmutz, J., Myers, R.M., Schluter, D., Kingsley, D.M., 2005. Widespread parallel evolution in sticklebacks by repeated fixation of ectodysplasin alleles. *Science.* **307**, 1928–1933. https://doi.org/10.1126/SCIENCE.1107239

Dean, L.L., Magalhaes, I.S., Foote, A., D'Agostino, D., McGowan, S., MacColl, A.D.C., 2019. Admixture between Ancient Lineages, Selection, and the Formation of Sympatric Stickleback Species-Pairs. *Mol. Biol. Evol.* **36**, 2481–2497. https://doi.org/10.1093/MOLBEV/MSZ161

Doerrier, C., Garcia-Souza, L.F., Krumschnabel, G., Wohlfarter, Y., Mészáros, A.T., Gnaiger, E., 2018. High-resolution fluorespirometry and oxphos protocols for human cells, permeabilized fibers from small biopsies of muscle, and isolated mitochondria. In: Palmeira, C., Moreno, A. (eds) Mitochondrial Bioenergetics. Methods in Molecular Biology, vol 1782. Humana Press, New York, NY. https://doi.org/10.1007/978-1-4939-7831-1_3

Ebanks, B., Kwiecinska, P., Moisoi, N., Chakrabarti, L., 2023. A method to assess the mitochondrial respiratory capacity of complexes I and II from frozen tissue using the Oroboros O2kFluoRespirometer. *PLoS One* **18**, e0276147. https://doi.org/10.1371/journal.pone.0276147

Ekström, A., Sandblom, E., Blier, P.U., Cyr, B.A.D., Brijs, J., Pichaud, N., 2017. Thermal sensitivity and phenotypic plasticity of cardiac mitochondrial metabolism in European perch, *Perca fluviatilis*. *J. Exp. Biol.* **220**, 386–396. https://doi.org/10.1242/jeb.150698

Ellison, C.K., Burton, R.S., 2008. Interpopulation hybrid breakdown maps to the mitochondrial genome. *Evolution.* **62**, 631–638. https://doi.org/10.1111/j.1558-5646.2007.00305.x

Gnaiger, E., 2020. Mitochondrial pathways and respiratory control. An introduction to OXPHOS analysis. 5th ed. *Bioenerg. Commun.* 2020.2. https://doi.org/10.26124/bec:2020-0002

Gómez-Durán, A., Pacheu-Grau, D., Martínez-Romero, I., López-Gallardo, E., López-Pérez, M.J., Montoya, J., Ruiz-Pesini, E., 2012. Oxidative phosphorylation differences between mitochondrial DNA haplogroups modify the risk of Leber's hereditary optic neuropathy. *BBA Molecular Basis of Disease.* **1822**, 1216–1222. https://doi.org/10.1016/J.BBADIS.2012.04.014

Gómez-Durán, A., Pacheu-Grau, D., López-Gallardo, E., Díez-Sánchez, C., Montoya, J., López-Pérez, M.J., Ruiz-Pesini, E., 2010. Unmasking the causes of multifactorial disorders: OXPHOS differences between mitochondrial haplogroups. *Hum. Mol. Genet.* **19**, 3343–3353. https://doi.org/10.1093/hmg/ddq246

Greenway, R., Barts, N., Henpita, C., Brown, A.P., Rodriguez, L.A., Rodríguez Peña, C.M., Arndt, S., Lau, G.Y., Murphy, M.P., Wu, L., Lin, D., Tobler, M., Kelley, J.L., Shaw, J.H., 2020. Convergent evolution of conserved mitochondrial pathways underlies repeated adaptation to extreme environments. *PNAS.* **117**, 16424–16430. https://doi.org/10.1073/pnas.2004223117

Guo, C.Y., Sun, L., Chen, X.P., Zhang, D.S., 2013. Oxidative stress, mitochondrial damage and neurodegenerative diseases. *Neural Regen. Res.* **8**, 2003–2014. https://doi.org/10.3969/j.issn.1673-5374.2013.21.009

Haenel, Q., Guerard, L., MacColl, A.D.C., Berner, D., 2022. The maintenance of standing genetic variation: Gene flow vs. selective neutrality in Atlantic stickleback fish. *Mol. Ecol.* **31**, 811–821. https://doi.org/10.1111/MEC.16269

Hatfield, T., 1997. Fluctuating asymmetry and reproductive isolation between two sticklebacks, *Environ. Biol. Fishes*. **49**, 63-69.

Hill, G.E., 2020. Mitonuclear Compensatory Coevolution. *Trends in Genetics.* **36**, 403–414. https://doi.org/10.1016/j.tig.2020.03.002

Hill, G.E., 2015. Mitonuclear ecology. *Mol. Biol. Evol*. **32**, 1917–1927. https://doi.org/10.1093/molbev/msv104

Hirst, J., 2013. Mitochondrial complex I. *Ann. Rev. Biochem.* **82**, 551–575. https://doi.org/10.1146/ANNUREV-BIOCHEM-070511-103700

Immonen, E., Berger, D., Sayadi, A., Liljestrand-Rönn, J., Arnqvist, G., 2020. An experimental test of temperature-dependent selection on mitochondrial haplotypes in *Callosobruchus* maculatus seed beetles*. Ecol. Evol*. **10**, 11387–11398. https://doi.org/10.1002/ECE3.6775

Ishikawa, A., Stuart, Y.E., Bolnick, D.I., Kitano, J., 2021. Copy number variation of a fatty acid desaturase gene Fads2 associated with ecological divergence in freshwater stickleback populations. *Biol. Lett.* **17**, 20210204. https://doi.org/10.1098/RSBL.2021.0204

Jones, F.C., Grabherr, M.G., Chan, Y.F., Russell, P., Mauceli, E., Johnson, J., Swofford, R., Pirun, M., Zody, M.C., White, S., Birney, E., Searle, S., Schmutz, J., Grimwood, J., Dickson, M.C., Myers, R.M., Miller, C.T., Summers, B.R., Knecht, A.K., Brady, S.D., Zhang, H., Pollen, A.A., Howes, T., Amemiya, C., Baldwin, J., Bloom, T., Jaffe, D.B., Nicol, R., Wilkinson, J., Lander, E.S., Di Palma, F., Lindblad-Toh, K., Kingsley, D.M., 2012. The genomic basis of adaptive evolution in threespine sticklebacks. *Nature*. **484**, 55–61. https://doi.org/10.1038/nature10944

Jørgensen, L.B., Hansen, A.M., Willot, Q., Overgaard, J., 2023. Balanced mitochondrial function at low temperature is linked to cold adaptation in *Drosophila* species. *J. Exp. Biol.* **15**, jeb245439. https://doi.org/10.1242/jeb.245439

Jorgensen, L.B., Overgaard, J., Hunter-Manseau, F., Pichaud, N., 2021. Dramatic changes in mitochondrial substrate use at critically high temperatures: a comparative study using *Drosophila*. *J. Exp. Biol.* **224**, jeb240960. https://doi.org/10.1242/jeb.240960

Kenney, M., Chwa, M., Atilano, S.R., Falatoonzadeh, P., Ramirez, C., Malik, D., Tarek, M., Cáceres-del-Carpio, J., Nesburn, A.B., Boyer, D.S., Kuppermann, B.D., Vawter, M., Jazwinski, S.M., Miceli, M., Wallace, D.C., Udar, N., 2014. Inherited mitochondrial DNA variants can affect complement, inflammation and apoptosis pathways: insights into mitochondrial-nuclear interactions. *Hum. Mol. Genet.* **23**, 3537–3551. https://doi.org/10.1093/HMG/DDU065

Liu, S., Hansen, M.M., Jacobsen, M.W., 2016. Region-wide and ecotype-specific differences in demographic histories of threespine stickleback populations, estimated from whole genome sequences. *Mol. Ecol.* **25**, 5187–5202. https://doi.org/10.1111/MEC.13827

Lui, M.A., Mahalingam, S., Patel, P., Connaty, A.D., Ivy, C.M., Cheviron, Z.A., Storz, J.F., McClelland, G.B., Scott, G.R., 2015. High-altitude ancestry and hypoxia acclimation have distinct effects on exercise capacity and muscle phenotype in deer mice. *Am. J. Physiol. Regul. Integr. Comp. Physiol.* **308**, R779-R791. https://doi.org/10.1152/AJPREGU.00362.2014

Luo, Y., Wang, W., Zhang, Y., Huang, Q., 2013. Effect of body size on organ-specific mitochondrial respiration rate of the largemouth bronze gudgeon. *Fish Physiol. Biochem.* **39**, 513–521. https://doi.org/10.1007/s10695-012-9716-z

Mäkinen, H.S., Merilä, J., 2008. Mitochondrial DNA phylogeography of the three-spined stickleback (*Gasterosteus aculeatus*) in Europe-Evidence for multiple glacial refugia. *Mol. Phylogenet. Evol.* **46**, 167–182. https://doi.org/10.1016/j.ympev.2007.06.011

Martínez-Reyes, I., Chandel, N.S., 2020. Mitochondrial TCA cycle metabolites control physiology and disease. *Nat. Commun.* **11**, 102. https://doi.org/10.1038/s41467-019-13668-3

Mcdonald, J.H., 2014. Handbook of Biological Statistics (3rd ed.). Sparky House Publishing, Baltimore, Maryland.

Menail, H.A., Cormier, S.B., Ben Youssef, M., Jørgensen, L.B., Vickruck, J.L., Morin, P., Boudreau, L.H., Pichaud, N., 2022. Flexible Thermal Sensitivity of Mitochondrial Oxygen Consumption and Substrate Oxidation in Flying Insect Species. *Front. Physiol.* **13**. https://doi.org/10.3389/fphys.2022.897174

Pichaud, N., Ballard, J.W.O., Tanguay, R.M., Blier, P.U., 2012. Naturally occurring mitochondrial DNA haplotypes exhibit metabolic differences: Insight into functional properties of mitochondria. *Evolution.* **66**, 3189–3197. https://doi.org/10.1111/j.1558-5646.2012.01683.x

Pichaud, N., Messmer, M., Correa, C.C., Ballard, J.W.O., 2013. Diet influences the intake target and mitochondrial functions of *Drosophila melanogaster* males. *Mitochondrion*. **13**, 817–822. https://doi.org/10.1016/J.MITO.2013.05.008

Ravinet, M., Harrod, C., Eizaguirre, C., Prod, P.A., Paulo Prod, C.A., 2013. Unique mitochondrial DNA lineages in Irish stickleback populations: cryptic refugium or rapid recolonization? *Ecol. Evol.* **4**, 2488–2504. https://doi.org/10.1002/ece3.853

Scott, G.R., Hawkes, L.A., Frappell, P.B., Butler, P.J., Bishop, C.M., Milsom, W.K., 2015. How bar-headed geese fly over the Himalayas. *Physiology*. **30**, 107–115. https://doi.org/10.1152/physiol.00050.2014

Scott, G.R., Schulte, P.M., Egginton, S., Scott, A.L.M., Richards, J.G., Milsom, W.K., 2011. Molecular Evolution of Cytochrome c Oxidase Underlies High-Altitude Adaptation in the Bar-Headed Goose. *Mol. Biol. Evol.* **28**, 351–363. https://doi.org/10.1093/MOLBEV/MSQ205

Tocher, D.R., 2003. Metabolism and Functions of Lipids and Fatty Acids in Teleost Fish. *Rev. Fish. Sci.* **11**, 107–184. https://doi.org/10.1080/713610925

Towarnicki, S.G., Ballard, J.W.O., 2020. Towards understanding the evolutionary dynamics of mtDNA. *Mitochondrial DNA Part A.* **31**, 355-364**.** https://doi.org/10.1080/24701394.2020.1830076

Twining, C.W., Bernhardt, J.R., Derry, A.M., Hudson, C.M., Ishikawa, A., Kabeya, N., Kainz, M.J., Kitano, J., Kowarik, C., Ladd, S.N., Leal, M.C., Scharnweber, K., Shipley, J.R., Matthews, B., 2021. The evolutionary ecology of fatty-acid variation: Implications for consumer adaptation and diversification. *Ecol. Lett.* **24**, 1709–1731. https://doi.org/10.1111/ele.13771

Wallace, D.C., 1999. Mitochondrial diseases in man and mouse. *Science.* **283**, 1482–1488. https://doi.org/10.1126/SCIENCE.283.5407.1482

Whitehead, A., 2009. Comparative mitochondrial genomics within and among species of killifish. *BMC Evol. Biol.* **9**, 11. https://doi.org/10.1186/1471-2148-9-11

Wilkins, H.M., Carl, S.M., Swerdlow, R.H., 2014. Cytoplasmic hybrid (cybrid) cell lines as a practical model for mitochondriopathies. *Redox Biol.* **2**, 619-631. https://doi.org/10.1016/J.REDOX.2014.03.006

Wirth, C., Brandt, U., Hunte, C., Zickermann, V., 2016. Structure and function of mitochondrial complex I. *BBA Bioenerg.* **1857**, 902–914. https://doi.org/10.1016/j.bbabio.2016.02.013

Wolff, J.N., Pichaud, N., Camus, M.F., Côté, G., Blier, P.U., Dowling, D.K., 2016. Evolutionary implications of mitochondrial genetic variation: Mitochondrial genetic effects on OXPHOS respiration and mitochondrial quantity change with age and sex in fruit flies. *J. Evol. Biol.* **29**, 736–747. https://doi.org/10.1111/jeb.12822

6.7 Supplementary Material

Table S6.1: Results of linear models fitted to three respiratory states ($LEAK_{CI}$, $OXPHOS_{CI}$, $OXPHOS_{CI+II}$) and to CI contribution to maximum uncoupled respiration rate. Temperature, mitochondrial lineage and an interaction between these as explanatory variables. df = degrees of freedom.

Tissue	Respiratory State	Treatment F Values (df)		
		Assay Temperature	Mitochondrial Lineage	Assay temperature x Mitochondrial Lineage
Heart	LEAK	4.7035 (1,26)	1.5413 (1,26)	1.1276 (1,26)
	$OXPHOS_{CI}$	2.5978 (1,26)	0.1447 (1,26)	0.0338 (1,26)
	$OXPHOS_{CI+II}$	7.3787 (1,26)	0.4296 (1,26)	0.8549 (1,26)
	CI contribution	1.8926 (1,26)	7.1166 (1,26)	6.2680 (1,26)
Brain	LEAK	9.7041 (1,26)	1.5179 (1,26)	1.1265 (1,26)
	$OXPHOS_{CI}$	8.9908 (1,26)	0.0101 (1,26)	0.0051 (1,26)
	$OXPHOS_{CI+II}$	13.0594 (1,26)	0.5781 (1,26)	0.0232 (1,26)
	CI contribution	1.8370 (1,26)	2.1163 (1,26)	0.3566 (1,26)

Table S6.2: Multiple comparisons testing of results. Reported in order of increasing P-value. P-values are from **Table 6.3**. P-values were given a rank (*i*) and compared to the Benjamini-Hochberg critical value (i/m)Q, where *i* is the rank, *m* is the total number of tests, and *Q* is the false discovery rate (FDR), set to 0.10. The largest P-value that is smaller than (*i*/*m*)*Q* is significant, as well as all P-vales smaller than it.

Tissue	Response	Test	P-value	Rank (*i*)	(*i*/*m*)*Q*	Benjamini & Hochberg Significance
Brain	$OXPHOS_{CI+CII}$	Temperature	0.001	1	0.004	Significant
Brain	$LEAK_{CI}$	Temperature	0.004	2	0.008	Significant
Brain	$OXPHOS_{CI}$	Temperature	0.006	3	0.013	Significant
Heart	$OXPHOS_{CI+CII}$	Temperature	0.012	4	0.017	Significant
Heart	CI contribution	Lineage	0.013	5	0.021	Significant
Heart	CI contribution	Interaction	0.019	6	0.025	Significant
Heart	$LEAK_{CI}$	Temperature	0.039	7	0.029	Not significant
Heart	$OXPHOS_{CI}$	Temperature	0.119	8	0.033	Not significant
Brain	CI contribution	Lineage	0.158	9	0.038	Not significant
Heart	CI contribution	Temperature	0.181	10	0.042	Not significant
Brain	CI contribution	Temperature	0.187	11	0.046	Not significant

Heart	$LEAK_{CI}$	Lineage	0.226	12	0.050	Not significant
Brain	$LEAK_{CI}$	Lineage	0.229	13	0.054	Not significant
Heart	$LEAK_{CI}$	Interaction	0.298	14	0.058	Not significant
Brain	$LEAK_{CI}$	Interaction	0.298	15	0.063	Not significant
Heart	$OXPHOS_{CI+CII}$	Interaction	0.364	16	0.067	Not significant
Brain	$OXPHOS_{CI+CII}$	Lineage	0.454	17	0.071	Not significant
Heart	$OXPHOS_{CI+CII}$	Lineage	0.518	18	0.075	Not significant
Brain	CI contribution	Interaction	0.556	19	0.079	Not significant
Heart	$OXPHOS_{CI}$	Lineage	0.707	20	0.083	Not significant
Heart	$OXPHOS_{CI}$	Interaction	0.856	21	0.088	Not significant
Brain	$OXPHOS_{CI+CII}$	Interaction	0.88	22	0.092	Not significant
Brain	$OXPHOS_{CI}$	Lineage	0.921	23	0.096	Not significant
Brain	$OXPHOS_{CI}$	Interaction	0.943	24	0.100	Not significant

Chapter 7: General Discussion

In this thesis I have looked at differences between mitochondrial lineages in the three-spined stickleback ('stickleback', *Gasterosteus aculeatus*). This work has involved describing the development of migratory stickleback, examination of the effect of anaesthetics on mitochondrial function and looking at the differences between the two lineages using phylogeographic and selection-based analysis and high-resolution respirometry (HRR).

7.1 Development of stickleback ecotypes

Much of my research was conducted on migratory three-spined stickleback from North Uist as these are an approximately equal mix of the two mitochondrial lineages. This involved comparing the morphology of wild caught stickleback (Chapter 4) and creating and raising crosses in the aquarium in order to compare mitochondrial function (Chapter 6). To my knowledge no previous research had looked at the development or hatching success of migratory stickleback and the only published work assessing stickleback development was on freshwater populations at 18°C, with line drawings showing the major developmental stages (Swarup, 1958). In comparison, my study of the development of saltwater resident and migratory stickleback from North Uist, in Chapter 2, offers additional information and novel findings: i) the assessment of stickleback development at a physiologically relevant temperature for North Uist, a well-studied system for stickleback ecology and evolution (Dean et al., 2019; MacColl et al., 2013; Magalhaes et al., 2016; Robertson et al., 2016), ii) a comparison of the development of two sympatric ecotypes that differ in morphology and genetics (Dean et al., 2019), identifying differences in time to hatch between ecotypes, iii) coloured photographs to help with the identification of the key stages of development. This not only informed raising stickleback in aquaria, but I believe that this will provide a framework for future work assessing the development of stickleback embryos, including a comparison of the two Atlantic mitochondrial lineages, and the assessment of any hybrid incompatibilities between ecotypes or mitochondrial haplotypes.

7.2 High-resolution respirometry

High-resolution respirometry (HRR) has been increasingly used in evolutionary ecology (McKenzie et al., 2019) as a tool to show the importance of mitochondria in adaptation (Devaux et al., 2019; Greenway et al., 2020; Willis et al., 2021) and in particular how fish may respond to changes in climate (Chouinard-Boisvert et al.,

2024; Gerber et al., 2020; Thoral et al., 2021). Most research measuring mitochondrial function in fish has used an anaesthetic during euthanasia (Leo et al., 2017; Pelster et al., 2020; Shama et al., 2014) without knowledge on how this can affect mitochondrial respiration. In Chapter 3 I determined the effect of euthanasia via an overdose of MS-222, a well-established method for fish, on mitochondrial respiratory parameters. I showed that mitochondrial respiration was generally lower in the brain of stickleback euthanised with MS-222, with significantly reduced LEAK state respiration. With HRR being increasingly conducted on fish, this research has been important in showing the need to consider the method used for euthanasia, in particular when comparing studies.

Although I have shown that MS-222 does affect some respiratory parameters, this does not necessarily mean that it should be avoided; additional factors should be considered, including how much stress the fish experiences prior to and during euthanasia (Animal Procedures Committee, 2009). In my comparison of mitochondrial respiration between the two Atlantic stickleback mitochondrial lineages (Chapter 6), I chose to continue euthanising stickleback using MS-222 as this method is effective, well-established, and I believed would reduce stress. As the main aim of this study was to compare the two mitochondrial lineages, using MS-222 would not bias results as any effects would be equal for *Eu* and *At* stickleback. While conducting my study on the effects of MS-222 on mitochondrial respiration, I was able to optimise substrate and inhibitor concentrations for the stickleback and compare two tissues which I used to inform my final protocol comparing *Eu* and *At* stickleback. I found that oxygen flux in the skeletal tail muscle was more variable than in the brain, and there was increased evidence of membrane damage from the preparation of skeletal muscle homogenates, so I instead used the heart when comparing mitochondrial lineages in Chapter 6. Like skeletal tail muscle, the heart resulted in higher OXPHOS flux control ratios (FCRs) with CI substrates than the brain (Chapters 3 and 6).

7.3 Ecological and evolutionary consequences of mtDNA variation

The adaptive significance of mtDNA variation, independent of the nuclear genome, has been substantially overlooked in natural populations. Despite research into the functional consequences of mitochondrial differences in model organisms including *Drosophila* and mice (Dowling and Wolff, 2023; Latorre-Pellicer et al., 2016; Scotece et al., 2021), where pure mitochondrial effects can be separated from nuclear genetic effects, this has rarely, if ever, been translated to studies of natural systems (Baris et

al., 2017, 2016). This is mainly due to a lack of populations or species wherein variation in the mtDNA can be studied independent of potentially confounding variation in the nuclear genetic background. Here, I describe a natural study system that allows pure mtDNA effects to be explored. Through Chapters 4 to 6 I demonstrate that the Atlantic three-spined stickleback is a valuable model to assess the ecological and evolutionary consequences of mtDNA variation. By combining ecology, phylogeography, phylogenetic selection analyses and mitochondrial physiology, I show that mtDNA variation between Atlantic stickleback mitochondrial lineages has physiological consequences for mitochondrial respiration independent to the nuclear genome, and that natural selection may have acted upon this variation, resulting in differences in adaptive potential between *Eu* and *At* stickleback. To my knowledge, this study is one of, if not the first, to explicitly link mtDNA variation to physiological mitochondrial differences and adaptive potential in natural populations.

7.3.1 Atlantic stickleback mitochondrial lineages

I first assessed the distribution of the two Atlantic mitochondrial lineages, providing evidence that *Eu* and *At* stickleback evolved in allopatry on opposite sides of the Atlantic Ocean during the last glacial maximum (Chapter 4). During this time, the two lineages likely experienced different environmental conditions as the ice sheets covered a much larger portion of the stickleback's current distribution in North America than in Europe (Dyke and Prest, 1987; Svendsen et al., 2004). Presumably, this severely restricted the distribution of the *At* lineage, while the *Eu* lineage likely had increased opportunity to colonise fresh water, resulting in different selective agents promoting mtDNA divergence between the lineages. The majority of present-day resident stickleback across the Atlantic had the *Eu* mtDNA while migratory populations were a mix of the *Eu* and *At* lineages, showing that the two mitochondrial lineages have different adaptive propensities, most likely due to the mtDNA itself.

7.3.2 Selection in the mitochondrial protein coding genes

To assess whether the variation in the mtDNA itself may be adaptive, in Chapter 5 I tested for evidence of natural selection acting on the mitochondrial protein coding genes (PCGs) of the stickleback using multiple phylogenetic methods. As in previous work (Baltazar-Soares et al., 2021; Shen et al., 2019; Wilson et al., 2020), selection acted primarily on complex I (CI) of the oxidative phosphorylation (OXPHOS) pathway. I identified long-term positive selection in sites within ND2 and ND5 of CI which likely occurred when the lineages evolved in allopatry. At these sites, *Eu* and *At* stickleback differed in amino acid sequence, and this was predicted to alter protein

structure. Unlike previous work finding evidence of selection across the mitogenome (Garvin et al., 2011; Mukundan et al., 2022), I was able to go on to explicitly test for any physiological effects of mtDNA variation (Chapter 6).

7.3.3 Functional consequences of mtDNA variation

The Atlantic stickleback is an ideal model to test whether mtDNA variation alone can influence mitochondrial physiology. North Uist is a point of secondary contact for the two mitochondrial lineages and migratory populations are an approximately equal mix of the two lineages (Chapter 4, Dean et al., 2019). As I found no evidence of divergence within the nuclear genome between mitochondrial lineages (Chapter 4), migratory stickleback are most likely from one panmictic population, segregating only by the mtDNA. This allows mtDNA variants to be compared in the same nuclear background, a system not too dissimilar to conplastic experiments in *Drosophila* (Aw et al., 2018; Dowling and Wolff, 2023; Wolff et al., 2016) and mice (Latorre-Pellicer et al., 2016; Scotece et al., 2021; Yu et al., 2009), but quite probably resulting from many more generations of stable interaction between the two genomes. This means that I could disentangle mitochondrial from nuclear effects, which is a major limitation to most current research into the ecological and evolutionary significance of mtDNA variation. An advantage to studying North Uist migratory stickleback in comparison to conplastic *Drosophila* and mice studies is that mitonuclear combinations are naturally occurring, and the fish are likely to possess a fairly equal mix of European (*Eu* associated) and North American (*At* associated) nuclear genetic ancestry, making it unlikely that the two lineages suffer from mitonuclear incompatibilities in this system (I have observed no evidence of hybrid breakdown when raising migratory North Uist stickleback in the aquarium). Whether offspring of *Eu* and *At* stickleback from opposite sides of the Atlantic with their own ancestral nuclear genome would display evidence of mitonuclear mismatch remains to be investigated. In comparison, in other natural systems such as the killifish (*Fundulus heteroclitus*), there may be ongoing local admixture between two lineages and some nuclear genes remain diverged (Baris et al., 2017, 2016). I cannot rule out with complete certainty that some linkage disequilibrium (LD) remains due to assortative mating or strong selection, although I have found no evidence of this to date and believe it to be unlikely. Further tests to confirm that there is no mitonuclear LD would require a larger nuclear SNP dataset and could include calculating LD coefficients between nuclear SNPs and the mitogenome (Sloan et al., 2015) or genome wide association studies (Lian et al., 2024; Wang et al., 2021).

To determine whether mtDNA variation had physiological consequences for mitochondria, I conducted high-resolution respirometry (HRR) to measure differences in OXPHOS between *Eu* and *At* stickleback from migratory North Uist populations (Chapter 6). I found temperature-dependent differences in CI respiration between the two lineages: *Eu* stickleback maintained the relative contribution of both complexes in the heart across the three assay temperatures, whereas *At* stickleback decreased the relative contribution of CI with increasing temperatures. This resulted in *At* stickleback having a larger CI contribution than *Eu* at 6°C. By designing a protocol to assess CI and CII respiration separately in frozen tissue, I was able to confirm that differences in enzyme contributions to flux were most likely due to differences in respiration via CI. As I compared migratory North Uist populations, differences in CI respiration between mitochondrial lineages were independent of the nuclear genetic background and most likely due to differences in mtDNA sequence between *Eu* and *At* stickleback. There were no differences in the respiratory control ratio, a measure of mitochondrial efficiency, calculated as $OXPHOS_{CI}/LEAK_{CI}$ (Salin et al., 2018), between *Eu* and *At* stickleback (data not presented), but differences in ATP production were not investigated in this study, so whether mtDNA variation or the observed differences in CI respiration effect the efficiency of ATP production requires further investigation. Even so, these results have shown clear measurable differences in CI respiration between mtDNA variants, particularly at colder temperatures.

HRR results are consistent with the finding that long-term positive selection was acting primarily on sites within the CI genes ND2 and ND5, where *Eu* and *At* stickleback differed in amino acid sequence at these positively selected sites (Chapter 5), implicating CI in adaptive evolution. Although I was unable to link a specific mtDNA substitution to these physiological consequences, this hints that variation at these positively selected sites could have altered CI respiration. When comparing the mitochondrial PCGs between *Eu* and *At* stickleback from North Uist migratory populations (Chapter 4) I identified four fixed amino acid substitutions between mitochondrial lineages: two in ND5 (including site 576 identified as evolving under positive selection in Chapter 5), one in ATP6, and one in COX1. As well as differing consistently between *Eu* and *At* migratory fish from North Uist, site 576 in ND5 showed evidence of evolving under positive selection using multiple methods and the amino acid substitution between mitochondrial lineages was predicted to be radical, likely altering protein structure (Chapter 5). This site therefore seems a strong candidate for being involved in the observed differences in CI respiration between *Eu* and *At* stickleback from these same populations. ND5 site 576 is in the piston arm of

ND5 (Chapter 5), which is predicted to be involved in proton pumping (Baradaran et al., 2013; Garvin et al., 2011; Hunte et al., 2010). Positive selection has been found in this region in other species (da Fonseca et al., 2008; Garvin et al., 2011; Mukundan et al., 2022; Pabijan et al., 2008), suggesting that it may be important in adaptive evolution across multiple taxa. *G. wheatlandi,* a close relative to the three-spined stickleback, has the same amino acid variant as the *At* lineage at this site in ND5. As the distribution of *G. wheatlandi* is restricted to salt water in the western Atlantic which is very similar to our predicted distribution of the *At* lineage during the last glacial maxima, this supports this variant being advantageous for CI function at colder temperatures. Although additional mitochondrial genes may be involved, our findings implement ND5 in adaptive processes.

In addition to affecting mitochondrial respiratory parameters, previous research into the functional consequences of mtDNA variation using model organisms have found that mitochondrial haplotype can affect multiple physiological and phenotypic variables, including reactive oxygen species generation, insulin signalling and longevity (Latorre-Pellicer et al., 2016). In natural populations this has begun to be explored (Dobelmann et al., 2019; Schwartz et al., 2015; Sun et al., 2019), although differences are often dependent on the nuclear genetic background. Using migratory North Uist populations, which allows a comparison between lineages in the same nuclear genetic background, I compared the standard length (SL) of stickleback, finding sex-dependent differences in SL between mitochondrial lineages: *At* females were longer than *Eu* females, but I observed no differences between males (Chapter 4). This finding is one of the first to our knowledge to identify phenotypic differences between mtDNA variants in natural populations, independent to the nuclear genome. As the differences in SL were only in females, as found in *Drosophila* (Camus et al., 2015), the extent to which the effects of mitochondrial haplotype on life-history traits are sex-dependent warrants further exploration. These findings open up a wealth of questions to explore the fitness effects of mtDNA variation further, including fecundity, mtDNA copy number and growth.

7.3.4 Ecological and evolutionary significance

I have provided strong evidence that variation within the mitochondrial PCGs of the stickleback has been acted upon by positive selection, and have shown that the mtDNA variation between Atlantic stickleback mitochondrial lineages affects mitochondrial function (in particular respiration via CI), physiology, and morphology. I have shown that this mtDNA variation has likely influenced the adaptive potential of

Eu and *At* stickleback as the two mitochondrial lineages differed in frequency between migratory (completely plated fish spending most of their lives in salt water) and resident (fish living year-round in fresh water or saltwater lagoons) stickleback across their Atlantic distribution, with the *Eu* lineage dominating in freshwater and saltwater resident populations. The nuclear genetic basis of freshwater adaptation has been well studied in the stickleback (Colosimo et al., 2005; Ishikawa et al., 2021, 2019; Jones et al., 2012), while the role of the mitochondrial genome has often been overlooked but may have also played an important role. The next question I considered is how the mitochondrial differences I have observed could result in different adaptive potential between the mitochondrial lineages. Not only do the lifestyles of migratory and resident stickleback differ in energy requirements due to differences in their tendency to migrate, but the environments inhabited by these ecotypes differ in temperature, diet, salinity and predation, all of which can alter metabolic demands.

From my results, I hypothesise that temperature has been a key driver of mitogenome evolution in the Atlantic stickleback, as in multiple other species of fish (Baltazar-Soares et al., 2021; Silva et al., 2014; Teacher et al., 2012). Temperature influences mitochondrial respiration (Chouinard-Boisvert et al., 2024; Pichaud et al., 2010) so variation in mtDNA that provides an advantage at specific temperatures could be selected for. I found that the measured differences in CI respiration between *Eu* and *At* stickleback were dependent on temperature, with differences in CI respiration most apparent at cold temperatures. When the two lineages diverged in allopatry, they likely experienced different environmental conditions and metabolic demands during this time. The *At* lineage likely diverged in North America in cold oceanic environments with restricted access to fresh water so mitochondrial variants that provided an advantage at cold temperatures could have been favoured. I found that *At* stickleback had higher CI respiration at cold temperatures than *Eu* stickleback, which may be advantageous, potentially increasing ATP production (Ahmad et al., 2023), although this would need further exploration. I conducted HRR on stickleback raised in the aquarium at approximately 14°C, so whether acclimation to warmer or cooler temperatures influences these findings could be investigated. The finding that *At* mitochondrial function differed to *Eu* stickleback in the cold is consistent with observations of stickleback at the southern edge of their range in eastern North America, where migratory stickleback breed in February or March when coastal sea surface temperatures are low, and the offspring then migrate northwards to remain in cold oceanic waters (Able and Fahay, 2010). These populations are likely to be

completely, or largely *At,* so these results add to the evidence that the *At* lineage is well-adapted to the cold as these temperatures are much lower than would be experienced by breeding stickleback on the eastern side of the Atlantic. The *Eu* lineage, in contrast, diverged in warmer southern European refugia (Defaveri et al., 2012; Mäkinen and Merilä, 2008; Sanz et al., 2015), with increased access to fresh water, so maintaining efficient mitochondrial function across a range of environmental conditions may have been beneficial, reflected by the finding that the *Eu* lineage maintained complex contributions across different temperatures. As the two mitochondrial lineages are found in approximately equal proportions in migratory populations on North Uist (Chapter 4), both are well suited to survive at temperatures experienced on North Uist, which likely do not get as cold as 6°C. Differences in adaptation to cold temperatures between *Eu* and *At* stickleback may not have influenced their present distribution on North Uist, but could have limited their spread further across the Atlantic.

Although I found no difference in CI contribution between *Eu* and *At* stickleback at 22°C, I observed a decline in CI contribution to oxygen flux with increasing temperatures in the *At* lineage. This could reflect a decrease in the function of CI at warm temperatures, where oxygen availability decreases, but HRR would need to be conducted at temperatures above 22°C to test whether this decline continues and results in a difference in CI respiration between the two lineages. If so, it is possible that this has restricted the *At* lineage from colonising fresh water and lagoons permanently, as these environments will reach much higher temperatures than the Atlantic Ocean. To test this hypothesis, further work measuring mitochondrial respiration and ATP production at temperatures above 22°C would be necessary, as well as assessing how the two lineages cope with increased temperatures. The hypothesis that mitochondrial differences between *Eu* and *At* stickleback result in different abilities to adapt to higher temperatures is supported by our finding that fewer *At* stickleback inhabit saltwater environments that experience higher maximum sea surface temperatures (Chapter 4), and observations of juvenile stickleback in North America (most likely the *At* lineage) moving northwards to remain in colder waters (Able and Fahay, 2010). Together, these findings show that variation in the mtDNA can have adaptive consequences, with temperature shaping the evolution of stickleback mitochondrial lineages in the Atlantic.

The fatty acid availability in the diet of freshwater (and most probably lagoon resident) stickleback is a lot lower than in the ocean (Twining et al., 2021), and previous research has found that freshwater stickleback have evolved duplications in fatty acid

desaturase 2 (*Fads2*), a nuclear gene which encodes a protein involved in the biosynthesis of long-chain polyunsaturated fatty acids, to adapt (Ishikawa et al., 2021, 2019). Differences in nutritional availability can also influence mitogenome evolution (Aw et al., 2018; Ballard and Youngson, 2015; Towarnicki and Ballard, 2018), so mtDNA variants that increase survival when stickleback experience lower nutritional quality would be promoted in freshwater populations. Whether the differences I observed in mtDNA sequence and CI respiration between *Eu* and *At* stickleback could be beneficial when fed a low nutrient or fatty acid diet would need further exploration. Resident stickleback populations are non-migratory, with altered energetics compared to migratory stickleback (Dalziel et al., 2012; Tudorache et al., 2007) so may require less efficient energy generation, and their mitogenome may have experienced relaxed purifying selection (Chapter 5). This may have allowed an increase in the biosynthesis of other molecules from the Krebs cycle (Martínez-Reyes and Chandel, 2020). If mitochondrial differences between *Eu* and *At* stickleback promote this increase in biosynthesis in the *Eu* lineage, this could be beneficial in fresh water where key nutrients may not be available from the diet. This idea is yet to be tested however. I also cannot rule out the smaller length of *Eu* stickleback in migratory North Uist populations providing an advantage when establishing freshwater populations, as having a smaller body size may be advantageous against freshwater predators and in nutrient poor environments (Dupont-Prinet et al., 2010), but it would be interesting to investigate whether this difference in SL persists across the Atlantic.

My findings suggest that temperature has had a role in the evolution of the two Atlantic stickleback mitochondrial lineages and I have provided strong evidence that the mtDNA itself is adaptive, but it is likely that a combination of variables that can influence the metabolic demands of the stickleback have influenced their current distribution. Potential selective agents, such as temperature and diet, that may have resulted in the *Eu* lineage dominating in resident populations could now be tested experimentally.

7.3.5 Conclusions

This research is one of the first to find evidence of positive selection acting on mtDNA variants, and to link this variation to physiological, phenotypic, and adaptive consequences independent of the nuclear genome. Most research to date has only part of this story. There has been increased interest in identifying signatures of positive selection across the mitochondrial PCGs or measuring the functional

consequences of mtDNA variation, and associating these with adaptation, but separating mitochondrial from nuclear genetic effects is challenging in most natural study systems. Learning from conplastic *Drosphila* and mice studies, research moved towards systems where a comparison of mtDNA variants could be carried out in the same nuclear genetic background. Although research in the small brown planthopper (*Laodelphax striatellus*) and killifish (*Fundulus heteroclitus*) were promising systems to assess pure mitochondrial effects, divergence in the nuclear genome remained between admixed mitochondrial lineages which affected mitochondrial function or fitness traits in the populations studied. Here, I have established the Atlantic three-spined stickleback as a model to assess the ecological and evolutionary significance of mtDNA variation. Using migratory stickleback from North Uist that segregate by the mtDNA but are otherwise panmictic, I have been able to assess mtDNA variation independent to the nuclear genome. I have identified physiological and morphological consequences of mtDNA variation, and shown that this results in different adaptive potential as both mtDNA variants were found in migratory populations, but one variant dominated in resident populations. From my findings, I show that CI of the OXPHOS pathway is involved in adaptive processes and suggest that temperature has been a major driver of the evolution of Atlantic stickleback mitochondrial lineages. I hope that in establishing the Atlantic stickleback as a model to assess mtDNA variation and evidencing the adaptive significance of the mitogenome, I have opened up an avenue for future research to address further questions on the evolutionary and ecological importance of mtDNA.

7.4 References

Able, K.W., Fahay, M.P., 2010. Ecology of Estuarine Fishes: Temperate waters of the North Atlantic. The John Hopkins University Press. Baltimore.

Ahmad, M., Wolberg, A., Kahwaji, C.I., 2023. Biochemistry, Electron Transport Chain. In: StatPearls [Internet]. Treasure Island (FL): StatPearls Publishing.

Animal Procedures Committee, 2009. Supplementary Review of Schedule 1 of the Animals (Scientific Procedures) Act 1986 Appropriate methods of humane killing for fish.

Aw, W.C., Towarnicki, S.G., Melvin, R.G., Youngson, N.A., Garvin, M.R., Hu, Y., Nielsen, S., Thomas, T., Pickford, R., Bustamante, S., Vila-Sanjurjo, A., Smyth, G.K., Ballard, J.W.O., 2018. Genotype to phenotype: Diet-by-mitochondrial DNA

haplotype interactions drive metabolic flexibility and organismal fitness. *PLoS Genet.* **14**, e1007735. https://doi.org/10.1371/JOURNAL.PGEN.1007735

Ballard, J.W., Youngson, N.A., 2015. Review: can diet influence the selective advantage of mitochondrial DNA haplotypes? *Biosci. Rep.* **35**, e00277. https://doi.org/10.1042/BSR20150232

Baltazar-Soares, M., Lima, A.R. de A., Silva, G., 2021. Targeted sequencing of mitochondrial genes reveals signatures of molecular adaptation in a nearly panmictic small pelagic fish species. *Genes*. **12**, 91. https://doi.org/10.3390/genes12010091

Baradaran, R., Berrisford, J.M., Minhas, G.S., Sazanov, L.A., 2013. Crystal structure of the entire respiratory complex I. *Nature*. **494**, 443–448. https://doi.org/10.1038/nature11871

Baris, T.Z., Blier, P.U., Pichaud, N., Crawford, D.L., Oleksiak, M.F., 2016. Gene by environmental interactions affecting oxidative phosphorylation and thermal sensitivity. *Am. J. Physiol. Regul. Integr. Comp. Physiol.* **311**, R157–R165. https://doi.org/10.1152/ajpregu.00008.2016

Baris, T.Z., Wagner, D.N., Dayan, D.I., Du, X., Blier, P.U., Pichaud, N., Oleksiak, M.F., Crawford, D.L., 2017. Evolved genetic and phenotypic differences due to mitochondrial-nuclear interactions. *PLoS Genet.* **13**, e1006517. https://doi.org/10.1371/journal.pgen.1006517

Camus, M.F., Wolf, J.B.W., Morrow, E.H., Dowling, D.K., 2015. Single Nucleotides in the mtDNA Sequence Modify Mitochondrial Molecular Function and Are Associated with Sex-Specific Effects on Fertility and Aging. *Curr. Biol.* **25**, 2717–2722. https://doi.org/10.1016/J.CUB.2015.09.012

Chouinard-Boisvert, S., Ghinter, L., St-Pierre, A., Mortz, M., Desrosiers, V., Dufresne, F., Tardif, J.-C., Huard, J., Sirois, P., Fortin, S., Blier, P.U., 2024. Mitochondrial functions and fatty acid profiles in fish heart: an insight into physiological limitations linked with thermal tolerance and age. *J. Exp. Biol*. **227**, jeb247502. https://doi.org/10.1242/JEB.247502

Colosimo, P.F., Hosemann, K.E., Balabhadra, S., Villarreal, G., Dickson, H., Grimwood, J., Schmutz, J., Myers, R.M., Schluter, D., Kingsley, D.M., 2005. Widespread parallel evolution in sticklebacks by repeated fixation of ectodysplasin alleles. *Science.* **307**, 1928–1933. https://doi.org/10.1126/SCIENCE.1107239

da Fonseca, R.R., Johnson, W.E., O'Brien, S.J., Ramos, M.J., Antunes, A., 2008. The adaptive evolution of the mammalian mitochondrial genome. *BMC Genomics.* **9**, 119. https://doi.org/10.1186/1471-2164-9-119

Dalziel, A.C., Ou, M., Schulte, P.M., 2012. Mechanisms underlying parallel reductions in aerobic capacity in non-migratory threespine stickleback (*Gasterosteus aculeatus*) populations. *J. Exp. Biol*. **215**, 746–759. https://doi.org/10.1242/JEB.065425

Dean, L.L., Magalhaes, I.S., Foote, A., D'Agostino, D., McGowan, S., MacColl, A.D.C., 2019. Admixture between Ancient Lineages, Selection, and the Formation of Sympatric Stickleback Species-Pairs. *Mol. Biol. Evol.* **36**, 2481–2497. https://doi.org/10.1093/MOLBEV/MSZ161

Defaveri, J., Zanella, L.N., Zanella, D., Mrakovčić, M., Merilä, J., 2012. Phylogeography of isolated freshwater three-spined stickleback *Gasterosteus aculeatus* populations in the Adriatic Sea basin. *J. Fish Biol.* **80**, 61–85. https://doi.org/10.1111/J.1095-8649.2011.03147.X

Devaux, J.B.L., Hedges, C.P., Birch, N., Herbert, N., Renshaw, G.M.C., Hickey, A.J.R., 2019. Acidosis Maintains the Function of Brain Mitochondria in Hypoxia-Tolerant Triplefin Fish: A Strategy to Survive Acute Hypoxic Exposure? *Front. Physiol.* **9**. https://doi.org/10.3389/FPHYS.2018.01941

Dobelmann, J., Alexander, A., Baty, J.W., Gemmell, N.J., Gruber, M.A.M., Quinn, O., Wenseleers, T., Lester, P.J., 2019. The association between mitochondrial genetic variation and reduced colony fitness in an invasive wasp. *Mol. Ecol.* **28**, 3324–3338. https://doi.org/10.1111/MEC.15159

Dowling, D.K., Wolff, J.N., 2023. Evolutionary genetics of the mitochondrial genome: insights from Drosophila. *Genetics*. **224**, iyad036. https://doi.org/10.1093/GENETICS/IYAD036

Dupont-Prinet, A., Chatain, B., Grima, L., Vandeputte, M., Claireaux, G., McKenzie, D.J., 2010. Physiological mechanisms underlying a trade-off between growth rate and tolerance of feed deprivation in the European sea bass (*Dicentrarchus labrax*). *J. Exp. Biol.* **213**, 1143–1152. https://doi.org/10.1242/JEB.037812

Dyke, A.S., Prest, V.K., 1987. Late Wisconsinan and Holocene history of the Laurentide Ice Sheet. *Geographie Physique et Quaternaire* **41**, 237–263. https://doi.org/10.7202/032681ar

Garvin, M.R., Bielawski, J.P., Gharrett, A.J., 2011. Positive Darwinian Selection in the Piston That Powers Proton Pumps in Complex I of the Mitochondria of Pacific Salmon. *PLoS One.* **6**, e24127. https://doi.org/10.1371/JOURNAL.PONE.0024127

Gerber, L., Clow, K.A., Mark, F.C., Gamperl, A.K., 2020. Improved mitochondrial function in salmon (*Salmo salar*) following high temperature acclimation suggests that there are cracks in the proverbial 'ceiling.' *Sci. Rep.* **10**, 21636. https://doi.org/10.1038/s41598-020-78519-4

Greenway, R., Barts, N., Henpita, C., Brown, A.P., Rodriguez, L.A., Rodríguez Peña, C.M., Arndt, S., Lau, G.Y., Murphy, M.P., Wu, L., Lin, D., Tobler, M., Kelley, J.L., Shaw, J.H., 2020. Convergent evolution of conserved mitochondrial pathways underlies repeated adaptation to extreme environments. *PNAS.* **117**, 16424–16430. https://doi.org/10.1073/pnas.2004223117

Hunte, C., Zickermann, V., Brandt, U., 2010. Functional modules and structural basis of conformational coupling basis of conformational coupling in mitochondrial complex I. *Science.* **329**, 448–451. https://doi.org/10.1126/SCIENCE.1191046

Ishikawa, A., Kabeya, N., Ikeya, K., Kakioka, R., Cech, J.N., Osada, N., Leal, M.C., Inoue, J., Kume, M., Toyoda, A., Tezuka, A., Nagano, A.J., Yamasaki, Y.Y., Suzuki, Y., Kokita, T., Takahashi, H., Lucek, K., Marques, D., Takehana, Y., Naruse, K., Mori, S., Monroig, O., Ladd, N., Schubert, C.J., Matthews, B., Peichel, C.L., Seehausen, O., Yoshizaki, G., Kitano, J., 2019. A key metabolic gene for recurrent freshwater colonization and radiation in fishes. *Science*. **364**, 886–889. https://doi.org/10.1126/SCIENCE.AAU5656

Ishikawa, A., Stuart, Y.E., Bolnick, D.I., Kitano, J., 2021. Copy number variation of a fatty acid desaturase gene Fads2 associated with ecological divergence in freshwater stickleback populations. *Biol. Lett.* **17**, 20210204. https://doi.org/10.1098/RSBL.2021.0204

Jones, F.C., Grabherr, M.G., Chan, Y.F., Russell, P., Mauceli, E., Johnson, J., Swofford, R., Pirun, M., Zody, M.C., White, S., Birney, E., Searle, S., Schmutz, J., Grimwood, J., Dickson, M.C., Myers, R.M., Miller, C.T., Summers, B.R., Knecht, A.K., Brady, S.D., Zhang, H., Pollen, A.A., Howes, T., Amemiya, C., Baldwin, J., Bloom, T., Jaffe, D.B., Nicol, R., Wilkinson, J., Lander, E.S., Di Palma, F., Lindblad-Toh, K., Kingsley, D.M., 2012. The genomic basis of adaptive evolution in threespine sticklebacks. *Nature*. **484**, 55–61. https://doi.org/10.1038/nature10944

Latorre-Pellicer, A., Moreno-Loshuertos, R., Lechuga-Vieco, A.V., Sánchez-Cabo, F., Torroja, C., Acín-Pérez, R., Calvo, E., Aix, E., González-Guerra, A., Logan, A., Bernad-Miana, M.L., Romanos, E., Cruz, R., Cogliati, S., Sobrino, B., Carracedo, Á., Pérez-Martos, A., Fernández-Silva, P., Ruíz-Cabello, J., Murphy, M.P., Flores, I., Vázquez, J., Enríquez, J.A., 2016. Mitochondrial and nuclear DNA matching shapes metabolism and healthy ageing. *Nature.* **535**, 561–565. https://doi.org/10.1038/nature18618

Leo, E., Kunz, K.L., Schmidt, M., Storch, D., Pörtner, H.O., Mark, F.C., 2017. Mitochondrial acclimation potential to ocean acidification and warming of Polar cod (*Boreogadus saida*) and Atlantic cod (*Gadus morhua*). *Front. Zool.* **14**, 21. https://doi.org/10.1186/S12983-017-0205-1

Lian, Q., Li, S., Kan, S., Liao, X., Huang, S., Sloan, D.B., Wu, Z., 2024. Association Analysis Provides Insights into Plant Mitonuclear Interactions. *Mol. Biol. Evol.* **41**, msae028. https://doi.org/10.1093/MOLBEV/MSAE028

MacColl, A.D.C., Nagar, A. El, De Roij, J., 2013. The evolutionary ecology of dwarfism in three-spined sticklebacks. *J. Anim. Ecol.* **82**, 642-652. https://doi.org/10.1111/1365-2656.12028

Magalhaes, I.S., D'Agostino, D., Hohenlohe, P.A., MacColl, A.D.C., 2016. The ecology of an adaptive radiation of three-spined stickleback from North Uist, Scotland. *Mol. Ecol.* **25**, 4319–4336. https://doi.org/10.1111/MEC.13746

Mäkinen, H.S., Merilä, J., 2008. Mitochondrial DNA phylogeography of the three-spined stickleback (*Gasterosteus aculeatus*) in Europe-Evidence for multiple glacial refugia. *Mol. Phylogenet. Evol.* **46**, 167–182. https://doi.org/10.1016/j.ympev.2007.06.011

Martínez-Reyes, I., Chandel, N.S., 2020. Mitochondrial TCA cycle metabolites control physiology and disease. *Nat. Commun.* **11**, 102. https://doi.org/10.1038/s41467-019-13668-3

McKenzie, J.L., Chung, D.J., Healy, T.M., Brennan, R.S., Bryant, H.J., Whitehead, A., Schulte, P.M., 2019. Mitochondrial Ecophysiology: Assessing the Evolutionary Forces That Shape Mitochondrial Variation. *Integr. Comp. Biol.* **59**, 925–937. https://doi.org/10.1093/ICB/ICZ124

Mukundan, L.P., Sukumaran, S., Raj, N., Jose, A., Gopalakrishnan, A., 2022. Positive selection in the mitochondrial protein coding genes of teleost regional

endotherms: Evidence for adaptive evolution. *J. Mar. Biol. Ass. India.* **64**, 1. https://doi.org/10.6024/jmbai.2022.64.1.2320-02

Pabijan, M., Spolsky, C., Uzzell, T., Szymura, J.M., 2008. Comparative analysis of mitochondrial genomes in *Bombina* (Anura; Bombinatoridae). *J. Mol. Evol.* **67**, 246–256. https://doi.org/10.1007/S00239-008-9123-3

Pelster, B., Wood, C.M., Campos, D.F., Val, A.L., 2020. Cellular oxygen consumption, ROS production and ROS defense in two different size-classes of an Amazonian obligate air-breathing fish (*Arapaima gigas*). *PLoS One*. **15**, e0236507. https://doi.org/10.1371/JOURNAL.PONE.0236507

Pichaud, N., Chatelain, E.H., Ballard, J.W.O., Tanguay, R., Morrow, G., Blier, P.U., 2010. Thermal sensitivity of mitochondrial metabolism in two distinct mitotypes of *Drosophila simulans*: evaluation of mitochondrial plasticity. *J. Exp. Biol.* 213, 1665–1675. https://doi.org/10.1242/JEB.040261

Robertson, S., Bradley, J.E., Maccoll, A.D.C., 2016. Measuring the immune system of the three-spined stickleback - investigating natural variation by quantifying immune expression in the laboratory and the wild. *Mol. Ecol. Resour.* **16**, 701-713. https://doi.org/10.1111/1755-0998.12497

Salin, K., Villasevil, E.M., Anderson, G.J., Selman, C., Chinopoulos, C., Metcalfe, N.B., 2018. The RCR and ATP/O Indices Can Give Contradictory Messages about Mitochondrial Efficiency. *Integr. Comp. Biol.* **58**, 486–494. https://doi.org/10.1093/ICB/ICY085

Sanz, N., Araguas, R.M., Vidal, O., Viñas, J., 2015. Glacial refuges for three-spined stickleback in the Iberian Peninsula: mitochondrial DNA phylogeography. *Freshw. Biol.* **60**, 1794–1809. https://doi.org/10.1111/FWB.12611

Schwartz, T.S., Arendsee, Z.W., Bronikowski, A.M., 2015. Mitochondrial divergence between slow- and fast-aging garter snakes. *Exp. Gerontol.* **71**, 135–146. https://doi.org/10.1016/J.EXGER.2015.09.004

Scotece, M., Rego-Pérez, I., Lechuga-Vieco, A.V., Cortés, A.C., Jiménez-Gómez, M.C., Filgueira-Fernández, P., Vaamonde-García, C., Enríquez, J.A., Blanco, F.J., 2021. Mitochondrial DNA impact on joint damaged process in a conplastic mouse model after being surgically induced with osteoarthritis. *Sci. Rep.* **11**, 9112. https://doi.org/10.1038/s41598-021-88083-0

Shama, L.N.S., Strobel, A., Mark, F.C., Wegner, K.M., 2014. Transgenerational plasticity in marine sticklebacks: Maternal effects mediate impacts of a warming ocean. *Funct. Ecol.* **28**, 1482–1493. https://doi.org/10.1111/1365-2435.12280

Shen, X., Pu, Z., Chen, X., Murphy, R.W., Shen, Y., 2019. Convergent Evolution of Mitochondrial Genes in Deep-Sea Fishes. *Front. Genet.* **10**, 925. https://doi.org/10.3389/FGENE.2019.00925

Silva, G., Lima, F.P., Martel, P., Castilho, R., 2014. Thermal adaptation and clinal mitochondrial DNA variation of European anchovy. *Proc. R. Soc. B.* **281**, 20141093. https://doi.org/10.1098/rspb.2014.1093

Sloan, D.B., Fields, P.D., Havird, J.C., 2015. Mitonuclear linkage disequilibrium in human populations. *Proc. R. Soc. B.* **282**, 20151704. https://doi.org/10.1098/RSPB.2015.1704

Sun, J.T., Duan, X.Z., Hoffmann, A.A., Liu, Y., Garvin, M.R., Chen, L., Hu, G., Zhou, J.C., Huang, H.J., Xue, X.F., Hong, X.Y., 2019. Mitochondrial variation in small brown planthoppers linked to multiple traits and probably reflecting a complex evolutionary trajectory. *Mol. Ecol.* **28**, 3306–3323. https://doi.org/10.1111/MEC.15148

Svendsen, J.I., Alexanderson, H., Astakhov, V.I., Demidov, I., Dowdeswell, J.A., Funder, S., Gataullin, V., Henriksen, M., Hjort, C., Houmark-Nielsen, M., Hubberten, H.W., Ingólfsson, Ó., Jakobsson, M., Kjær, K.H., Larsen, E., Lokrantz, H., Lunkka, J.P., Lyså, A., Mangerud, J., Matiouchkov, A., Murray, A., Möller, P., Niessen, F., Nikolskaya, O., Polyak, L., Saarnisto, M., Siegert, C., Siegert, M.J., Spielhagen, R.F., Stein, R., 2004. Late Quaternary ice sheet history of northern Eurasia. *Quat. Sci. Rev*. **23**, 1229–1271. https://doi.org/10.1016/j.quascirev.2003.12.008

Swarup, H., 1958. Stages in the Development of the Stickleback *Gasterosteus aculeatus* (L.). *Development*. **6**, 373–383. https://doi.org/10.1242/DEV.6.3.373

Teacher, A.G., André, C., Merilä, J., Wheat, C.W., 2012. Whole mitochondrial genome scan for population structure and selection in the Atlantic herring. *BMC Evol. Biol.* **12**, 248. https://doi.org/10.1186/1471-2148-12-248

Thoral, E., Roussel, D., Chinopoulos, C., Teulier, L., Salin, K., Thoral, E., 2021. Low oxygen levels can help to prevent the detrimental effect of acute warming on mitochondrial efficiency in fish. *Biol. Lett.* **17**, 20200759 https://doi.org/10.1098/RSBL.2020.0759

Towarnicki, S.G., Ballard, J.W.O., 2018. Mitotype Interacts With Diet to Influence Longevity, Fitness, and MitochondriaTowarnicki, S. G., & Ballard, J. W. O. (2018). Mitotype Interacts With Diet to Influence Longevity, Fitness, and Mitochondrial Functions in Adult Female *Drosophila. Front. Genet.* **9**. https://doi.org/10.3389/FGENE.2018.00593

Tudorache, C., Blust, R., De Boeck, G., 2007. Swimming capacity and energetics of migrating and non-migrating morphs of three-spined stickleback Gasterosteus aculeatus L. and their ecological implications. *J. Fish Biol.* **71**, 1448–1456. https://doi.org/10.1111/j.1095-8649.2007.01612.x

Twining, C.W., Bernhardt, J.R., Derry, A.M., Hudson, C.M., Ishikawa, A., Kabeya, N., Kainz, M.J., Kitano, J., Kowarik, C., Ladd, S.N., Leal, M.C., Scharnweber, K., Shipley, J.R., Matthews, B., 2021. The evolutionary ecology of fatty-acid variation: Implications for consumer adaptation and diversification. *Ecol. Lett.* **24**, 1709–1731. https://doi.org/10.1111/ele.13771

Wang, S., Ore, M.J., Mikkelsen, E.K., Lee-Yaw, J., Toews, D.P.L., Rohwer, S., Irwin, D., 2021. Signatures of mitonuclear coevolution in a warbler species complex. *Nat. Commun.* **12**, 4279. https://doi.org/10.1038/s41467-021-24586-8

Willis, J.R., Hickey, A.J.R., Devaux, J.B.L., 2021. Thermally tolerant intertidal triplefin fish (*Tripterygiidae*) sustain ATP dynamics better than subtidal species under acute heat stress. *Sci. Rep.* **11**, 11074. https://doi.org/10.1038/s41598-021-90575-y

Wilson, R.E., Sonsthagen, S.A., Smé, N., Gharrett, A.J., Majewski, A.R., Wedemeyer, K., Nelson, R.J., Talbot, S.L., 2020. Mitochondrial genome diversity and population mitogenomics of polar cod (*Boreogadus saida*) and Arctic dwelling gadoids. *Polar Biology.* **43**, 979–994. https://doi.org/10.1007/S00300-020-02703-5

Wolff, J.N., Pichaud, N., Camus, M.F., Côté, G., Blier, P.U., Dowling, D.K., 2016. Evolutionary implications of mitochondrial genetic variation: Mitochondrial genetic effects on OXPHOS respiration and mitochondrial quantity change with age and sex in fruit flies. *J. Evol. Biol.* **29**, 736–747. https://doi.org/10.1111/jeb.12822

Yu, X., Gimsa, U., Wester-Rosenlöf, L., Kanitz, E., Otten, W., Kunz, M., Ibrahim, S.M., 2009. Dissecting the effects of mtDNA variations on complex traits using mouse conplastic strains. *Genome Res.* **19**, 159–165. https://doi.org/10.1101/GR.078865.108